Mathematical Models for Dispersal of Aerosol Droplets in an Agricultural Setting

A thesis presented in partial fulfilment of the requirements

for the degree of

Doctor of Philosophy in Mathematics

at Massey University, Albany,

New Zealand

Sharleen Anne Harper

2008

Abstract

Agrichemical spray drift is an issue of concern for the orcharding industry. Shelterbelts surrounding orchard blocks can significantly reduce spray drift by intercepting droplets from the airflow. At present, there is little information available with which to predict drift deposits downwind, particularly in the case of a fully-sheltered orchard block.

In this thesis, we develop a simple mathematical model for the transport of airborne drifting spray droplets, including the effects of droplet evaporation and interception by a shelterbelt. The object is for the model to capture the major features of the droplet transport, yet be simple enough to determine an analytic solution, so that the deposit on the ground may be easily calculated and the effect of parameter variations observed.

We model the droplet transport using an advection-dispersion equation, with a trapping term added to represent the shelterbelt. In order to proceed analytically, we discretise the shelterbelt by dividing it into a three-dimensional array of blocks, with the trapping in each block concentrated to the point at its centre. First, we consider the more straightforward case where the droplets do not evaporate; solutions are presented in one, two and three dimensions, along with explicit expressions for the total amount trapped and the deposit on the ground. With evaporation, the model is more difficult to solve analytically, and the solutions obtained are nestled in integral equations which are evaluated numerically. In both cases, examples are presented to show the deposition profile on the ground downwind of the shelterbelt, and the corresponding reduction in deposit from the same scenario without the shelterbelt.

Acknowledgements

I would like to sincerely thank my supervisors, Robert McKibbin and Graeme Wake, for their invaluable guidance and support during my PhD study. I could not have asked for better supervisors.

Next, I would like to thank Massey University for providing me with a three year Doctoral Scholarship, and Lincoln Ventures Ltd for generously providing additional financial support which has allowed me to attend conferences during this time.

Several people have contributed their time and knowledge, and I would like to express my gratitude to them: John-Paul Praat and Simon Woodward, formerly of Lincoln Ventures Ltd, and Alison Forster of Plant Protection Chemistry New Zealand. Special thanks also to Peter Jaques for patiently reading this thesis and providing much-appreciated feedback.

Last, but certainly not least, I would like to say a huge thank you to my family, Mum and Dad, Andrea and Damien and my grandparents, for all their love and support. Special thanks also to all of my friends, particularly my fellow PhD students who have been with me on this journey.

Contents

Abstract i

Acknowledgements ii

Contents iii

List of Figures vi

List of Tables viii

Notation ix

1 General Introduction 1

1.1 Background and Research Motivation 1

1.2 Literature Review 4

1.3 Research Objective 6

1.4 Methodology 6

1.5 Thesis Overview 9

2 Preliminaries: Single Droplet Kinetics and Thermodynamics 11

2.1 Equation of Motion 11

2.2 Terminal Velocity 12

2.3 Some Example Trajectories 13

2.4 Droplet Evaporation 15

2.5 An Example Trajectory with Evaporation 22

2.6 Chapter Summary 23

3 Advection-Dispersion Model Framework 26

3.1 Model Derivation 26

3.2 Initial and Boundary Conditions 32
3.3 The Background Trapping Rate k_b 34
3.4 Parameter Values 36
3.5 Chapter Summary 38

4 A Point Representation for Trapping 40
4.1 Advection-Dispersion Model 41
4.2 Total Droplet Trapping and Deposition 42
4.3 Case 1: Zero Vertical Dispersion 43
4.4 Case 2: Non-Zero Vertical Dispersion 57
4.5 Chapter Summary 72

5 Trapping in a Discretised Shelterbelt 74
5.1 Discretising a Shelterbelt 74
5.2 Advection-Dispersion Model 76
5.3 Total Trapping in the Shelterbelt and Deposit on the Ground 76
5.4 Case 1: Zero Vertical Dispersion 78
5.5 Case 2: Non-Zero Vertical Dispersion 99
5.6 Chapter Summary 112

6 Trapping With Evaporation 115
6.1 Advection-Dispersion Model with Trapping and Evaporation 115
6.2 Total Droplet Trapping and Deposition 117
6.3 Approximations for the Mass and Settling Speed 118
6.4 Case 1: Zero Vertical Dispersion 119
6.5 Case 2: Non-Zero Vertical Dispersion 131
6.6 Partial Evaporation (Solid Core) 144
6.7 Chapter Summary 145

7 Thesis Summary 148
7.1 Summary 148
7.2 Analyses 149
7.3 Further Research 150
7.4 Publications 150

A Selected Workings **152**

A.1 The Dispersion Tensor 152

A.2 A Point Representation for Trapping with $D_V \neq 0$ 154

A.3 A Point Representation for Trapping With Evaporation and $D_V \neq 0$ 159

B Laplace and Fourier Transforms **164**

B.1 Laplace Transforms 164

B.2 Fourier Transforms 166

References **167**

List of Figures

1.1 Spray released from an airblast sprayer 2
1.2 An airblast sprayer in an avocado orchard 2
1.3 An orchard block surrounded by a shelterbelt 3
1.4 Conceptual illustration of droplet transport 8

2.1 Droplet settling speed for a range of different diameters 14
2.2 Trajectory of a small droplet in an ambient wind 16
2.3 Velocity components of the droplet in Figure 2.2 16
2.4 Trajectory of a larger individual droplet in an ambient wind 17
2.5 Velocity components of the droplet in Figure 2.4 17
2.6 Ventilation coefficient for droplets falling at terminal velocity 22
2.7 Trajectory of an individual evaporating droplet in an ambient wind 23
2.8 Falling speed of the evaporating droplet in Figure 2.7 24
2.9 Diameter of the evaporating droplet in Figure 2.7 24

3.1 Theoretical profiles of the horizontal windspeed for a single row shelterbelt . . . 28
3.2 Values of the background trapping rate for a broadleaf shelterbelt 37
3.3 Values of the background trapping rate for a fine-needled shelterbelt 37

4.1 Conceptual illustration of trapping at a plane 44
4.2 Conceptual illustration of trapping at a line 47
4.3 Cross sections of the mass concentration with $D_V = 0$ and a trapping line 50
4.4 Cross-section of the deposit with $D_V = 0$ and a trapping line 53
4.5 Cross-section of the reduction in deposit due to the trapping line 53
4.6 Cross-section of the deposit with $D_V \neq 0$ and a trapping line 66
4.7 Cross-section of the reduction in deposit due to the line 66
4.8 Contours of the deposit with $D_V \neq 0$ and no trapping 71

4.9 Contours of the deposit with $D_V \neq 0$ and a trapping point 71
4.10 Contours of the reduction deposit due to the point 72

5.1 A rectangular shelterbelt discretised using a 3-D array of trapping points 75
5.2 A shelterbelt "slab" discretised using multiple trapping planes 79
5.3 Comparisons between continuous and discretised trapping with $D_V = 0$ 87
5.4 Accuracy of the discretised solution with $D_V = 0$ 88
5.5 An infinitely long shelterbelt discretised using a 2-D array of trapping lines . . . 88
5.6 Cross-section of the deposit with $D_V = 0$ and an array of trapping lines 96
5.7 Cross-section of the reduction deposit due to the trapping lines 96
5.8 Accuracy of the discretised solution with $D_V \neq 0$ 104
5.9 Cross-section of the deposit with $D_V \neq 0$ and an array of trapping lines 109
5.10 Cross-section of the reduction in deposit due to the trapping lines 109
5.11 Contours of the deposit with $D_V \neq 0$ and no trapping 113
5.12 Contours of the deposit with $D_V \neq 0$ and an array of trapping points 113
5.13 Contours of the reduction deposit due to the trapping points 114

6.1 Actual and Stokes flow settling speeds plotted against droplet diameter 120
6.2 Illustration of the moving coordinate system 121
6.3 Cross-sections of the deposit with evaporation, $D_V = 0$ and a trapping line . . . 128
6.4 Solution space in moving coordinates 135
6.5 Accuracy of the deposit with no evaporation and no trapping. 142
6.6 Cross-section of the deposit with evapoation, $D_V \neq 0$ and a trapping line 142
6.7 Number density of deposit with partial evaporation 146
6.8 Mass density of deposit with partial evaporation 146

A.1 Mean wind velocity $\mathbf{u}$ in the horizontal plane 152

List of Tables

2.1 Droplet settling speed for a range of different diameters 14

2.2 Temperature of an evaporating droplet for various relative humidities 20

3.1 Some typical parameter values 38

4.1 Parameter set used to generate Figures 4.4 and 4.5 52

4.2 Parameter set used to generate Figures 4.6 and 4.7 65

4.3 Parameter set used to generate Figures 4.8, 4.9 and 4.10 70

5.1 Transformed concentration for a number of consecutive trapping planes 82

5.2 Parameter set used to generate Figures 5.6 and 5.7. 95

5.3 Parameter set used to generate Figures 5.9 and 5.10. 107

5.4 Parameter set used to generate Figures 5.11, 5.12 and 5.13. 112

6.1 Parameter set used to generate Figure 6.3. 127

6.2 Parameter set used to generate Figure 6.3. 141

B.1 Table of Laplace transforms 164

B.2 Table of Fourier transforms 166

Notation

Upper Case

C	Droplet number concentration [# m^{-3}]
D_L	Alongwind (longitudinal) dispersion coefficient [m^2 s^{-1}]
D_T	Crosswind (transverse) dispersion coefficient [m^2 s^{-1}]
D_V	Vertical dispersion coefficient [m^2 s^{-1}]
D_W	Diffusivity of water vapour in air [m^2 s^{-1}]
H	Release height [m]
L_L	Dominant alongwind (longitudinal) turbulence length scale [m]
L_T	Dominant crosswind (transverse) turbulence length scale [m]
L_V	Dominant vertical turbulence length scale [m]
L_v	Latent heat of vaporisation [J kg^{-1}]
M_W	Molecular mass of water [kg mol^{-1}]
Q	Mass release [kg]
R	Dimensionless function non-zero only within a region of trapping [-]
R_g	Universal gas constant [J mol^{-1} K^{-1}]
S	Droplet settling speed [m s^{-1}]
T	Absolute temperature [K]
X_0	release x coordinate [m]
Y_0	release y coordinate [m]

Lower Case

a	Droplet radius [m]
c	Droplet mass concentration [kg m^{-3}]
c_p	Specific heat of water [J kg^{-1} K^{-1}]
d	Droplet diameter [m]
f_h	Ventilation coefficient for heat [-]
f_w	Ventilation coefficient for water vapour [-]
g	Gravitational acceleration [m s^{-2}]
k_a	Thermal conductivity of moist air [W m^{-1} K^{-1}]
k_b	Background trapping rate [s^{-1}]
k	Effective trapping rate [m^3 s^{-1}]
m	Droplet mass [kg]
p	Laplace transform variable [s^{-1}]
p_{sat}	Saturation pressure [Pa]
t	Time [s]
u	Mean wind speed (positive x direction) [m s^{-1}]
x, y, z	Cartesian coordinate system [m]

Bold

$\underline{\mathbf{D}}$	Dispersion tensor [$\mathrm{m}^2\ \mathrm{s}^{-1}$]
$\mathbf{i}$	Unit vector in the positive x direction [-]
$\mathbf{j}$	Unit vector in the positive y direction [-]
$\mathbf{k}$	Unit vector in the positive z direction [-]
$\mathbf{u}$	Mean wind velocity [$\mathrm{m\ s}^{-1}$]
$\mathbf{v}$	Droplet velocity relative to the origin [$\mathrm{m\ s}^{-1}$]

Greek

μ_a	Dynamic viscosity of air [$\mathrm{kg\ m}^{-1}\ \mathrm{s}^{-1}$]
ρ_a	Air density [$\mathrm{kg\ m}^{-3}$]
ρ_w	Droplet density (water) [$\mathrm{kg\ m}^{-3}$]
ϕ	Relative humidity (expressed as a fraction) [-]
ψ	Spatial Fourier transform variable [m^{-1}]
ω	Spatial Fourier transform variable [m^{-1}]

Chapter 1

General Introduction

1.1 Background and Research Motivation

Crop spraying is a valuable production tool for the agricultural industry. In New Zealand, estimates of the worth of hydrogen cyanamide (HC) spraying to the kiwifruit industry are as high as \$60−\$200 million per year (Manktelow *et al.*, 2006; Ministry of Agriculture and Forestry, 2006). Yet the issue is often highly controversial: sprays contain a wide range of droplet sizes and, because of their light weight, smaller droplets often remain airborne for a long time and can be carried great distances by the wind. The issue is a particular concern for orchardists, who use airblast sprayers such as the ones shown in Figures 1.1 and 1.2; the photographs in these figures, courtesy of Plant Protection Chemistry NZ, are from a series of spray drift trials in kiwifruit and avocado orchards in New Zealand. Airblast sprayers propel droplets upwards and into fruit trees with the assistance of air jets, so the potential for drift is high. Off-target drift of sprays containing chemicals may be hazardous to human or animal health in the surrounding environment, therefore it is important to minimise such drift.

Most orchard blocks are surrounded by shelterbelts, such as the kiwifruit block shown in Figure 1.3. Not only do these protect crops from wind damage, they also provide one of the most effective means of reducing spray drift, by lowering windspeeds and filtering droplets from the airflow. Windspeed is reduced by varying amounts both upwind and downwind of a shelterbelt; experiments have found the zone of influence to be between about $5h$ upwind and $20h$ downwind, where h is the shelterbelt height (Ucar & Hall, 2001). The porosity of a shelterbelt is one of the major factors affecting both the zone of influence on windspeed, and the filtration of droplets from the air. For example, most of the airflow is deflected up and over the top of a very

Figure 1.1: Spray released from an airblast sprayer. Photograph courtesy of Plant Protection Chemistry New Zealand.

Figure 1.2: An airblast sprayer in an avocado orchard. Photograph courtesy of Plant Protection Chemistry New Zealand.

Figure 1.3: A kiwifruit orchard block surrounded by a shelterbelt. Photograph courtesy of Plant Protection Chemistry New Zealand.

dense shelterbelt, carrying any droplets with it to be deposited farther downwind, whereas a very porous shelterbelt has little effect on the airflow, but also does not have enough vegetation elements with which to filter the droplets (Mercer, n.d.). Other influencing factors include shelterbelt species and droplet size. Various experimental studies have confirmed the effectiveness of shelterbelts in reducing spray drift. Despite differences in experimental methods, there is a general agreement that reductions in drift of up to 90 % are possible downwind of a porous shelterbelt. Artificial netting is observed to be similarly, though slightly less, effective, with reductions of up to 75 % (Hewitt, 2001; Ucar & Hall, 2001). In New Zealand, in a series of field trials carried out in kiwifruit and apple orchards, measured drift levels with shelter were up to 8 times lower than those without shelter (P. Holland & Maber, 1991).

Whilst there has been some research aimed at evaluating drift reduction by shelterbelts, very little information is available to quantify drift deposits downwind, particularly in the case of a fully-sheltered orchard block. The more information that can be provided about predicted drift deposits, the better growers and local or regional authorities will be able to identify hazards and minimise drift impacts.

The research presented in this thesis came about following a problem brought to the Mathematics-

in-Industry Study Group (MISG)[1] in 2005, in which the author was a participant. The problem, entitled "Predicting Off-Site Deposition of Spray Drift from Horticultural Spraying Through Porous Barriers on Soil and Plant Surfaces", was presented by Lincoln Ventures Ltd[2] and Plant Protection Chemistry New Zealand (PPCNZ)[3]. The MISG was tasked with investigating a mathematical model for the spray capture efficiency of a shelterbelt, in order to produce a better working model for use in a spray drift management system; the report may be found in Mercer & Roberts (2005). With a continued interest in further study in the area of spray drift reduction by shelterbelts, Lincoln Ventures Ltd have provided support for the research in this thesis.

1.2 Literature Review

Spray Drift Modelling

The transport of spray droplets (with no shelterbelt) has been extensively studied. Models for droplet transport from a sprayer may be broadly divided into Lagrangian, or particle-tracking, models and Gaussian plume models. Lagrangian models simulate the trajectories of many individual droplets; examples include Thompson & Ley (1983), Miller & Hadfield (1989), Walklate (1992) and Holterman *et al.* (1997). Gaussian plume models are generally more applicable away from the source, but can be used to provide an estimate of drift in the near-field (Craig, 2004). Further discussion of computer models and software packages for modelling spray drift may be found in Ucar & Hall (2001), who point out that, without quantification of off-site transport under shelterbelt or windbreak conditions, tactics to minimise spray drift cannot be fully exploited.

Shelterbelts as a Drift Mitigation Strategy

Published research into drift reduction by shelterbelts is comprehensively reviewed up to 2001 by Hewitt (2001) and Ucar & Hall (2001). These reviews cover theoretical considerations and experimental results on: (i) windspeed attenuation and shelterbelt aerodynamics, (ii) the amount by which drift can be reduced, (iii) the influence of shelterbelt species and structure, and (iv) computational models and software packages for spray drift.

[1] Mathematics-in-Industry Study Group 2005 website http://misg2005.massey.ac.nz
[2] Lincoln Ventures Ltd website http://www.lvl.co.nz
[3] Plant Protection Chemistry New Zealand website http://www.ppcnz.co.nz

There has been considerable research into the airflow through and around a shelterbelt. Experimental results on windspeed attenuation are summarised by Hewitt (2001). Models to simulate the airflow are numerical and computationally intensive, requiring solutions to the Navier-Stokes equations with turbulence. H. Wang *et al.* (2001), for example, use a quasi-three-dimensional model where the shelterbelt is infinitely long across-wind but the airflow may be fully three-dimensional. Mercer & Roberts (2005) and Mercer (n.d.) use two-dimensional models which are simpler but still capture the main features of the airflow.

While there have been a number of experimental studies measuring the reduction in spray drift downwind of a shelterbelt (P. T. Holland *et al.*, 1997; Hewitt, 2001; Ucar & Hall, 2001), there is very little information available to predict the reduction efficiency of a shelterbelt from its physical characteristics. Raupach *et al.* (2000, 2001) developed a model relating the particle transmittance of a shelterbelt σ (the fraction of particles which pass through without being trapped) to its optical porosity τ. They found that the relationship depended on particle size and the diameter of the shelterbelt vegetation elements, but that for most applications involving spray drift the approximation $\sigma = \tau$ works well. Mercer & Roberts (2005) evaluated the model for use in a spray drift management system, and concluded that it was suitable over the typical range of expected droplet sizes, windspeeds and vegetation element sizes.

There are also very few models which can be used to predict spray drift deposits downwind of a shelterbelt. For particulates in general, Raupach *et al.* (2000) gain an idea of the concentration in the air downwind of a shelterbelt using a very simple two-dimensional steady-state model, in which particles are advected by the wind and disperse only vertically. The shelterbelt is assumed to be immersed in a particle-laden airflow, so that the upwind concentration is approximately uniform with height. Lazzaro *et al.* (2008) take an empirical approach, using experimental data to fit an exponential decay model for the variation in the amount of spray drift with distance downwind. There are several assumptions which must hold for this model to apply; these include that sprayer operating conditions are similar to those of the experiments, and that none of the spray passes over the shelterbelt.

There is certainly scope for more investigation into modelling spray drift deposition, particularly in the case of a fully-sheltered orchard block. The simplified model in Raupach *et al.* (2000) is only intended to provide an idea of particle concentration; it does not include detail such as gravitational settling, nor does it allow for evaporation. The empirical model of Lazzaro *et al.* (2008) may not be applicable if conditions are too dissimilar to those in the experiments upon which it is based. Also, both of the models above are two-dimensional, so that the shelterbelt

is modelled as infinitely long across-wind; a three-dimensional model would be beneficial, as it would allow for finite-size orchard blocks.

1.3 Research Objective

The aim of this research is to develop a simple mathematical model for the transport of airborne drifting spray droplets, including the effects of droplet evaporation and capture by a shelterbelt. We seek, if possible, analytic solutions so that the capture of droplets by the shelterbelt and the subsequent deposit on the ground may be easily calculated, and the effect of parameter variations estimated. We do not consider the spraying process itself, nor the crop; our focus is on the small droplets which remain airborne and are carried by the wind.

Whilst the accuracy of analytical models is often limited by a number of inherent assumptions, their simplicity gives them several advantages over numerical models. The effects of parameter variations are more readily observed, since all of the influencing parameters are explicitly expressed in a mathematically closed form (Lin & Hildemann, 1996; Essa *et al.*, 2007). Lindstrom & Boersma (1989) also note that:

- Analytical methods are probably the most efficient alternative when the data necessary for identification of the system are sparse and uncertain.
- Where applicable, these methods are the most economical approach.
- They are always the most useful means for an initial order-of-magnitude estimation.
- Experienced modellers and complex numerical codes are not required.

1.4 Methodology

As stated above, our objective is to develop a simple analytic model for the transport of airborne drifting spray droplets, including the trapping of these droplets by a shelterbelt. Our approach is to consider the cloud of spray droplets as a continuum and formulate an advection-dispersion model, including a sink term to represent the trapping. This approach is based upon previous analysis of particle transport within a forest canopy by McKibbin (2006).

A cloud of spray droplets in the air is advected by the wind and dispersed by turbulence, all while falling under the influence of gravity. If the droplets are also evaporating, the loss of mass will cause them to fall more slowly as time goes on. Within a shelterbelt, some of the droplets may be trapped by impacting on the foliage, and these trapped droplets are removed from the airflow. Conceptually, the number of droplets trapped will depend upon how many are in the shelterbelt and thus have the potential to be trapped. The situation is depicted in Figure 1.4a; initially the droplet cloud is small and concentrated, then at later times it has been blown further by the wind, fallen nearer to the ground, and become more spread due to turbulence. Downwind of the shelterbelt, because some of the droplets have been trapped, there is a smaller proportion to go on and deposit on the ground.

We model the droplet transport using an advection-dispersion equation. This type of equation is widely-used in modelling particulate transport, as in many cases analytic solutions are possible. Just a few examples of its application include contaminant transport in aquifers, pollen and dust transport, and volcanic ashfall (Lindstrom & Boersma, 1989; Eltayeb & Hassan, 2000; McKibbin, 2006; Lim, 2005). We include the shelterbelt in our model as a block within which droplets are trapped at a rate proportional to the local concentration. The proportionality constant, termed the background trapping rate, is a measure of the droplet capture efficiency of the shelterbelt, and is related to physical properties such as the foliage size and density.

Figure 1.4b is a conceptual illustration of our model as it is described above, with the shelterbelt represented by a block of trapping. Continuous trapping of droplets throughout the block would be the ideal scenario from a continuum viewpoint, unfortunately however it is difficult to obtain an analytic solution with this approach. Instead, we look to obtain an analytic solution by discretising the shelterbelt as shown in Figure 1.4c: the discretisation is achieved by dividing the block representing the shelterbelt into a three-dimensional array of smaller blocks, where the effect of trapping in each smaller block is concentrated to the point at its centre.

We solve the model for a cohort of droplets that are all of the same size, and released instantaneously from a point. The distribution of droplet sizes released from a sprayer would be simulated by superposing solutions to the model, each for a different droplet size. Also, solutions for other releases such as a line source can be constructed from the point release (in the manner of Lim, 2005, and McKibbin, 2006).

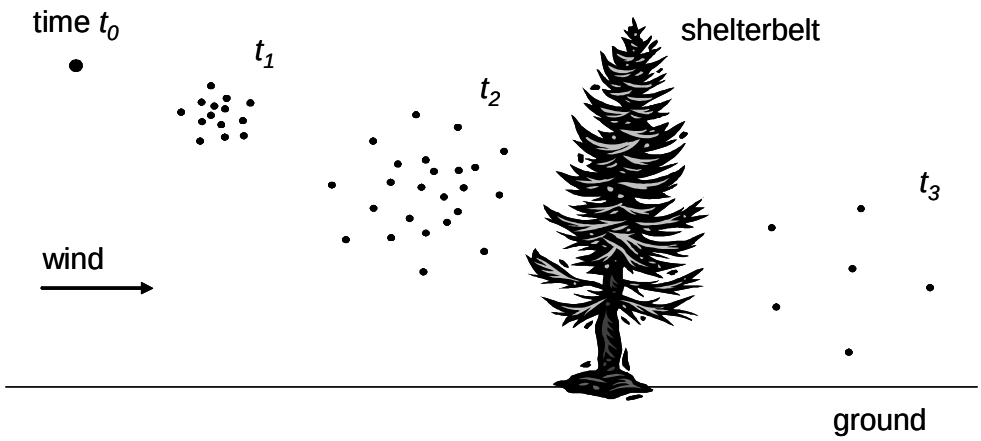

(a) Conceptual illustration of droplet transport with trapping by a shelterbelt.

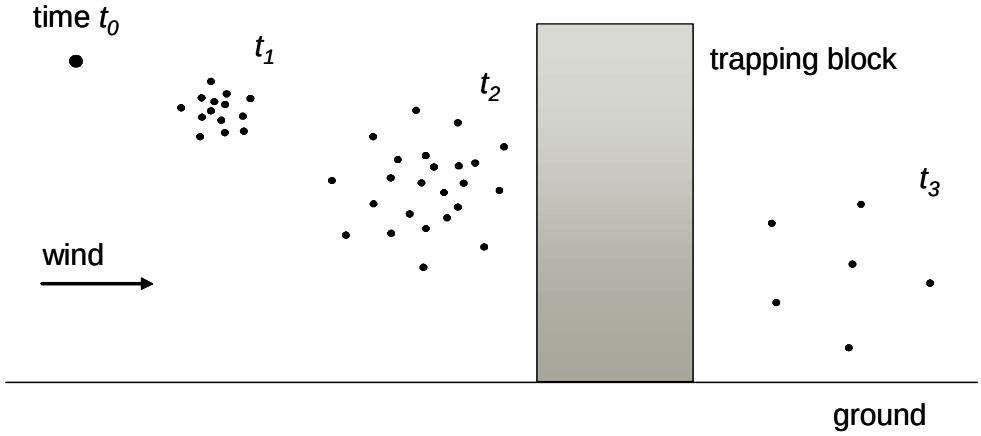

(b) Conceptual illustration of modelling droplet transport with a shelterbelt represented by a block of trapping.

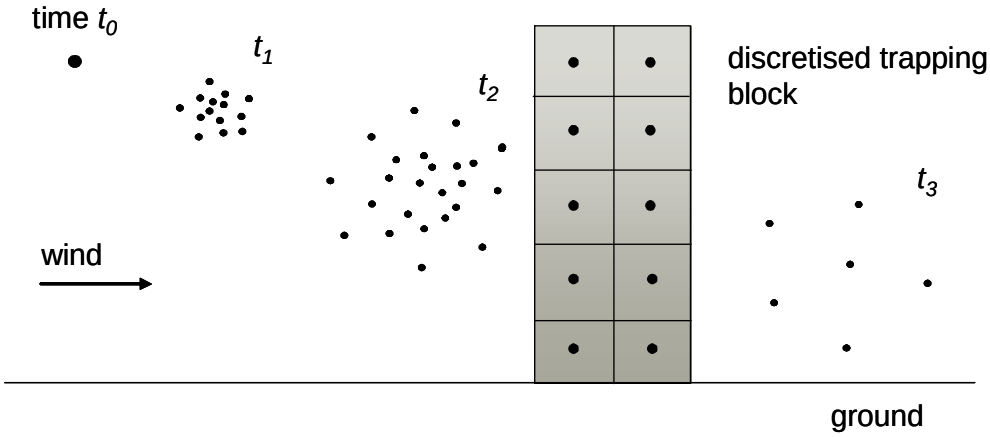

(c) Conceptual illustration showing the trapping block above discretised using an array of trapping "points".

Figure 1.4: Sketches illustrating the advection-dispersion model for droplet transport with trapping in a shelterbelt. t_0 is the release time, and t_1, t_2 and t_3 are later times.

1.5 Thesis Overview

This thesis presents details of the development of our continuum model for spray drift transport as outlined above. We begin in Chapter 2 with background information on the kinetics and thermodynamics of individual droplets in the air. This material lays a foundation for the continuum models in subsequent chapters. The first part of the chapter is devoted to the kinetics of moving droplets; it includes the equations of motion describing a droplet's trajectory and the rate at which it falls towards the ground (that is, its settling speed), and also includes calculated examples of droplet trajectories illustrating why small droplets are of the greatest concern for spray drift. The second part of the chapter is devoted to the thermodynamics of evaporating droplets; it includes expressions for the evaporation rate and droplet temperature as a function of the relative humidity and ambient temperature, and also includes a calculated example showing the effect of evaporation on a droplet's trajectory.

Chapters 3 – 5 cover the development of, and solutions to, our advection-dispersion model in the more straightforward case where there is no evaporation of the droplets. Chapter 3 contains a full derivation of the model, along with the initial and boundary conditions used and some discussion of the boundary condition on the ground. This is our idealised model where the shelterbelt is represented by a block of continuous trapping (as per Figure 1.4b). The chapter also features a summary of some typical parameter values, and an expression for the background trapping rate determined from the Raupach, Woods, *et al.* (2001) model for the droplet capture efficiency of a shelterbelt.

Chapter 4 introduces the point representation for trapping, which will later be used to discretise the shelterbelt. Two separate cases are considered: first, a special case where droplets disperse only horizontally, followed by the general case where droplets disperse both horizontally and vertically. In each case, we present solutions to the model with a single point representation for trapping in one, two and three dimensions, along with explicit expressions for the total amount trapped and the deposit on the ground. An interesting artefact of the point representation becomes apparent: the droplet mass concentration is negative for a short time in a localised area beneath the trapping point. Whilst a negative concentration is conceptually wrong, the issue is magnified by the unrealistically high trapping rates used for illustrative purposes, and is shown to be of little consequence with realistic trapping rates in Chapter 5.

Chapter 5 is the culminating chapter for the model in the absence of evaporation; in it we describe the discretisation of the shelterbelt via the point representation from Chapter 4. Using

the solutions that were obtained in that chapter, we construct the corresponding solutions for trapping in the discretised shelterbelt. The resulting expressions for the total amount trapped and the deposit on the ground allow us to plot deposition profiles, and to calculate the reduction in deposit downwind of the shelterbelt.

We draw to a close in Chapter 6 by introducing evaporation into our advection-dispersion model. Attention is restricted to the single point representation for trapping, which could later be used to construct solutions for the discretised trapping block in the same manner as in Chapter 5. The same two cases are considered as in Chapter 4; that is, the special case of horizontal dispersion only, followed by the general case of both horizontal and vertical dispersion. Obtaining analytic solutions to the model with evaporation in the special case is relatively straightforward, whereas the latter case is much more difficult.

Finally, we conclude the thesis with Chapter 7, which contains a summary of the main points from the development and analysis of the models in Chapters 3 – 6, and offers some suggestions for future research.

Chapter 2

Preliminaries: Single Droplet Kinetics and Thermodynamics

This chapter examines the kinetics and thermodynamics of an individual droplet moving in the air; it is intended to provide background information to assist in understanding the continuum models developed in the next and subsequent chapters. All of the theoretical material in the chapter may be found in literature sources (as cited in the text), and the equations of the kinetics are those upon which Lagrangian, or particle-tracking, models for spray drift are based (see Bilanin *et al.*, 1989; Brown & Sidhamed, 2001).

The chapter is divided roughly in two. Firstly, Sections 2.1 - 2.3 relate to the kinetics: we look at the equation of motion which governs the droplet flight, and the terminal velocity at which it no longer accelerates. We also provide some calculated examples of droplet trajectories without evaporation. The material in these three sections leads on to the continuum models in Chapters 3, 4 and 5, which do not include evaporation. Secondly, Sections 2.4 - 2.5 relate to the thermodynamics when there is evaporation: we show how expressions are derived for the rate of mass loss and temperature of the droplet, and give a further example illustrating the effect of evaporation on the droplet trajectory. The material in these two sections leads on to Chapter 6, which sees the introduction of evaporation to the continuum models.

2.1 Equation of Motion

An individual droplet in the air is subject to three external forces: a drag force due to relative motion between the droplet and the air, a weight force due to gravity, and a buoyancy force

due to the air displaced by the droplet. The droplet is much heavier than the air it displaces, therefore the buoyancy force is negligible and can be ignored. Assuming that the droplet is spherical, and behaves like a solid particle, these forces sum according to Newton's second law to give the following differential equation for the velocity:

$$\begin{aligned} m\frac{d\mathbf{v}}{dt} &= -\frac{\pi}{8}C_D\rho_a d^2\left|\mathbf{v}-\mathbf{u}\right|(\mathbf{v}-\mathbf{u}) - mg\mathbf{k} \\ &= -\frac{\pi}{8}C_D\rho_a d^2\left|\mathbf{v}-\mathbf{u}\right|(\mathbf{v}-\mathbf{u}) - \frac{\pi}{6}\rho_w d^3 g\mathbf{k} \end{aligned} \tag{2.1}$$

where m [kg], ρ_w [kg m^{-3}], d [m] and $\mathbf{v}$ [m s^{-1}] are the droplet's mass, density, diameter and its velocity relative to the ground, respectively, C_D is the drag coefficient [-], $\mathbf{u}$ is the wind velocity [m s^{-1}], ρ_a is the air density [kg m^{-3}], g is the gravitational acceleration [m s^{-2}] and $\mathbf{k}$ is a unit vector pointing vertically upwards.

The drag coefficient C_D is a function of the Reynolds number Re; for a spherical droplet, Green & Perry (2008, p. 6-52) give

$$C_D = \begin{cases} \dfrac{24}{\mathrm{Re}}, & \mathrm{Re} < 0.1, \\ \dfrac{24}{\mathrm{Re}}\left(1 + 0.14\,\mathrm{Re}^{0.7}\right), & 0.1 < \mathrm{Re} < 1000, \\ 0.447, & 1000 < \mathrm{Re} < 350000. \end{cases} \tag{2.2}$$

The Reynolds number Re is the ratio of inertial forces to viscous forces, and is given by

$$\mathrm{Re} = \frac{\rho_a\left|\mathbf{v}-\mathbf{u}\right|d}{\mu_a} \tag{2.3}$$

where μ_a is the dynamic viscosity of air [kg m^{-1} s^{-1}]. In the region of flow for which $C_D = \dfrac{24}{\mathrm{Re}}$, known as Stokes flow, Equation (2.1) may be solved analytically to give the droplet velocity and subsequently its displacement; according to Equation (2.2), Stokes flow applies for $\mathrm{Re} < 0.1$, however some texts extend this to $\mathrm{Re} < 1$ (for example Reist, 1993, p. 51).

2.2 Terminal Velocity

A droplet released into the air accelerates according to Equation (2.1) until the drag force balances its weight, after which it continues at a constant terminal velocity denoted $\mathbf{v}_T$. Setting the drag force equal to the weight in Equation (2.1) gives

$$\mathbf{v}_T = \mathbf{u} - \frac{4\rho_w g d}{3\rho_a C_D\left|\mathbf{v}_T-\mathbf{u}\right|}\mathbf{k}. \tag{2.4}$$

We write this as $\mathbf{v}_T = \mathbf{u} - S\mathbf{k}$, where S is the downward settling speed. At its terminal velocity, the droplet is therefore travelling with the wind horizontally and falling at speed S. From Equation (2.4):

$$S = \sqrt{\frac{4\rho_w g d}{3\rho_a C_D}}. \tag{2.5}$$

The drag coefficient C_D is itself dependent upon the droplet speed S, thus Equation (2.5) has to be solved numerically. Figure 2.1 on page 14 shows the settling speed S for droplets with diameter between 10 μm and 1000 μm; some specific values between 10 μm and 200 μm, along with the corresponding Reynolds numbers, are then given in Table 2.1. The parameter values used are $\rho_a = 1.23$ kg m^{-3}, $\mu_a = 1.46 \times 10^{-5}$ kg m^{-1} s^{-1}, $\rho_w = 998.29$ kg m^{-3} and $g = 9.8$ m s^{-2} (at standard atmospheric temperature and pressure).

2.3 Some Example Trajectories

Here we present some calculated examples of individual droplet trajectories. The trajectory is determined from the coupled system of differential equations, for the droplet velocity $\mathbf{v} = (v_x, v_y, v_z)$ and displacement $\mathbf{x} = (x, y, z)$, obtained from Equation (2.1):

$$\begin{aligned} \frac{d\mathbf{x}}{dt} &= \mathbf{v}, \\ \frac{d\mathbf{v}}{dt} &= -\frac{3\rho_a C_D}{4\rho_w d} |\mathbf{v} - \mathbf{u}| (\mathbf{v} - \mathbf{u}) - g\mathbf{k}. \end{aligned} \tag{2.6}$$

In the examples below, this system is solved numerically with MATLAB® Version 7 (The MathWorks™, n.d.), using the in-built solver ode15s designed for stiff problems. The stiff solver is more efficient here because there are two distinct time scales involved: droplets reach their terminal velocity quickly, but then take comparatively much longer to fall to the ground. In both examples, the droplet is released horizontally with initial velocity $\mathbf{v}_0 = (18, 0, 0)$ m s^{-1} (a typical release speed from a spray nozzle), from a height of 3 m above the ground into an ambient wind with velocity $\mathbf{u} = (1, 0, 0)$ m s^{-1}.

The first example (Figures 2.2 and 2.3 on page 16) is for a small droplet, with diameter $d = 10$ μm and settling speed $S = 0.003$ m s^{-1}. Figure 2.2 shows the droplet trajectory, and Figure 2.3 shows the individual components of the droplet velocity scaled to appear on the same axes. The horizontal component initially decreases as the droplet decelerates from its release speed to the ambient windspeed, and the vertical component initially increases as the droplet begins to fall and then attains its settling speed S. Note that the droplet reaches terminal velocity almost

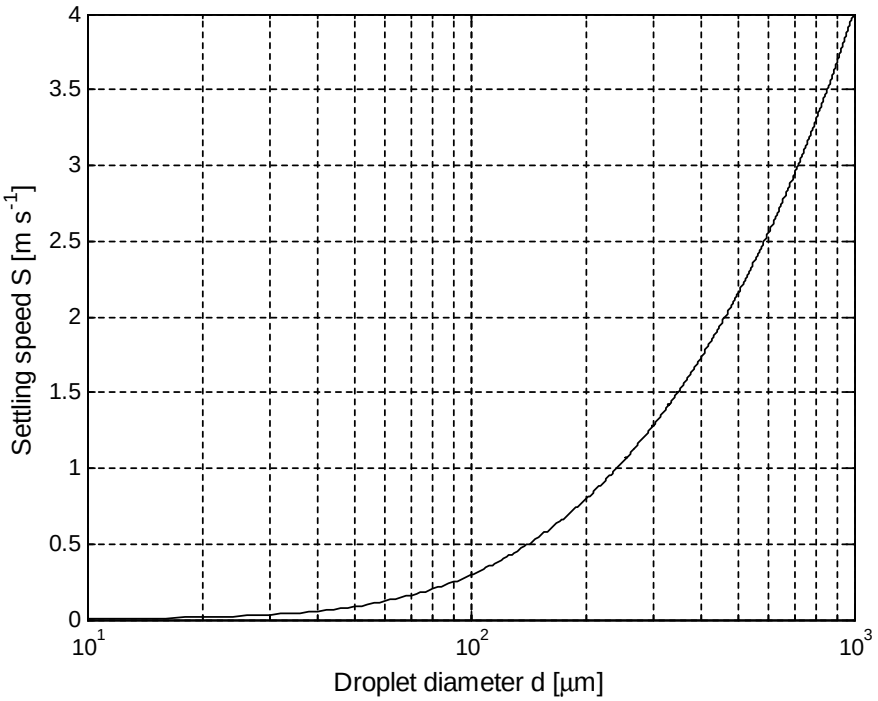

Figure 2.1: Settling speed, as calculated from Equation (2.5), for a range of different droplet diameters.

Table 2.1: Settling speed, as calculated from Equation (2.5), for a range of droplet diameters between 100 μm and 200 μm.

Droplet diameter d [μm]	Settling speed S [m s^{-1}]	Reynolds number Re [-]
10	0.003	0.003
20	0.015	0.025
50	0.087	0.366
70	0.161	0.947
100	0.294	2.478
120	0.392	3.960
150	0.544	6.868
170	0.646	9.247
200	0.798	13.448

immediately (both components of the velocity are constant after around 2 ms in Figure 2.3); it then takes 807 s to hit the ground, by which time it has travelled just over 800 m horizontally.

The second example (Figures 2.4 and 2.5 on page 17) is for a larger droplet, with diameter $d = 200$ μm and settling speed $S = 0.798$ m s^{-1}. Once again, Figure 2.4 shows the droplet trajectory, and Figure 2.5 shows the individual components of the droplet velocity scaled to appear on the same axes. The 200 μm droplet in this example retains its initial velocity for longer, but settles to the ground much quicker, than the 10 μm droplet in the first example: the larger droplet takes around 0.4 s to reach terminal velocity, but it hits the ground after only 3.9 s and travels just under 4.5 m horizontally. These two examples illustrate why small droplets pose the greatest risk for spray drift: large droplets settle quickly and so do not travel far horizontally, whereas small droplets settle slowly and are carried long distances by the wind.

2.4 Droplet Evaporation

As a droplet evaporates, liquid water at the droplet's surface becomes water vapour which diffuses out through the surrounding air, and there is also a heat exchange which results in a decrease in droplet temperature. The rate of evaporation and droplet temperature are interdependent; formulae based on the diffusion of water vapour are common and may be found, for example, in Davies (1978), Pruppacher & Klett (1978, Chap. 13), Asman *et al.* (2003, Chap. 4) and Lorenzini (2006). The analysis assumes that the droplet is evaporating in a large volume of air, so that there is no effect on the ambient conditions (that is, the ambient relative humidity and temperature remain uniformly constant and are unaffected by the evaporative mass and heat loss).

Rate of Mass Loss by Evaporation

An expression for the rate at which a droplet loses mass by evaporation is found by examining the diffusion of water vapour from the droplet's surface out through the surrounding air. This is done by assuming that the droplet is stationary in still air; relative motion is accounted for by introducing a ventilation coefficient, as described later in the section.

The following derivation is adapted from Davies (1978, pp. 136-138). When the droplet begins to evaporate, a changing distribution of water vapour is established around it, but this quickly

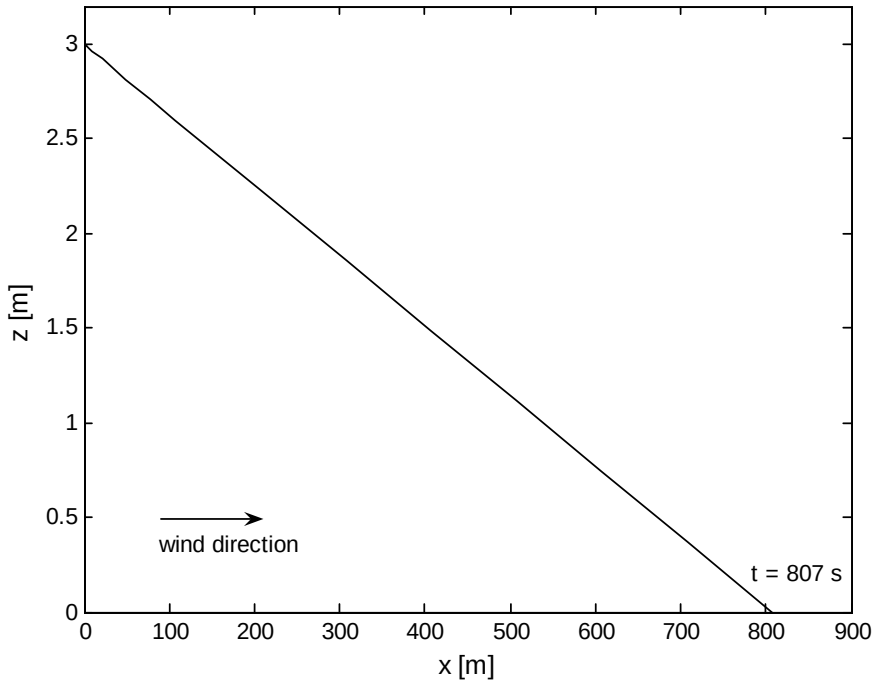

Figure 2.2: The trajectory of an individual droplet, 10 μm in diameter, released horizontally at speed 18 m s^{-1} from a height of 3 m in a 1 m s^{-1} wind. The displayed time $t = 807$ s is the time at which the droplet reaches the ground.

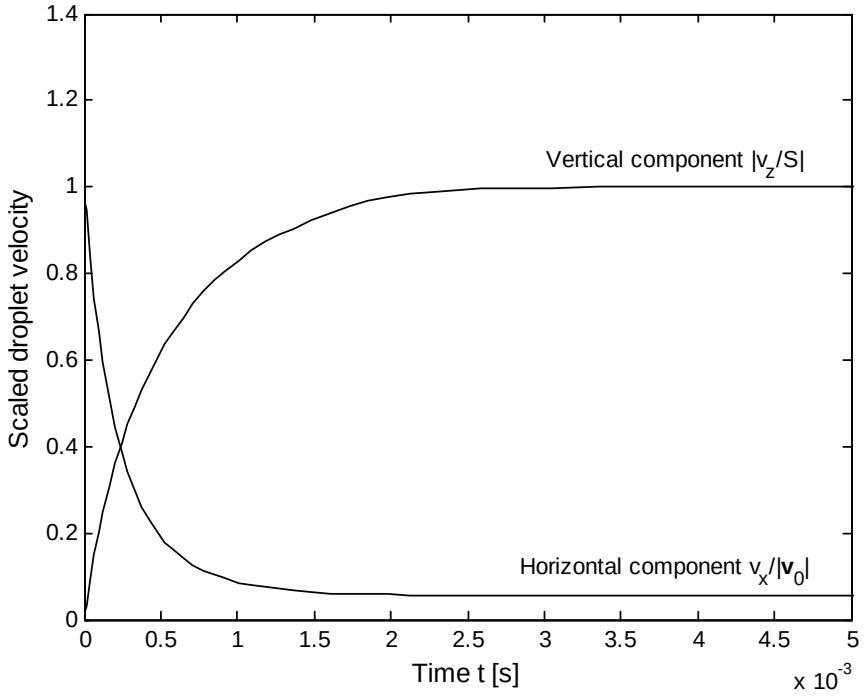

Figure 2.3: Individual components of the droplet velocity over time, scaled to be displayed on the same axes, for the release in Figure 2.2. v_x is the horizontal component of the droplet velocity, and $|\mathbf{v}_0|$ is the release speed. v_z is the vertical component of the droplet velocity, and S is the settling speed. Parameter values are as for Figure 2.2.

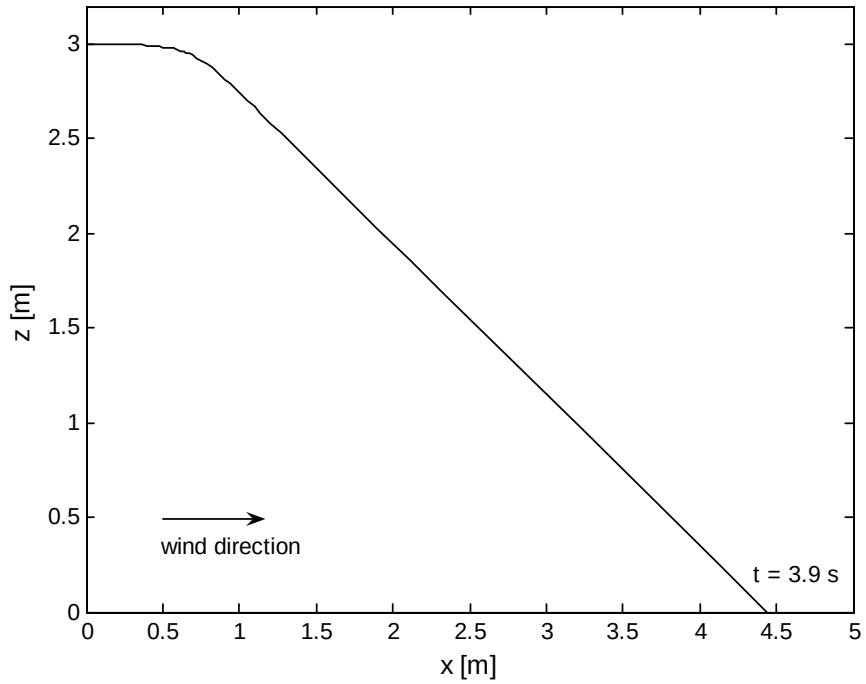

Figure 2.4: The trajectory of an individual droplet, 200 μm in diameter, released horizontally at speed 18 m s^{-1} from a height of 3 m in a 1 m s^{-1} wind. The displayed time $t = 3.9$ s is the time at which the droplet reaches the ground.

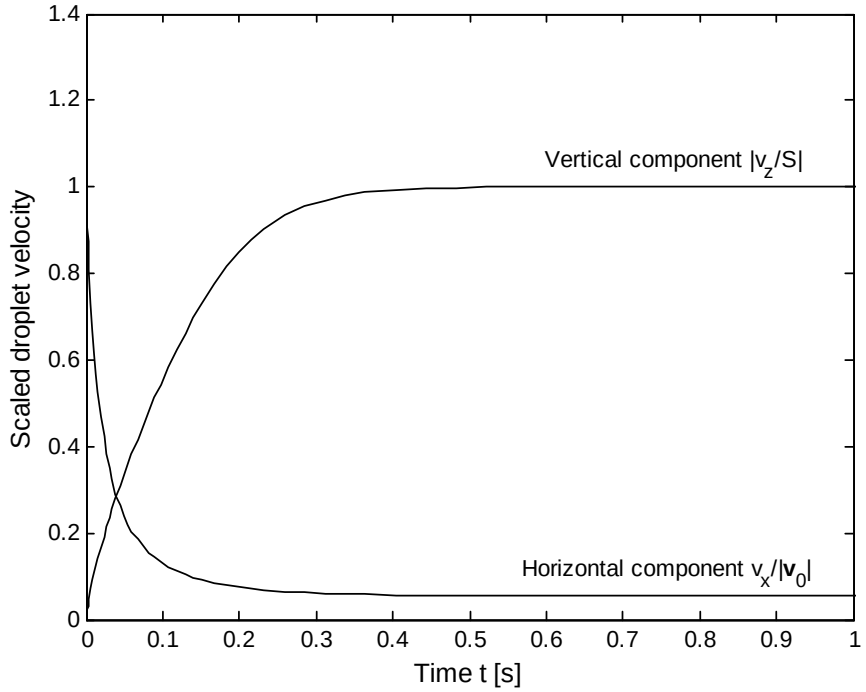

Figure 2.5: Individual components of the droplet velocity over time, scaled to be displayed on the same axes, for the release in Figure 2.4. v_x is the horizontal component of the droplet velocity, and $|\mathbf{v}_0|$ is the release speed. v_z is the vertical component of the droplet velocity, and S is the settling speed. Parameter values are the same as for Figure 2.4.

becomes steady over a distance from the surface of up to a few radii. Assuming that it does not vary with angle, the distribution of water vapour is described by the diffusion equation in spherical coordinates:

$$\frac{\partial w}{\partial t} = D_W \left(\frac{2}{r} \frac{\partial w}{\partial r} + \frac{\partial^2 w}{\partial r^2} \right) \tag{2.7}$$

where w is the mass concentration of water vapour [kg m^{-3}], D_W is the diffusivity of water vapour in air [m^2 s^{-1}], and r is the radial distance from the centre of the droplet [m]. When the distribution becomes steady so that $\dfrac{\partial w}{\partial t} = 0$, integrating the right-hand side of Equation (2.7) gives

$$w(r) = w_\infty + \frac{a}{r}(w_a - w_\infty) \tag{2.8}$$

where a is the droplet radius, $w_a = w(a)$ is the water vapour concentration at the droplet surface, and $w_\infty = w(\infty)$ is the water vapour concentration at $r = \infty$ (that is the ambient value). Using Fick's law, the outward diffusive mass flux of water vapour per unit area is $-D_W \dfrac{dw}{dr}$; the rate of change in the droplet mass with respect to time is then

$$\begin{aligned} \frac{dm}{dt} &= 4\pi a^2 \left(D_W \frac{dw}{dr} \right)_{r=a} \\ &= -4\pi a D_W (w_a - w_\infty). \end{aligned} \tag{2.9}$$

Since the water vapour is almost a perfect gas, the concentration can be expressed in terms of the vapour pressure and temperature:

$$w = \frac{p M_W}{R_g T} \tag{2.10}$$

where M_W is the molecular weight of water [18×10^{-3} kg mol^{-1}], R_g is the universal gas constant [8.315 J mol^{-1} K^{-1}], p is the vapour pressure [Pa] and T is the absolute temperature [K]. Equation (2.9) then becomes

$$\frac{dm}{dt} = -\frac{4\pi a M_W D_W}{R_g} \left(\frac{p_a}{T_a} - \frac{p_\infty}{T_\infty} \right). \tag{2.11}$$

Environmental conditions are usually measured in terms of relative humidity, the ratio of the actual amount of water in the air to the maximum amount it could hold at that temperature; the relative humidity ϕ is related to the vapour pressure p by $p = \phi p_{sat}(T)$, so that

$$\frac{dm}{dt} = -\frac{4\pi a M_W D_W}{R_g} \left(\frac{p_{sat}(T_a)}{T_a} - \phi \frac{p_{sat}(T_\infty)}{T_\infty} \right) \tag{2.12}$$

where p_{sat} is the saturation pressure (which is a function of temperature). In Equation (2.12) above, the relative humidity at the droplet surface is equal to one (since conditions there are saturated), and ϕ represents the relative humidity at $r = \infty$, or in other words the ambient value.

The change in droplet size with respect to time may also be found from Equation (2.12). The mass of the droplet in terms of its radius is $m(t) = \frac{4}{3}\pi\rho_w a(t)^3$, thus

$$\frac{dm}{dt} = 4\pi\rho_w a^2 \frac{da}{dt}. \tag{2.13}$$

Substituting Equation (2.12) for the rate of change in the mass with respect to time, the corresponding rate of change in the droplet radius with respect to time is

$$\frac{da}{dt} = -\frac{M_W D_W}{R_g \rho_w a}\left(\frac{p_{sat}(T_a)}{T_a} - \phi\frac{p_{sat}(T_\infty)}{T_\infty}\right). \tag{2.14}$$

So, both the rate at which a droplet evaporates and the subsequent rate at which it decreases in size are dependent upon the relative humidity, and the ambient and droplet temperatures. The temperature of an evaporating droplet is cooler than that of the surrounding air, as is discussed further below.

Droplet Temperature

During evaporation, there is a heat exchange between the droplet and the surrounding air: heat is lost from the droplet in order to evaporate some of the water, which results in a decrease in the temperature of the droplet, and heat is then conducted to the cooler droplet from the surrounding air. A steady state is rapidly reached where there is zero net heat exchange, and the droplet remains at constant temperature but cooler than the surrounding air.

An expression for the droplet temperature is found by examining the heat exchange; once again this is done assuming that the droplet is stationary in still air. Similar to the water vapour concentration, when the droplet begins to evaporate a temperature gradient is established around it, described by the heat equation in spherical coordinates:

$$\frac{\partial T}{\partial t} = \frac{k_a}{\rho_w c_p}\left(\frac{2}{r}\frac{\partial T}{\partial r} + \frac{\partial^2 T}{\partial r^2}\right) \tag{2.15}$$

where k_a is the thermal conductivity of moist air [W m^{-1} K^{-1}], and c_p is the specific heat of water [4190 J kg^{-1} K^{-1}]. Once the steady-state has been reached where $\frac{\partial T}{\partial t} = 0$, the right-hand side integrates to give

$$T(r) = T_\infty + \frac{a}{r}(T_a - T_\infty). \tag{2.16}$$

The total thermal energy of the droplet is mc_pT_a; in the steady state, the rate of change in the thermal energy is

$$\frac{dm}{dt}c_pT_a = \frac{dm}{dt}L_v + \frac{dm}{dt}c_pT_a + 4\pi k_a a^2\left(\frac{dT}{dr}\right)_{r=a}. \tag{2.17}$$

Table 2.2: Temperature of an evaporating droplet for various relative humidities and an ambient temperature of $T_\infty = 20$ °C.

Relative Humidity ϕ	Droplet Temperature T_a
2 %	5.2 °C
20 %	8.5 °C
40 %	11.8 °C
60 %	14.7 °C
80 %	17.5 °C
100 %	20.0 °C

The first term on the right-hand side is the rate of change in thermal energy due to evaporation of water from the droplet surface; L_v is the latent heat of vaporisation [J kg^{-1}]. The second term on the right-hand side is the rate of change in thermal energy due to the change in droplet mass (the water evaporated from the droplet surface is diffused out through the surrounding air, taking its thermal energy with it), and the third term is the rate of change in thermal energy due to heat conduction to the droplet from the surrounding air. Substituting for $\frac{dT}{dr}$ from Equation (2.16) and $\frac{dm}{dt}$ from Equation (2.11), and simplifying, gives

$$T_\infty - T_a = \frac{M_W D_W L_v}{k_a R_g} \left(\frac{p_{sat}(T_a)}{T_a} - \phi \frac{p_{sat}(T_\infty)}{T_\infty} \right). \tag{2.18}$$

Because the saturation pressure p_{sat} is a function of temperature, this equation has to be solved numerically to obtain the droplet temperature T_a. It turns out that this temperature is very close to the wet-bulb temperature (Asman *et al.*, 2003, Chap. 4).

Table 2.2 above lists the temperature of an evaporating droplet, calculated from Equation (2.18), for various relative humidities and an ambient temperature of $T_\infty = 20$ °C. The temperature depression at low relative humidity (dry air) is much greater than that at high relative humidity (moist air).

Correction for a Moving Droplet

With relative motion between an evaporating droplet and the surrounding air, the transfer of water vapour becomes convective rather than diffusive, which tends to increase the rate of evaporation, and the transfer of heat also becomes convective rather than conductive (Davies, 1978, p. 144). The effect is described using ventilation coefficients: f_w [-], the ventilation

coefficient for water vapour, is the ratio of the mass flux of water vapour for the moving droplet to that of a stationary droplet, and similarly f_h [-], the ventilation coefficient for heat, is the ratio of the thermal energy flux for the moving droplet to that of a stationary droplet. For the moving droplet, the expressions for the evaporation rate and droplet temperature become:

$$\frac{dm}{dt} = -\frac{4\pi a f_w M_W D_W}{R_g}\left(\frac{p_{sat}\left(T_a\right)}{T_a} - \phi\frac{p_{sat}\left(T_\infty\right)}{T_\infty}\right), \tag{2.19}$$

$$\text{and } T_a - T_\infty = -\frac{M_W D_W L_v f_w}{k_a R_g f_h}\left(\frac{p_{sat}\left(T_a\right)}{T_a} - \phi\frac{p_{sat}\left(T_\infty\right)}{T_\infty}\right). \tag{2.20}$$

The ratio f_w/f_h in Equation (2.20) is very close to one and changes little with droplet size (Asman *et al.*, 2003, Chap. 4), so the effect of relative motion on the temperature of an evaporating droplet is negligible and may be ignored. For f_w, Figure 2.6 shows values calculated using three different empirical formulae (given in Davies (1978, p. 146), Asman *et al.* (2003, Chap. 4) and Bhalwankar *et al.* (2004)), for droplets with a range of diameters which are falling at terminal velocity. For droplets less than around 100 μm in diameter, f_w is close to one so there is little effect on the rate of evaporation, however, above 100 μm in diameter f_w is greater than one and the rate of evaporation is increased. Subsequently in this thesis, we use the formula for f_w given in Davies:

$$f_w = 1 + 0.276\ \mathrm{Re}^{1/2}\mathrm{Sc}^{1/3} \tag{2.21}$$

where Re is the Reynolds number (see Equation 2.3) and $\mathrm{Sc} = \dfrac{\mu_a}{\rho_a D_W}$ is the Schmidt number.

Temperature-Dependent Parameters

In the expressions above for the droplet temperature and rate of evaporation, the parameters D_W, p_{sat}, k_a and L_v are all temperature-dependent. For D_W and k_a we use the following formulae from Asman *et al.* (2003, App. F), where T is the absolute temperature [K]:

$$D_W = 2.5007 \times 10^{-5}\left(\frac{T}{298.15}\right)^{1.94}, \tag{2.22}$$

$$\text{and } k_a = 0.43812 \times 10^{-2} + 7.11756 \times 10^{-5}T. \tag{2.23}$$

For p_{sat} and L_v we fitted a curve to data from steam tables in Rogers & Mayhew (1980) over the temperature range $0 - 30$ °C:

$$p_{sat} = 1.7785 \times 10^{-5}e^{0.0637T}, \tag{2.24}$$

$$\text{and } L_v = 3144 \times 10^3 - 2.3556 \times 10^3 T \tag{2.25}$$

where T is once again the absolute temperature [K].

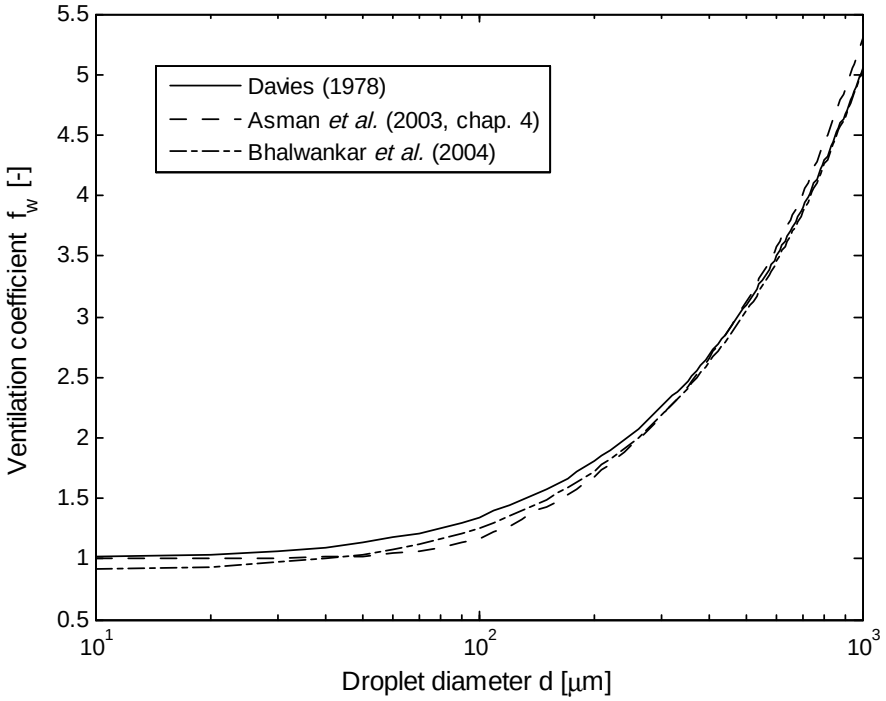

Figure 2.6: Ventilation coefficient for water vapour f_w [-], calculated using three different empirical formulae, for droplets of various diameters falling in air at their terminal velocity.

2.5 An Example Trajectory with Evaporation

Here we present a calculated example of the trajectory of an individual evaporating droplet at five different relative humidities. The trajectory is determined by solving the coupled system of differential equations for the droplet radius a, velocity $\mathbf{v} = (v_x, v_y, v_z)$ and displacement $\mathbf{x} = (x, y, z)$, all obtained from Equation (2.1) and Equation (2.14):

$$\begin{aligned}
\frac{da}{dt} &= -\frac{M_W D_W f_w}{R_g \rho_w a}\left(\frac{p_{sat}(T_a)}{T_a} - \phi\frac{p_{sat}(T_\infty)}{T_\infty}\right), \\
\frac{d\mathbf{x}}{dt} &= \mathbf{v}, \\
\frac{d\mathbf{v}}{dt} &= -\frac{3\rho_a C_D}{8\rho_w a}|\mathbf{v}-\mathbf{u}|(\mathbf{v}-\mathbf{u}) - g\mathbf{k}.
\end{aligned} \tag{2.26}$$

As for the earlier examples without evaporation, this system was solved numerically using the in-built solver ode15s from MATLAB®, Version 7. The droplet in this example is of medium size, with initial diameter $d_0 = 100$ μm, and the ambient temperature is $T_\infty = 20$ °C. The release parameters are the same as for the earlier examples (see page 13).

Figure 2.7 shows the droplet trajectory. The effect of evaporation on the trajectory is clearly

visible: as the droplet becomes smaller its falling speed decreases, therefore it is blown further by the wind before reaching the ground, and, if ϕ is small enough it evaporates completely. Termination of the trajectory lines above $z = 0$ indicates that the droplet has evaporated completely before reaching the ground. Figure 2.8 shows the falling speed of the droplet, $|v_z|$, over time: initially the falling speed increases as the droplet begins to fall and quickly accelerates towards its settling speed, but then evaporation takes effect and the falling speed starts to decrease as the droplet becomes smaller and lighter. Finally, Figure 2.9 shows the change in droplet diameter over time; termination of the line above $d = 0$ for $\phi = 80$ % indicates that the droplet does reach the ground before evaporating completely.

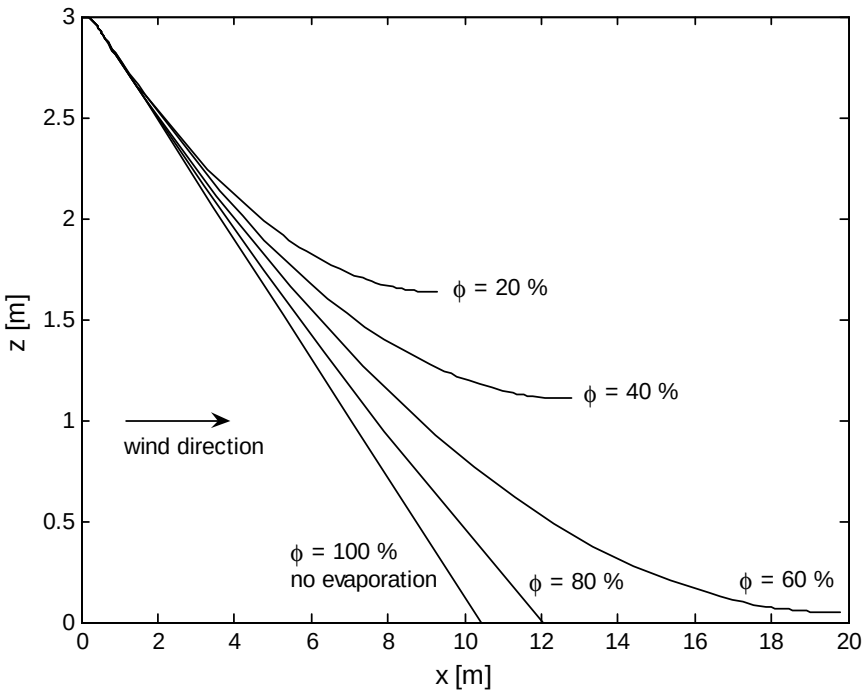

Figure 2.7: Trajectory of an individual evaporating droplet, with initial diameter 100 μm, for five different relative humidities. The droplet is released horizontally at speed 18 m s^{-1} from a height of 3 m in a 1 m s^{-1} wind. See the text for additional parameter values.

2.6 Chapter Summary

In this chapter we provided details of the kinetics and thermodynamics of an individual droplet, in order to better understand the continuum models which are the focus of this thesis. The material is widely available in the literature, and is included here as background information.

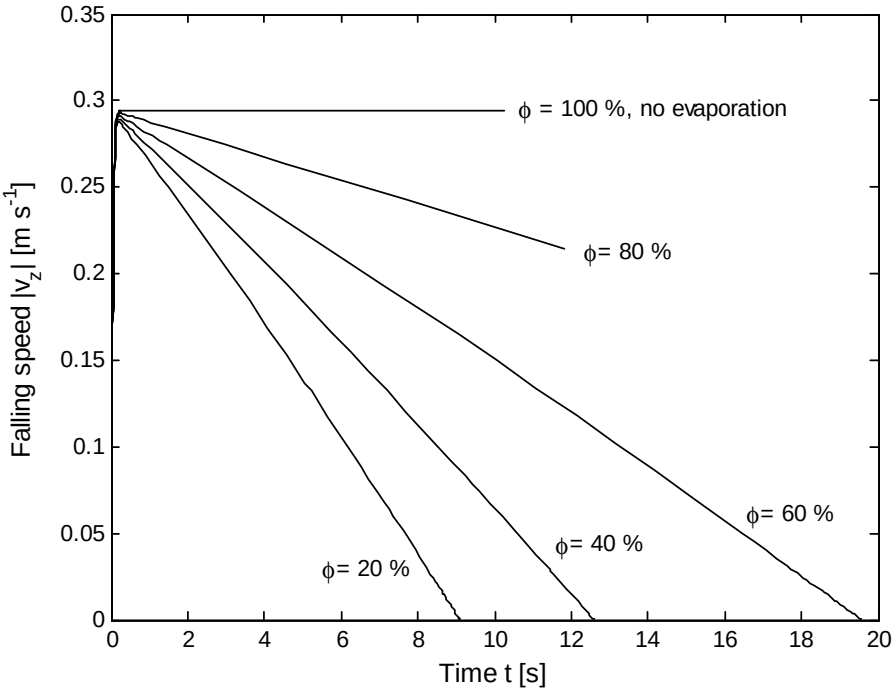

Figure 2.8: Falling speed over time for the individual evaporating droplet in Figure 2.7. Parameter values are the same as for Figure 2.7.

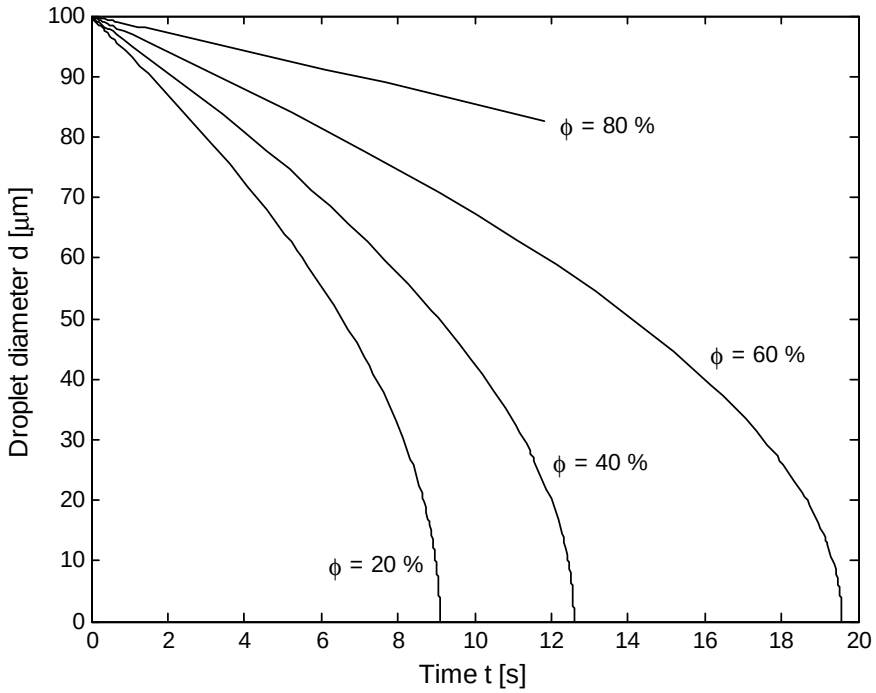

Figure 2.9: Diameter over time for the individual evaporating droplet in Figure 2.7. Parameter values are the same as for Figure 2.7.

For the kinetics, we looked at the equation of motion governing the droplet flight, found by summing the forces acting according to Newton's law, and the terminal velocity at which the droplet no longer accelerates. At terminal velocity, the droplet is travelling with the wind horizontally and falling towards the ground at its settling speed. To conclude, we showed two calculated examples of trajectories, which illustrate that droplets in the size range of interest reach their terminal velocity almost immediately, and that small droplets pose a greater threat for spray drift because they settle slowly, and therefore travel long distances before depositing on the ground.

For the thermodynamics, we showed how expressions are derived for the rate of mass loss and temperature when the droplet is evaporating. The expressions are derived assuming the droplet is stationary relative to the surrounding air, with a scaling factor introduced when the droplet is moving; we observed that the effect of relative motion on the droplet temperature is negligible, and that the rate of evaporation is increased only for droplets greater than around 100 μm in diameter. Finally, we gave an example of the trajectory of an evaporating droplet, which illustrated that in some cases droplets can evaporate completely before depositing, whilst in other cases the travel distances are increased.

To reiterate, the material in Sections 2.1 - 2.3 (covering the droplet kinematics) leads on to Chapters 3, 4 and 5 where we develop continuum models without evaporation, and the material in Sections 2.4 - 2.5 (covering the thermodynamics) leads on to Chapter 6 where we introduce evaporation.

Chapter 3

Advection-Dispersion Model Framework

In this chapter, we set up our advection-dispersion model to describe the transport of airborne drifting spray droplets and their removal by trapping within a shelterbelt, in the more straightforward case where the droplets are not evaporating. The majority of the chapter covers a full derivation of the model, with some discussion of the initial and boundary conditions used. One of the key parameters appearing in the model is the background trapping rate, which is a measure of the rate at which droplets are removed within the shelterbelt; this parameter is not easily measured, so we show how it can be related to a recent model for the capture efficiency of a shelterbelt as a function of its more easily-measured optical porosity.

3.1 Model Derivation

A cloud of airborne droplets is advected by the wind and dispersed by turbulence, all whilst falling towards the ground (settling) under the influence of gravity. Within a shelterbelt, some of the droplets may impact on the foliage and adhere; this is referred to as trapping, and trapped droplets are removed from the airflow. The transport of airborne droplets may be modelled using an advection-dispersion equation, and we represent the shelterbelt as a block in which droplets are trapped at a rate proportional to the local concentration. Here we present a derivation of this advection-dispersion model, obtained by applying the principle of conservation of mass.

We use a Cartesian coordinate system (x, y, z), such that the (x, y) plane is on the ground, the positive x-axis points in the direction of the mean wind velocity, and z measures the height above

the ground. The mass of droplets in the air per unit volume is denoted $c(x, y, z, t)$ [kg m^{-3}], a function of both position and time; we assume that the droplets are all of the same size, and therefore of the same mass, and that their volume fraction in the air is small (so that the motion of the air is unaffected). We also assume that the droplets are at terminal velocity immediately upon release; since only small droplets contribute to drift (those with diameter less than around 200 μm, Thompson & Ley, 1983), and we showed in Chapter 2 that these small droplets reach their terminal velocity very quickly.

Consider an arbitrary fixed volume of air, V, with surface area A. The mass of droplets contained in V is

$$\iiint_V c \, dV. \tag{3.1}$$

The rate of change in the mass of droplets contained in V with respect to time is equal to the net mass flux through its surface area A due to advection, gravitational settling and dispersion, plus the rates of mass addition by sources and removal by trapping.

Advection by the Wind

Advection describes the transport of droplets by the wind. The wind profile is considerably influenced by the presence of a shelterbelt: windspeed within the shelterbelt is reduced, forcing some of it to accelerate over the top, and leaving a "quiet zone" of reduced windspeed for some distance downstream. Figure 3.1 on page 28, sourced from Cleugh (1998), shows a theoretical profile of the airflow for a single row shelterbelt; the streamlines show the reduced windspeed through the shelterbelt, the accelerated flow over the top, and the quiet zone downstream. Experimental results indicate that the windspeed is most significantly reduced between distances of about $5h$ upwind and $20h$ downwind, where h is the shelterbelt height; the effectiveness of the shelterbelt in reducing windspeed, however, is dependent upon many factors such as its height, length, width, foliage type and foliage density (Ucar & Hall, 2001).

Accurate simulation of the wind through and around a shelterbelt is difficult and computationally intensive (see for example H. Wang *et al.*, 2001). It would be impossible to include the full dynamics of the wind in our advection-dispersion model and still hope to gain an analytic solution; thus, to simplify, we assume that the wind in our model is horizontal and uniform, and flows through the shelterbelt undisturbed. This may not be too significant a simplification, as we are mostly concerned with a fully-sheltered orchard block, and therefore the windspeed

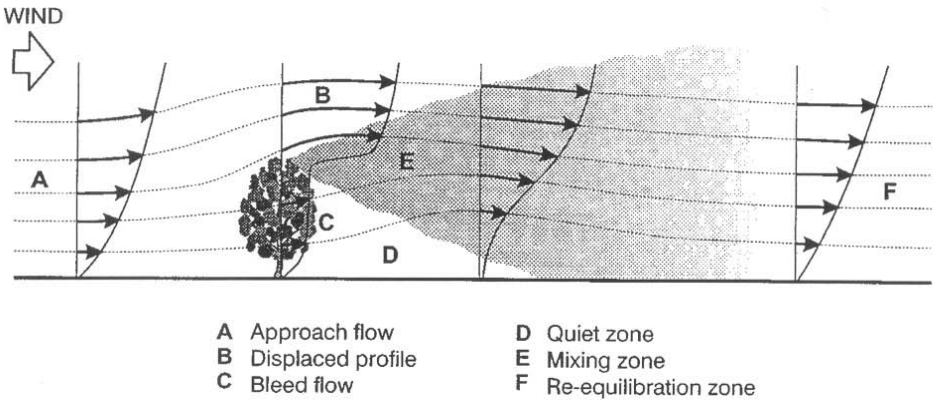

Figure 3.1: Theoretical profiles of the mean horizontal windspeed and streamlines for a single row shelterbelt oriented normal to the incoming wind. Source: Cleugh (1998).

will be low within the block and for some considerable distance downwind. Also, numerical investigations by Mercer & Roberts (2005) indicate that for shelterbelts most likely to be used to capture spray drift, most of the incoming wind will go through the full width of the shelterbelt, therefore accelerating flow over the top is unlikely to be a problem.

Returning now to our derivation, the mean wind velocity is denoted $\mathbf{u} = (u, 0, 0)$. For our volume V, let dA be a small element of surface area A with outward unit normal $\mathbf{n}$; the mean wind velocity in the direction of $\mathbf{n}$ is then $\mathbf{u} \cdot \mathbf{n}$; this may be considered as a volume flux of air per unit area [$\mathrm{m}^3\ \mathrm{s}^{-1}\ \mathrm{m}^{-2}$], thus the inward mass flux of droplets through surface element dA is $-c\,(\mathbf{u} \cdot \mathbf{n})\,dA$. Integrating over the entire surface area A, the total inward mass flux of droplets into volume V via advection is

$$\oiint_A -c\,(\mathbf{u} \cdot \mathbf{n})\ dA. \tag{3.2}$$

Gravitational Settling

Droplets fall towards the ground under the influence of gravity at a rate dependent upon their shape, mass and size (diameter), and the air density; this rate is known as the settling speed, denoted here by S. We have assumed that the droplets are identical, therefore they all have the same settling speed. Since they are not evaporating the droplets do not change in size or mass, thus the settling speed S remains constant.

In the direction of $\mathbf{n}$, the settling velocity is $-S\mathbf{k} \cdot \mathbf{n}$, where $\mathbf{k}$ is a unit vector in the positive z direction; thus, the inward mass flux of droplets through surface element dA is $c\,(S\mathbf{k} \cdot \mathbf{n})\,dA$.

Integrating over the entire surface area A, the total inward mass flux of droplets into volume V via gravitational settling is

$$\oiint_A c\,(S\mathbf{k}\cdot\mathbf{n})\;\,dA. \tag{3.3}$$

Dispersion due to Turbulence

Dispersion describes the spreading of a cloud of droplets due to turbulence in the airflow. We closely follow the treatment by McKibbin (2006): the turbulence eddy structures are assumed to have some dominant length scales in the alongwind, crosswind and vertical directions, and the dispersion coefficients are defined as these length scales multiplied by the mean windspeed.

A dispersion tensor $\underline{\mathbf{D}}$ reflects the ability of the droplets to spread in the x, y and z directions. Using a Fickian model for the dispersion, the mass flux per unit area in the direction of $\mathbf{n}$ is $-(\underline{\mathbf{D}}\nabla c)\cdot\mathbf{n}$; thus, the inward mass flux of droplets through surface element dA is $(\underline{\mathbf{D}}\nabla c)\cdot\mathbf{n}\;dA$. Integrating over the entire surface area A, the total inward mass flux of droplets into volume V via turbulent dispersion is

$$\oiint_A (\underline{\mathbf{D}}\nabla c)\cdot\mathbf{n}\;dA. \tag{3.4}$$

Following McKibbin (2006), in general form the dispersion tensor may be written as

$$\underline{\mathbf{D}} = \begin{bmatrix} D_{xx} & D_{xy} & 0 \\ D_{yx} & D_{yy} & 0 \\ 0 & 0 & D_{zz} \end{bmatrix} \tag{3.5}$$

where the zero components arise because the mean wind velocity is assumed to be horizontal. If the mean wind direction is at angle θ to the x-axis, then under the Fickian model the dispersion tensor becomes

$$\underline{\mathbf{D}} = \begin{bmatrix} D_L\cos^2\theta + D_T\sin^2\theta & (D_L - D_T)\sin\theta\cos\theta & 0 \\ (D_L - D_T)\sin\theta\cos\theta & D_L\sin^2\theta + D_T\cos^2\theta & 0 \\ 0 & 0 & D_V \end{bmatrix} \tag{3.6}$$

where D_L, D_T and D_V are the dispersion coefficients alongwind, crosswind and vertically. These dispersion coefficients are defined as $(D_L, D_T, D_V) = |\mathbf{u}|\,(L_L, L_T, L_V)$, where $|\mathbf{u}|$ is the mean windspeed and L_L, L_T and L_V are the dominant turbulence length scales. Left as it is, this form of the dispersion tensor gives rise to cross-derivative terms which are difficult to deal with in

our final advection-dispersion model. To eliminate these terms, the coordinate axes are aligned such that the positive x-axis points directly downwind (that is $\theta = 0$); the dispersion tensor then simplifies to

$$\underline{\mathbf{D}} = \begin{bmatrix} D_L & 0 & 0 \\ 0 & D_T & 0 \\ 0 & 0 & D_V \end{bmatrix}. \tag{3.7}$$

In general, the rate of turbulent dispersion of a particulate cloud depends upon the cloud dimensions and turbulence intensity. It has been observed that as a particulate cloud becomes larger, larger eddies come into play and so the rate of dispersion increases; accounting for this effect would require the dispersion coefficients to depend upon the travel time or distance from the source, which is very difficult to deal with analytically (Moreira *et al.*, 2005). Typically, the dispersion coefficients D_L, D_T and D_V vary with height above the ground, and they are often assumed to follow a power law profile. Here, we treat them as constant throughout the domain; this assumption gives us much more traction analytically, and while it will limit the accuracy of the model it will not greatly alter the qualitative behaviour.

Mass Source Term

Given a source of droplets with mass release rate per unit volume $q(x, y, z, t)$ [kg s^{-1} m^{-3}], the rate of increase in the mass of droplets contained in volume V will be

$$\iiint_V q \, dV. \tag{3.8}$$

In this thesis we use an instantaneous point release: mass Q is released at time $t = 0$ from the point (X_0, Y_0, H). This can be expressed in terms of Dirac delta functions as

$$q = Q\delta(x - X_0)\,\delta(y - Y_0)\,\delta(z - H)\,\delta(t). \tag{3.9}$$

The Dirac delta function $\delta(x - a)$ is non-zero only at $x = a$, it has dimensions of $[x]^{-1}$ (that is the inverse of the dimensions of x), and the fundamental property that

$$\int_{-\infty}^{\infty} f(x)\,\delta(x - a)\; dx = f(a) \tag{3.10}$$

for all functions which are continuous at $x = a$. With such a simple source term we are able to seek analytic solutions to our advection-dispersion model, and other mass releases may later be constructed by using a number of individual point releases and integrating the results, such as in Lim (2005, Chap. 4) and McKibbin (2006).

Trapping Within a Shelterbelt

Trapping occurs when droplets impact on the foliage of a shelterbelt and adhere. Trapped droplets are removed from the airflow, thus the shelterbelt acts like a mass sink. The conceptual model here is that the trapping is proportional to the concentration c; this is because the amount of material which is removed by trapping must be proportional to how much is actually available to be trapped. Under this model, there is no decrease in the trapping ability of the shelterbelt due to saturation. We also assume that the droplets either pass through the shelterbelt or are trapped by the foliage; they are not "splashed" or disintegrated into smaller droplets with a different settling speed.

The rate of droplet mass removal by trapping, per unit volume of air, is given by $k_b R c$. The rate of mass removal from volume V is therefore

$$\iiint_V k_b R c \; dV. \tag{3.11}$$

The parameter k_b reflects the ability of the shelterbelt to trap droplets; it is called the background trapping rate, and defined as the mass fraction of droplets trapped per unit time [s^{-1}]. The size of k_b will depend upon factors such as the foliage type, windspeed and droplet size (for more information see Section 3.3). The function R is dimensionless, and non-zero only within the block which represents the shelterbelt; it is like a switching function which turns the trapping on within the shelterbelt and off elsewhere.

Governing Equation for the Model

The rate of change in the mass of droplets contained in volume V with respect to time is equal to the net mass flux through its surface area A (due to advection, gravitational settling and dispersion) plus the rates of mass addition by sources and removal by trapping. Combining Equations (3.1)–(3.4), (3.8) and (3.11) accordingly:

$$\frac{\partial}{\partial t} \iiint_V c \; dV = - \oiint_A (c\mathbf{u} - cS\mathbf{k} - \underline{\mathbf{D}} \nabla c) \cdot \mathbf{n} \; dA + \iiint_V (q - k_b R c) \; dV. \tag{3.12}$$

Using Gauss' divergence theorem to convert the surface integral to a volume integral then gives

$$\frac{\partial}{\partial t} \iiint_V c \; dV = - \iiint_V (\nabla \cdot (c\mathbf{u} - cS\mathbf{k} - \underline{\mathbf{D}} \nabla c) - q + k_b R c) \; dV. \tag{3.13}$$

Volume V is fixed in space, so the time derivative may be moved inside the integral on the left-hand side. On the right-hand side, we have $\nabla \cdot (S\mathbf{k}) = 0$ because the settling speed

S is constant, and $\nabla \cdot \mathbf{u} = 0$ because the airflow is incompressible (we are dealing only with windspeeds of around $1-5$ m s^{-1}, and air at 20 °C is incompressible at velocities up to 102 m s^{-1}, "Incompressible Flow", n.d.). Thus, Equation (3.13) simplifies to

$$\iiint_V \left(\frac{\partial c}{\partial t} + \mathbf{u} \cdot \nabla c - S\mathbf{k} \cdot \nabla c - \nabla \cdot (\underline{\mathbf{D}} \nabla c) - q + k_b R c \right) \, dV = 0 \tag{3.14}$$

and since V is arbitrary, this implies

$$\frac{\partial c}{\partial t} + \mathbf{u} \cdot \nabla c - S\mathbf{k} \cdot \nabla c - \nabla \cdot (\underline{\mathbf{D}} \nabla c) - q + k_b R c = 0 \tag{3.15}$$

or

$$\frac{\partial c}{\partial t} + u\frac{\partial c}{\partial x} - S\frac{\partial c}{\partial z} = D_L \frac{\partial^2 c}{\partial x^2} + D_T \frac{\partial^2 c}{\partial y^2} + D_V \frac{\partial^2 c}{\partial z^2} + q - k_b R c. \tag{3.16}$$

Finally, substituting the rate of mass release per unit volume for an instantaneous point source as given by Equation (3.9),

$$\frac{\partial c}{\partial t} + u\frac{\partial c}{\partial x} - S\frac{\partial c}{\partial z} = D_L \frac{\partial^2 c}{\partial x^2} + D_T \frac{\partial^2 c}{\partial y^2} + D_V \frac{\partial^2 c}{\partial z^2} + Q\delta\left(x - X_0\right)\delta\left(y - Y_0\right)\delta\left(z - H\right)\delta\left(t\right) - k_b R c \tag{3.17}$$

over the domain

$$t > 0, \ -\infty < x, y < \infty, \text{ and } 0 \leq z < \infty.$$

Equation (3.17) is the advection-dispersion model upon which the remainder of this thesis is based; it is to be solved subject to the initial and boundary conditions described in Section 3.2 below.

In the model as it stands above, the trapping is continuous throughout the block which represents the shelterbelt; this is ideal from a continuum viewpoint but unfortunately it is difficult to proceed analytically. As a way around the difficulty, we discretise the shelterbelt by instead representing it as an array of smaller blocks, with the effect of trapping in each block concentrated to the point at its centre. This point representation for trapping is a mathematical tool which allows us to solve the model analytically and write explicit expressions for the total trapping and the deposit on the ground. We begin in Chapter 4 with an analysis of the model for a single trapping point, then consider the discretised shelterbelt in Chapter 5.

3.2 Initial and Boundary Conditions

The initial, horizontal and upper boundary conditions for Equation (3.17) are

$$c\left(x, y, z, 0^-\right) = 0, \text{ and} \tag{3.18}$$

$$c\left(x, y, z, t\right) \to 0 \text{ as } x, y \to \pm\infty, \text{ and } z \to +\infty. \tag{3.19}$$

These are straightforward conditions stating that the concentration is zero everywhere until the instant of release, and that for any given time the concentration should drop to zero far away in the domain.

The boundary condition on the ground is less clear. We assume that the ground is impervious to the droplets, so that they cannot disperse through it; consequently, the vertical dispersive flux on the ground surface must be zero, which leads to the final boundary condition that

$$D_V \frac{\partial c}{\partial z}(x, y, 0, t) = 0. \tag{3.20}$$

There are two possibilities here: If vertical dispersion of the droplets is negligible compared to horizontal dispersion, such that D_V may be considered zero, then the boundary condition is automatically satisfied. Otherwise, if vertical dispersion of the droplets is significant, then the boundary condition must be satisfied by setting $\frac{\partial c}{\partial z}(x, y, 0, t) = 0$. Realistically, vertical dispersion is likely to be significant because, this close to the ground, the airflow will be affected by the surface topography (that is the crop and the shelterbelt) and will also have been disturbed by the air-assisted spraying process.

Since the downward vertical flux [kg m^{-2}] is given by $Sc + D_V \frac{\partial c}{\partial z}$, Equation (3.20) implies that in our model droplets deposit on the ground via gravitational settling only. According to literature sources, particle deposition to a vegetated ground surface is more complicated as roughness elements (such as leaves and stems) protrude from the surface. It is generally thought that the ground surface will act as a "mass sink" proportional to the local concentration, so that the boundary condition is of the form (Calder, 1961):

$$Sc(x, y, 0, t) + D_V \frac{\partial c}{\partial z}(x, y, 0, t) = Wc(x, y, 0, t) \tag{3.21}$$

where W is the proportionality constant [m s^{-1}] for the particle removal at the ground surface. This is commonly written as

$$D_V \frac{\partial c}{\partial z}(x, y, 0, t) = v_d c(x, y, 0, t) \tag{3.22}$$

where $v_d = (W - S)$ is the deposition velocity (Calder, 1961; Lin & Hildemann, 1997; Raupach, Briggs, *et al.*, 2001; Essa *et al.*, 2007). Raupach, Briggs, *et al.* (2001) present a model for the deposition velocity as the sum of contributions from three processes: gravitational settling, inertial impaction and Brownian diffusion. They show a comparison of their predicted values (for a range of particle diameters) against experimental data and also the settling speed; this comparison indicates that Equation (3.20), which implies that the droplets in our model deposit with their settling speed, is not unreasonable over the applicable diameter range.

3.3 The Background Trapping Rate k_b

As introduced in Section 3.1, our conceptual model is that the trapping of droplets within a shelterbelt is proportional to the local concentration. The proportionality constant is denoted k_b; we call this the background trapping rate, and it is defined as the mass fraction of droplets trapped per unit time [s^{-1}]. In this section we provide more information on k_b, and show how it can be related to the recent Raupach, Woods, *et al.* (2001) model for the droplet capture efficiency of a shelterbelt.

The capture efficiency of a shelterbelt depends upon factors such as windspeed and droplet size, and also upon physical characteristics of the shelterbelt such as its porosity and foliage type. The porosity of a shelterbelt affects the proportion of the airflow which travels through it. There is a trade-off between porosity and capture efficiency: Raupach, Woods, *et al.* (2001) note that the shelterbelt must be dense enough to collect droplets efficiently, but sparse enough to allow airflow through it so that droplets may enter and be trapped. Inside the shelterbelt, large droplets are more efficiently captured than small droplets; as droplet-laden air flows around the foliage elements, small droplets are carried with the flow, whilst large droplets which have greater inertia are more likely to deviate from the flow and impact on the foliage (Mercer & Roberts, 2005). It has also been observed that small foliage elements have a better capture efficiency, thus fine-needled species are more efficient than broadleaf species (Ucar *et al.*, 2003).

The background trapping rate k_b in our model is a measure of the capture efficiency of the shelterbelt; in the paragraphs below we show how it can be related to the recent Raupach, Woods, *et al.* (2001) model for the capture efficiency. First, an outline of the Raupach, Woods, *et al.* (2001) model is as follows. Their assumptions are that the wind flows horizontally through the shelterbelt, and that both the wind flow and droplet concentration are uniform with height. Deposition to the foliage elements occurs via gravitational settling, inertial impaction and Brownian diffusion; of these three processes only impaction is considered significant, since large droplets with appreciable settling speeds do not contribute to drift, and Brownian diffusion is only significant for droplets smaller than the range of interest. The model is formulated as

$$\frac{DC}{Dt} = -\alpha g_p C \tag{3.23}$$

where C is the droplet number concentration per unit volume [# m^{-3}], α is the frontal area of the foliage elements per unit volume [m^{-1}], and g_p is the impaction conductance onto the foliage elements [m s^{-1}]. We use a capital D to indicate that this is a material derivative, because

the model is formulated from a Lagrangian viewpoint. Equation (3.23) is integrated along a trajectory to give

$$C_1 = C_0 e^{-\alpha g_p \frac{MX_b}{u_b}} \tag{3.24}$$

where C_1 and C_0 are the droplet number concentrations directly upwind and downwind of the shelterbelt. The fraction $\frac{MX_b}{u_b}$ represents a typical time for the droplets to cross the shelterbelt; u_b is the windspeed through the shelterbelt, known as the bleed velocity, X_b is the width of the shelterbelt, and M is a meander factor set at 1.2 which accounts for the droplets following a meandering path due to turbulence. Most field measurements of shelterbelt density are in terms of the optical porosity τ, which is related to α and X_b by $\tau = e^{-\alpha X_b}$; the transmittance of the shelterbelt $\sigma = \frac{C_1}{C_0}$ is thus written as

$$\sigma = \tau^{ME} \tag{3.25}$$

where $E = \frac{g_p}{u_b}$ is the impaction efficiency. An empirical formula for E based on the Stokes number St is taken from Peters & Eiden (1992):

$$E = \left(\frac{St}{St + 0.8}\right)^2. \tag{3.26}$$

The Stokes number St is given by

$$St = \frac{\rho_w d^2}{18\rho_a \nu_a} \frac{2u_b}{d_e} \tag{3.27}$$

where ρ_a and ν_a are the density and kinematic viscosity of the air, ρ_w and d are the density and diameter of the droplets, and d_e is the average diameter of the foliage elements. It is noted that, for d larger than around 30 μm and for d_e smaller than 30 mm, $ME \approx 1$ and the simple approximation $\sigma = \tau$ works well.

Now to determine an expression for k_b. Recall that in our model, the rate of mass removal per unit volume within the shelterbelt is $k_b c$ (setting $R = 1$ within the shelterbelt). Thus, from a Lagrangian viewpoint

$$\frac{Dc}{Dt} = -k_b c. \tag{3.28}$$

The number concentration of droplets is given by $C = \frac{c}{m}$, where m is the mass of an individual droplet. With m constant, Equation (3.28) becomes

$$\frac{DC}{Dt} = -k_b C. \tag{3.29}$$

Direct comparison with Equation (3.23) shows that k_b is related to the Raupach, Woods, *et al.* model by $k_b = \alpha g_p$; rewriting this in terms of the optical porosity $\tau = e^{-\alpha X_b}$ and the impaction efficiency $E = \frac{g_p}{u_b}$ gives

$$k_b = \frac{u_b E}{X_b} \ln\left(\frac{1}{\tau}\right). \tag{3.30}$$

According to this equation, the background trapping rate k_b depends upon the windspeed through the shelterbelt, the optical porosity and width of the shelterbelt, and also the droplet size (via the impaction efficiency E).

Figures 3.2 and 3.3 on page 37 show the value of k_b, as calculated from Equation (3.30), for various droplet sizes and five different windspeeds through the shelterbelt. Figure 3.2 is for a poplar shelterbelt with $\tau = 0.2$ and $d_e = 100$ mm; this is a moderately dense broadleaf shelterbelt. Figure 3.3 is for a casuarina shelterbelt with $\tau = 0.2$ and $d_e = 2$ mm; this is a fine needled shelterbelt, also moderately dense. In both cases, the width of the shelterbelt is $X_b = 2$ m. The values used for τ and d_e are taken from Mercer & Roberts (2005).

3.4 Parameter Values

Table 3.1 (page 38) summarises some likely values for the parameters involved in our model. Crop spraying usually takes place in low to moderate windspeeds, around $1 - 5$ m s^{-1}, and growers are recommended to avoid spraying in windspeeds greater than 5 m s^{-1} (P. Holland *et al.*, n.d.; Wolf, 1997). Sprays contain a wide range of droplet sizes, approximately 10 μm – 1000 μm in diameter; we limit our attention to diameters less than 200 μm, since droplets larger than this rarely contribute to drift as they have significant settling speeds and therefore deposit quickly (Thompson & Ley, 1983).

Analysis of the structure of turbulence within plant canopies has shown large coherent eddy structures with length scales $\sim h$ horizontally and $\sim h/3$ vertically, where h is the canopy height (Finnigan, 2000). There are few specific measurements of turbulence length scales within orchard blocks, however some values from an apple orchard and an almond orchard which agree roughly with these length scales may be found in Walklate (1993) and Y. S. Wang *et al.* (1992).

Crop heights and shelterbelt characteristics naturally vary between different orchard blocks. Some typical values for kiwifruit orchards are given in Palmer *et al.* (1993): crops are usually around 3 m tall, and shelterbelts are frequently deciduous species such as poplar or willow, or evergreen species such as casuarina; they can be as much as 20 m tall, but are generally around $8 - 10$ m tall, with a width of approximately $2 - 4$ m. Using Equation (3.30), the background trapping rate k_b is then likely to be < 2 s^{-1}.

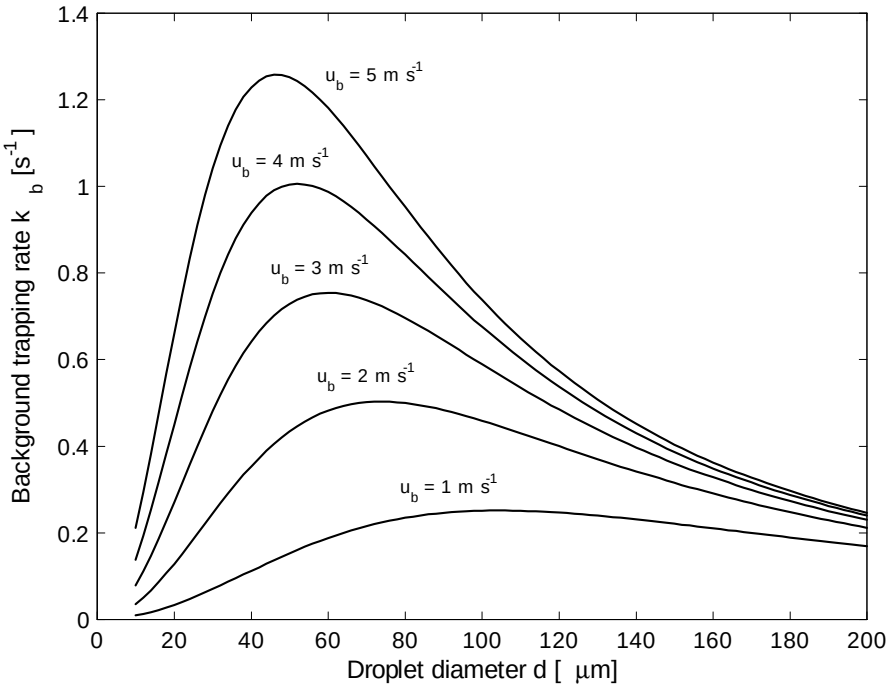

Figure 3.2: Values of the background trapping rate k_b [s^{-1}], calculated from Equation (3.30), for various droplet sizes and five different windspeeds through a moderately dense poplar (broadleaf) shelterbelt. See the text for parameter values

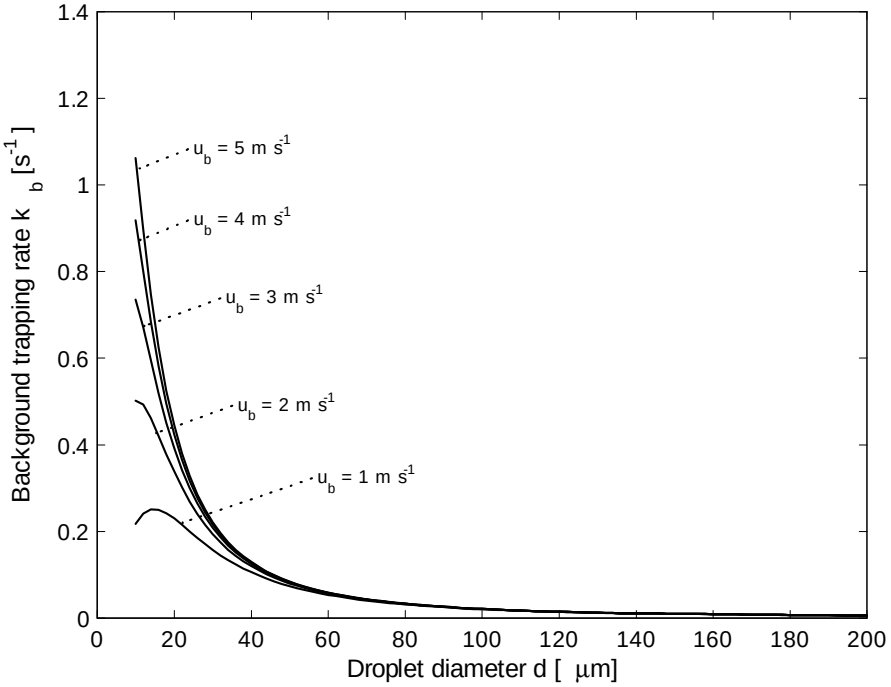

Figure 3.3: Values of the background trapping rate k_b [s^{-1}], calculated from Equation (3.30), for various droplet sizes and five different windspeeds through a moderately dense casuarina (fine needled) shelterbelt. See the text for parameter values

Table 3.1: Some typical parameter values

Parameter	Description	Range
u	mean windspeed	$1 - 5$ m s^{-1}
d	droplet diameter	$10 - 200$ μm
S	settling speed	$0.003 - 1.2$ m s^{-1}
L_L, L_T	horizontal turbulence length scales	$\sim 8 - 10$ m
L_V	vertical turbulence length scales	$\sim 2 - 3$ m
k_b	background trapping rate	< 2 s^{-1}

3.5 Chapter Summary

In this chapter, we set up the framework for our advection-dispersion model to describe the transport of airborne drifting spray droplets, in the absence of evaporation, including trapping within a shelterbelt. The model is intended to be simple, in order to make an analytic solution possible, yet still capture the major features of the droplet transport. A summary of the main features and assumptions of the model, as described earlier in the chapter, is as follows:

- Drifting spray droplets are advected by the wind and dispersed by turbulence, all whilst falling under the influence of gravity. Within the shelterbelt, droplets are removed by trapping at a rate proportional to the local concentration there.
- The wind is assumed to be horizontal, and uniform in both speed and direction. It is also assumed to flow through the shelterbelt undisturbed.
- Turbulence in the airflow is modelled as having some dominant length scales in the along-wind, crosswind and vertical directions. These length scales are taken to be constant throughout the flow.
- The ground is approximately horizontal; it is assumed to be impervious to the droplets, therefore they cannot disperse through it. As a result, there is zero vertical dispersive flux at ground level.

It remains, now, to determine an analytic solution for the model. As introduced earlier, the ideal scenario of continuous trapping throughout the block representing the shelterbelt is difficult to

deal with analytically, so instead we proceed by discretising the shelterbelt using an array of smaller blocks with the trapping in each block concentrated to the point at its centre. The next two chapters cover the process of obtaining an analytic solution to the model for the discretised shelterbelt, beginning with just a single point representation for trapping.

Chapter 4

A Point Representation for Trapping

Recollect that in our advection-dispersion model for the transport of airborne drifting spray droplets in the absence of evaporation (Chapter 3), a shelterbelt is represented by a block of continuous trapping. Seeking an analytic solution, we begin by looking at a mathematically simplified problem where the effect of continuous trapping throughout a block is concentrated to the point at its centre; this point representation for trapping gives us much more traction analytically, and allows us to write explicit expressions for the total trapping and the subsequent deposit on the ground. Later we will use the results from this point representation to construct an analytic solution to the model with trapping in a discretised shelterbelt (see Chapter 5).

In this chapter we analyse our advection-dispersion model with a point representation for trapping. We consider two separate cases: the first is a special case where vertical dispersion of the droplets is negligible compared to horizontal dispersion, and the second is the more realistic case where vertical dispersion is significant. In each case the ultimate objective is a full three-dimensional (3-D) solution to the model, but we also show solutions in one and two dimensions (1-D and 2-D). The 1-D and 2-D solutions are stepping-stones towards the full 3-D solution, but are also interesting in their own right: the 1-D solution behaves a little differently from the 2-D and 3-D solutions, and the 2-D solution is useful for comparison, as other models for spray drift deposition, described in the literature, are also 2-D.

As is explained in further detail in this chapter, an interesting artefact of the point representation arises whereby the droplet mass concentration is negative for a short time in the vicinity of the trapping point; this is a consequence of using Dirac delta functions to define the point. Whilst the issue seems alarming at first, it is magnified in this chapter by the unrealistically high trapping rates used for demonstrative purposes. In Chapter 5 we show that the issue is of

negligible effect with realistic trapping rates, as the localised area in which the concentration is negative becomes very small.

4.1 Advection-Dispersion Model

Let us begin by clarifying what is meant by a point representation for trapping: we assume that there is continuous trapping of droplets within a small block, and then concentrate the trapping to the single point at the centre of this block using Dirac delta functions.

Recall from Chapter 3 that the rate of mass removal by trapping per unit volume of air is $k_b R c$, where k_b is the background trapping rate, and R is a dimensionless function which is non-zero only where trapping occurs. Let the small block of continuous trapping have dimensions $\Delta x \times \Delta y \times \Delta z$, and the point at its centre be denoted (X_1, Y_1, Z_1); then R is defined as

$$R = \Delta x \Delta y \Delta z \delta\left(x - X_1\right) \delta\left(y - Y_1\right) \delta\left(z - Z_1\right) \tag{4.1}$$

which is dimensionless and non-zero only at (X_1, Y_1, Z_1). In this way, the rate of mass removal per unit volume of air is $k_b c \Delta x \Delta y \Delta z \delta\left(x - X_1\right) \delta\left(y - Y_1\right) \delta\left(z - Z_1\right)$. Lastly, we define

$$k = k_b \Delta x \Delta y \Delta z \tag{4.2}$$

as the effective trapping rate for the point (with dimensions of volume per unit time [$\mathrm{m}^3\ \mathrm{s}^{-1}$]). Substituting Equations (4.1) and (4.2) into (3.17), our advection-dispersion model with a point representation for trapping is

$$\begin{aligned} \frac{\partial c}{\partial t} + u\frac{\partial c}{\partial x} - S\frac{\partial c}{\partial z} &= D_L \frac{\partial^2 c}{\partial x^2} + D_T \frac{\partial^2 c}{\partial y^2} + D_V \frac{\partial^2 c}{\partial z^2} + Q\delta\left(x - X_0\right) \delta\left(y - Y_0\right) \delta\left(z - H\right) \delta\left(t\right) \\ &\quad - kc\left(X_1, Y_1, Z_1, t\right) \delta\left(x - X_1\right) \delta\left(y - Y_1\right) \delta\left(z - Z_1\right). \end{aligned} \tag{4.3}$$

This is to be solved subject to the initial and boundary conditions given in Chapter 3, Section 3.2. If the vertical dispersion coefficient $D_V = 0$, then the boundary condition on the ground is automatically satisfied and Equation (4.3) is relatively simple to solve analytically. However, if $D_V \neq 0$ then the boundary condition on the ground makes the solution process much more complicated, and the solutions we obtain are nestled in integral equations.

4.2 Total Droplet Trapping and Deposition

The quantities of particular interest are the total mass of droplets trapped at the point and the subsequent deposit on the ground. Both of these quantities are found from the solution to the advection-dispersion model; we will make frequent use of Laplace transforms in evaluating them, via the property that

$$\int_0^\infty c\,(x,y,z,t)\ dt = \int_0^\infty e^{-pt} c\,(x,y,z,t)\ dt \Big|_{p=0} = \overline{c}\,(x,y,z,0) \tag{4.4}$$

where $\overline{c}\,(x,y,z,p)$ is the Laplace transform of $c\,(x,y,z,t)$ with respect to t.

Total Droplet Trapping

The total mass of droplets trapped at the point, M_{TT} [kg], is found by integrating the trapping rate per unit volume with respect to space and time. The trapping rate per unit volume of air is $k_b R c$; with substitution of Equations (4.1) and (4.2) for the point representation, this becomes $kc\,(X_1,Y_1,Z_1,t)\,\delta\,(x-X_1)\,\delta\,(y-Y_1)\,\delta\,(z-Z_1)$. Integrating with respect to space and time:

$$\begin{aligned} M_{TT} &= \int_0^\infty \int_0^\infty \int_{-\infty}^\infty \int_{-\infty}^\infty kc\,(X_1,Y_1,Z_1,t)\,\delta\,(x-X_1)\,\delta\,(y-Y_1)\,\delta\,(z-Z_1)\ dx\ dy\ dz\ dt \\ &= \int_0^\infty kc\,(X_1,Y_1,Z_1,t)\ dt \\ &= k\overline{c}\,(X_1,Y_1,Z_1,0)\,. \end{aligned} \tag{4.5}$$

The total mass of droplets deposited on the ground, M_{DT} [kg], is simply what remains of the original release after trapping, that is

$$\begin{aligned} M_{DT} &= Q - M_{TT} \\ &= Q - k\overline{c}\,(X_1,Y_1,Z_1,0)\,. \end{aligned} \tag{4.6}$$

Droplet Deposition

The total mass of droplets deposited on the ground per unit area, M_D [kg m^{-2}], is found by integrating the downward mass flux per unit area with respect to time. At height z, the downward mass flux per unit area is $Sc + D_V \dfrac{\partial c}{\partial z}$ (made up of a settling flux and a dispersive

flux). At ground level ($z = 0$) the boundary condition asserts that the dispersive flux is zero, thus droplets will only deposit via gravitational settling, and the downward mass flux per unit area is $Sc(x, y, 0, t)$. Integrating with respect to time:

$$\begin{aligned} M_D(x, y) &= \int_0^\infty Sc(x, y, 0, t)\ dt \\ &= S\overline{c}(x, y, 0, 0). \end{aligned} \tag{4.7}$$

This method of evaluating the total trapping and deposition is particularly convenient, as we make considerable use of Laplace transforms in solving our advection-dispersion model, and in most cases the required transforms are readily available. Tables of the Laplace (and Fourier) transforms used in this thesis may be found in Appendix B.

4.3 Case 1: Zero Vertical Dispersion

In this section we analyse our advection-dispersion model with a point representation for trapping, in the case where vertical dispersion of the droplets is very small compared to horizontal dispersion, such that the vertical dispersion coefficient D_V may be considered zero. This is a special case of the model where the droplets can disperse only horizontally; the boundary condition of zero vertical dispersive flux on the ground is automatically satisfied, and it is relatively simple to determine an analytic solution. We present solutions in 1-D and 2-D, building up to a full 3-D solution.

One-Dimensional Solution

In 1-D, and with $D_V = 0$, our advection-dispersion model with a point representation for trapping becomes

$$\frac{\partial c}{\partial t} - S\frac{\partial c}{\partial z} = Q\delta(z - H)\,\delta(t) - kc(Z_1, t)\,\delta(z - Z_1) \tag{4.8}$$

with initial and boundary conditions

$$c\left(z, 0^-\right) = 0 \text{ and } c(\infty, t) = 0.$$

Conceptually this is now trapping at a plane, as shown in Figure 4.1. Mass Q per unit area is released at time $t = 0$ from the plane $(x, y, z) = (x, y, H)$. A thin layer of continuous trapping, with thickness Δz, removes droplets at mass rate per unit volume $k_b Rc$. We concentrate this

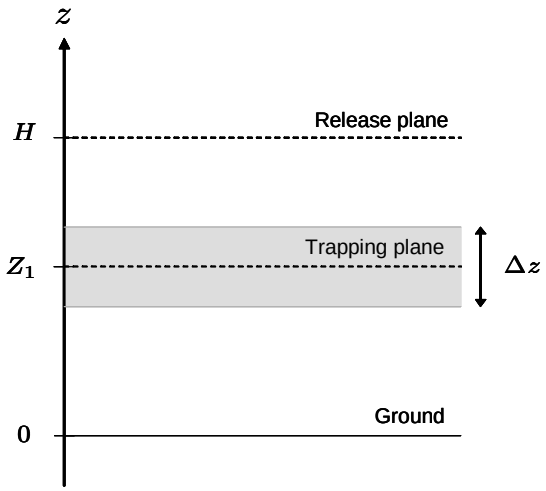

Figure 4.1: Conceptual illustration of the 1-D model with trapping at a plane.

trapping to the plane $(x, y, z) = (x, y, Z_1)$ at the centre of the layer, so that $R = \Delta z \delta(z - Z_1)$, and the effective trapping rate for the plane is $k = k_b \Delta z$. After release, the droplets simply fall towards the ground with settling speed S; they do not disperse as they fall.

An analytic solution to Equation (4.8) may be found by taking Laplace transforms with respect to t. The transformed solution is

$$\overline{c}(z,p) = \frac{Q}{S}\mathcal{H}(H-z)\, e^{-\frac{p(H-z)}{S}} - \frac{k}{S}\overline{c}(Z_1,p)\,\mathcal{H}(Z_1-z)\, e^{-\frac{p(Z_1-z)}{S}} \tag{4.9}$$

where the bar accent denotes the Laplace transform, and $\mathcal{H}(z)$ is the Heaviside function

$$\mathcal{H}(z) = \begin{cases} 0, & z < 0, \\ 1, & z > 0. \end{cases} \tag{4.10}$$

Note that this transformed solution contains the, as yet, unknown $\overline{c}(Z_1, p)$ and has discontinuities at $z = H$ and $z = Z_1$. To determine $\overline{c}(Z_1, p)$ we let $z \to Z_1^+$ (that is, we let z approach Z_1 from above), since this corresponds to the droplet mass concentration which arrives at the trapping plane, thereby influencing the amount trapped.

$$\begin{aligned} \overline{c}(Z_1,p) &= \lim_{z \to Z_1^+} \overline{c}(z,p) \\ &= \frac{Q}{S}\mathcal{H}(H-Z_1)\, e^{-\frac{p(H-Z_1)}{S}}. \end{aligned} \tag{4.11}$$

Inverting the Laplace transforms:

$$\text{For } Z_1 > H, \quad c(z,t) = \begin{cases} 0, & z > H, \\ Q\,\delta(z-(H-St)), & z < H, \end{cases} \tag{4.12}$$

$$\text{and for } Z_1 < H, \quad c\,(z,t) = \begin{cases} 0, & z > H, \\ Q\ \delta\,(z-(H-St))\,, & Z_1 < z < H, \\ Q\left(1-\dfrac{k}{S}\right)\ \delta\,(z-(H-St))\,, & z < Z_1. \end{cases} \tag{4.13}$$

Above the release height the concentration is always zero; this is because there is no dispersion, so the droplets do not move upwards. Below the release the concentration is non-zero only at height $z = H - St$, which is the height the droplets have fallen to after time t. Because the droplets simply fall downwards the concentration is the same at all heights, until the trapping plane (provided it is below the release), whereupon some of the droplets are removed leaving a lower concentration below.

Total Droplet Trapping and Deposition

The total trapping at the plane and the deposit on the ground are calculated by setting $p = 0$ in the transformed solution, as described in Section 4.2. The total mass trapped at the plane per unit area [kg m^{-2}] is

$$\begin{aligned} M_{TT} &= k\overline{c}\,(Z_1,0) \\ &= \begin{cases} 0, & Z_1 > H, \\ \dfrac{kQ}{S}, & Z_1 < H, \end{cases} \end{aligned} \tag{4.14}$$

and the density of deposit on the ground (mass deposited per unit area) [kg m^{-2}] is

$$\begin{aligned} M_D &= S\overline{c}\,(0,0) \\ &= \begin{cases} Q, & Z_1 > H, \\ Q\left(1-\dfrac{k}{S}\right), & Z_1 < H. \end{cases} \end{aligned} \tag{4.15}$$

Some points to note:

- There is no trapping if $Z_1 > H$, that is, if the trapping plane is higher than the release. This is because the droplets do not move upwards, therefore none will reach the trapping plane if it is higher than the release.
- For $Z_1 < H$ the total mass trapped is independent of Z_1. This is because, for $Z_1 < H$, all of the droplets will encounter the trapping plane no matter where it is, therefore the same mass is always available to be trapped.

A Physical Restriction on the Size of the Trapping Rate

For the model to remain physically sensible, the rate of mass removal at the trapping plane must not exceed the rate of mass arrival; this places an upper limit on the size of the effective trapping rate k, and consequently on Δz, the thickness of the layer which the trapping plane represents. The rate of mass arrival at the trapping plane is $Sc\left(Z_1^+, t\right)$ and the rate of mass removal is $kc\left(Z_1^+, t\right)$, therefore we must have $kc\left(Z_1^+, t\right) \leq Sc\left(Z_1^+, t\right)$ which requires

$$k \leq S. \tag{4.16}$$

Since $k = k_b \Delta z$, this condition implies

$$\Delta z \leq \frac{S}{k_b}. \tag{4.17}$$

Equation (4.17) says that, given background trapping rate k_b, the maximum thickness of trapping layer which may be represented by a single trapping plane is $\dfrac{S}{k_b}$. Satisfying Equation (4.17) also ensures that $M_{TT} \leq Q$ and $M_D \geq 0$; in other words, that the total mass trapped does not exceed the original release and the density of deposit is non-negative.

Two-Dimensional Solution

In 2-D, and with $D_V = 0$, our advection-dispersion model with a point representation for trapping becomes

$$\frac{\partial c}{\partial t} + u\frac{\partial c}{\partial x} - S\frac{\partial c}{\partial z} = D_L \frac{\partial^2 c}{\partial x^2} + Q\delta\left(x - X_0\right)\delta\left(z - H\right)\delta\left(t\right) - kc\left(X_1, Z_1, t\right)\delta\left(x - X_1\right)\delta\left(z - Z_1\right) \tag{4.18}$$

with initial and boundary conditions

$$c\left(x, z, 0^-\right) = 0, \text{ and}$$

$$c\left(x, z, t\right) \to 0 \text{ as } x \to \pm\infty, \text{ and } z \to +\infty.$$

The conceptual situation is now trapping at a line of infinite crosswind length, as shown in Figure 4.2. Mass Q per unit length is released at time $t = 0$ from the line $(x, y, z) = (X_0, y, H)$. A rectangular prism of continuous trapping with infinite length, and cross-sectional area $\Delta x \times \Delta z$, removes droplets at mass rate per unit volume $k_b Rc$. We concentrate this trapping to the line $(x, y, z) = (X_1, y, Z_1)$ through the centre of the prism, so that $R = \Delta x \Delta z \delta\left(x - X_1\right)\delta\left(z - Z_1\right)$ and the effective trapping rate for the line is $k = k_b \Delta x \Delta z$. After release, the droplets disperse alongwind whilst travelling with the mean windspeed u and falling at settling speed S.

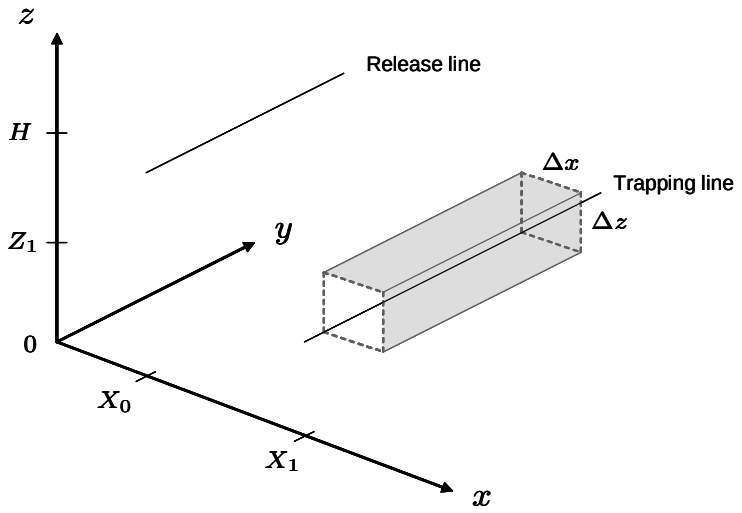

Figure 4.2: Conceptual illustration of the 2-D model with trapping at a line.

An analytic solution to Equation (4.18) may be found using a combination of Laplace transforms with respect to t and Fourier transforms with respect to x. The transformed solution is

$$\begin{aligned}\widehat{\overline{c}}\,(\omega,z,p) &= \frac{Q}{S}\mathcal{H}\,(H-z)\,e^{-\frac{p(H-z)}{S}-i\omega\left(X_0+\frac{u(H-z)}{S}\right)-\frac{\omega^2 D_L(H-z)}{S}} \\ &\quad -\frac{k}{S}\overline{c}\,(X_1,Z_1,p)\,\mathcal{H}\,(Z_1-z)\,e^{-\frac{p(Z_1-z)}{S}-i\omega\left(X_1+\frac{u(Z_1-z)}{S}\right)-\frac{\omega^2 D_L(Z_1-z)}{S}} \qquad (4.19)\end{aligned}$$

where the bar accent denotes the Laplace transform with respect to t, and the hat accent denotes the Fourier transform with respect to x, as defined by $\widehat{f}\,(\omega) = \int_{-\infty}^{\infty} f\,(x)\,e^{-i\omega x}\,dx$. Inverting the Fourier transforms:

$$\begin{aligned}\overline{c}\,(x,z,p) &= \frac{Q}{2\sqrt{\pi S D_L\,(H-z)}}\mathcal{H}\,(H-z)\,e^{-\frac{p(H-z)}{S}-\frac{S(x-X_0-u(H-z)/S)^2}{4D_L(H-z)}} \\ &\quad -\frac{k\overline{c}\,(X_1,Z_1,p)}{2\sqrt{\pi S D_L\,(Z_1-z)}}\mathcal{H}\,(Z_1-z)\,e^{-\frac{p(Z_1-z)}{S}-\frac{S(x-X_1-u(Z_1-z)/S)^2}{4D_L(Z_1-z)}}. \qquad (4.20)\end{aligned}$$

To determine the, as yet, unknown $\overline{c}\,(X_1,Z_1,p)$ we set $x = X_1$ and let $z \to Z_1^+$, since this corresponds to the concentration which arrives at the trapping line, thereby influencing the amount trapped.

$$\begin{aligned}\overline{c}\,(X_1,Z_1,p) &= \lim_{z\to Z_1^+}\overline{c}\,(X_1,z,p) \\ &= \frac{Q}{2S\sqrt{\pi D_L t_1}}\mathcal{H}\,(H-Z_1)\,e^{-pt_1-\frac{(X_1-X_0-ut_1)^2}{4D_L t_1}} \qquad (4.21)\end{aligned}$$

where $t_1 = \dfrac{H-Z_1}{S}$ is the time for the droplets to fall to the height of the trapping line, assuming it is below the release height. Inverting the Laplace transforms:

For $Z_1 > H$,

$$c\left(x,z,t\right) = \begin{cases} 0, & z > H, \\ \dfrac{Q}{2\sqrt{\pi D_L t}} e^{-\frac{(x-X_0-ut)^2}{4D_L t}} \delta\left(z-(H-St)\right), & z < H, \end{cases} \tag{4.22}$$

and for $Z_1 < H$,

$$c\left(x,z,t\right) = \begin{cases} 0, & z > H, \\ \dfrac{Q}{2\sqrt{\pi D_L t}} e^{-\frac{(x-X_0-ut)^2}{4D_L t}} \delta\left(z-(H-St)\right), & Z_1 < z < H, \\ \left[\dfrac{Q}{2\sqrt{\pi D_L t}} e^{-\frac{(x-X_0-ut)^2}{4D_L t}} - \dfrac{kQ}{4\pi S D_L \sqrt{t_1\left(t-t_1\right)}} \times \right. & \\ \left. e^{-\frac{(X_1-X_0-ut_1)^2}{4D_L t_1} - \frac{(x-X_1-u(t-t_1))^2}{4D_L(t-t_1)}} \right] \delta\left(z-(H-St)\right), & z < Z_1. \end{cases} \tag{4.23}$$

This solution is similar to the 1-D solution, in that the concentration above the release height is zero and the concentration below the release is only non-zero at height $z = H - St$ (the height the droplets have fallen to after time t). Here, though, the use of delta functions in the model to define the trapping line results in a locally negative concentration beneath the trapping line. This phenomenon was mentioned in the opening of the chapter, and is explained further below.

Examining the Negative Concentration

An artefact of using Dirac delta functions as we have done in this model to focus the trapping to a single line, is that the droplet mass concentration becomes negative in a localised area beneath the trapping line. For instance, consider the concentration immediately below the height of the trapping line, that is, at $z = Z_1^-$. The time at which the droplets reach this height is $t = t_1^+$, and the concentration there as given by Equation (4.23) is

$$c\left(x, Z_1^-, t_1^+\right) = \left[\frac{Q}{2\sqrt{\pi D_L t_1}} e^{-\frac{(x-X_0-ut_1)^2}{4D_L t_1}} - \frac{kQ}{2S\sqrt{\pi D_L t_1}} e^{-\frac{(X_1-X_0-ut_1)^2}{4D_L t_1}} \delta\left(x-X_1\right)\right] \delta\left(Z_1^- - \left(H - St_1^+\right)\right) \tag{4.24}$$

using the property that

$$\lim_{\sigma \to 0^+} \frac{e^{-\frac{a^2}{\sigma^2}}}{\sigma\sqrt{\pi}} = \delta(a). \tag{4.25}$$

It is apparent from Equation (4.24) that, because of the $\delta(x - X_1)$ term, the concentration immediately beneath the trapping line at $(x, z) = \left(X_1, Z_1^-\right)$ is infinitely negative (unless $k = 0$ in which case there is no trapping).

The negative concentration occurs because we have focussed all of the trapping to an infinitely thin line. Essentially, the trapping is a negative release of strength $kc(X_1, Z_1, t_1)$ which occurs from the line $(x, z) = (X_1, Z_1)$ at time $t = t_1$. Looking at Equation (4.23), the concentration below Z_1 is a superposition of the original release and this negative release. Immediately below the trapping line, the negative release dominates and so the concentration is negative, but then as the droplets continue to fall and disperse, after a while the original release dominates and the concentration becomes positive everywhere again. The time it takes for the concentration to recover and become positive again depends on the size of $kc(X_1, Z_1, t_1)$; the larger this is the longer it takes, and therefore the larger the localised area beneath the trapping line where the concentration is negative.

As an example, Figure 4.3 shows the finite part of the mass concentration (the terms inside the square brackets in Equation (4.23)) as a superposition of the original release and the negative release which represents the trapping. The two heights, $z = 1.9$ m and $z = 1.5$ m, are below the trapping line which is located at $(X_1, Z_1) = (4, 2)$ m. The effective trapping rate is $k = 1$ m^2 s^{-1}, which comes from $k_b = 25$ s^{-1} and $\Delta x \Delta z = 0.04$ m^2; this k value is unrealistically high and is used only for demonstration purposes. The remaining parameters used are summarised in Table 4.1 (page 52). At $z = 1.9$ m the negative release overpowers the original release and the concentration is negative in the vicinity of X_1, but by $z = 1.5$ m the original release is dominant and the concentration is positive everywhere.

We recognise that a negative concentration is a physical impossibility, thus the model does not accurately describe the situation immediately beneath the trapping line. However, the issue is only significant for unrealistically high values of k which result in a long recovery time. As shown in the next chapter, for realistic values of k the concentration recovers very quickly, so the localised area in which the concentration is negative is very small and the issue has negligible effect.

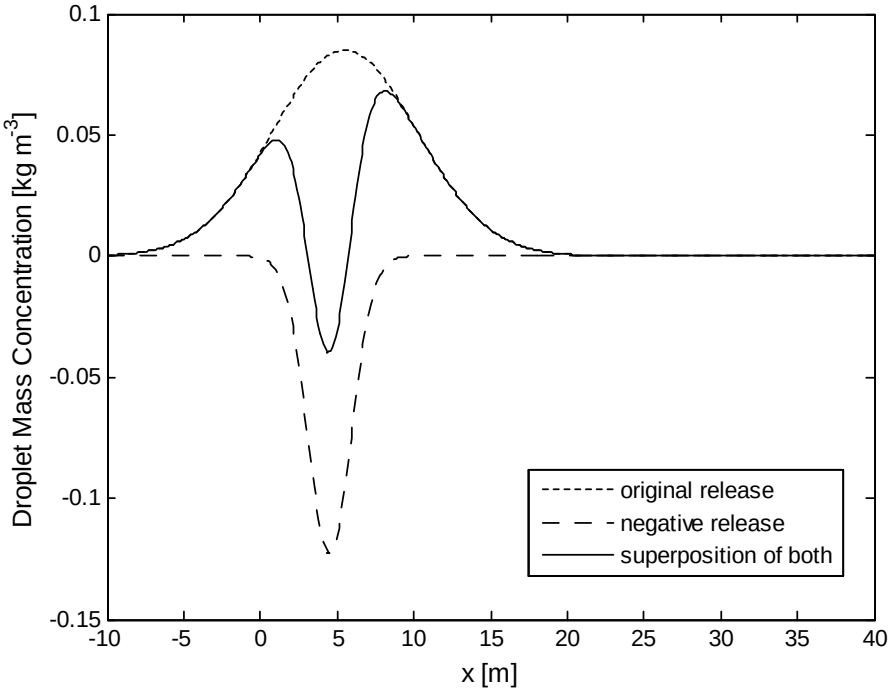

(a) Finite part of the droplet mass concentration at height $z = 1.9$ m and time $t = 5.5$ s.

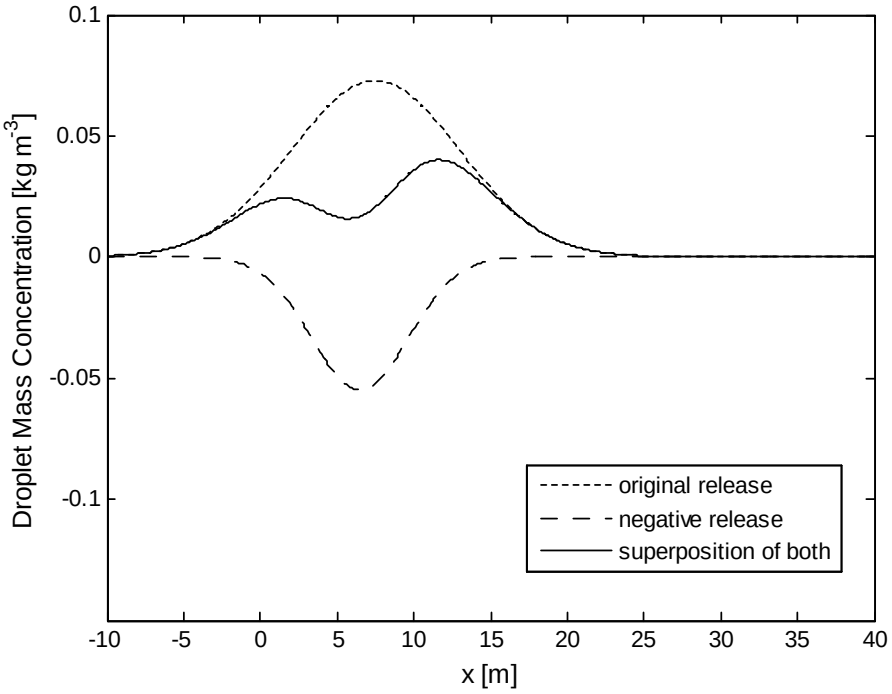

(b) Finite part of the droplet mass concentration at height $z = 1.5$ m and time $t = 7.5$ s.

Figure 4.3: Cross-sections of the finite part of the mass concentration c [kg m^{-3}] at two different heights below the trapping line which is at $(X_1, Z_1) = (4, 2)$ m. The mass concentration is a superposition of the original release, and a negative release (representing the trapping). At $z = 1.9$ m the negative release dominates and the concentration is negative near the trapping line. By $z = 1.5$ m the original release dominates and the concentration is positive everywhere.

Total Droplet Trapping and Deposition

Following the procedure described in Section 4.2, the total mass of droplets trapped at the line per unit length [kg m^{-1}] is

$$\begin{aligned} M_{TT} &= k\overline{c}\,(X_1, Z_1, 0) \\ &= \begin{cases} 0, & Z_1 > H, \\ \dfrac{kQ}{2S\sqrt{\pi D_L t_1}} e^{-\frac{(X_1 - X_0 - ut_1)^2}{4D_L t_1}}, & Z_1 < H, \end{cases} \end{aligned} \tag{4.26}$$

leaving a total deposit on the ground per unit crosswind length of $M_{DT} = Q - M_{TT}$ [kg m^{-1}]. The density of deposit on the ground [kg m^{-2}] is

$$\begin{aligned} M_D\,(x) &= S\overline{c}\,(x, 0, 0) \\ &= \begin{cases} \dfrac{Q\sqrt{S}}{2\sqrt{\pi H D_L}} e^{-\frac{S(x - X_0 - uH/S)^2}{4D_L H}}, & Z_1 > H, \\ \dfrac{Q\sqrt{S}}{2\sqrt{\pi H D_L}} e^{-\frac{S(x - X_0 - uH/S)^2}{4D_L H}} - \\ \dfrac{kQ}{4\pi D_L \sqrt{S Z_1 t_1}} e^{-\frac{(X_1 - X_0 - ut_1)^2}{4D_L t_1} - \frac{S(x - X_1 - uZ_1/S)^2}{4D_L Z_1}}, & Z_1 < H. \end{cases} \end{aligned} \tag{4.27}$$

Some points to note:

- As in the 1-D solution there is no trapping if $Z_1 > H$, that is, if the trapping line is higher than the release.
- If $Z_1 < H$ then the total mass trapped decreases with increasing separation between the trapping line and the release. For instance, if the alongwind separation $|X_0 - X_1|$ is large then few droplets will encounter the trapping line as most will deposit before travelling far enough. Alternatively, if the vertical separation $(H - Z_1)$ is large then few droplets will encounter the trapping line as they will be well-dispersed by the time they fall to that height.
- For $Z_1 < H$ the total mass trapped increases with increasing trapping rate k. To ensure that $M_{TT} \leq Q$, in other words that the total trapping does not exceed the original release, requires

$$k \leq 2S\sqrt{\pi D_L t_1}\, e^{\frac{(X_1 - X_0 - ut_1)^2}{4D_L t_1}} \tag{4.28}$$

and consequently, since $k = k_b \Delta x \Delta z$,

$$\Delta x \Delta z \leq \frac{2S\sqrt{\pi D_L t_1}}{k_b} e^{\frac{(X_1 - X_0 - ut_1)^2}{4D_L t_1}}. \tag{4.29}$$

An Illustrative Example of the Two-Dimensional Solution

The following example illustrates the 2-D solution described above. The parameter set used here is given in Table 4.1. A settling speed of $S = 0.2$ m s^{-1} corresponds to droplets of approximate diameter $d = 44$ μm, and a dominant alongwind turbulence length scale of $L_L = 2$ m gives dispersion coefficient $D_L = uL_L = 2$ m^2 s^{-1}. In this example the position of the trapping line, (X_1, Z_1), is slightly upstream of the centre of mass of the droplets at time t_1, and the effective trapping rate for the line is $k = k_b \Delta x \Delta z = 1$ m^2 s^{-1}. According to Equation (4.28), the maximum allowable effective trapping rate is 2.30 m^2 s^{-1}. Note that the value of the the background trapping rate k_b is unrealistically high and used only so that the effect of trapping may be more clearly observed.

Table 4.1: Parameter set used to generate Figures 4.4 and 4.5

u	S	L_L	Q	(X_0, H)	k_b	$\Delta x \Delta z$	(X_1, Z_1)
1 m s^{-1}	0.2 m s^{-1}	2 m	1 kg m^{-1}	$(0, 3)$ m	25 s^{-1}	0.04 m^2	$(4, 2)$ m

Figure 4.4 shows cross-sections of the density of deposit [kg m^{-2}], as calculated from Equation (4.27). The density of deposit with trapping is denoted M_D and the value without trapping (found by setting $k = 0$) is denoted M_D^*. The corresponding percentage reduction in the density of deposit as a result of this trapping is shown in Figure 4.5. There is a shadow region of significant reduction just downwind of the trapping line, then less effect further downwind. In this example the maximum reduction in density of deposit is 55 % which occurs at $x = 12$ m. According to Equation (4.26) the total mass trapped at the line is $M_{TT} = 0.44$ kg m^{-1}.

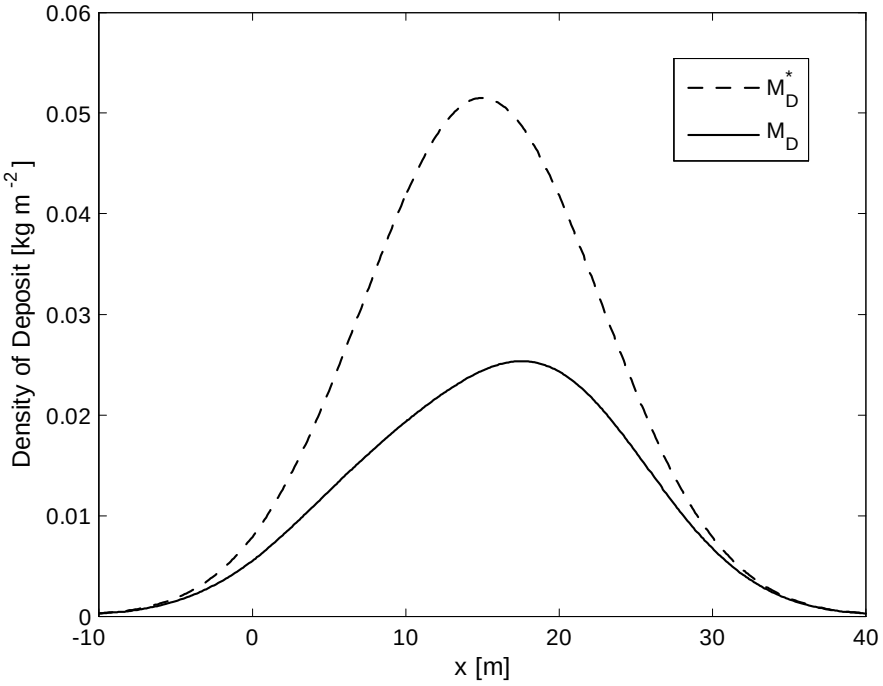

Figure 4.4: Cross-section of the density of deposit [kg m^{-2}], resulting from a line release with zero vertical dispersion and a line of trapping. M_D denotes the density of deposit with trapping, and M_D^* denotes the corresponding value without trapping. Parameter values are given in Table 4.1.

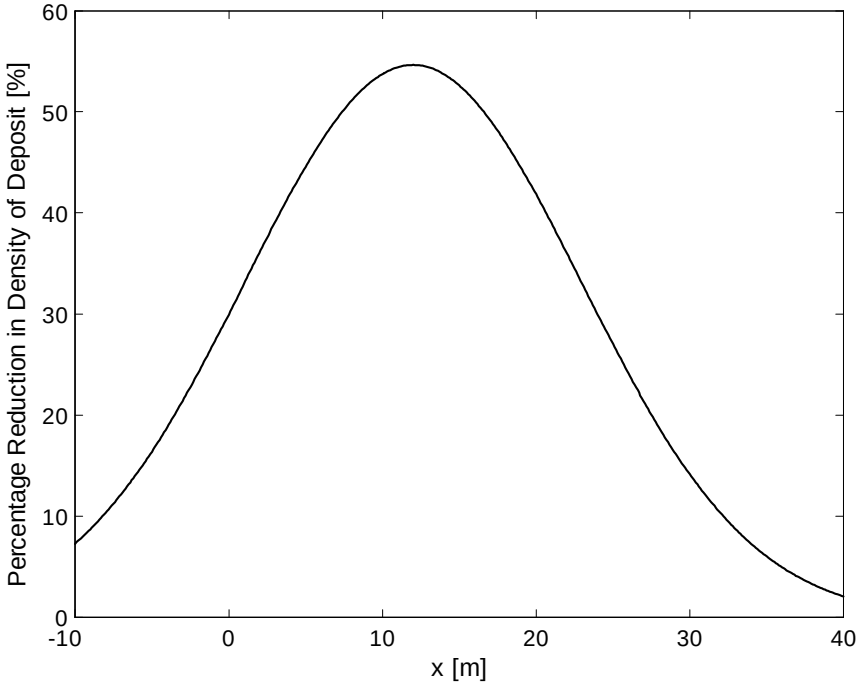

Figure 4.5: Cross-section of the percentage reduction in density of deposit as a result of the trapping in Figure 4.4. Parameter values are the same as for Figure 4.4.

Three-Dimensional Solution

In all three spatial dimensions, but with $D_V = 0$, our advection-dispersion model with a point representation for trapping becomes

$$\begin{aligned}\frac{\partial c}{\partial t} + u\frac{\partial c}{\partial x} - S\frac{\partial c}{\partial z} &= D_L\frac{\partial^2 c}{\partial x^2} + D_T\frac{\partial^2 c}{\partial y^2} + Q\delta(x - X_0)\,\delta(y - Y_0)\,\delta(z - H)\,\delta(t) \\ &\quad -kc(X_1, Y_1, Z_1, t)\,\delta(x - X_1)\,\delta(y - Y_1)\,\delta(z - Z_1) \end{aligned} \tag{4.30}$$

with initial and boundary conditions

$$c\left(x, y, z, 0^-\right) = 0, \text{ and}$$
$$c(x, y, z, t) \to 0 \text{ as } x, y \to \pm\infty, \text{ and } z \to +\infty.$$

Recapping the conceptual scenario: mass Q is released at time $t = 0$ from the point $(x, y, z) = (X_0, Y_0, H)$, and a small block of continuous trapping with dimensions $\Delta x \times \Delta y \times \Delta z$ removes droplets at mass rate per unit volume $k_b R c$. We concentrate this trapping to the point $(x, y, z) = (X_1, Y_1, Z_1)$ at the centre of the block, so that $R = \Delta x \Delta y \Delta z \delta(x - X_1)\,\delta(y - Y_1)\,\delta(z - Z_1)$ and the effective trapping rate for the point is $k = k_b \Delta x \Delta y \Delta z$. After release, the droplets disperse horizontally (both alongwind and crosswind) whilst travelling with the mean wind speed u and falling at settling speed S.

An analytic solution to Equation (4.76) may be found using a combination of Laplace transforms with respect to t and Fourier transforms with respect to x and y; this is really just an extension of the previous 2-D solution. The transformed solution here is

$$\begin{aligned}\widetilde{\widehat{\overline{c}}}(\omega, \psi, z, p) &= \frac{Q}{S}\mathcal{H}(H - z)\, e^{-\frac{p(H-z)}{S} - i\omega\left(X_0 + \frac{u(H-z)}{S}\right) - i\psi Y_0 - \frac{\left(\omega^2 D_L + \psi^2 D_T\right)(H-z)}{S}} \\ &\quad -\frac{k}{S}\overline{c}(X_1, Y_1, Z_1, p)\,\mathcal{H}(Z_1 - z)\, e^{-\frac{p(Z_1-z)}{S} - i\omega\left(X_1 + \frac{u(Z_1-z)}{S}\right) - i\psi Y_1 - \frac{\left(\omega^2 D_L + \psi^2 D_T\right)(Z_1-z)}{S}}. \end{aligned} \tag{4.31}$$

The bar accent denotes the Laplace transform with respect to t, the hat accent denotes the Fourier transform with respect to x, and the tilde accent denotes the Fourier transform with respect to y. Inverting the Fourier transforms:

$$\begin{aligned}\overline{c}(x, y, z, p) &= \frac{Q}{4\pi\sqrt{D_L D_T}\,(H - z)}\mathcal{H}(H - z)\, e^{-\frac{p(H-z)}{S} - \frac{S(x - x_0 - u(H-z)/S)^2}{4D_L(H-z)} - \frac{S(y-Y_0)^2}{4D_T(H-z)}} \\ &\quad -\frac{k\overline{c}(X_1, Y_1, Z_1, p)}{4\pi\sqrt{D_L D_T}\,(Z_1 - z)}\mathcal{H}(Z_1 - z)\, e^{-\frac{p(Z_1-z)}{S} - \frac{S(x - X_1 - u(Z_1-z)/S)^2}{4D_L(Z_1-z)} - \frac{S(y-Y_1)^2}{4D_T(Z_1-z)}}. \end{aligned} \tag{4.32}$$

To determine $\overline{c}\,(X_1, Y_1, Z_1, p)$ we set $(x, y) = (X_1, Y_1)$ and let $z \to Z_1^+$ to correspond with the concentration which arrives at the trapping point, thereby influencing the amount trapped.

$$\begin{aligned}\overline{c}\,(X_1, Y_1, Z_1, p) &= \lim_{z \to Z_1^+} \overline{c}\,(X_1, Y_1, z, p) \\ &= \frac{Q}{4\pi S t_1 \sqrt{D_L D_T}} \mathcal{H}\,(H - Z_1)\, e^{-pt_1 - \frac{(X_1 - X_0 - ut_1)^2}{4D_L t_1} - \frac{(Y_1 - Y_0)^2}{4D_T t_1}} \end{aligned} \tag{4.33}$$

where $t_1 = \dfrac{H - Z_1}{S}$ is the time for the droplets to fall to the height of the trapping point. Inverting the Laplace transforms:

For $Z_1 > H$

$$c\,(x, y, z, t) = \begin{cases} 0, & z \geq H, \\ \dfrac{Q}{4\pi t \sqrt{D_L D_T}} e^{-\frac{(x - X_0 - ut)^2}{4D_L t} - \frac{(y - Y_0)^2}{4D_T t}} \delta\,(z - (H - St))\,, & z < H, \end{cases} \tag{4.34}$$

and for $Z_1 < H$

$$c\,(x, y, z, t) = \begin{cases} 0, & z \geq H, \\ \dfrac{Q}{4\pi t \sqrt{D_L D_T}} e^{-\frac{(x - X_0 - ut)^2}{4D_L t} - \frac{(y - Y_0)^2}{4D_T t}} \delta\,(z - (H - St))\,, & Z_1 \leq z < H, \\ \left[\dfrac{Q}{4\pi t \sqrt{D_L D_T}} e^{-\frac{(x - X_0 - ut)^2}{4D_L t} - \frac{(y - Y_0)^2}{4D_T t}} - \dfrac{kQ}{16\pi^2 S D_L D_T t_1 (t - t_1)} \times \right. & \\ \left. e^{-\frac{(X_1 - X_0 - ut_1)^2}{4D_L t_1} - \frac{(Y_1 - Y_0)^2}{4D_T t_1} - \frac{(x - X_1 - u(t - t_1))^2}{4D_L (t - t_1)} - \frac{(y - Y_1)^2}{4D_T (t - t_1)}} \right] \delta\,(z - (H - St))\,, & z < Z_1. \end{cases} \tag{4.35}$$

As in both the 1-D and 2-D solutions previously, the concentration is always zero above the release height and only non-zero below the release at height $z = H - St$ (the height the droplets have fallen to after time t).

Being an extension from 2-D, this solution also exhibits a negative concentration in a localised region beneath the trapping point. This may be explained as for the 2-D solution (refer to page 48) by noting that, here, the trapping is essentially a negative release of strength $kc\,(X_1, Y_1, Z_1, t_1)$ which occurs from the point $(x, y, z) = (X_1, Y_1, Z_1)$ at time $t = t_1$. As such,

the concentration below Z_1 is a superposition of the original release and this negative release, and immediately beneath the trapping point the negative release is dominant. Once again, though a negative concentration is physically wrong, the issue is only of significance for unrealistically high trapping rates.

Total Droplet Trapping and Deposition

Following Section 4.2, the total mass of droplets trapped at the point [kg] is

$$\begin{aligned} M_{TT} &= k\overline{c}\,(X_1, Y_1, Z_1, 0) \\ &= \begin{cases} 0, & Z_1 > H, \\ \dfrac{kQ}{4\pi S t_1 \sqrt{D_L D_T}} e^{-\frac{(X_1 - X_0 - ut_1)^2}{4D_L t_1} - \frac{(Y_1 - Y_0)^2}{4D_T t_1}}, & Z_1 < H, \end{cases} \end{aligned} \tag{4.36}$$

leaving a total deposit on the ground of $M_{DT} = Q - M_{TT}$ [kg]. The density of deposit on the ground [kg m^{-2}] is

$$\begin{aligned} M_D\,(x, y) &= S\overline{c}\,(x, y, 0, 0) \\ &= \begin{cases} \dfrac{SQ}{4\pi H \sqrt{D_L D_T}} e^{-\frac{S(x - X_0 - uH/S)^2}{4D_L H} - \frac{S(y - Y_0)^2}{4D_T H}}, & Z_1 > H, \\ \dfrac{SQ}{4\pi H \sqrt{D_L D_T}} e^{-\frac{S(x - X_0 - uH/S)^2}{4D_L H} - \frac{S(y - Y_0)^2}{4D_T H}} - & \\ \dfrac{kQ}{16\pi^2 t_1 Z_1 D_L D_T} e^{-\frac{(X_1 - X_0 - ut_1)^2}{4D_L t_1} - \frac{(Y_1 - Y_0)^2}{4D_T t_1} - \frac{S(x - X_1 - uZ_1/S)^2}{4D_L Z_1} - \frac{S(y - Y_1)^2}{4D_T Z_1}}, & Z_1 < H. \end{cases} \end{aligned} \tag{4.37}$$

Some points to note:

- There is no trapping if $Z_1 > H$, that is, if the trapping point is higher than the release.
- For $Z_1 < H$, the total mass trapped decreases as the trapping point is moved farther from the release. For instance, if either the alongwind separation $|X_0 - X_1|$ or the crosswind separation $|Y_1 - Y_0|$ is large, then few of the droplets will travel far enough to reach the trapping point before depositing. Alternatively, if the vertical separation $(H - Z_1)$ is large then the droplets will be well dispersed by the time they reach the trapping point.

- For $Z_1 < H$ the total mass trapped increases with increasing trapping rate k. To keep $M_{TT} \leq Q$ requires

$$k \leq 4\pi St_1 \sqrt{D_L D_T} e^{\frac{(X_1 - X_0 - ut_1)^2}{4D_L t_1} + \frac{(Y_1 - Y_0)^2}{4D_T t_1}} \tag{4.38}$$

and therefore, since $k = k_b \Delta x \Delta y \Delta z$,

$$\Delta x \Delta y \Delta z \leq \frac{4\pi St_1 \sqrt{D_L D_T}}{k_b} e^{\frac{(X_1 - X_0 - ut_1)^2}{4D_L t_1} + \frac{(Y_1 - Y_0)^2}{4D_T t_1}}. \tag{4.39}$$

4.4 Case 2: Non-Zero Vertical Dispersion

In this section we analyse our advection-dispersion model with a point representation for trapping, in the case where vertical dispersion of the droplets is significant compared to horizontal dispersion (that is $D_V \neq 0$). This is more likely to be the case in reality, because the airflow will have been disturbed by the sprayer, and with the proximity to the ground it will also be affected by the surface topography.

Finding an analytic solution to the model with $D_V \neq 0$ is much more complicated due to the boundary condition on the ground. This boundary condition, established in Section 3.2, requires zero vertical dispersive flux at ground level, that is

$$D_V \frac{\partial c}{\partial z}(x, y, 0, t) = 0. \tag{4.40}$$

For $D_V \neq 0$ this implies $\dfrac{\partial c}{\partial z}(x, y, 0, t) = 0$. A similar model, with the same boundary conditions, has been applied to volcanic ashfall (McKibbin *et al.*, 2005; Lim, 2005). McKibbin *et al.* use an alternative boundary condition $c(x, y, z, t) \to 0$ as $z \to -\infty$; this does not ensure zero vertical dispersive flux on the ground, but the overall dispersion pattern is not greatly changed and the resulting analytic solution is simpler. Lim presents a method for finding an analytic solution with the original boundary condition via the use of a Greens function; we follow this method and extend it to include the effect of trapping. As in Case 1 where $D_V = 0$, we build up to a full 3-D solution by first finding solutions in 1-D and 2-D.

One-Dimensional Solution

In 1-D, and with $D_V \neq 0$, our advection-dispersion model with a point representation for trapping becomes

$$\frac{\partial c}{\partial t} - S\frac{\partial c}{\partial z} = D_V \frac{\partial^2 c}{\partial z^2} + Q\delta(z - H)\,\delta(t) - kc(Z_1, t)\,\delta(z - Z_1) \tag{4.41}$$

with initial and boundary conditions

$$c\left(z,0^{-}\right)=0,\ c\left(\infty,t\right)=0 \text{ and } \frac{\partial c}{\partial z}\left(0,t\right)=0.$$

See page 43 for a description of the conceptual situation, which is now trapping at a plane. After release the droplets disperse vertically, whilst falling towards the ground with settling speed S.

A solution to Equation (4.41) may be found by following the method presented by Lim (2005, Chap. 2), though the solution we obtain is nestled in an integral equation. The process is rather lengthy; a brief outline is given here, with a full working in Appendix A.2. We begin by writing

$$c\left(z,t\right)=U\left(z,t\right)e^{-\frac{Sz}{2D_V}-\frac{S^2t}{4D_V}} \tag{4.42}$$

in Equation (4.41), so that

$$\frac{\partial U}{\partial t}-D_V\frac{\partial^2 U}{\partial z^2}=P\left(z,t\right) \tag{4.43}$$

where

$$P\left(z,t\right)=Qe^{\frac{SH}{2D_V}}\delta\left(z-H\right)\delta\left(t\right)-kc\left(Z_1,t\right)e^{\frac{SZ_1}{2D_V}-\frac{S^2t}{4D_V}}. \tag{4.44}$$

Next, we write

$$V\left(z,t\right)=\frac{\partial U}{\partial z}-\frac{SU}{2D_V} \tag{4.45}$$

and apply the operator $\left(\frac{\partial}{\partial t}-D_V\frac{\partial^2}{\partial z^2}\right)$ to obtain a diffusion equation with homogeneous boundary conditions, that is

$$\frac{\partial V}{\partial t}-D_V\frac{\partial^2 V}{\partial z^2}=\frac{\partial P}{\partial z}-\frac{S}{2D_V}P \tag{4.46}$$

with $V\left(z,0^{-}\right)=V\left(0,t\right)=V\left(\infty,t\right)=0$. The Greens function solution for $V\left(z,t\right)$ is

$$V\left(z,t\right)=\int_0^t d\tau\int_0^\infty\left(\frac{\partial P}{\partial\xi}\left(\xi,\tau\right)-\frac{S}{2D_V}P\left(\xi,\tau\right)\right)G_{X10}\left(z,t|\xi,\tau\right)\ d\xi \tag{4.47}$$

(Beck *et al.*, 1992, p. 43) where $G_{X10}\left(z,t|\xi,\tau\right)$ is given by

$$G_{X10}\left(z,t|\xi,\tau\right)=\frac{1}{2\sqrt{\pi D_V\left(t-\tau\right)}}\left(e^{-\frac{(z-\xi)^2}{4D_V(t-\tau)}}-e^{-\frac{(z+\xi)^2}{4D_V(t-\tau)}}\right). \tag{4.48}$$

Integrating Equation (4.45) with respect to z gives $U\left(z,t\right)$ in terms of $V\left(z,t\right)$, then direct substitution back into Equation (4.42) yields the desired solution $c\left(z,t\right)$. The solution is

$$c\left(z,t\right)=Qf\left(z,t;H\right)-\int_0^t kc\left(Z_1,\tau\right)f\left(z,t-\tau;Z_1\right)\ d\tau \tag{4.49}$$

where

$$f(z,t;Z) = \frac{e^{-\frac{S^2 t}{4D_V} - \frac{S(z-Z)}{2D_V}}}{2\sqrt{\pi D_V t}} \left(e^{-\frac{(z-Z)^2}{4D_V t}} + e^{-\frac{(z+Z)^2}{4D_V t}} \right) - \frac{S e^{\frac{SZ}{D_V}}}{2D_V} \operatorname{erfc}\left(\frac{z+Z+St}{2\sqrt{D_V t}} \right) \tag{4.50}$$

and $\operatorname{erfc}(z)$ is the complementary error function. Note that the solution in Equation (4.49) contains the, as yet, unknown concentration at the trapping plane $c(Z_1,t)$ in the integrand. Setting $z = Z_1$ gives

$$c(Z_1,t) = Qf(Z_1,t;H) - \int_0^t kc(Z_1,\tau)\, f(Z_1,t-\tau;Z_1)\ d\tau \tag{4.51}$$

which is a linear Volterra equation of the second kind. Linz (1985) provides a good introduction to these kinds of equations, and details various analytical and numerical solution methods. For equations like this one where the integral is a convolution, analytic solutions can sometimes be found by taking Laplace transforms, but in most cases the inversion is tricky and it is easier to solve the equation numerically to begin with. Conveniently in our case, the quantities of particular interest are evaluated directly using Laplace transforms (see Section 4.2), so there is no need for inversion.

Total Droplet Trapping and Deposition

The total droplet trapping and deposition are found by taking Laplace transforms with respect to t and then setting the transform variable to zero, as described in Section 4.2. The total mass of droplets trapped at the plane per unit area [kg m^{-2}] is

$$\begin{aligned} M_{TT} &= k\overline{c}(Z_1,0) \\ &= \frac{kQ\overline{f}(Z_1,0;H)}{1+k\overline{f}(Z_1,0;Z_1)} \\ &= \begin{cases} \dfrac{kQ}{S+k} e^{-\frac{S(Z_1-H)}{D_V}}, & Z_1 > H, \\ \dfrac{kQ}{S+k}, & Z_1 < H, \end{cases} \end{aligned} \tag{4.52}$$

and the density of deposit on the ground (mass deposited per unit area) [kg m^{-2}] is

$$\begin{aligned} M_D &= S\overline{c}(0,0) \\ &= SQ\overline{f}(0,0;H) - Sk\overline{c}(Z_1,0)\,\overline{f}(0,0;Z_1) \\ &= \begin{cases} Q - \dfrac{kQ}{S+k} e^{-\frac{S(Z_1-H)}{D_V}}, & Z_1 > H, \\ \dfrac{QS}{S+k}, & Z_1 < H. \end{cases} \end{aligned} \tag{4.53}$$

Some points to note:

- If $Z_1 > H$, so that the trapping plane is above the release height, then the total mass trapped decreases with increasing Z_1. This is to be expected, since the droplets only move upwards via dispersion, therefore the higher the trapping plane is, the less droplets will disperse high enough to reach it.
- For $Z_1 < H$ the total mass trapped is independent of Z_1. This is because, for $Z_1 < H$, all of the droplets must eventually encounter the trapping plane and so the total mass available to be trapped over all time is the same.
- The total mass trapped increases with increasing trapping rate k. Contrary to the 1-D solution with $D_V = 0$ though, it does not continue to increase as k gets large; in fact

$$\lim_{k\to\infty} M_{TT} = \begin{cases} Qe^{-\frac{S(Z_1-H)}{D_V}}, & Z_1 > H, \\ Q, & Z_1 < H, \end{cases} \tag{4.54}$$

  so it is not possible to trap more than the original release. This, in turn, ensures that $M_D \geq 0$ (the density of deposit is non-negative).

A Numerical Solution Method

It may be of interest to evaluate the mass concentration $c(z,t)$ as given by Equation (4.49); however this equation cannot be evaluated directly because of the, as yet, unknown $c(Z_1,t)$ in the integrand. In this section we present a simple numerical method to determine the concentration $c(z,t)$ at a number of discrete time steps.

Given discrete time steps

$$t_1 = 0,\ t_2 = \Delta t,\ t_3 = 2\Delta t,\ \ldots\ t_i = (i-1)\,\Delta t,$$

the first step is to solve for the unknown at each time step, that is $c(Z_1,t_i)$, using Equation (4.51). The integrand in this equation is singular at the upper end-point $\tau = t_i$. Applying the technique of product integration as in Linz (1985, Chap. 8), the integrand is split into two parts: a non-singular part and a singular part. We write

$$c(Z_1,t_i) = Qf(Z_1,t_i;H) - \int_0^{t_i} kc(Z_1,\tau)\,K(t_i,\tau)\,P(t_i,\tau)\ d\tau. \tag{4.55}$$

The non-singular part is $kc(Z_1,\tau)\,K(t_i,\tau)$ and the singular part is $P(t_i,\tau)$, where

$$K(t_i,\tau)=\frac{e^{-\frac{S^2(t_i-\tau)}{4D_V}}}{2\sqrt{\pi D_V}}\left(1-e^{-\frac{Z_1^2}{D_V(t_i-\tau)}}\right)-\frac{S\sqrt{t_i-\tau}e^{\frac{SZ_1}{D_V}}}{2D_V}\operatorname{erfc}\left(\frac{2Z_1+S(t_i-\tau)}{2\sqrt{D_V(t_i-\tau)}}\right) \tag{4.56}$$

and

$$P(t_i,\tau)=\frac{1}{\sqrt{t_i-\tau}}. \tag{4.57}$$

The well-behaved part $kc(Z_1,\tau)K(t_i,\tau)$ is approximated by its value at the beginning of each time step. Thus, for the integral in Equation (4.55),

$$\int_0^{t_i} kc(Z_1,\tau)K(t_i,\tau)P(t_i,\tau)\ d\tau \simeq \sum_{j=1}^{i-1} kc(Z_1,t_j)K(t_i,t_j)\int_{t_j}^{t_{j+1}} P(t_i,\tau)\ d\tau. \tag{4.58}$$

As there is no contribution to the summation from the first time step ($c(Z_1,t_1)=c(Z_1,0)=0$ from the initial condition), $c(Z_1,t_i)$ is approximated by

$$\begin{aligned} c(Z_1,t_i) &\simeq Qf(Z_1,t_i;H)-\sum_{j=2}^{i-1} kc(Z_1,t_j)K(t_i,t_j)\int_{t_j}^{t_{j+1}} P(t_i,\tau)\ d\tau \\ &\simeq Qf(Z_1,t_i;H)-\sum_{j=2}^{i-1} 2kc(Z_1,t_j)K(t_i,t_j)\left[\sqrt{t_i-t_j}-\sqrt{t_i-t_{j+1}}\ \right]. \end{aligned} \tag{4.59}$$

Thus, successive values for the concentration at the trapping plane are determined using values from previous time steps. According to Linz this method (usually called Euler's method) can be expected to be of order $O(\Delta t)$. Other higher-order methods could also be used, such as product integration based on the trapezium rule, but the advantage of this one is its simplicity.

The next step is to numerically evaluate Equation (4.49) for the concentration $c(z,t_i)$, using the approximated values for $c(Z_1,t_i)$. According to that equation

$$c(z,t_i)=Qf(z,t_i;H)-\int_0^{t_i} kc(Z_1,\tau)f(z,t_i-\tau;Z_1)\ d\tau \tag{4.60}$$

where $f(z,t;Z)$ is given by Equation (4.50). For $z\neq Z_1$ the integrand is zero at each of the end-points $\tau=0$ (because of the initial condition) and $\tau=t_i$. We apply a method based on the trapezium integration rule, as in Linz (1985, Chap. 7), so that $c(z,t_i)$ is approximated by

$$c(z,t_i)\simeq Qf(z,t_i;H)-\Delta t\sum_{j=2}^{i-1} kc(Z_1,t_j)f(z,t_i-t_j;Z_1). \tag{4.61}$$

Thus, successive values for the concentration are determined using values at the trapping plane from previous time steps. According to Linz, this method can be expected to be of order $O(\Delta t)^2$, but in this case the accuracy is probably reduced because the approximated values for $c(Z_1,t_i)$ already contain some error.

Two-Dimensional Solution

In 2-D, and with $D_V \neq 0$, our advection-dispersion model with a point representation for trapping becomes

$$\begin{aligned}\frac{\partial c}{\partial t} + u\frac{\partial c}{\partial x} - S\frac{\partial c}{\partial z} &= D_L\frac{\partial^2 c}{\partial x^2} + D_V\frac{\partial^2 c}{\partial z^2} + Q\delta(x - X_0)\,\delta(z - H)\,\delta(t) \\ &\quad -kc(X_1, Z_1, t)\,\delta(x - X_1)\,\delta(z - Z_1) \end{aligned} \tag{4.62}$$

with initial and boundary conditions

$$\begin{gathered} c\left(x, z, 0^-\right) = 0, \\ c(x, z, t) \to 0 \text{ as } x \to \pm\infty, \text{ and } z \to +\infty, \text{ and} \\ \frac{\partial c}{\partial z}(x, 0, t) = 0. \end{gathered}$$

Conceptually this is now trapping at a line of infinite crosswind length, as described on page 46. After release the droplets disperse alongwind and vertically, whilst travelling with the mean windspeed u and falling at settling speed S.

An analytic solution to Equation (4.62) may be found by taking Fourier transforms with respect to x and then following the method used to obtain the 1-D solution. The transformed equation is

$$\begin{aligned}\frac{\partial \widehat{c}}{\partial t} - S\frac{\partial \widehat{c}}{\partial z} + \left(\omega^2 D_L + i\omega u\right)\widehat{c} &= D_V\frac{\partial^2 \widehat{c}}{\partial z^2} + Qe^{-i\omega X_0}\delta(z - H)\,\delta(t) \\ &\quad -kc(X_1, Z_1, t)\,e^{-i\omega X_1}\delta(z - Z_1). \end{aligned} \tag{4.63}$$

We then write

$$\widehat{c}(\omega, z, t) = \widehat{U}(\omega, z, t)\,e^{-\frac{Sz}{2D_V} - \frac{S^2 t}{4D_v} - \left(\omega^2 D_L + i\omega u\right)t} \tag{4.64}$$

so that the transformed equation becomes

$$\frac{\partial \widehat{U}}{\partial t} - D_V\frac{\partial^2 \widehat{U}}{\partial z^2} = \widehat{P}(\omega, z, t) \tag{4.65}$$

where

$$\begin{aligned}\widehat{P}(\omega, z, t) &= Qe^{\frac{SH}{2D_V} - i\omega X_0}\delta(z - H)\,\delta(t) \\ &\quad -kc(X_1, Z_1, t)\,e^{\frac{SZ_1}{2D_V} + \frac{S^2 t}{4D_V} + \omega^2 D_L t - i\omega(X_1 - ut)}\delta(z - Z_1). \end{aligned} \tag{4.66}$$

Equation (4.65) is now in the same form as Equation (4.43) in the 1-D solution, thus to find an expression for $\widehat{U}(\omega, z, t)$, and subsequently $\widehat{c}(\omega, z, t)$, we follow the steps outlined in the 1-D solution. The result is

$$\widehat{c}(\omega, z, t) = Q\widehat{f}(\omega, z, t; X_0, H) - \int_0^t kc(X_1, Z_1, \tau)\,\widehat{f}(\omega, z, t - \tau; X_1, Z_1)\;d\tau \tag{4.67}$$

where

$$\widehat{f}\left(\omega,z,t;X,Z\right) = e^{-i\omega(X+ut)-\omega^2 D_L t}\left[\frac{e^{-\frac{S^2 t}{4D_V}-\frac{S(z-Z)}{2D_V}}}{2\sqrt{\pi D_V t}}\left(e^{-\frac{(z-Z)^2}{4D_V t}}+e^{-\frac{(z+Z)^2}{4D_V t}}\right)\right.$$
$$\left.-\frac{Se^{-\frac{SZ}{D_V}}}{2D_V}\operatorname{erfc}\left(\frac{z+Z+St}{2\sqrt{D_V t}}\right)\right]. \tag{4.68}$$

At this point we would like to invert the Fourier transforms, but a difficulty arises at $z = Z_1$ where the integrand in Equation (4.67) has a singularity of the form $(t-\tau)^{-1/2}$ at the upper endpoint. Ignoring this for now and simply inverting under the integral:

$$c\left(x,z,t\right) = Qf\left(x,z,t;X_0,H\right) - \int_0^t kc\left(X_1,Z_1,\tau\right) f\left(x,z,t-\tau;X_1,Z_1\right)\ d\tau \tag{4.69}$$

where

$$f\left(x,z,t;X,Z\right) = \frac{e^{-\frac{(x-X-ut)^2}{4D_L t}}}{2\sqrt{\pi D_L t}}\left[\frac{e^{-\frac{S^2 t}{4D_V}-\frac{S(z-Z)}{2D_V}}}{2\sqrt{\pi D_V t}}\left(e^{-\frac{(z-Z)^2}{4D_V t}}+e^{-\frac{(z+Z)^2}{4D_V t}}\right)\right.$$
$$\left.-\frac{Se^{\frac{SZ}{D_V}}}{2D_V}\operatorname{erfc}\left(\frac{z+Z+St}{2\sqrt{D_V t}}\right)\right]. \tag{4.70}$$

Once again we observe that the concentration becomes negative as an artefact of using Dirac delta functions to focus all of the trapping to an infinitely thin line. In this case the concentration is negative in a localised area around the trapping line (both above and below), whereas for $D_V = 0$ it was only negative below. Similar to the explanation on page 48, the trapping here is essentially a continuous negative release of strength $kc\left(X_1,Z_1,t\right)$ from the line $(x,z) = (X_1,Z_1)$, and the concentration as given by Equation (4.69) is a superposition of the original release and the summed effect (up to the present time) of this negative release. Near the trapping line the negative release overpowers the original release for a short time; the size of the area over which this occurs depends on the size of k.

The solution in Equation (4.69) contains the, as yet, unknown $c\left(X_1,Z_1,t\right)$ in the integrand. Setting $(x,z) = (X_1,Z_1)$ gives

$$c\left(X_1,Z_1,t\right) = Qf\left(X_1,Z_1,t;X_0,H\right) - \int_0^t kc\left(X_1,Z_1,\tau\right) f\left(X_1,Z_1,t-\tau;X_1,Z_1\right)\ d\tau, \tag{4.71}$$

and now the difficulty mentioned in regard to inverting the Fourier transform becomes apparent: $f\left(X_1,Z_1,t-\tau;X_1,Z_1\right)$ has a singularity of the form $(t-\tau)^{-1}$ at the upper endpoint, thus the integral is divergent, and the Laplace transform $\overline{f}\left(X_1,Z_1,p;X_1,Z_1\right)$ is not defined classically. However, an expression may be found for the transform via distribution theory as covered by Zemanian (1987, Chap. 8).

Total Droplet Trapping and Deposition

Following Section 4.2, the total mass of droplets trapped at the line per unit crosswind length [kg m^{-1}] is

$$\begin{aligned} M_{TT} &= k\overline{c}\left(X_1, Z_1, 0\right) \\ &= \frac{kQ\overline{f}\left(X_1, Z_1, 0; X_0, H\right)}{1 + k\overline{f}\left(X_1, Z_1, 0; X_1, Z_1\right)}, \end{aligned} \tag{4.72}$$

which leaves a total mass deposit per unit crosswind length of $M_{DT} = Q - M_{TT}$ [kg m^{-1}], and the density of deposit on the ground (mass of droplets deposited per unit area) [kg m^{-2}] is

$$\begin{aligned} M_D\left(x\right) &= S\overline{c}\left(x, 0, 0\right) \\ &= SQ\overline{f}\left(x, 0, 0; X_0, H\right) - Sk\overline{c}\left(X_1, Z_1, 0\right)\overline{f}\left(x, 0, 0; X_1, Z_1\right) \\ &= SQ\overline{f}\left(x, 0, 0; X_0, H\right) - \frac{SkQ\overline{f}\left(X_1, Z_1, 0; X_0, H\right)\overline{f}\left(x, 0, 0; X_1, Z_1\right)}{1 + k\overline{f}\left(X_1, Z_1, 0; X_1, Z_1\right)}. \end{aligned} \tag{4.73}$$

Provided $(x, z) \neq (X, Z)$, the required transform is

$$\begin{aligned} \overline{f}\left(x, z, 0; X, Z\right) &= \frac{e^{\frac{u(x-X)}{2D_L}}}{2\pi\sqrt{D_L D_V}}\left(e^{-\frac{S(z-Z)}{2D_V}}\left[K_0\left(\frac{\alpha\beta_1\left(x, z\right)}{2}\right) + K_0\left(\frac{\alpha\beta_2\left(x, z\right)}{2}\right)\right]\right. \\ &\quad \left. - \frac{S}{D_V}\int_z^\infty e^{-\frac{S(\xi-Z)}{2D_V}} K_0\left(\frac{\alpha\beta_2\left(x, \xi\right)}{2}\right)\, d\xi\right) \end{aligned} \tag{4.74}$$

where

$$\alpha = \sqrt{\frac{u^2}{D_L} + \frac{S^2}{D_V}},\ \beta_1\left(x, z\right) = \sqrt{\frac{\left(x - X\right)^2}{D_L} + \frac{\left(z - Z\right)^2}{D_V}},\ \beta_2\left(x, z\right) = \sqrt{\frac{\left(x - X\right)^2}{D_L} + \frac{\left(z + Z\right)^2}{D_V}},$$

and K_0 is a modified Bessel function of the second kind of order zero (Weisstein, 2002). The transform $\overline{f}\left(X_1, Z_1, 0; X_1, Z_1\right)$ is not defined classically because it requires the Laplace transform of t^{-1}. Using the formula for the Laplace transform of t^{-1} given by Zemanian (1987, p. 348 No. 4) we obtain

$$\begin{aligned} \overline{f}\left(X_1, Z_1, 0; X_1, Z_1\right) &= \frac{1}{2\pi\sqrt{D_L D_V}}\left[-\frac{1}{2}\left(\ln\left(\frac{\alpha^2}{4}\right) + \gamma\right) + K_0\left(\frac{\alpha Z_1}{\sqrt{D_V}}\right)\right. \\ &\quad \left. - \frac{S}{D_V}\int_{Z_1}^\infty e^{-\frac{S(\xi-Z_1)}{2D_V}} K_0\left(\frac{\alpha\left(\xi + Z_1\right)}{2\sqrt{D_V}}\right)\, d\xi\right] \end{aligned} \tag{4.75}$$

where γ = Euler's constant = 0.57722… (Zemanian, 1987, p. 346). It is not so easy to analyse the total trapping directly from Equation (4.72) because of the more complicated transforms.

However, looking at various calculated examples we observe the expected behaviour; that is, the total trapping increases with increasing trapping rate k, and decreases if the trapping line is moved further from the release.

An Illustrative Example for the Two-Dimensional Solution

The following example illustrates the 2-D solution with $D_V \neq 0$ described above. The parameter set used here is given in Table 4.2; these are the same values as used previously for the 2-D solution with $D_V = 0$. A settling speed of 0.2 m s^{-1} corresponds to droplets of approximate diameter $d = 44$ μm, and dominant turbulence length scales of $(L_L, L_V) = (2, 1)$ m give dispersion coefficients $(D_L, D_V) = u\,(L_L, L_V) = (2, 1)$ m^2 s^{-1}. The effective trapping rate for the line is $k = k_b \Delta x \Delta z = 1$ m^2 s^{-1}; note that the value used for k_b is unrealistically high, and is used only for demonstration purposes.

Table 4.2: Parameter set used to generate Figures 4.6 and 4.7

u	S	(L_L, L_V)	Q	(X_0, H)	k_b	$\Delta x \Delta z$	(X_1, Z_1)
1 m s^{-1}	0.2 m s^{-1}	$(2, 1)$ m	1 kg m^{-1}	$(0, 3)$ m	25 s^{-1}	0.04 m^2	$(4, 2)$ m

Figure 4.6 shows cross-sections of the density of deposit [kg m^{-2}], as calculated from Equation (4.73); the density of deposit with trapping is denoted M_D, and the value without trapping is denoted M_D^* (found by setting $k = 0$). One notable feature is the "elongated tail", that is, the deposition profile is not symmetric. This is because of the vertical dispersion: droplets which are dispersed upwards spend longer in the air, and therefore travel further with the wind before depositing.

The corresponding percentage reduction in density of deposit as a result of the trapping is shown in Figure 4.7. In the previous example for $D_V = 0$ there was significant reduction just downwind of the trapping line; but then strength of reduction decreased quite rapidly with increasing downwind distance. Here, though the deposit is not reduced by as great a percentage, the effect persists much further downwind. According to Equation (4.72), the total trapping in this case is $M_{TT} = 0.13$ kg m^{-1}; this is considerably less than the previous example for $D_V = 0$ where it was 0.44 kg m^{-1}.

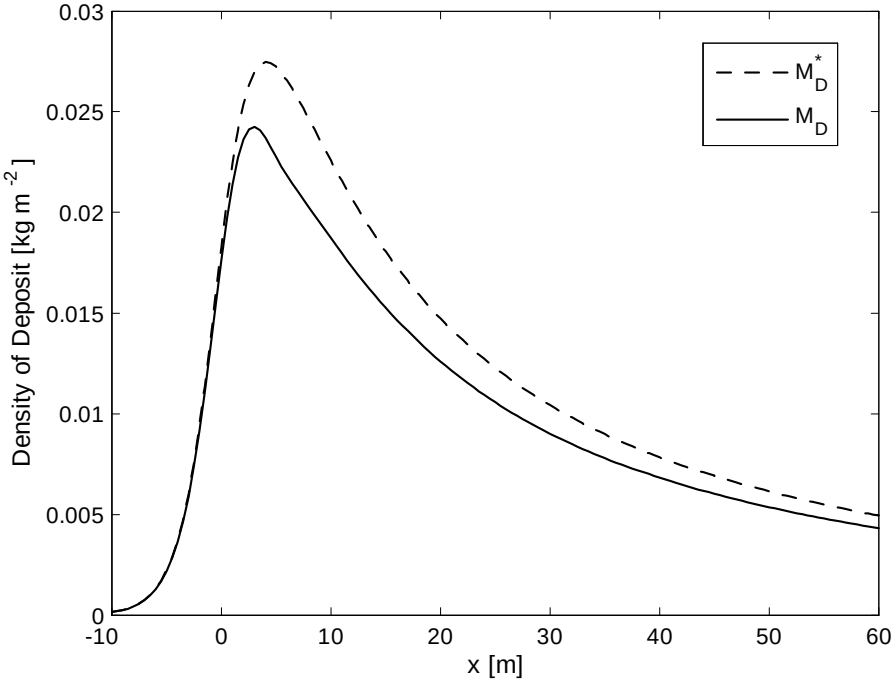

Figure 4.6: Cross-section of the density of deposit [kg m^{-2}], resulting from a line release with non-zero vertical dispersion and a line of trapping. M_D denotes the density of deposit with trapping, and M_D^* denotes the corresponding value without trapping. Parameter values are given in Table 4.2.

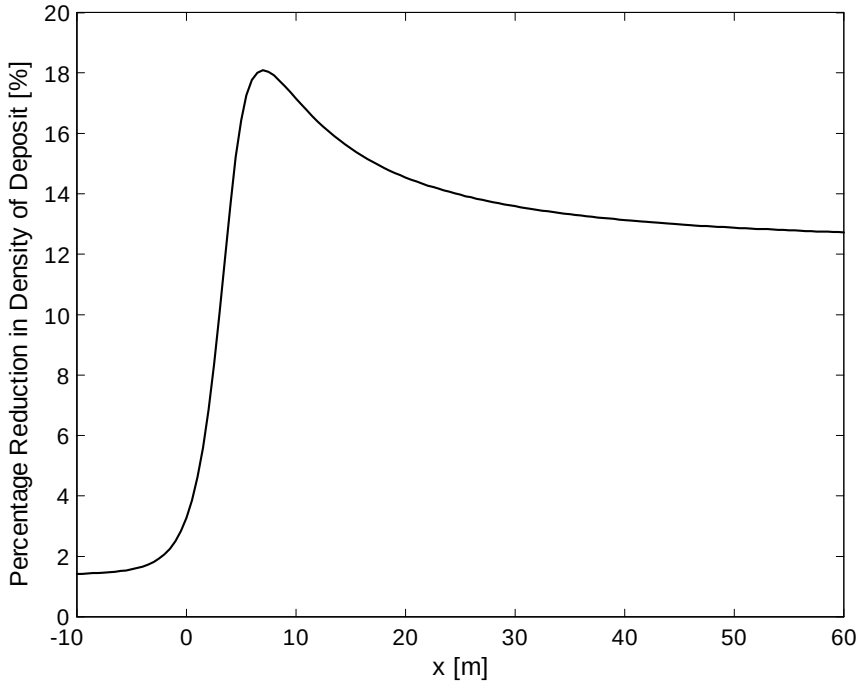

Figure 4.7: Cross-section of the percentage reduction in density of deposit as a result of the trapping in Figure 4.6. Parameter values are the same as for Figure 4.6.

Three-Dimensional Solution

In all three spatial dimensions, our advection-dispersion model with a point representation for trapping is as given by Equation (4.3); that is

$$\begin{aligned}\frac{\partial c}{\partial t}+u\frac{\partial c}{\partial x}-S\frac{\partial c}{\partial z} &= D_L\frac{\partial^2 c}{\partial x^2}+D_T\frac{\partial^2 c}{\partial y^2}+D_V\frac{\partial^2 c}{\partial z^2}+Q\delta\left(x-X_0\right)\delta\left(y-Y_0\right)\delta\left(z-H\right)\delta\left(t\right)\\ &\quad -kc\left(X_1,Y_1,Z_1,t\right)\delta\left(x-X_1\right)\delta\left(y-Y_1\right)\delta\left(z-Z_1\right)\end{aligned} \tag{4.76}$$

with initial and boundary conditions

$$\begin{gathered}c\left(x,y,z,0^-\right)=0\\ c\left(x,y,z,t\right)\to 0 \text{ as } x,y\to\pm\infty \text{ and } z\to+\infty, \text{ and}\\ \frac{\partial c}{\partial z}\left(x,y,0,t\right)=0.\end{gathered}$$

The conceptual scenario is recapped on page 54. After release the droplets disperse horizontally (both alongwind and crosswind) and vertically, whilst travelling with the mean windspeed u and falling at settling speed S.

An implicit analytic solution to Equation (4.76) may be found by taking Fourier transforms with respect to x and y then following the method used to obtain the 1-D solution; this procedure is really just an extension from that used in 2-D. The transformed equation is

$$\begin{aligned}\frac{\partial\widetilde{\widehat{c}}}{\partial t}-S\frac{\partial\widetilde{\widehat{c}}}{\partial z}+\left(\omega^2D_L+i\omega u+\psi^2D_T\right)\widetilde{\widehat{c}} &= D_V\frac{\partial^2\widetilde{\widehat{c}}}{\partial z^2}+Qe^{-i\omega X_0-i\psi Y_0}\delta\left(z-H\right)\delta\left(t\right)\\ &\quad -kc\left(X_1,Y_1,Z_1,t\right)e^{-i\omega X_1-i\psi Y_1}\delta\left(z-Z_1\right).\end{aligned} \tag{4.77}$$

We then write

$$\widetilde{\widehat{c}}(\omega,\psi,z,t)=\widetilde{\widehat{U}}\left(\omega,\psi,z,t\right)e^{-\frac{Sz}{2D_V}-\frac{S^2t}{4D_V}-\left(\omega^2D_L+i\omega u+\psi^2D_T\right)t} \tag{4.78}$$

so that the transformed equation becomes

$$\frac{\partial\widetilde{\widehat{U}}}{\partial t}-D_V\frac{\partial^2\widetilde{\widehat{U}}}{\partial z^2}=\widetilde{\widehat{P}}\left(\omega,\psi,z,t\right) \tag{4.79}$$

where

$$\begin{aligned}\widetilde{\widehat{P}}\left(\omega,\psi,z,t\right) &= Qe^{\frac{SH}{2D_V}-i\omega X_0-i\psi Y_0}\delta\left(z-H\right)\delta\left(t\right)\\ &\quad -kc\left(X_1,Y_1,Z_1,t\right)e^{\frac{SZ_1}{2D_V}+\frac{S^2t}{4D_V}+\omega^2D_Lt-i\omega(X_1-ut)+v^2D_Tt-i\psi Y_1}\delta\left(z-Z_1\right).\end{aligned} \tag{4.80}$$

Equation (4.79) is now in the same form as Equation (4.43) in the 1-D solution; thus to find an expression for $\widetilde{\widehat{U}}\left(\omega,\psi,z,t\right)$, and subsequently $\widetilde{\widehat{c}}(\omega,\psi,z,t)$, we once again follow the steps outlined in the 1-D solution. The result is

$$\widetilde{\widehat{c}}(\omega,\psi,z,t) = Q\widetilde{\widehat{f}}(\omega,\psi,z,t;X_0,Y_0,H) - \int_0^t kc\,(X_1,Y_1,Z_1,\tau)\,\widetilde{\widehat{f}}(\omega,\psi,z,t-\tau;X_1,Y_1,Z_1)\;d\tau \tag{4.81}$$

where

$$\begin{aligned}\widetilde{\widehat{f}}\,(\omega,\psi,z,t;X,Y,Z) &= e^{-i\omega(X+ut)-\omega^2 D_L t - i\psi Y - \psi^2 D_T t}\left[\frac{e^{-\frac{S^2 t}{4D_V}-\frac{S(z-Z)}{2D_V}}}{2\sqrt{\pi D_V t}}\left(e^{-\frac{(z-Z)^2}{4D_V t}}\right.\right.\\ &\qquad \left.\left. + e^{-\frac{(z+Z)^2}{4D_V t}}\right) - \frac{Se^{\frac{SZ}{D_V}}}{2D_V}\,\mathrm{erfc}\left(\frac{z+Z+St}{2\sqrt{D_V t}}\right)\right].\end{aligned} \tag{4.82}$$

As in the 2-D solution, at this point we would like to invert the Fourier transforms, but a difficulty arises at $z = Z_1$ where the integrand in Equation (4.81) has a singularity of the form $(t-\tau)^{-1/2}$ at the upper endpoint. Ignoring the singularity and inverting the transforms:

$$c\,(x,y,z,t) = Qf\,(x,y,z,t;X_0,Y_0,H) - \int_0^t kc\,(X_1,Y_1,Z_1,\tau)\,f\,(x,y,z,t-\tau;X_1,Y_1,Z_1)\;d\tau \tag{4.83}$$

where

$$\begin{aligned}f\,(x,y,z,t;X,Y,Z) &= \frac{e^{-\frac{(x-X-ut)^2}{4D_L t}-\frac{(y-Y)^2}{4D_T t}}}{4\pi t\sqrt{D_L D_T}}\left[\frac{e^{-\frac{S^2 t}{4D_V}-\frac{S(z-Z)}{2D_V}}}{2\sqrt{\pi D_V t}}\left(e^{-\frac{(z-Z)^2}{4D_V t}} + e^{-\frac{(z+Z)^2}{4D_V t}}\right)\right.\\ &\qquad \left. - \frac{Se^{-\frac{SZ}{D_V}}}{2D_V}\,\mathrm{erfc}\left(\frac{z+Z+St}{2\sqrt{D_V t}}\right)\right].\end{aligned} \tag{4.84}$$

Being an extension from 2-D, this solution also exhibits a negative concentration for a short time in the vicinity of the trapping point (refer to page 63).

Setting $(x,y,z) = (X_1,Y_1,Z_1)$ to determine the, as yet, unknown $c\,(X_1,Y_1,Z_1,t)$ which appears in the integrand of Equation (4.83) gives

$$\begin{aligned}c\,(X_1,Y_1,Z_1,t) &= Qf\,(X_1,Y_1,Z_1,t;X_0,Y_0,H)\\ &\qquad - \int_0^t kc\,(X_1,Y_1,Z_1,\tau)\,f\,(X_1,Y_1,Z_1,t-\tau;X_1,Y_1,Z_1)\;d\tau.\end{aligned} \tag{4.85}$$

In Equation (4.85), $f\,(X_1,Y_1,Z_1,t-\tau;X_1,Y_1,Z_1)$ has a singularity of the form $(t-\tau)^{-3/2}$ at the upper endpoint, thus the integral is divergent, and the Laplace transform $\overline{f}\,(X_1,Y_1,Z_1,p;X_1,Y_1,Z_1)$ does not exist classically. As in the 2-D solution an expression may be found for the transform by using distribution theory, and in this way we are still able to directly evaluate the total trapping and deposition.

Total Droplet Trapping and Deposition

Following Section 4.2, the total mass of droplets trapped at the point [kg] is

$$\begin{aligned} M_{TT} &= k\overline{c}\left(X_1, Y_1, Z_1, 0\right) \\ &= \frac{kQ\overline{f}\left(X_1, Y_1, Z_1, 0; X_0, Y_0, H\right)}{1 + k\overline{f}\left(X_1, Y_1, Z_1, 0; X_1, Y_1, Z_1\right)}, \end{aligned} \tag{4.86}$$

leaving a total mass deposit on the ground of $M_{DT} = Q - M_{TT}$ [kg]. The density of deposit on the ground [kg m^{-2}] is

$$\begin{aligned} M_D\left(x, y\right) &= S\overline{c}\left(x, y, 0, 0\right) \\ &= SQ\overline{f}\left(x, y, 0, 0; X_0, Y_0, H\right) - Sk\overline{c}\left(X_1, Y_1, Z_1, 0\right)\overline{f}\left(x, y, 0, 0; X_1, Z_1\right) \\ &= SQ\overline{f}\left(x, y, 0, 0; X_0, Y_0, H\right) - \frac{SkQ\overline{f}\left(X_1, Y_1, Z_1, 0; X_0, Y_0, H\right)\overline{f}\left(x, y, 0, 0; X_1, Y_1, Z_1\right)}{1 + k\overline{f}\left(X_1, Y_1, Z_1, 0; X_1, Y_1, Z_1\right)}. \end{aligned} \tag{4.87}$$

Provided $(x, y, z) \neq (X, Y, Z)$, the required transform is

$$\begin{aligned} \overline{f}\left(x, y, z, 0; X, Y, Z\right) &= \frac{e^{\frac{u(x-X)}{2D_L}}}{4\pi\sqrt{D_L D_T D_V}}\left[e^{-\frac{S(z-Z)}{2D_V}}\left(\frac{e^{-\frac{1}{2}\alpha\beta_1(x,y,z)}}{\beta_1\left(x, y, z\right)} + \frac{e^{-\frac{1}{2}\beta_2(x,y,z)}}{\beta_2\left(x, y, z\right)}\right)\right. \\ &\quad \left. - \frac{S}{D_V}\int_z^\infty e^{-\frac{S(\xi-Z)}{2D_V}}\frac{e^{-\frac{1}{2}\alpha\beta_2(x,y,\xi)}}{\beta_2\left(x, y, \xi\right)}\, d\xi\right] \end{aligned} \tag{4.88}$$

where

$$\alpha = \sqrt{\frac{u^2}{D_L} + \frac{S^2}{D_V}}, \quad \beta_1\left(x, y, z\right) = \sqrt{\frac{\left(x-X\right)^2}{D_L} + \frac{\left(y-Y\right)^2}{D_T} + \frac{\left(z-Z\right)^2}{D_V}}, \text{ and}$$

$$\beta_2\left(x, y, z\right) = \sqrt{\frac{\left(x-X\right)^2}{D_L} + \frac{\left(y-Y\right)^2}{D_T} + \frac{\left(z+Z\right)^2}{D_V}}.$$

The transform $\overline{f}\left(X_1, Y_1, Z_1, p; X_1, Y_1, Z_1\right)$ is not defined classically because it requires the Laplace transform of $t^{-3/2}$; using the expression obtained via distribution theory in Zemanian (1987, p. 348 No. 2) gives

$$\begin{aligned} \overline{f}\left(X_1, Y_1, Z_1, 0; X_1, Y_1, Z_1\right) &= \frac{1}{4\pi\sqrt{D_L D_T D_V}}\left[-\frac{\alpha}{2} + \frac{\sqrt{D_V}}{2Z_1}e^{-\frac{\alpha Z_1}{\sqrt{D_V}}}\right. \\ &\quad \left. - \frac{S}{\sqrt{D_V}}\int_{Z_1}^\infty \frac{1}{\left(\xi + Z_1\right)}e^{-\frac{S(\xi-Z_1)}{2D_V} - \frac{\alpha(\xi+Z_1)}{2\sqrt{D_V}}}\, d\xi\right]. \end{aligned} \tag{4.89}$$

Again, it is not so easy to analyse the total trapping directly from Equation (4.86) because of the more complicated transforms, but looking at various calculated examples the total trapping increases with increasing trapping rate, and decreases if the trapping point is moved further from the release as expected.

An Illustrative Example for the Three-Dimensional Solution

The following example illustrates the 3-D solution with $D_V \neq 0$ described above. The parameter set used here is given in Table 4.3. A settling speed of 0.2 m s^{-1} corresponds to droplets of approximate diameter $d = 44$ μm, and dominant turbulence length scales of $(L_L, L_T, L_V) = (2, 2, 1)$ m give dispersion coefficients $(D_L.D_T, D_V) = u\,(L_L, L_T, L_V) = (2, 2, 1)$ m^2 s^{-1}. The effective trapping rate for the point is $k = k_b \Delta x \Delta y \Delta z = 10$ m^3 s^{-1}; this comes from an unrealistically high background trapping rate k_b, which we use only to make the effect of trapping more easily observed.

Table 4.3: Parameter set used to generate Figures 4.8, 4.9 and 4.10

u	S	(L_L, L_T, L_V)	Q	(X_0, Y_0, H)	k_b	$\Delta x \Delta y \Delta z$	(X_1, Y_1, Z_1)
1 m s^{-1}	0.2 m s^{-1}	$(2, 2, 1)$ m	1 kg	$(0, 0, 3)$ m	1250 s^{-1}	0.008 m^3	$(4, 2, 2)$ m

Figure 4.8 shows contours of the density of deposit [kg m^{-2}] without trapping, calculated by setting $k = 0$ in Equation (4.87). The corresponding contours with trapping are shown in Figure 4.9; there is not much visible effect on the contour lines, but they are bent slightly near the trapping point. Note the oval shape of the contours in both figures; they are elongated in the downwind direction as a result of the vertical dispersion - droplets which are dispersed upwards spend longer in the air, and are blown further by the wind before depositing. Figure 4.10 shows the percentage reduction in density of deposit as a result of the trapping. The maximum reduction in density of deposit is around 31 %, which occurs in the clearly evident shadow area behind the trapping point. According to Equation (4.86), the total mass trapped is $M_{TT} = 0.14$ kg.

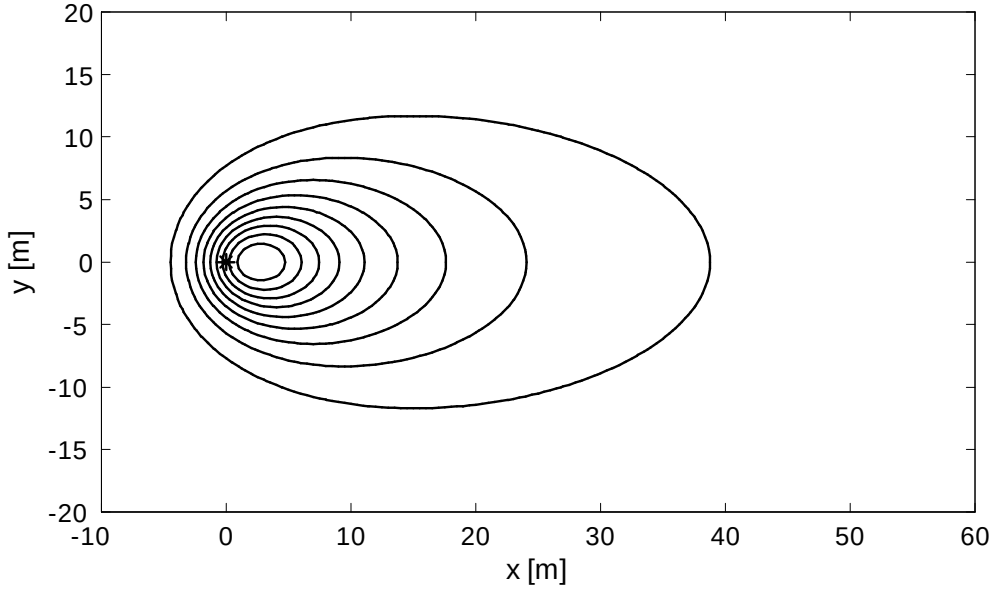

Figure 4.8: Contours of the density of deposit [kg m^{-2}], resulting from a point release (marked with a $*$) with non-zero vertical dispersion and no trapping. The spacing between contours is 0.00027 kg m^{-2}, with the outer contour at 0.00027 kg m^{-2} and the inner contour at 0.00243 kg m^{-2}. Parameter values are given in Table 4.3.

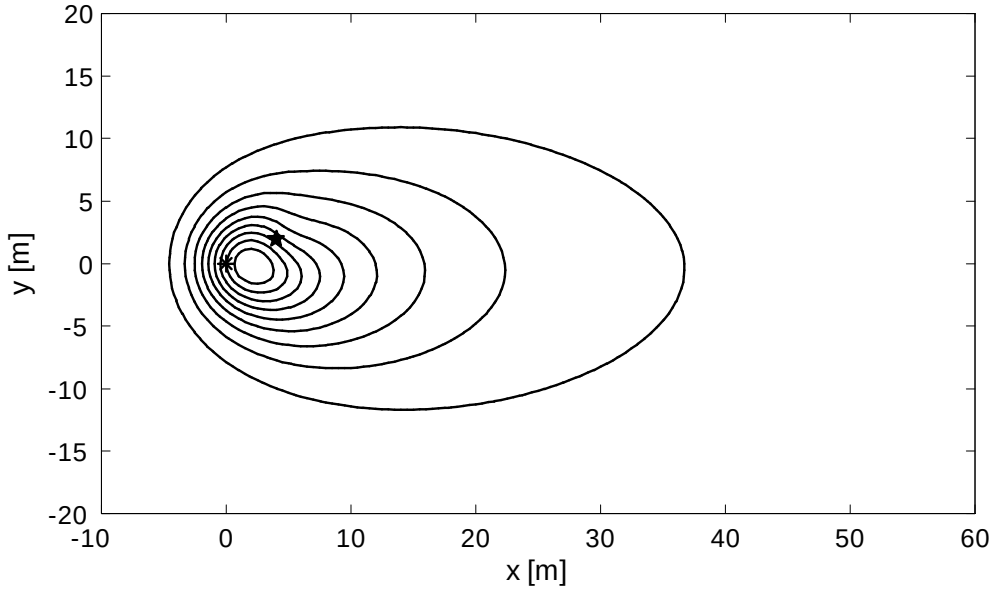

Figure 4.9: Contours of the density of deposit [kg m^{-2}], resulting from a point release (marked with a $*$), with non-zero vertical dispersion and trapping at a point (marked with a $\star$). The spacing between contours is 0.00025 kg m^{-2}, with the outer contour at 0.00025 kg m^{-2} and the inner contour at 0.00225 kg m^{-2}. Parameter values are given in Table 4.3.

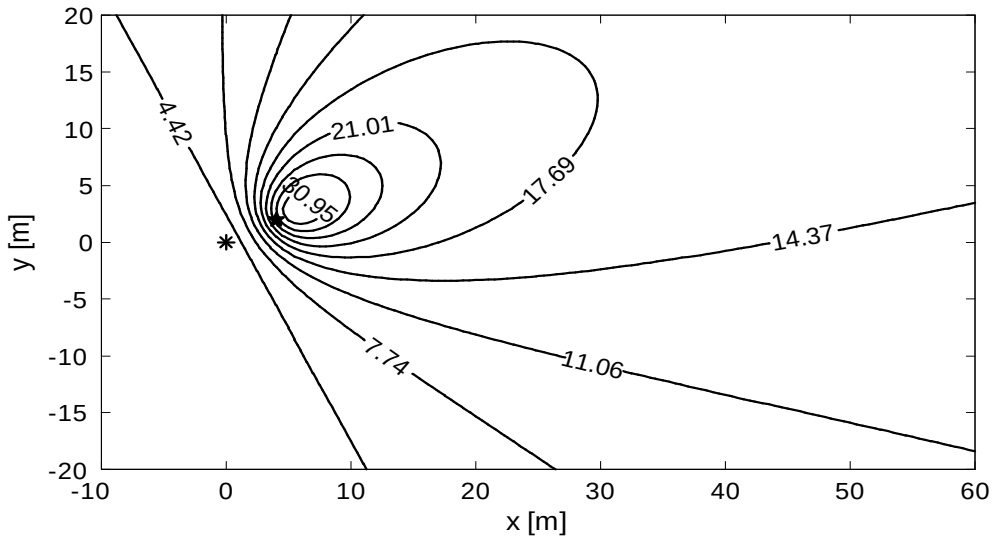

Figure 4.10: Contours of the reduction in density of deposit between Figures 4.8 and 4.9 as a result of the trapping. The maximum reduction is 30.95 % (the inner contour). The release point is marked with a $*$, and the trapping point is marked with a $\star$. Parameter values are the same as for Figures 4.8 and 4.9.

4.5 Chapter Summary

In this chapter we simplified our advection-dispersion model, which was derived in Chapter 3, so that the effect of trapping is concentrated at a single point. The benefit of this point representation for trapping is that it allowed us to solve the model analytically, and find explicit expressions for the total trapping and the resulting deposit downwind. The material presented in subsequent chapters is built upon this point representation.

We analysed the model in two cases: first the simple case of negligible vertical dispersion, and second the more realistic case of significant vertical dispersion. In each case we found solutions to the model in one- and two-dimensions, building up to a full three-dimensional solution. For the case of zero vertical dispersion, the solutions were readily obtained following standard Laplace and Fourier transform methods; but for non-zero vertical dispersion the process was more complicated and involved the use of Green functions. Although the solutions obtained for the model with non-zero vertical dispersion turned out to be nestled in integral equations, we were still able to find explicit expressions for the total trapping and deposition.

It was found that an artefact of the point representation for trapping is that it causes the droplet mass concentration to become negative in the vicinity of the trapping. We recognise that in this vicinity the model does not accurately represent the conceptual situation, however the unrealistically high trapping rates in this chapter exaggerate the issue. In the next chapter we will use the point representation to construct a discretised shelterbelt, and it becomes clear that the issue of a negative concentration has negligible effect with realistic trapping rates.

Chapter 5

Trapping in a Discretised Shelterbelt

Here we use the results obtained in the previous chapter to construct an analytic solution to our advection-dispersion model with trapping in a discretised shelterbelt (in the absence of evaporation). Recall that the shelterbelt in our model as it was originally derived in Chapter 3 is represented by a block of continuous trapping, but since it is difficult to solve the model analytically with this approach we discretise the shelterbelt as a way in which to advance.

In this chapter we analyse our advection-dispersion model with trapping in a discretised shelterbelt. We consider the same two cases as for the single trapping point in the previous chapter: first, a special case where the droplets can disperse only horizontally, and second, the more realistic case where the droplets also disperse vertically. Once again, the ultimate objective in each case is a full three-dimensional (3-D) solution, which we work towards by first determining solutions in one and two dimensions (1-D and 2-D).

The solutions in this chapter inherit the issue identified in the previous chapter (refer to pages 48 – 49), whereby the concentration becomes negative as an artefact of using Dirac delta functions to focus the effect of trapping in each block to an infinitely small point. We show how this issue may be avoided by making the trapping continuous horizontally within the shelterbelt (that is, only discretising it vertically), however it becomes clear that there is very little effect on the total trapping and deposit.

5.1 Discretising a Shelterbelt

We discretise a shelterbelt by building upon the point representation for trapping in the previous chapter. The shelterbelt is conceptualised as a three-dimensional array of small equally-sized

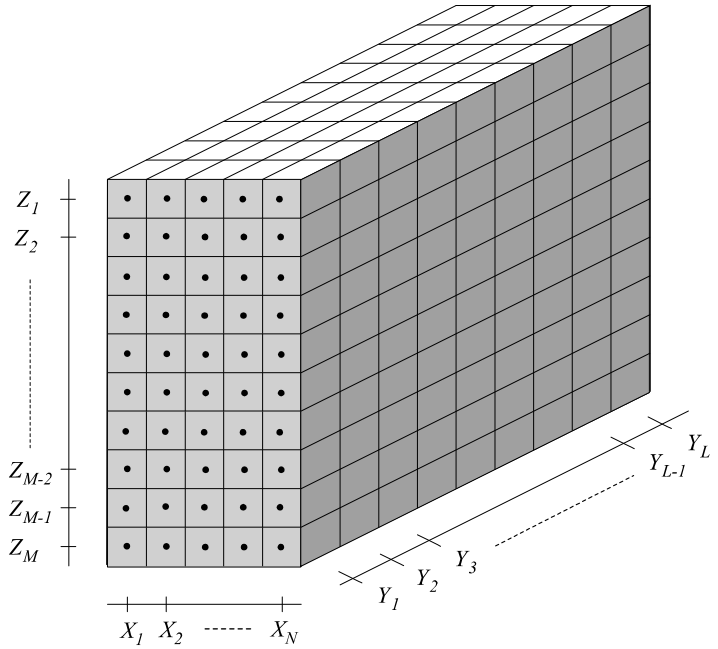

Figure 5.1: A rectangular shelterbelt discretised by dividing it into a three-dimensional array of blocks, N blocks wide $\times$ L blocks long $\times$ M high, with a trapping point at the centre of each block.

blocks of continuous trapping. Following the approach in Chapter 4, we concentrate the effect of trapping in each block to the point at its centre, so that the shelterbelt is represented by a three-dimensional array of trapping points. Figure 5.1 shows a rectangular shelterbelt discretised in such a manner; each small block has dimensions $\Delta x \times \Delta y \times \Delta z$, the array is N blocks wide alongwind $\times$ L blocks long acrosswind $\times$ M blocks high vertically, and the point at the centre of each block is denoted (X_n, Y_l, Z_m), $1 \leq n \leq N,\ 1 \leq l \leq L,\ 1 \leq m \leq M$.

In each block, the rate of mass removal by trapping per unit volume is $k_b Rc$, where k_b is the background trapping rate and R is a dimensionless function which is non-zero only where trapping occurs. Following the approach in Chapter 4, we concentrate the effect of trapping in each block to the point at its centre by defining

$$R_{nlm} = \Delta x \Delta y \Delta z \delta\left(x - X_n\right) \delta\left(y - Y_l\right) \delta\left(z - Z_m\right), \tag{5.1}$$

which is dimensionless and non-zero only at (X_n, Y_l, Z_m). The effective trapping rate $k = k_b \Delta x \Delta y \Delta z$ is the same for each point, because k_b is assumed constant and all of the blocks are equally-sized. In this way, the rate of mass removal per unit volume of air for each point

is $kc\left(X_n, Y_l, Z_m, t\right)\delta\left(x - X_n\right)\delta\left(y - Y_l\right)\delta\left(z - Z_m\right)$. The total rate of mass removal per unit volume of air by the discretised shelterbelt is the summed effect of all of the points; that is

$$\sum_{n=1}^{N}\sum_{l=1}^{L}\sum_{m=1}^{M} kc\left(X_n, Y_l, Z_m, t\right)\delta\left(x - X_n\right)\delta\left(y - Y_l\right)\delta\left(z - Z_m\right). \tag{5.2}$$

5.2 Advection-Dispersion Model

Our advection-dispersion model with trapping in a discretised shelterbelt is

$$\begin{aligned}\frac{\partial c}{\partial t} + u\frac{\partial c}{\partial x} - S\frac{\partial c}{\partial z} &= D_L\frac{\partial^2 c}{\partial x^2} + D_T\frac{\partial^2 c}{\partial y^2} + D_V\frac{\partial^2 c}{\partial z^2} + Q\delta\left(x - X_0\right)\delta\left(y - Y_0\right)\delta\left(z - H\right)\delta\left(t\right) \\ &\quad - \sum_{n=1}^{N}\sum_{l=1}^{L}\sum_{m=1}^{M} kc\left(X_n, Y_l, Z_m, t\right)\delta\left(x - X_n\right)\delta\left(y - Y_l\right)\delta\left(z - Z_m\right).\end{aligned} \tag{5.3}$$

This is to be solved subject to the initial and boundary conditions given in Chapter 3, Section 3.2. As for the analysis of a single trapping point in Chapter 4: if $D_V = 0$ then the boundary condition on the ground is automatically satisfied and Equation (5.3) is relatively simple to solve analytically, otherwise, if $D_V \neq 0$ the boundary condition is not automatically satisfied and the solution is more complicated.

5.3 Total Trapping in the Shelterbelt and Deposit on the Ground

The quantities of particular interest are the total trapping by the discretised shelterbelt and the subsequent deposit on the ground. Both of these quantities are found from the solution to the advection-dispersion model, we evaluate them using Laplace transforms via the property

$$\int_0^\infty c\left(x, y, z, t\right)\ dt = \int_0^\infty e^{-pt}c\left(x, y, z, t\right)\ dt\ \Big|_{p=0} = \overline{c}\left(x, y, z, 0\right) \tag{5.4}$$

where $\overline{c}\left(x, y, z, p\right)$ is the Laplace transform of $c\left(x, y, z, t\right)$ with respect to t.

Total Droplet Trapping by the Shelterbelt

The total mass of droplets trapped by the discretised shelterbelt, M_{TT} [kg], is found by integrating the rate of mass removal per unit volume of air with respect to space and time. The rate of mass removal per unit volume of air is given by Equation (5.2); integrating with respect to space and time:

$$M_{TT} = \int_0^\infty \int_0^\infty \int_{-\infty}^\infty \int_{-\infty}^\infty \sum_{n=1}^{N} \sum_{l=1}^{L} \sum_{m=1}^{M} kc\left(X_n, Y_l, Z_m, t\right) \delta\left(x - X_n\right) \delta\left(y - Y_l\right) \delta\left(z - Z_m\right) \, dx \, dy \, dz \, dt \tag{5.5}$$

which simplifies to

$$\begin{aligned} M_{TT} &= \sum_{n=1}^{N} \sum_{l=1}^{L} \sum_{m=1}^{M} \int_0^\infty kc\left(X_n, Y_l, Z_m, t\right) \, dt \\ &= \sum_{n=1}^{N} \sum_{l=1}^{L} \sum_{m=1}^{M} k\overline{c}\left(X_n, Y_l, Z_m, 0\right). \end{aligned} \tag{5.6}$$

The total mass of droplets deposited on the ground, M_{DT} [kg], is simply what remains of the original release:

$$\begin{aligned} M_{DT} &= Q - M_{TT} \\ &= Q - \sum_{n=1}^{N} \sum_{l=1}^{L} \sum_{m=1}^{M} k\overline{c}\left(X_n, Y_l, Z_m, 0\right). \end{aligned} \tag{5.7}$$

Droplet Deposit on the Ground

The total mass of droplets deposited on the ground per unit area, M_D [kg m^{-2}], is found by integrating the downward mass flux per unit area on the ground with respect to time. At height z the downward mass flux per unit area is $Sc + D_V \dfrac{\partial c}{\partial z}$; on the ground this reduces to Sc, because of the boundary which requires zero vertical dispersive flux at ground level. Integrating with respect to time:

$$\begin{aligned} M_D\left(x, y\right) &= \int_0^\infty Sc\left(x, y, 0, t\right) \, dt \\ &= S\overline{c}\left(x, y, 0, 0\right). \end{aligned} \tag{5.8}$$

The transforms required here are the same as those for the single trapping point. Most are standard formulae readily available in transform tables, but for $D_V \neq 0$ some of the transforms must be sourced from generalized calculus.

5.4 Case 1: Zero Vertical Dispersion

In this section we analyse our advection-dispersion model with trapping in a discretised shelterbelt, in the case where vertical dispersion of the droplets is very small compared to horizontal dispersion, such that the vertical dispersion coefficient may be considered zero. This is a special case of the model, where the droplets can disperse only horizontally and the boundary condition on the ground is automatically satisfied.

We present solutions to the model with $D_V = 0$ in 1-D and 2-D, building up to a full 3-D solution. The 1-D case is conceptually very simple, and in fact we can determine a solution with continuous trapping in that particular case. A common feature of all of these $D_V = 0$ solutions, as for those with $D_V = 0$ in the previous chapter, is that the concentration is always zero above the release height and only non-zero below the release height at the level of the droplets after time t. This is because the droplets do not spread vertically; they fall as a sheet.

One-Dimensional Solution with Discretised Trapping

In 1-D, and with $D_V = 0$, our advection-dispersion model with trapping in a discretised shelterbelt becomes

$$\frac{\partial c}{\partial t} - S\frac{\partial c}{\partial z} = Q\delta\left(z - H\right)\delta\left(t\right) - \sum_{m=1}^{M} kc\left(Z_m, t\right)\delta\left(z - Z_m\right) \tag{5.9}$$

with initial and boundary conditions

$$c\left(z, 0^-\right) = 0 \text{ and } c\left(\infty, t\right) = 0.$$

The conceptual situation here is a plane release with trapping at a number of planes stacked atop each other, as shown in Figure 5.2. Mass Q per unit area is released at time $t = 0$ from the plane at $(x, y, z) = (x, y, H)$. A shelterbelt "slab" of infinite length and width is discretised by dividing it into M layers of equal thickness Δz; these are labelled $m = 1, \ldots, M$, and the midpoint of each is denoted $z = Z_m$. The highest layer is $m = 1$ and the lowest is $m = M$.

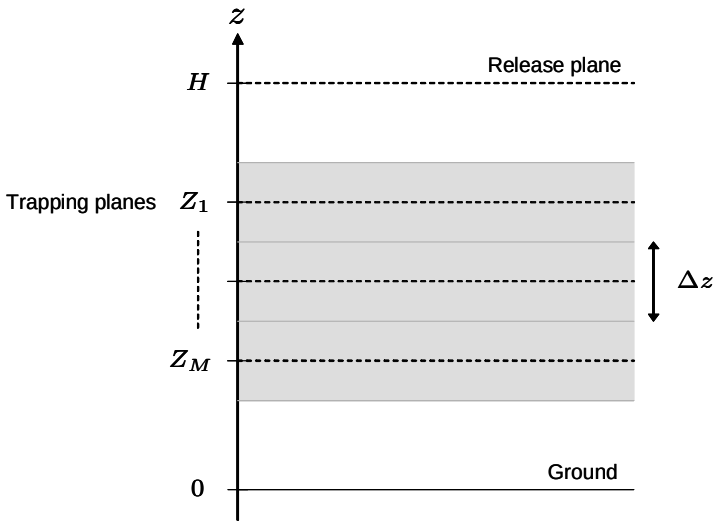

Figure 5.2: Illustration of a shelterbelt "slab", shaded in grey, discretised by dividing it into M layers with the trapping in each layer concentrated to the mid-plane.

Each layer removes droplets at mass rate per unit volume $k_b R_m c$; we concentrate the effect of trapping in each layer to the plane at $(x, y, z) = (x, y, Z_m)$, so that $R_m = \Delta z \delta(z - Z_m)$ and the effective trapping rate for the plane is $k = k_b \Delta z$. After release the droplets simply fall towards the ground with settling speed S; they do not disperse as they fall.

The solution to the Laplace transform of Equation (5.9) with respect to t may be constructed from the transformed solution for a single trapping plane on page 44:

$$\overline{c}(z,p) = \frac{Q}{S}\mathcal{H}(H-z)\, e^{-\frac{p(H-z)}{S}} - \sum_{m=1}^{M} \frac{k}{S}\overline{c}(Z_m,p)\,\mathcal{H}(Z_m - z)\, e^{-\frac{p(Z_m-z)}{S}} \tag{5.10}$$

where $\mathcal{H}(z)$ is the Heaviside function

$$\mathcal{H}(z) = \begin{cases} 0, & z < 0, \\ 1, & z > 0. \end{cases} \tag{5.11}$$

Equation (5.10) contains the M, as yet, unknowns $\overline{c}(Z_1,p), \ldots, \overline{c}(Z_M,p)$, and has discontinuities at $z = H$ and $z = Z_1, \ldots, Z_M$. To determine $\overline{c}(Z_m,p)$ we let $z \to Z_m^+$ to correspond with the concentration which arrives at the m^{th} trapping plane.

$$\begin{aligned} \overline{c}(Z_m,p) &= \lim_{z \to Z_m^+} \overline{c}(z,p) \\ &= \frac{Q}{S}\mathcal{H}(H-Z_m)\, e^{-pt_m} - \sum_{i=1}^{m-1} \frac{k}{S}\overline{c}(Z_i,p)\, e^{-p(t_m - t_i)} \end{aligned} \tag{5.12}$$

where $t_m = \dfrac{(H - Z_m)}{S}$ is the time for the droplets to fall to the m^{th} trapping plane. If the m^{th} trapping plane is above the release height, then the concentration there is zero because no droplets move upwards from the release. Otherwise, if the m^{th} trapping plane is below the release height, then the concentration there depends upon the trapping planes between it and the release.

Some values of Equation (5.12) at consecutive trapping planes below the release height are given in Table 5.1. It is assumed that $m = J$ is the highest trapping plane below the release height; this accounts for the possibility that some of the trapping planes are above the release height and some are below. Note that the values at consecutive trapping planes in Table 5.1 give a sequence of polynomials in $\dfrac{k}{S}$ of increasing degree; in fact we can write the following:

For $Z_1, \ldots, Z_M > H$, so that all of the trapping planes are above the release height,

$$\overline{c}\,(Z_m, p) = \ 0, \quad m = 1, \ldots, M, \tag{5.13}$$

and for $Z_M, \ldots, Z_J < H$, $1 \leq J \leq M$, so that the highest $J - 1$ trapping planes are above the release height and the remaining $M - (J - 1)$ trapping planes are below,

$$\overline{c}\,(Z_m, p) = \begin{cases} 0, & m = 1, \ldots, J-1, \\ \dfrac{Q}{S} e^{-pt_m} \left(1 - \dfrac{k}{S}\right)^{m-J}, & m = J, \ldots, M. \end{cases} \tag{5.14}$$

Equation (5.14) may be proven by induction, though the details are not included here. Finally, using the formula for the finite sum of a geometric progression (Gradshteyn & Ryzhik, 2000, p. 1)

$$\sum_{m=1}^{M} q^{m-1} = \frac{q^M - 1}{q - 1}, \quad q \neq 1 \tag{5.15}$$

and inverting the Laplace transforms, we obtain the following:

For $Z_1, \ldots, Z_M > H$, so that all of the trapping planes are above the release height,

$$c\,(z, t) = \begin{cases} 0, & z > H, \\ Q\delta\left(z - (H - St)\right), & z < H, \end{cases} \tag{5.16}$$

and for $Z_M, \ldots, Z_J < H$, $1 \leq J \leq M$, so that the highest $J-1$ trapping planes are above the release height and the remaining $M-(J-1)$ trapping planes are below

$$c(z,t) = \begin{cases} 0, & z > H, \\ Q\delta\left(z-(H-St)\right), & Z_J < z < H, \\ Q\left(1-\dfrac{k}{S}\right)^{m-J}\delta\left(z-(H-St)\right), & \underset{m=J+1,\ldots,M-1}{Z_{m+1} < z < Z_m}, \\ Q\left(1-\dfrac{k}{S}\right)^{M-J}\delta\left(z-(H-St)\right), & z < Z_M. \end{cases} \tag{5.17}$$

Droplets are removed at each successive trapping plane below the release height, leaving a smaller concentration underneath.

Total Droplet Trapping and Deposition

As described in Section 5.3, the total mass of droplets trapped and the subsequent deposit on the ground are calculated by setting $p = 0$ in the transformed solution. The total mass of droplets trapped by the discretised shelterbelt "slab" per unit area [kg m^{-2}] is

$$\begin{aligned} M_{TT} &= \sum_{m=1}^{M} k\overline{c}\left(Z_m, 0\right) \\ &= \begin{cases} 0, & Z_1, \ldots, Z_M > H, \\ Q - Q\left(1-\dfrac{k}{S}\right)^{M-J+1}, & \underset{1\leq J\leq M}{H > Z_J, \ldots, Z_M} \end{cases} \end{aligned} \tag{5.18}$$

leaving a density of deposit on the ground [kg m^{-2}] of $M_D = Q - M_{TT}$. The notes on the total trapping for a single plane (page 45 in the previous chapter) also apply here:

- Nothing is trapped if all of the trapping planes are above the release height.
- If all of the trapping planes are below the release height, then the total trapping is independent of their placement.
- The total trapping increases with increasing trapping rate k. A restriction on the size of k is necessary in order to keep the trapping within its physical bounds (see below).

Table 5.1: Transformed concentration at a number of consecutive trapping planes below the release height. $\overline{c}(Z_m, p)$ is the Laplace transform with respect to t of the concentration at the m^{th} trapping plane. It is assumed that $m = J$, $1 \leq J \leq M$, is the highest trapping plane below the release height.

m	$\overline{c}(Z_m, p)$
J	$\overline{c}(Z_J, p) = \frac{Q}{S} e^{-pt_J}$
$J+1$	$\overline{c}(Z_{J+1}, p) = \frac{Q}{S}\left(1 - \frac{k}{S}\right) e^{-pt_{J+1}}$
$J+2$	$\overline{c}(Z_{J+2}, p) = \frac{Q}{S}\left(1 - \frac{2k}{S} + \frac{k^2}{S^2}\right) e^{-pt_{J+2}}$
$J+3$	$\overline{c}(Z_{J+3}, p) = \frac{Q}{S}\left(1 - \frac{3k}{S} + \frac{3k^2}{S^2} - \frac{k^3}{S^3}\right) e^{-pt_{J+3}}$
$J+4$	$\overline{c}(Z_{J+4}, p) = \frac{Q}{S}\left(1 - \frac{4k}{S} + \frac{6k^2}{S^2} - \frac{4k^3}{S^3} + \frac{k^4}{S^4}\right) e^{-pt_{J+4}}$
$J+5$	$\overline{c}(Z_{J+5}, p) = \frac{Q}{S}\left(1 - \frac{5k}{S} + \frac{10k^2}{S^2} - \frac{10k^3}{S^3} + \frac{5k^4}{S^4} - \frac{k^5}{S^5}\right) e^{-pt_{J+5}}$

A Physical Restriction on the Trapping

For the model to remain physically sensible, the rate of mass removal at each trapping plane must not exceed the rate of mass arrival; this places an upper limit on the size of the effective trapping rate k, and consequently on the thickness of the layers into which the shelterbelt is divided, Δz. The rate of mass arrival at the m^{th} trapping plane is $Sc\left(Z_m^+, t\right)$, and the rate of mass removal there is $kc\left(Z_m^+, t\right)$. As a consequence we must have

$$kc\left(Z_m^+, t\right) \leq Sc\left(Z_m^+, t\right), \text{ which requires } k \leq S. \tag{5.19}$$

Since k is positive, this condition also ensures that $0 \leq M_{TT} \leq Q$ in Equation (5.18), in other words that the total trapping is no greater than the original release.

Recall that the effective trapping rate is defined as $k = k_b \Delta z$; since the value of the background trapping rate k_b is intrinsic to the shelterbelt and we have no control over it, the condition of $k \leq S$ must be satisfied by an appropriate choice for Δz, the thickness of the layers into which the shelterbelt is divided. In other words the number of layers M must be chosen so that the thickness of each layer satisfies

$$\Delta z \leq \frac{S}{k_b}. \tag{5.20}$$

One-Dimensional Solution with Continuous Trapping

It is generally difficult to solve our advection-dispersion model analytically with continuous trapping, however, in this particular 1-D case we can determine a solution and it is presented here for comparison with the discretised solution obtained above.

Suppose the shelterbelt "slab" shown in Figure 5.2 extends vertically between $z = Z_B$ and $z = Z_A$, where $Z_A > Z_B$. The rate of mass removal per unit volume of air is $k_b R c$, where R is a dimensionless function which is non-zero only within the shelterbelt; here R can be expressed in terms of Heaviside functions as

$$R = \mathcal{H}\left(z - Z_B\right) - \mathcal{H}\left(z - Z_A\right). \tag{5.21}$$

With the droplet mass concentration denoted $c_c\left(z, t\right)$ [kg m^{-3}] to indicate continuous trapping, our advection-dispersion model in 1-D and with $D_V = 0$ becomes

$$\frac{\partial c_c}{\partial t} - S\frac{\partial c_c}{\partial z} = Q\delta\left(z - H\right)\delta\left(t\right) - k_b c_c\left(\mathcal{H}\left(z - Z_B\right) - \mathcal{H}\left(z - Z_A\right)\right) \tag{5.22}$$

with initial and boundary conditions

$$c_c\left(z, 0^-\right) = 0 \text{ and } c_c\left(\infty, t\right) = 0.$$

We solve Equation (5.22) in three regions: above the shelterbelt, within the shelterbelt and below the shelterbelt; matching the downward flux $Sc\left(z,t\right)$ at the interface between each region. There are three possible scenarios: (i) the release height is below the shelterbelt, (ii) the release height is within the shelterbelt, and (iii) the release height is above the shelterbelt.

(i). For $H < Z_B$, so that the release height is below the shelterbelt,

$$c_c\left(z,t\right) = \begin{cases} 0, & z > H, \\ Q\delta\left(z - \left(H - St\right)\right), & z < H. \end{cases} \tag{5.23}$$

(ii). For $Z_B < H < Z_A$, so that the release height is within the shelterbelt,

$$c_c\left(z,t\right) = \begin{cases} 0, & z > H, \\ Qe^{-k_b t}\delta\left(z - \left(H - St\right)\right), & Z_B < z < H, \\ Qe^{-k_b t_B}\delta\left(z - \left(H - St\right)\right), & z < Z_B. \end{cases} \tag{5.24}$$

(iii). For $Z_A < H$, so that the release height is above the shelterbelt,

$$c_c\left(z,t\right) = \begin{cases} 0, & z > H, \\ Q\delta\left(z - \left(H - St\right)\right), & Z_A < z < H, \\ Qe^{-k_b\left(t - t_A\right)}\delta\left(z - \left(H - St\right)\right), & Z_B < z < Z_A, \\ Qe^{-k_b\left(t_B - t_A\right)}\delta\left(z - \left(H - St\right)\right), & z < Z_B, \end{cases} \tag{5.25}$$

where $t_A = \dfrac{H - Z_A}{S}$ and $t_B = \dfrac{H - Z_B}{S}$ are the times for the droplets to fall to heights Z_A and Z_B respectively. From Equations (5.24) and (5.25) it is clear that with continuous trapping the concentration decreases exponentially as the droplets fall through the shelterbelt.

Total Droplet Trapping and Deposition

With continuous trapping, the total mass of droplets trapped by the shelterbelt per unit area, denoted M_{TTc} [kg m^{-2}], is the integral of the mass rate of removal per unit volume with respect to space and time:

$$\begin{aligned} M_{TTc} &= \int_0^\infty \int_0^\infty k_b c_c(z,t) \left(\mathcal{H}(z-Z_B) - \mathcal{H}(z-Z_A)\right) \, dz \, dt \\ &= \begin{cases} 0, & Z_B > H, \\ Q\left(1 - e^{-k_b t_B}\right), & Z_A > H > Z_B, \\ Q\left(1 - e^{-k_b (t_B - t_A)}\right), & H > Z_A. \end{cases} \end{aligned} \tag{5.26}$$

The density of deposit on the ground, M_{Dc} [kg m^{-2}], is simply what remains of the original release, that is $Q - M_{TTc}$.

Note the parallels between the total trapping here and in the discretised solution: once again there is no trapping if the shelterbelt is completely above the release height, or, if the shelterbelt is completely below the release height its position has no effect on the total trapping. In Equation (5.26) however, $0 \leq M_{TTc} \leq Q$ so it is not possible to trap more than the original release.

Comparison with the Discretised Solution

In this section we compare the solutions with continuous and discretised tapping, for a varying number of trapping planes M in the discretised solution. The shelterbelt "slab"extends between $Z_B = 0.5$ m and $Z_A = 2.5$ m, with background trapping rate $k_b = 0.5$ s^{-1}, and the release parameters are $S = 0.2$ m s^{-1}, $Q = 1$ kg m^{-2} and $H = 3$ m.

Figure 5.3 (page 87) shows the finite part of the concentration (which appears at height z only at time $t = \dfrac{H-z}{S}$) as the droplets fall through the shelterbelt. The solid line represents the solution with continuous trapping, $c_c(z,t)$, and the asterisks represent the solution with discretised trapping, $c(z,t)$ (calculated midway between each trapping plane). Note that $M = 5$ is the minimum number of trapping planes required for the effective trapping rate to satisfy $k \leq$

S. This figure illustrates that the discretised solution does indeed approximate the continuous solution, and that the fit between the two improves as M increases.

A measure of the accuracy of the discretised solution is shown by the dimensionless ratio M_{TT}/M_{TTc} in Figure 5.4, where M_{TT} is the total trapping in the discretised solution [kg m^{-2}] and M_{TTc} is the corresponding value in the continuous solution. The accuracy of the discretised solution increases with the number of trapping planes, though the total trapping always remains a little higher than in the continuous solution. In this example, even with the minimum number of trapping planes M_{TT} is only larger than M_{TTc} by 0.7 %.

Two-Dimensional Solution with Discretised Trapping

In 2-D, and with $D_V = 0$, our advection-dispersion model with trapping in a discretised shelterbelt becomes

$$\begin{aligned} \frac{\partial c}{\partial t} + u\frac{\partial c}{\partial x} - S\frac{\partial c}{\partial z} &= D_L\frac{\partial^2 c}{\partial x^2} + Q\delta\left(x - X_0\right)\delta\left(z - H\right)\delta\left(t\right) \\ &\quad - \sum_{n=1}^{N}\sum_{m=1}^{M} kc\left(X_n, Z_m, t\right)\delta\left(x - X_n\right)\delta\left(z - Z_m\right) \end{aligned} \tag{5.27}$$

with initial and boundary conditions

$$c\left(x, z, 0^-\right) = 0, \text{ and}$$

$$c\left(x, z, t\right) \to 0 \text{ as } x \to \pm\infty \text{ and } z \to +\infty.$$

As shown in Figure 5.5 on page 88, this is now a line release with trapping at a number of lines stacked in a 2-D array. Mass Q per unit length is released at time $t = 0$ from the line $(x, y, z) = (X_0, y, H)$. A rectangular shelterbelt of infinite crosswind length is discretised by dividing it into a 2-D array of prisms, each with cross-sectional area $\Delta x \Delta z$; these are labelled by alongwind index $n = 1, \ldots, N$ and vertical index $m = 1, \ldots, M$, and the midline of each is denoted (X_n, y, Z_m). The highest row of prisms in the array is $m = 1$ and the lowest is $m = M$. Each prism removes droplets at mass rate per unit volume $k_b R_{nm} c$; we concentrate the effect of this trapping to the line $(x, y, z) = (X_n, y, Z_m)$, so that $R_{nm} = \Delta x \Delta z \delta\left(x - X_n\right)\delta\left(z - Z_m\right)$ and the effective trapping rate for the line is $k = k_b \Delta x \Delta z$. After release the droplets disperse alongwind, whilst travelling with the mean windspeed u and falling at settling speed S.

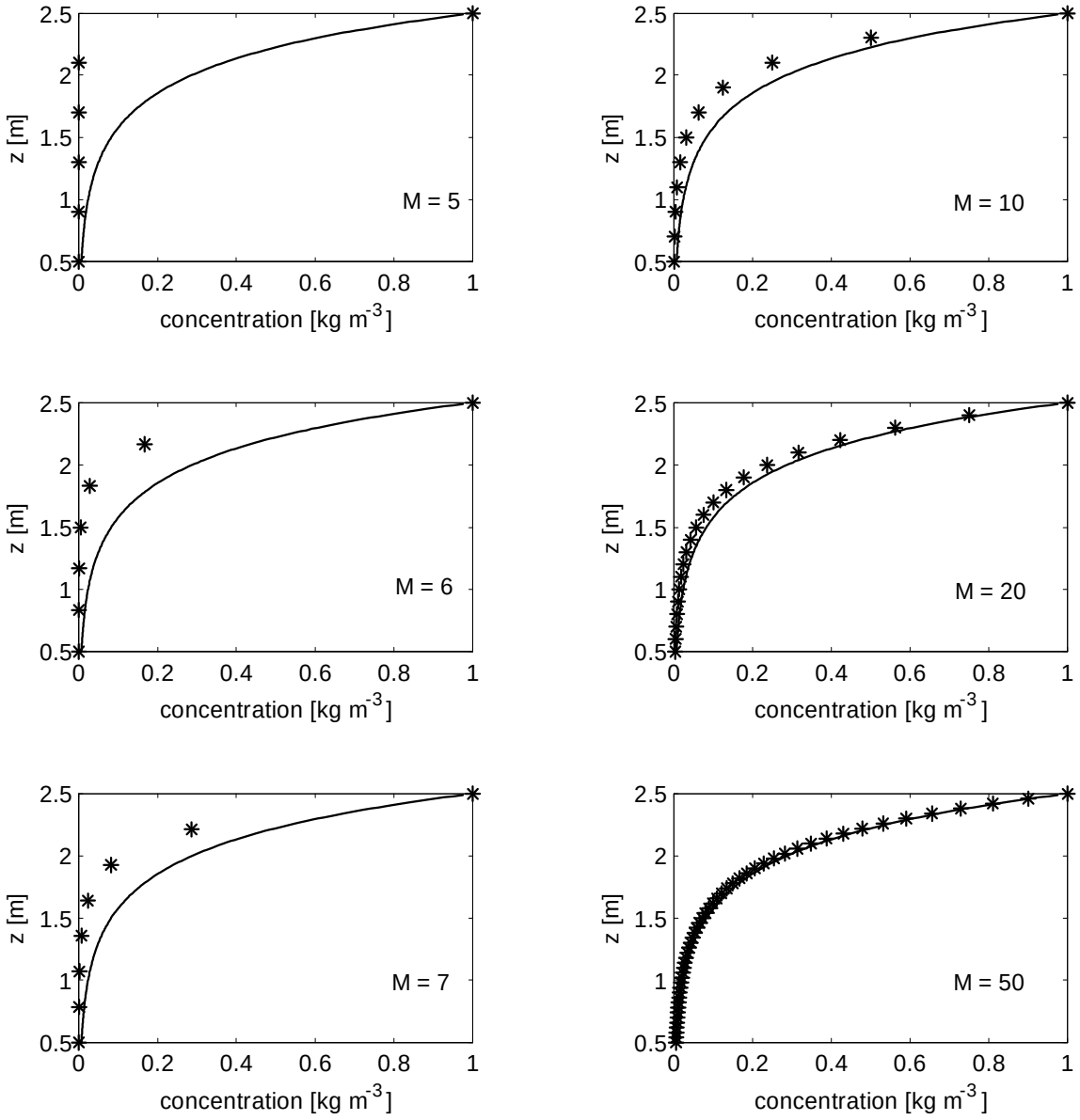

Figure 5.3: Comparisons between the solutions for continuous and discretised trapping, with a varying number of trapping planes M in the discretised solution. The solid line represents the solution with continuous trapping, and the asterisks represent the solution with discretised trapping (calculated midway between each trapping plane). See the text for parameter values.

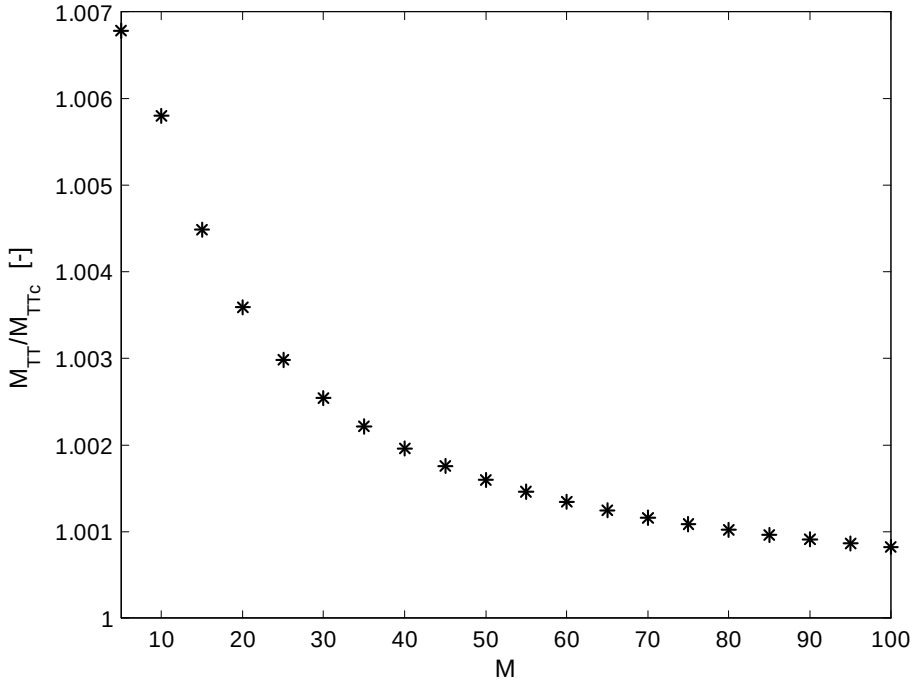

Figure 5.4: A measure of the accuracy of the discretised solution, illustrated by the dimensionless ratio M_{TT}/M_{TTc}, as the number of trapping planes M increases. M_{TT} [kg m^{-2}] denotes the total trapping in the discretised solution, and M_{TTc} is the corresponding value in the continuous solution. Parameter values are as for Figure 5.3.

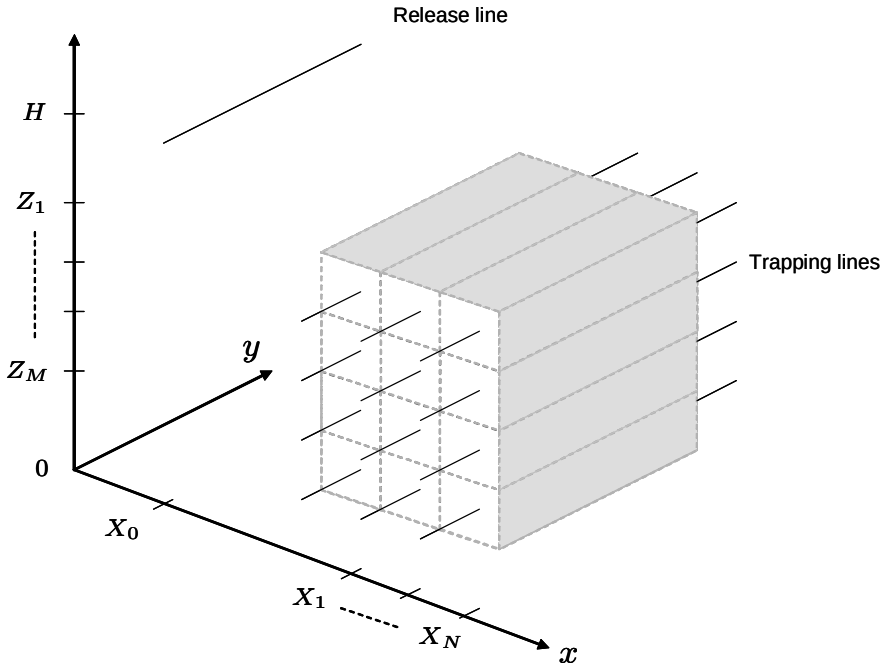

Figure 5.5: Illustration of an infinitely long rectangular shelterbelt, shaded in grey, discretised by dividing it into $N \times M$ prisms with the trapping in each concentrated to the mid-line.

The solution to the Laplace transform of Equation (5.27) with respect to t may be constructed from the transformed solution for a single trapping line on page 47:

$$\begin{aligned}\overline{c}\,(x,z,p) &= \frac{Q}{2\sqrt{\pi S D_L\,(H-z)}}\mathcal{H}\,(H-z)\,e^{-\frac{p(H-z)}{S}-\frac{S(x-X_0-u(H-z)/S)^2}{4D_L(H-z)}} \\ &\quad -\sum_{n=1}^{N}\sum_{m=1}^{M}\frac{k\overline{c}\,(X_n,Z_m,p)}{2\sqrt{\pi S D_L\,(Z_m-z)}}\mathcal{H}\,(Z_m-z)\,e^{-\frac{p(Z_m-z)}{S}-\frac{S(x-X_n-u(Z_m-z)/S)^2}{4D_L(Z_m-z)}}.\end{aligned} \tag{5.28}$$

This transformed solution contains the $N \times M$, as yet unknowns $\overline{c}\,(X_1,Z_1,p),\ldots,c\,(X_N,Z_M,p)$ and has discontinuities at $z = H$ and $z = Z_1,\ldots,Z_M$. To determine $\overline{c}\,(X_n,Z_m,p)$ we set $x = X_n$ and let $z \to Z_m^+$, since this represents the concentration which arrives at the n,m^{th} trapping line.

$$\begin{aligned}\overline{c}\,(X_n,Z_m,p) &= \lim_{z\to Z_m^+}\overline{c}\,(X_n,z,p) \\ &= \frac{Q}{2S\sqrt{\pi D_L t_m}}\mathcal{H}\,(H-Z_m)\,e^{-pt_m-\frac{(X_n-X_0-ut_m)^2}{4D_L t_m}} \\ &\quad -\sum_{j=1}^{N}\sum_{i=1}^{m-1}\frac{k\overline{c}\,(X_j,Z_i,p)}{2S\sqrt{\pi D_L\,(t_m-t_i)}}e^{-p(t_m-t_i)-\frac{\left(X_n-X_j-u(t_m-t_i)\right)^2}{4D_L(t_m-t_i)}}\end{aligned} \tag{5.29}$$

where $t_m = \dfrac{H-Z_m}{S}$ is the time for the droplets to fall to the height of the m^{th} row of trapping lines. If the n,m^{th} trapping line is above the release height, then the concentration there is zero because no droplets move upwards from the release. Otherwise, if the n,m^{th} trapping line is below the release height, then the concentration there depends upon the rows of trapping lines between it and the release (note that other trapping lines at the same level have no influence).

In the 1-D solution we were able to write an explicit expression for $\overline{c}$ at each trapping plane, but because of the alongwind dispersion here it is difficult to go any further than the recursive formula above. The first term corresponds to the concentration at the n,m^{th} trapping line due purely to the original release, and the second term compensates for the mass which has been removed at the trapping lines above.

Inverting the Laplace transforms:

For $Z_1, \ldots, Z_M > H$, so that all of the rows of trapping lines are above the release height,

$$c(x,z,t) = \begin{cases} 0, & z > H, \\ \dfrac{Q}{2\sqrt{\pi D_L t}} e^{-\frac{(x-X_0-ut)^2}{4D_L t}} \delta\left(z-(H-St)\right), & H > z, \end{cases} \tag{5.30}$$

and for $Z_M, \ldots, Z_J < H$, $1 \leq J \leq M$, so that the highest $J-1$ rows of trapping lines are above the release height and the remaining $M-(J-1)$ rows are below,

$$c(x,z,t) = \begin{cases} 0, & z > H, \\ \dfrac{Q}{2\sqrt{\pi D_L t}} e^{-\frac{(x-X_0-ut)^2}{4D_L t}} \delta\left(z-(H-St)\right), & Z_J < z < H, \\ \dfrac{Q}{2\sqrt{\pi D_L t}} e^{-\frac{(x-X_0-ut)^2}{4D_L t}} \delta\left(z-(H-St)\right) & \\ -\displaystyle\sum_{n=1}^{N}\sum_{m=J}^{j}\left[\frac{kc\left(X_n, Z_m, t-(Z_m-z)/S\right)}{2\sqrt{\pi S D_L\left(Z_m-z\right)}} e^{-\frac{S(x-X_n-u(Z_m-z)/S)^2}{4D_L(Z_m-z)}}\right], & \\ & Z_{j+1} < z < Z_j, \\ & {\scriptstyle (j=J,\ldots,M-1)} \\ \dfrac{Q}{2\sqrt{\pi D_L t}} e^{-\frac{(x-X_0-ut)^2}{4D_L t}} \delta\left(z-(H-St)\right) & \\ -\displaystyle\sum_{n=1}^{N}\sum_{m=J}^{M}\left[\frac{kc\left(X_n, Z_m, t-(Z_m-z)/S\right)}{2\sqrt{\pi S D_L\left(Z_m-z\right)}} e^{-\frac{S(x-X_n-u(Z_m-z)/S)^2}{4D_L(Z_m-z)}}\right], & z < Z_M. \end{cases} \tag{5.31}$$

Below the release height the concentration distribution alongwind is Gaussian until the level of the trapping lines, where some of the droplets are removed at each successive row of trapping lines, leaving a smaller concentration underneath and altering the distribution.

This solution inherits the issue identified in Chapter 4 (see page 48), where, due to the interaction of delta functions, the concentration becomes negative as one nears the trapping lines from below. In the next section we show how this issue can be resolved by making the trapping continuous alongwind (thus spreading it out over a finite width which removes one of the delta functions). After performing some comparative examples however, it becomes clear that the issue has very little effect on the total trapping and deposit.

Total Droplet Trapping and Deposition

Following Section 5.3, the mass of droplets trapped by the discretised shelterbelt per unit length [kg m^{-1}] is

$$M_{TT} = \sum_{n=1}^{N} \sum_{m=1}^{M} k\overline{c}\,(X_n, Z_m, 0) \tag{5.32}$$

where $\overline{c}\,(X_n, Z_m, 0)$ is given by Equation (5.29) with $p = 0$. This leaves a total mass deposit on the ground per unit crosswind length of $M_{DT} = Q - M_{TT}$ [kg m^{-1}]. The density of deposit on the ground (mass of droplets deposited per unit area) [kg m^{-2}] is

$$\begin{aligned} M_D\,(x) &= S\overline{c}\,(x, 0, 0) \\ &= \frac{Q\sqrt{S}}{2\sqrt{\pi D_L H}} e^{-\frac{S(x - X_0 - uH/S)^2}{4D_L H}} \\ &\quad - \sum_{n=1}^{N} \sum_{m=1}^{M} \frac{k\sqrt{S}\overline{c}\,(X_n, Z_m, 0)}{2\sqrt{\pi D_L Z_m}} e^{-\frac{S(x - X_n - uZ_m/S)^2}{4D_L Z_m}}. \end{aligned} \tag{5.33}$$

To evaluate the total trapping M_{TT} and the density of deposit M_D, one must solve the system of $N \times M$ equations formed by Equation (5.29) at each of the trapping lines. For each trapping line, Equation (5.29) is calculated using only values from higher rows of trapping lines; thus the system does not have to be solved simultaneously, it can be solved directly by forward substitution (working downwards from the highest row of trapping lines).

Two-Dimensional Solution With Continuous Trapping Alongwind

In this section, we show how the issue of the concentration becoming negative in the discretised solution can be resolved by making the trapping continuous alongwind. In the discretised solution, the shelterbelt was divided into an $N \times M$ array of prisms (each with cross-sectional area $\Delta x \Delta z$), with the trapping in each prism concentrated to the mid-line at $(x, y, z) = (X_n, y, Z_m)$. To make the trapping continuous alongwind we let $N \to \infty$ which, in turn, makes $\Delta x \to 0$. Conceptually, this means that the shelterbelt is now divided into M layers vertically, with the trapping in each layer concentrated to the sheet through the middle of the layer.

Here, we denote the Laplace transform of the concentration with respect to t by $\overline{c}_c\,(x, z, p)$, to indicate that it applies to continuous trapping alongwind. Letting $\Delta x \to 0$ in Equation (5.28)

gives

$$\begin{aligned}\overline{c}_c\left(x,z,p\right) &= \frac{Q}{2\sqrt{\pi S D_L\left(H-z\right)}}\mathcal{H}\left(H-z\right)e^{-\frac{p(H-z)}{S}-\frac{S(x-X_0-u(H-z)/S)^2}{4D_L(H-z)}} \\ &\quad - \lim_{\Delta x\to 0}\sum_{n=1}^{N}\sum_{m=1}^{M}\frac{k_b\Delta x\Delta z\;\overline{c}\left(X_n,Z_m,p\right)}{2\sqrt{\pi S D_L\left(Z_m-z\right)}}\mathcal{H}\left(Z_m-z\right)e^{-\frac{p(Z_m-z)}{S}-\frac{S(x-X_n-u(Z_m-z)/S)^2}{4D_L(Z_m-z)}}.\end{aligned} \tag{5.34}$$

Note the use of the background trapping rate k_b, rather than the effective trapping rate $k = k_b\Delta x\Delta z$. The second term above is the limit of a Riemann sum, and can be written as a definite integral; assuming that the shelterbelt extends alongwind between $x = X_A$ on the left and $x = X_B$ on the right:

$$\begin{aligned}\overline{c}_c\left(x,z,p\right) &= \frac{Q}{2\sqrt{\pi S D_L\left(H-z\right)}}\mathcal{H}\left(H-z\right)e^{-\frac{p(H-z)}{S}-\frac{S(x-X_0-u(H-z)/S)^2}{4D_L(H-z)}} \\ &\quad - \sum_{m=1}^{M}\int_{X_A}^{X_B}\frac{k_b\Delta z\;\overline{c}_c\left(\chi,Z_m,p\right)}{2\sqrt{\pi S D_L\left(Z_m-z\right)}}\mathcal{H}\left(Z_m-z\right)e^{-\frac{p(Z_m-z)}{S}-\frac{S(x-\chi-u(Z_m-z)/S)^2}{4D_L(Z_m-z)}}\,d\chi\end{aligned} \tag{5.35}$$

which contains the M, as yet, unknowns $\overline{c}_c\left(x,Z_1,p\right),\ldots,\overline{c}_c\left(x,Z_M,p\right)$, and has discontinuities at $z = H$ and $z = Z_1,\ldots,Z_M$. To determine $\overline{c}_c\left(x,Z_m,p\right)$ we let $z\to Z_m^+$, to correspond with the concentration which arrives at the m^{th} trapping sheet.

$$\begin{aligned}\overline{c}_c\left(x,Z_m,p\right) &= \lim_{z\to Z_m^+}\overline{c}_c\left(x,z,p\right) \\ &= \frac{Q}{2S\sqrt{\pi D_L t_m}}\mathcal{H}\left(H-Z_m\right)e^{-pt_m-\frac{(x-X_0-ut_m)^2}{4D_L t_m}} \\ &\quad - \sum_{i=1}^{m-1}\int_{X_A}^{X_B}\frac{k_b\Delta z\;\overline{c}_c\left(\chi,Z_i,p\right)}{2S\sqrt{\pi D_L\left(t_m-t_i\right)}}e^{-p(t_m-t_i)-\frac{(x-\chi-u(t_m-t_i))^2}{4D_L(t_m-t_i)}}\,d\chi\end{aligned} \tag{5.36}$$

where $t_m = \dfrac{H-Z_m}{S}$ is the time for the droplets to fall to the height of the m^{th} trapping sheet. If the m^{th} trapping sheet is above the release height, then the concentration there is zero. Otherwise, if the m^{th} trapping sheet is below the release height, then the concentration there depends upon the trapping sheets between it and the release. We can calculate Equation (5.36) analytically for the first two trapping sheets which are below the release height, but beyond that the integral has to be evaluated numerically.

Inverting the Laplace transforms:

For $Z_1, \ldots, Z_M > H$, so that all of the trapping sheets are above the release height,

$$c_c(x,z,t) = \begin{cases} 0, & z > H, \\ \dfrac{Q}{2\sqrt{\pi D_L t}} e^{-\frac{(x-X_0-ut)^2}{4D_L t}} \delta\left(z-(H-St)\right), & z < H \end{cases} \tag{5.37}$$

and for $Z_M, \ldots, Z_J < H$, $1 \leq J \leq M$, so that the highest $J-1$ trapping sheets are above the release height and the remaining $M-(J-1)$ sheets are below,

$$c_c(x,z,t) = \begin{cases} 0, & z > H, \\ \dfrac{Q}{2\sqrt{\pi D_L t}} e^{-\frac{(x-X_0-ut)^2}{4D_L t}} \delta\left(z-(H-St)\right), & Z_J < z < H, \\ \dfrac{Q}{2\sqrt{\pi D_L t}} e^{-\frac{(x-X_0-ut)^2}{4D_L t}} \delta\left(z-(H-St)\right) & \\ \quad - \displaystyle\sum_{m=J}^{j} \int_{X_A}^{X_B} \left[\frac{k_b \Delta z \; c\left(\chi, Z_m, t-(Z_m-z)/S\right)}{2\sqrt{\pi S D_L (Z_m - z)}} e^{-\frac{S(x-\chi-u(Z_m-z)/S)^2}{4D_L(Z_m-z)}} \right] d\chi, & \\ & Z_{j+1} < z < Z_j, \\ & (j=J,\ldots,M-1) \\ \dfrac{Q}{2\sqrt{\pi D_L t}} e^{-\frac{(x-X_0-ut)^2}{4D_L t}} \delta\left(z-(H-St)\right) & \\ \quad - \displaystyle\sum_{m=J}^{M} \int_{X_A}^{X_B} \left[\frac{k_b \Delta z \; c\left(\chi, Z_m, t-(Z_m-z)/S\right)}{2\sqrt{\pi S D_L (Z_m - z)}} e^{-\frac{S(x-\chi-u(Z_m-z)/S)^2}{4D_L(Z_m-z)}} \right] d\chi, & \\ & z < Z_M. \end{cases} \tag{5.38}$$

This solution behaves in much the same way as the discretised solution: the concentration distribution alongwind is Gaussian below the release height, until the level of the trapping sheets, where some of the droplets are removed at each successive sheet. Here, though, the concentration does not become negative provided the number of layers (and also trapping sheets) M is chosen such that $\Delta z \leq \dfrac{S}{k_b}$. This is the same condition as for the discretised solution in 1-D.

Total Droplet Trapping and Deposition

With continuous trapping alongwind, we denote the total mass of droplets trapped per unit crosswind length by M_{TTc} [kg m^{-1}]. It is given by the limit as $\Delta x \to 0$ in Equation (5.32):

$$\begin{aligned} M_{TTc} &= \lim_{\Delta x \to 0} \sum_{n=1}^{N} \sum_{m=1}^{M} k_b \Delta x \Delta z \; \overline{c}_c \left(X_n, Z_m, 0\right) \\ &= \sum_{m=1}^{M} \int_{X_A}^{X_B} k_b \Delta z \; \overline{c}_c \left(x, Z_m, 0\right) \; dx \end{aligned} \tag{5.39}$$

where $\overline{c}_c \left(x, Z_m, 0\right)$ is found from Equation (5.36) with $p = 0$. The total deposit on the ground per unit crosswind length is $M_{DTc} = Q - M_{TTc}$ [kg m^{-1}], and the density of deposit on the ground [kg m^{-2}] is

$$\begin{aligned} M_{Dc}\left(x\right) &= S\overline{c}_c \left(x, 0, 0\right) \\ &= \frac{Q\sqrt{S}}{2\sqrt{\pi D_L H}} e^{-\frac{S(x - X_0 - uH/S)^2}{4D_L H}} \\ &\quad - \sum_{m=1}^{M} \int_{X_A}^{X_B} \frac{k_b \Delta z \sqrt{S} \; \overline{c}_c \left(\chi, Z_m, 0\right)}{2\sqrt{\pi D_L Z_m}} e^{-\frac{S(x - \chi - uZ_m/S)^2}{4D_L Z_m}} \; d\chi. \end{aligned} \tag{5.40}$$

To evaluate the total trapping M_{TTc} and the density of deposit M_{Dc}, one must solve the system of M integral equations formed by Equation (5.36) at each trapping sheet. As in the discretised solution, Equation (5.36) is calculated for each trapping sheet using only values from higher trapping sheets, thus the system does not have to be solved simultaneously.

An Illustrative Example for the Two-Dimensional Solution

The following example illustrates the 2-D solution with discretised trapping. It also shows that the issue of the concentration becoming negative has negligible effect given the realistic trapping rate used. The parameter set is given in Table 5.2: a settling speed of $S = 0.2$ m s^{-1} corresponds to droplets of approximate diameter $d = 44$ μm, and a dominant alongwind turbulence length scale of $L_L = 2$ m gives dispersion coefficient $D_L = uL_L = 2$ m^2 s^{-1}. The shelterbelt extends vertically between $Z_B = 0.5$ m and $Z_A = 8.5$ m, and alongwind between $X_A = 4$ m and $X_B = 8$ m.

Table 5.2: Parameter set used to generate Figures 5.6 and 5.7.

u	S	L_L	Q	(X_0, H)	k_b
1 m s^{-1}	0.2 m s^{-1}	2 m	1 kg m^{-1}	$(0, 4)$ m	0.5 s^{-1}

Figure 5.6 shows cross-sections of the density of deposit [kg m^{-2}] for both discretised trapping, with $M = 40$ and $N = 2$, and continuous trapping alongwind (that is $N = \infty$) also with $M = 40$. The densities of deposit with discretised and with continuous trapping alongwind are denoted M_D and M_{Dc} respectively, and the corresponding value without trapping is denoted M_D^*. Note that with continuous trapping alongwind, $M = 20$ is the minimum number of trapping sheets required to ensure that the concentration does not become negative. The percentage reduction in density of deposit as a result of the trapping is shown in Figure 5.7.

Looking at these two figures, the values for discretised and for continuous trapping alongwind are almost identical, which shows that the issue of the concentration becoming negative in the discretised solution has very little effect. In fact, the total mass of droplets trapped is the same: $M_{TT} = M_{TTc} = 0.78$ kg m^{-1} according to Equations (5.32) and (5.39). There is significant reduction in the density of deposit downwind of the shelterbelt; in this example the maximum reduction is 87 % which occurs at $x = 11.5$ m.

Three-Dimensional Solution

In all three spatial dimensions, but with $D_V = 0$, our advection-dispersion model with trapping in a discretised shelterbelt becomes

$$\begin{aligned} \frac{\partial c}{\partial t} + u\frac{\partial c}{\partial x} - S\frac{\partial c}{\partial z} &= D_L\frac{\partial^2 c}{\partial x^2} + D_T\frac{\partial^2 c}{\partial y^2} + Q\delta\left(x - X_0\right)\delta\left(y - Y_0\right)\delta\left(z - H\right)\delta\left(t\right) \\ &\quad - \sum_{m=1}^{M}\sum_{n=1}^{N}\sum_{l=1}^{L} kc\left(X_n, Y_l, Z_m, t\right)\delta\left(x - X_n\right)\delta\left(y - Y_l\right)\delta\left(z - Z_m\right) \end{aligned} \tag{5.41}$$

with initial and boundary conditions

$$c\left(x, y, z, 0^-\right) = 0, \text{ and}$$

$$c\left(x, y, z, t\right) \to 0 \text{ as } x, y \to \pm\infty \text{ and } z \to +\infty.$$

The conceptual situation is as described in Section 5.1. To recap: a rectangular shelterbelt is divided into a 3-D array of blocks, each with volume $\Delta x \Delta y \Delta z$; these are labelled by alongwind

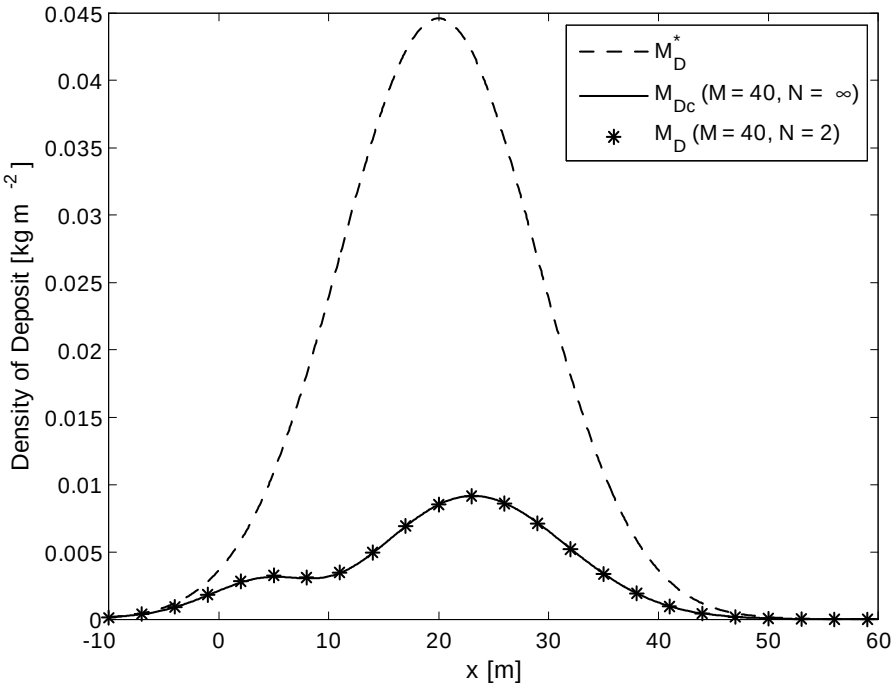

Figure 5.6: Cross-section of the density of deposit [kg m^{-2}], resulting from a line release with zero vertical dispersion and an $N \times M$ array of trapping lines. M_D and M_{Dc} are the densities of deposit with discretised, and continuous trapping alongwind, and M_D^* is the corresponding value without trapping. Parameter values are as given in Table 5.2.

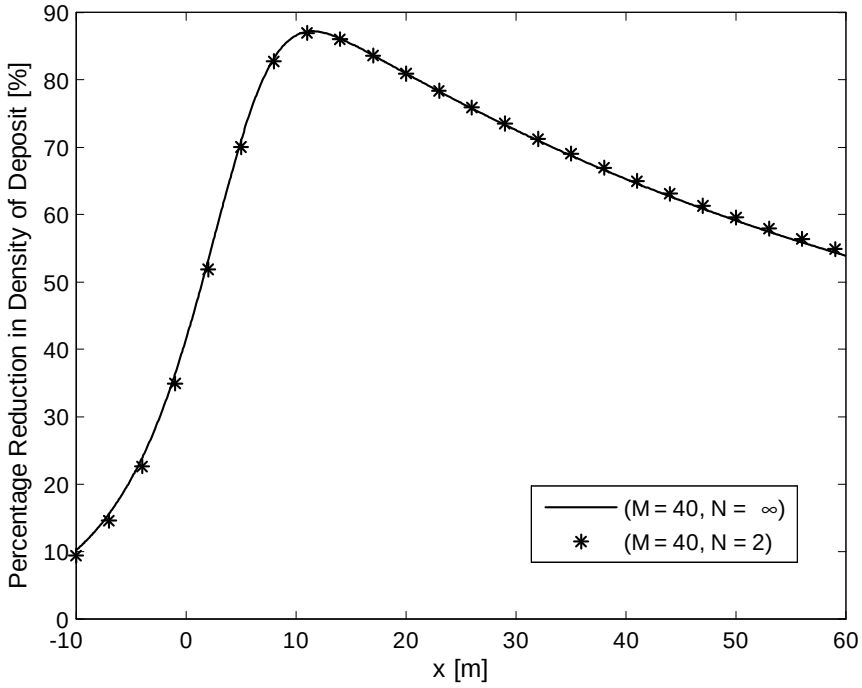

Figure 5.7: Cross-section of the percentage reduction in density of deposit as a result of the trapping in Figure 5.6. Parameter values are the same as for Figure 5.6.

index $n = 1, \ldots, N$, crosswind index $l = 1, \ldots, L$ and vertical index $m = 1, \ldots, M$. The effect of trapping in each block is concentrated to the midpoint (X_n, Y_l, Z_m). After release from the source the droplets disperse horizontally (both alongwind and crosswind), whilst travelling with the mean wind speed u and falling at settling speed S.

The solution to the Laplace transform of Equation (5.41) with respect to t is constructed from the transformed solution for a single trapping point on page 54:

$$\begin{aligned}\overline{c}\,(x,y,z,p) &= \frac{Q}{4\pi\sqrt{D_L D_T}\,(H-z)}\mathcal{H}\,(H-z)\,e^{-\frac{p(H-z)}{S}-\frac{S(x-X_0-u(H-z)/S)^2}{4D_L(H-z)}-\frac{S(y-Y_0)^2}{4D_T(H-z)}} \\ &\quad -\sum_{n=1}^{N}\sum_{l=1}^{L}\sum_{m=1}^{M}\left[\frac{k\overline{c}\,(X_n,Y_l,Z_m,p)}{4\pi\sqrt{D_L D_T}\,(Z_m-z)}\mathcal{H}\,(Z_m-z)\times\right. \\ &\qquad \left. e^{-\frac{p(Z_m-z)}{S}-\frac{S(x-X_n-u(Z_m-z)/S)^2}{4D_L(Z_m-z)}-\frac{S(y-Y_l)^2}{4D_T(Z_m-z)}}\right]. \qquad (5.42)\end{aligned}$$

The transformed solution above contains the $N \times L \times M$, as yet unknown values of $\overline{c}\,(X_1, Y_1, Z_1, p)$ $\ldots, \overline{c}\,(X_N, Y_L, Z_M, p)$ and has discontinuities at $z = H$ and $z = Z_1, \ldots, Z_M$. Setting $(x, y) = (X_1, Y_1)$ and letting $z \to Z_m^+$ to correspond with the concentration which arrives at the n, l, m^{th} trapping point:

$$\begin{aligned}\overline{c}\,(X_n,Y_l,Z_m,p) &= \lim_{z\to Z_m^+}\overline{c}\,(X_n,Y_l,z,p) \\ &= \frac{Q}{4\pi S t_m\sqrt{D_L D_T}}\mathcal{H}\,(H-Z_m)\,e^{-pt_m-\frac{(X_n-X_0-ut_m)^2}{4D_L t_m}-\frac{(y-Y_0)^2}{4D_T t_m}} \\ &\quad -\sum_{j=1}^{N}\sum_{r=1}^{L}\sum_{i=1}^{m-1}\left[\frac{k\overline{c}\,(X_j,Y_r,Z_i,p)}{4\pi S\,(t_m-t_i)\,\sqrt{D_L D_T}}\times\right. \\ &\qquad \left. e^{-p(t_m-t_i)-\frac{\left(X_n-X_j-u(t_m-t_i)\right)^2}{4D_L(t_m-t_i)}-\frac{(Y_l-Y_r)^2}{4D_T(t_m-t_i)}}\right] \qquad (5.43)\end{aligned}$$

where $t_m = \dfrac{H - Z_m}{S}$ is the time for the droplets to fall to the height of the m^{th} sheet of trapping points. If the n, l, m^{th} trapping point is above the release height, then the concentration there is zero. Otherwise, if the n, l, m^{th} trapping point is below the release height, then the concentration there depends upon the sheets of trapping points between it and the release.

As in the 2-D solution, the dispersion both alongwind and crosswind makes it difficult to go any further than the recursive formula above. The first term corresponds to the concentration at the n, l, m^{th} trapping point due purely to the original release, and the second term compensates for the mass which has been removed at at higher trapping points.

Inverting the Laplace transforms:

For $Z_1, \ldots, Z_M > H$, so that all of the sheets of trapping points are above the release height,

$$c\left(x,y,z,t\right) = \begin{cases} 0, & z > H, \\ \dfrac{Q}{4\pi t\sqrt{D_L D_T}} e^{-\frac{(x-X_0-ut)^2}{4D_L t} - \frac{(y-Y_0)^2}{4D_T t}} \delta\left(z-(H-St)\right), & H > z, \end{cases} \tag{5.44}$$

and for $Z_M, \ldots, Z_J < H$, $1 \leq J \leq M$, so that the highest $J-1$ sheets of trapping points are above the release height and the remaining $M-(J-1)$ sheets are below,

$$c\left(x,y,z,t\right) = \begin{cases} 0, & z > H, \\ \dfrac{Q}{4\pi t\sqrt{D_L D_T}} e^{-\frac{(x-X_0-ut)^2}{4D_L t} - \frac{(y-Y_0)^2}{4D_T t}} \delta\left(z-(H-St)\right), & Z_J < z < H, \\ \dfrac{Q}{4\pi t\sqrt{D_L D_T}} e^{-\frac{(x-X_0-ut)^2}{4D_L t} - \frac{(y-Y_0)^2}{4D_T t}} \delta\left(z-(H-St)\right) & \\ \quad - \displaystyle\sum_{n=1}^{N}\sum_{l=1}^{L}\sum_{m=J}^{j} \left[\frac{kc\left(X_n, Y_l, Z_m, t-\left(Z_m-z\right)/S\right)}{4\pi\sqrt{D_L D_T}\left(Z_m-z\right)} \times \right. & \\ \qquad \left. e^{-\frac{S(x-X_n-u(Z_m-z)/S)^2}{4D_L(Z_m-z)} - \frac{S(y-Y_l)^2}{4D_T(Z_m-z)}} \right], & Z_{j+1} < z < Z_j, \\ & (j=J,\ldots,M-1) \\ \dfrac{Q}{4\pi t\sqrt{D_L D_T}} e^{-\frac{(x-X_0-ut)^2}{4D_L t} - \frac{(y-Y_0)^2}{4D_T t}} \delta\left(z-(H-St)\right) & \\ \quad - \displaystyle\sum_{n=1}^{N}\sum_{l=1}^{L}\sum_{m=J}^{M} \left[\frac{kc\left(X_n, Y_l, Z_m, t-\left(Z_m-z\right)/S\right)}{4\pi\sqrt{D_L D_T}\left(Z_m-z\right)} \times \right. & \\ \qquad \left. e^{-\frac{S(x-X_n-u(Z_m-z)/S)^2}{4D_L(Z_m-z)} - \frac{S(y-Y_l)^2}{4D_T(Z_m-z)}} \right], & z < Z_M. \end{cases} \tag{5.45}$$

Similar to the 2-D solution, the horizontal concentration distribution is Gaussian until the level of the trapping points, where some of the droplets are removed at each successive layer of points, leaving a reduced concentration underneath and altering the distribution.

This 3-D solution also inherits the issue of the concentration becoming negative. It is possible to resolve the issue by making the trapping continuous horizontally (both alongwind and crosswind), and this can be done by letting both N and $L \to \infty$ following the procedure described in 2-D. The solution with continuous trapping horizontally is not included here, however, as again it makes little difference to the total trapping and deposit.

Total Droplet Trapping and Deposition

Following Section 5.3, the total mass of droplets trapped by the discretised shelterbelt [kg] is

$$M_{TT} = \sum_{n=1}^{N} \sum_{l=1}^{L} \sum_{m=1}^{M} k\overline{c}\,(X_n, Y_l, Z_m, 0) \tag{5.46}$$

where $\overline{c}\,(X_n, Y_l, Z_m, 0)$ is given by Equation (5.43) with $p = 0$. This leaves a total mass deposit on the ground of $M_{DT} = Q - M_{TT}$ [kg]. The density of deposit on the ground [kg m^{-2}] is

$$\begin{aligned} M_D\,(x,y) &= S\overline{c}\,(x,y,0,0) \\ &= \frac{Q}{4\pi H\sqrt{D_L D_T}} e^{-\frac{S(x-X_0-uH/S)^2}{4D_L H} - \frac{S(y-Y_0)^2}{4D_T H}} \\ &\quad - \sum_{n=1}^{N}\sum_{l=1}^{L}\sum_{m=1}^{M} \frac{k\overline{c}\,(X_n, Y_l, Z_m, 0)}{4\pi Z_m\sqrt{D_L D_T}} e^{-\frac{S(x-X_n-uZ_m/S)^2}{4D_L Z_1} - \frac{S(y-Y_l)^2}{4D_T Z_m}}. \end{aligned} \tag{5.47}$$

To evaluate the total trapping M_{TT} and the density of deposit M_D, one must solve the system of $N \times L \times M$ equations formed from Equation (5.43) at each of the trapping points. For each trapping point, Equation (5.43) is calculated using only values at the sheets of trapping points above it; this means that the system can be solved by working downwards from the highest sheet of trapping points, without having to solve simultaneously.

5.5 Case 2: Non-Zero Vertical Dispersion

In this section we analyse our advection-dispersion model, with trapping in a discretised shelterbelt, in the more realistic case where vertical dispersion of the droplets is significant compared to horizontal dispersion (that is $D_V \neq 0$). In this case the boundary condition of zero vertical dispersive flux on the ground requires $\dfrac{\partial c}{\partial z}(x, y, 0, t) = 0$, and the form of the solution is more complicated.

As in Case 1 where $D_V = 0$, we present solutions in 1-D and 2-D, building up to a full 3-D solution. Once again, the 2-D and 3-D solutions inherit the issue identified in Chapter 4, where, due to the interaction of delta functions, the concentration is negative for a short time in the vicinity of the trapping. The issue can be resolved by making the trapping continuous horizontally in the same manner as for the $D_V = 0$ solutions, though the computation process is made much more difficult by the vertical dispersion. Whilst we have determined solutions with continuous trapping horizontally in this case, they are not included here as it was shown in Case 1 that there is little effect on the total trapping and deposit with a realistic trapping rate (thus no benefit to the extra computational difficulty).

One-Dimensional Solution With Discretised Trapping

In 1-D, and with $D_V \neq 0$, our advection-dispersion model with trapping in a discretised shelterbelt becomes

$$\frac{\partial c}{\partial t} - S\frac{\partial c}{\partial z} = D_V \frac{\partial^2 c}{\partial z^2} + Q\delta\left(z - H\right)\delta\left(t\right) - \sum_{m=1}^{M} kc\left(Z_m, t\right)\delta\left(z - Z_m\right) \tag{5.48}$$

with initial and boundary conditions

$$c\left(z, 0^-\right) = 0,\ c\left(\infty, t\right) = 0 \text{ and } \frac{\partial c}{\partial z}\left(0, t\right) = 0. \tag{5.49}$$

The conceptual situation is now a shelterbelt "slab" discretised using a number of trapping planes, as described on page 78. After release from the source the droplets disperse vertically, whilst falling towards the ground with settling speed S.

A solution to Equation (5.48) is constructed from the solution for a single trapping plane on page 58:

$$c\left(z, t\right) = Qf\left(z, t; H\right) - \sum_{m=1}^{M} \int_0^t kc\left(Z_m, \tau\right) f\left(z, t - \tau; Z_m\right)\ d\tau \tag{5.50}$$

where

$$f\left(z, t; Z\right) = \frac{e^{-\frac{S^2 t}{4D_V} - \frac{S(z-Z)}{2D_V}}}{2\sqrt{\pi D_V t}}\left(e^{-\frac{(z-Z)^2}{4D_V t}} + e^{-\frac{(z+Z)^2}{4D_V t}}\right) - \frac{Se^{\frac{SZ}{D_V}}}{2D_V}\operatorname{erfc}\left(\frac{z + Z + St}{2\sqrt{D_V t}}\right). \tag{5.51}$$

Note that the M, as yet, unknowns $c\left(Z_1, t\right), \ldots, c\left(Z_M, t\right)$ appear inside the integrand in Equation (5.50). Setting $z = Z_m$ gives

$$c\left(Z_m, t\right) = Qf\left(Z_m, t; H\right) - \sum_{i=1}^{M} \int_0^t kc\left(Z_i, \tau\right) f\left(Z_m, t - \tau; Z_i\right)\ d\tau. \tag{5.52}$$

Thus, the concentration at the m^{th} trapping plane depends upon all of the other trapping planes (both above and below it). The first term represents the concentration at the m^{th} trapping plane due purely to the original release, and the second term compensates for the mass removed at all of the trapping planes up until the present time.

The concentration $c(z,t)$ can be evaluated numerically, by solving Equation (5.52) at each trapping plane using the procedure described for the single trapping plane in Chapter 4 (see page 60). The advantage of that particular method is that the concentration at each time step is calculated using values already calculated at previous time steps, thus the system does not have to be solved simultaneously. Other higher order methods which could also be applied may be found for instance in Linz (1985, Chap. 8); as the order increases however, so too does the complexity involved in the computation.

Total Droplet Trapping and Deposition

The total trapping and deposition are found by taking Laplace transforms with respect to t and then setting the transform variable to zero, as described in Section 5.3. The total mass of droplets trapped by the discretised shelterbelt "slab" per unit area is

$$M_{TT} = \sum_{m=1}^{M} k\overline{c}\,(Z_m, 0) \tag{5.53}$$

where

$$\begin{aligned} \overline{c}\,(Z_m,0) &= \frac{Q\overline{f}\,(Z_m,0;H)}{1+k\overline{f}\,(Z_m,0;Z_m)} - \sum_{\substack{i=1\\ i\neq m}}^{M} \frac{k\overline{c}\,(Z_i,0)\,\overline{f}\,(Z_m,0;Z_i)}{1+k\overline{f}\,(Z_m,0;Z_m)} \\ &= \frac{Q}{S+k} e^{-\frac{S(Z_m-H+|Z_m-H|)}{2D_V}} - \sum_{\substack{i=1\\ i\neq m}}^{M} \frac{k\overline{c}\,(Z_i,0)}{S+k} e^{-\frac{S(Z_m-Z_i+|Z_m-Z_i|)}{2D_V}}. \end{aligned} \tag{5.54}$$

The density of deposit on the ground (mass of droplets deposited per unit area) [kg m^{-2}] is then $Q - M_{TT}$. To evaluate the total trapping and the density of deposit, one must solve the system of simultaneous equations formed by Equation (5.54) at each trapping plane.

One-Dimensional Solution With Continuous Trapping

Though complicated by the vertical dispersion, it is still possible in 1-D to determine an analytic solution with continuous trapping. We present this solution here for comparison with the discretised solution obtained above.

The rate of mass removal by the shelterbelt "slab" per unit volume is $k_b R c$, where R is dimensionless and non-zero only within the shelterbelt. As in Case 1 where $D_V = 0$, assuming that the shelterbelt extends vertically between $z = Z_B$ at the base and $z = Z_A$ at the top, R can be expressed in terms of Heaviside functions as

$$R = \mathcal{H}(z - Z_B) - \mathcal{H}(z - Z_A). \tag{5.55}$$

With the concentration denoted by $c_c(z,t)$ [kg m^{-3}] to indicate that it is for continuous trapping, our advection-dispersion model in 1-D and with $D_V = 0$ becomes

$$\frac{\partial c_c}{\partial t} - S\frac{\partial c_c}{\partial z} = D_V \frac{\partial^2 c_c}{\partial z^2} + Q\delta(z - H)\,\delta(t) - k_b c_c\left(\mathcal{H}(z - Z_B) - \mathcal{H}(z - Z_A)\right) \tag{5.56}$$

with initial and boundary conditions

$$c_c\left(z, 0^-\right) = 0,\ c_c(\infty, t) = 0 \text{ and } \frac{\partial c_c}{\partial z}(0,t) = 0.$$

We solve Equation (5.56) by taking Laplace transforms with respect to t in three regions: above the shelterbelt, within the shelterbelt and below the shelterbelt. The concentration $c_c(z,t)$ and the downward vertical flux $Sc_c(z,t) + D_V\frac{\partial c_c}{\partial z}(z,t)$ must match at the interface between each region. The Laplace transform is

$$\overline{c}_c(z,t) = \begin{cases} \alpha_1(p)\,e^{r_2 z} + \dfrac{Qe^{-r_1(H-z)}}{D_V(r_1 - r_2)}\mathcal{H}(H - z) - \dfrac{Qe^{-r_2(H-z)}}{D_V(r_1 - r_2)}\mathcal{H}(z - H), & z > Z_A, \\ \alpha_2(p)\,e^{r_3 z} + \alpha_3(p)\,e^{r_4 z} & \\ \quad -\dfrac{Q}{D_V(r_3 - r_4)}\left(e^{-r_3(H-z)} - e^{-r_4(H-z)}\right)\mathcal{H}(z - H), & Z_A > z > Z_B, \\ \alpha_4(p)\left(e^{r_1 z} - \dfrac{r_1}{r_2}e^{r_2 z}\right) & \\ \quad -\dfrac{Q}{D_V(r_1 - r_2)}\left(e^{-r_1(H-z)} - e^{-r_2(H-z)}\right)\mathcal{H}(z - H), & Z_B > z, \end{cases} \tag{5.57}$$

where

$$r_1 = \frac{1}{2D_V}\left(-S + \sqrt{S^2 + 4pD_V}\right),\ r_2 = \frac{1}{2D_V}\left(-S - \sqrt{S^2 + 4pD_V}\right),$$

$$r_3 = \frac{1}{2D_V}\left(-S + \sqrt{S^2 + 4(p + k_b)D_V}\right), \text{ and } r_4 = \frac{1}{2D_V}\left(-S - \sqrt{S^2 + 4(p + k_b)D_V}\right).$$

The four unknown functions $\alpha_1(p)$, $\alpha_2(p)$, $\alpha_3(p)$ and $\alpha_4(p)$ are determined by solving the following equations which come from the matching conditions between regions:

$$\begin{aligned}\overline{c}_c\left(Z_A^+,p\right) &= \overline{c}_c\left(Z_A^-,p\right) \text{ and } \frac{\partial\overline{c}_c}{\partial z}\left(Z_A^+,p\right)=\frac{\partial\overline{c}_c}{\partial z}\left(Z_A^-,p\right),\\ \overline{c}_c\left(Z_B^+,p\right) &= \overline{c}_c\left(Z_B^-,p\right) \text{ and } \frac{\partial\overline{c}_c}{\partial z}\left(Z_B^+,p\right)=\frac{\partial\overline{c}_c}{\partial z}\left(Z_B^-,p\right).\end{aligned}$$

The Laplace transform $\overline{c}_c(z,p)$ does not appear to be analytically invertible, however, it does lead directly to the quantities of particular interest, that is, the total trapping and deposit.

Total Droplet Trapping and Deposition

With continuous trapping, the total mass of droplets trapped by the shelterbelt "slab" per unit area is denoted M_{TTc} [kg m^{-2}], and it is found by integrating the rate of mass removal per unit volume with respect to space and time:

$$\begin{aligned}M_{TTc} &= \int_0^\infty\int_0^\infty k_b c_c(z,t)\left(\mathcal{H}(z-Z_B)-\mathcal{H}(z-Z_A)\right)\,dz\,dt\\ &= \int_{Z_B}^{Z_A} k_b\overline{c}_c(z,0)\,dz.\end{aligned} \tag{5.58}$$

There are three possible scenarios: (i) the release height is below the shelterbelt, (ii) the release height is within the shelterbelt, and (iii) the release height is above the shelterbelt.

(i). For $H < Z_B$, so that the release height is below the shelterbelt,

$$\begin{aligned}M_{TTc} = k_b\Bigg[&r_4\left(\alpha_2(p)-\frac{Qe^{-r_3H}}{D_V(r_3-r_4)}\right)\left(e^{r_3Z_A}-e^{r_3Z_B}\right)\\ &+r_3\left(\alpha_3(p)+\frac{Qe^{-r_4H}}{D_V(r_3-r_4)}\right)\left(e^{r_4Z_A}-e^{r_4Z_B}\right)\Bigg]_{p=0}.\end{aligned} \tag{5.59}$$

(ii). For $Z_B < H < Z_A$, so that the release height is within the shelterbelt,

$$\begin{aligned}M_{TTc} = k_b\Bigg[&r_4\left(\alpha_2(p)-\frac{Qe^{-r_3H}}{D_V(r_3-r_4)}\right)e^{r_3Z_A}+r_3\left(\alpha_3(p)+\frac{Qe^{-r_4H}}{D_V(r_3-r_4)}\right)e^{r_4Z_A}\\ &-\frac{Q}{D_V}-r_4\alpha_2(p)\,e^{r_3Z_B}-r_3\alpha_3(p)\,e^{r_4Z_B}\Bigg]_{p=0}.\end{aligned} \tag{5.60}$$

(iii). For $Z_A < H$, so that the shelterbelt is below the release height,

$$M_{TTc} = k_b\left[r_4\alpha_2(p)\left(e^{r_3Z_A}-e^{r_3Z_B}\right)+r_3\alpha_3(p)\left(e^{r_4Z_A}-e^{r_4Z_B}\right)\right]_{p=0}. \tag{5.61}$$

The density of deposit on the ground is then $M_{Dc} = Q - M_{TTc}$ [kg m^{-2}], that is, what remains of the original release.

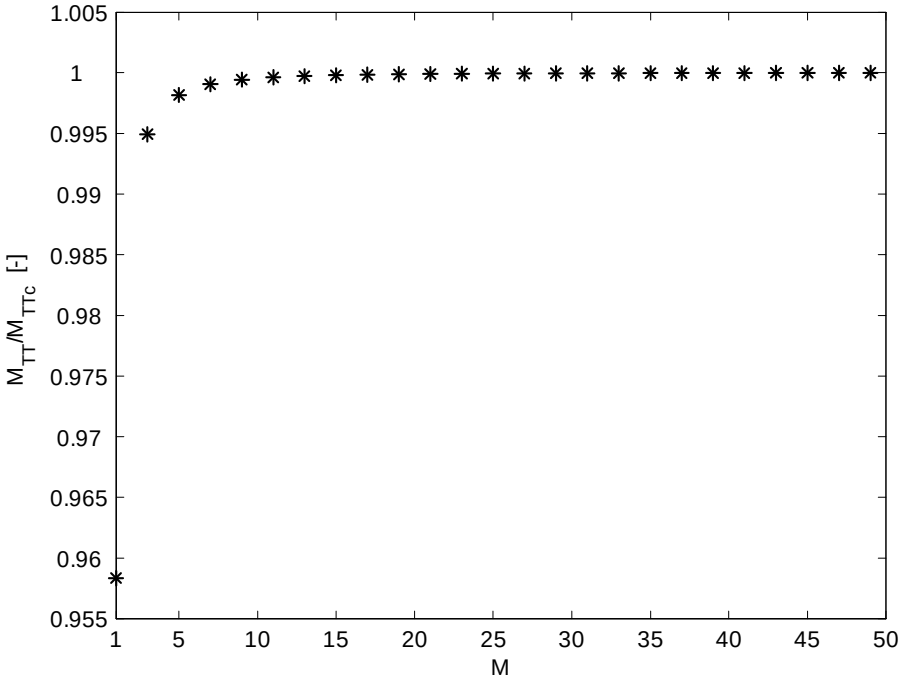

Figure 5.8: A measure of the accuracy of the discretised solution, illustrated by the ratio M_{TT}/M_{TTc}, as the number of trapping planes M increases. M_{TT} [kg m^{-2}] is the total trapping from the discretised solution, and M_{TTc} is the corresponding value from the continuous solution. See the text for parameter values.

Comparison with the Discretised Solution

Here we compare the total trapping from the discretised solution, for a varying number of trapping planes, against the total trapping from the continuous solution. The parameter values used are the same as those for the comparative example with $D_V = 0$ in Case 1; these are $S = 0.2$ m s^{-1}, $D_V = 1$ m^2 s^{-1}, $Q = 1$ kg m^{-2} and $H = 3$ m for the release, and $Z_B = 0.5$ m, $Z_A = 2.5$ m and $k_b = 0.5$ s^{-1} for the shelterbelt "slab".

Figure 5.8 shows the dimensionless ratio M_{TT}/M_{TTc} for a varying number of trapping planes M; M_{TT} is the total trapping [kg m^{-2}] from the discretised solution, and M_{TTc} is the corresponding value from the continuous solution. The accuracy of the discretised solution increases with the number of trapping planes, though it rapidly reaches a consistent level. In contrast to Case 1 where $D_V = 0$, M_{TT} is always a little lower here than M_{TTc}. In this example, even with only a single trapping plane M_{TT} is only less than M_{TTc} by 4.2 %.

Two-Dimensional Solution With Discretised Trapping

In 2-D, and with $D_V \neq 0$, our advection-dispersion model with trapping in a discretised shelterbelt becomes

$$\begin{aligned}\frac{\partial c}{\partial t} + u\frac{\partial c}{\partial x} - S\frac{\partial c}{\partial z} &= D_L\frac{\partial^2 c}{\partial x^2} + D_V\frac{\partial^2 c}{\partial z^2} + Q\delta\left(x - X_0\right)\delta\left(z - H\right)\delta\left(t\right) \\ &\quad - \sum_{n=1}^{N}\sum_{m=1}^{M} kc\left(X_n, Z_m, t\right)\delta\left(x - X_n\right)\delta\left(z - Z_m\right) \qquad (5.62)\end{aligned}$$

with initial and boundary conditions

$$\begin{gathered} c\left(x, z, 0^-\right) = 0, \\ c\left(x, z, t\right) \to 0 \text{ as } x \to \pm\infty, \text{ and } z \to \infty, \text{ and} \\ \frac{\partial c}{\partial z}\left(x, 0, t\right) = 0. \end{gathered}$$

Page 86 contains a description of the conceptual situation, which is now trapping at an infinitely long rectangular shelterbelt discretised using a 2-D array of trapping lines. After release from the source the droplets disperse alongwind and vertically, whilst travelling with the mean windspeed u and falling at settling speed S.

A solution to Equation (5.62) is constructed from the solution for a single trapping line on page 63:

$$c\left(x, z, t\right) = Qf\left(x, z, t; X_0, H\right) - \sum_{n=1}^{N}\sum_{m=1}^{M}\int_0^t kc\left(X_n, Z_m, \tau\right) f\left(x, z, t - \tau; X_n, Z_m\right)\, d\tau \qquad (5.63)$$

where

$$\begin{aligned} f\left(x, z, t; X, Z\right) &= \frac{e^{-\frac{(x-X-ut)^2}{4D_L t}}}{2\sqrt{\pi D_L t}}\left[\frac{e^{-\frac{S^2 t}{4D_V} - \frac{S(z-Z)}{2D_V}}}{2\sqrt{\pi D_V t}}\left(e^{-\frac{(z-Z)^2}{4D_V t}} + e^{-\frac{(z+Z)^2}{4D_V t}}\right)\right. \\ &\quad \left. - \frac{Se^{\frac{SZ}{D_V}}}{2D_V}\operatorname{erfc}\left(\frac{z + Z + St}{2\sqrt{D_V t}}\right)\right]. \qquad (5.64)\end{aligned}$$

Note that the $N \times M$, as yet unknown values of $c\left(X_1, Z_1, t\right), \ldots, c\left(X_N, Z_M, t\right)$ appear inside the integrand in Equation (5.63). Setting $(x, z) = (X_n, Z_m)$ gives

$$c\left(X_n, Z_m, t\right) = Qf\left(X_n, Z_m, t; X_0, H\right) - \sum_{j=1}^{N}\sum_{i=1}^{M}\int_0^t kc\left(X_n, Z_m, t - \tau; X_j, Z_i\right)\, d\tau. \qquad (5.65)$$

Thus, the concentration at the n, m^{th} trapping line depends upon all of the other trapping lines. The first term represents the concentration at the n, m^{th} trapping line due purely to the original

release, and the second term compensates for the mass which has been removed at all of the trapping lines up until the present time.

As mentioned in the opening of Case 2, this solution inherits the issue identified for the single trapping line in Chapter 4 (see page 63), where the concentration is negative for a short time in the vicinity of the trapping. It is possible to resolve the issue by making the trapping continuous alongwind following the procedure described in 2-D for Case 1, though this is not included here.

Total Droplet Trapping and Deposition

Following Section 5.3, the total mass of droplets trapped by the discretised shelterbelt per unit crosswind length [kg m^{-1}] is

$$M_{TT} = \sum_{n=1}^{N} \sum_{m=1}^{M} k\overline{c}\left(X_n, Z_m, 0\right) \tag{5.66}$$

where

$$\overline{c}\left(X_n, Z_m, 0\right) = \frac{Q\overline{f}\left(X_n, Z_m, 0; X_0, H\right)}{1 + k\overline{f}\left(X_n, Z_m, 0; X_n, Z_m\right)} - \sum_{\substack{j=1 \\ (j,i)\neq(n,m)}}^{N} \sum_{i=1}^{M} \frac{k\overline{c}\left(X_j, Z_i, 0\right)\overline{f}\left(X_n, Z_m, 0; X_j, Z_i\right)}{1 + k\overline{f}\left(X_n, Z_m, 0; X_n, Z_m\right)} \tag{5.67}$$

leaving a total mass deposit per unit crosswind length of $M_{DT} = Q - M_{TT}$ [kg m^{-1}]. The density of deposit on the ground [kg m^{-2}] is

$$\begin{aligned} M_D\left(x\right) &= S\overline{c}\left(x, 0, 0\right) \\ &= SQ\overline{f}\left(x, 0, 0; X_0, H\right) - \sum_{n=1}^{N} \sum_{m=1}^{M} Sk\overline{c}\left(X_n, Z_m, 0\right) f\left(x, 0, 0; X_n, Z_m\right). \end{aligned} \tag{5.68}$$

To evaluate the total trapping M_{TT} and the density of deposit M_D, one must solve the system of simultaneous equations formed by Equation (5.67) at each trapping line.

For $(x, z) \neq (X, Z)$, the required transform is

$$\begin{aligned} \overline{f}\left(x, z, 0; X, Z\right) = \frac{e^{\frac{u(x-X)}{2D_L}}}{2\pi\sqrt{D_L D_V}} \Bigg(& e^{-\frac{S(z-Z)}{2D_V}} \left[K_0\left(\frac{\alpha\beta_1\left(x, z\right)}{2}\right) + K_0\left(\frac{\alpha\beta_2\left(x, z\right)}{2}\right)\right] \\ & - \frac{S}{D_V}\int_z^{\infty} e^{-\frac{S(\xi-Z)}{2D_V}} K_0\left(\frac{\alpha\beta_2\left(x, \xi\right)}{2}\right) d\xi \Bigg) \end{aligned} \tag{5.69}$$

where

$$\alpha = \sqrt{\frac{u^2}{D_L} + \frac{S^2}{D_V}},\ \beta_1(x,z) = \sqrt{\frac{(x-X)^2}{D_L} + \frac{(z-Z)^2}{D_V}} \text{ and } \beta_2(x,z) = \sqrt{\frac{(x-X)^2}{D_L} + \frac{(z+Z)^2}{D_V}}.$$

Otherwise, for $(x,z) = (X,Z)$ the required transform is

$$\begin{aligned}\overline{f}(X,Z,0;X,Z) &= \frac{1}{2\pi\sqrt{D_L D_V}}\left[-\frac{1}{2}\left(\ln\left(\frac{\alpha^2}{4}\right)+\gamma\right) + K_0\left(\frac{\alpha Z}{\sqrt{D_V}}\right)\right. \\ &\quad \left. -\frac{S}{D_V}\int_Z^\infty e^{-\frac{S(\xi-Z)}{2D_V}} K_0\left(\frac{\alpha(\xi+Z)}{2\sqrt{D_V}}\right)\, d\xi\right]. \qquad (5.70)\end{aligned}$$

In Equations (5.69) and (5.70), γ = Euler's constant = 0.57722... (Zemanian, 1987, p. 346) and K_0 is a modified Bessel function of the second kind of order zero (Weisstein, 2002).

An Illustrative Example of the Two-Dimensional Solution

The following example illustrates the 2-D solution with discretised trapping. The parameter set used here is given in Table 5.3. A settling speed of $S = 0.2$ m s^{-1} corresponds to droplets of approximate diameter $d = 44$ μm, and dominant turbulence length scales of $(L_L, L_V) = (2,1)$ m give dispersion coefficients $(D_L, D_V) = u(L_L, L_V) = (2,1)$ m^2 s^{-1}. The shelterbelt extends vertically between $Z_B = 0.5$ m and $Z_A = 8.5$ m, and alongwind between $X_A = 4$ m and $X_B = 8$ m. The size of the array of trapping lines into which the shelterbelt is divided is $N \times M = 2 \times 40$, thus there are 80 trapping lines each with effective trapping rate $k = 0.2$ m^2 s^{-1}.

Table 5.3: Parameter set used to generate Figures 5.9 and 5.10.

u	S	(L_L, L_V)	Q	(X_0, H)	k_b	$N \times M$	$\Delta x \Delta z$
1 m s^{-1}	0.2 m s^{-1}	$(2,1)$ m	1 kg m^{-1}	$(0,4)$ m	0.5 s^{-1}	2×40	0.4 m^2

Figure 5.9 shows cross-sections of the density of deposit [kg m^{-2}] as calculated from Equation (5.66); the density of deposit with trapping is denoted M_D, and the corresponding value without trapping is denoted M_D^*. This figure features the "elongated tail" as a result of the vertical dispersion – the deposition profile is not symmetric because droplets which disperse upwards spend longer in the air and are blown further before depositing.

The corresponding percentage reduction in density of deposit as a result of the trapping is shown in Figure 5.10. There is significant reduction downwind of the shelterbelt, and this strength of reduction persists much further downwind than for the example with $D_V = 0$. According to

Equation (5.66), the total trapping here is $M_{TT} = 0.61$ kg m^{-1}, whereas in the example with $D_V = 0$ it was $M_{TT} = 0.78$ kg m^{-1}.

Three-Dimensional Solution With Discretised Trapping

In all three spatial dimensions, and with $D_V \neq 0$, our advection-dispersion model with trapping in a discretised shelterbelt is given by Equation (5.3); that is

$$\begin{aligned}\frac{\partial c}{\partial t} + u\frac{\partial c}{\partial x} - S\frac{\partial c}{\partial z} &= D_L\frac{\partial^2 c}{\partial x^2} + D_T\frac{\partial^2 c}{\partial y^2} + D_V\frac{\partial^2 c}{\partial z^2} + Q\delta\left(x - X_0\right)\delta\left(y - Y_0\right)\delta\left(z - H\right)\delta\left(t\right) \\ &\quad - \sum_{n=1}^{N}\sum_{l=1}^{L}\sum_{m=1}^{M} kc\left(X_n, Y_l, Z_m, t\right)\delta\left(x - X_n\right)\delta\left(y - Y_l\right)\delta\left(z - Z_m\right) \quad (5.71)\end{aligned}$$

with initial and boundary conditions

$$\begin{gathered} c\left(x, y, z, 0^-\right) = 0, \\ c\left(x, y, z, t\right) \to 0 \text{ as } x, y \to \pm\infty, \text{ and } z \to +\infty, \text{ and} \\ \frac{\partial c}{\partial z}\left(x, y, 0, t\right) = 0. \end{gathered}$$

To recap, a rectangular shelterbelt is discretised by dividing it into a 3-D array of blocks with the trapping in each block concentrated to the mid-point (see Section 5.1). After release from the source the droplets disperse horizontally (both alongwind and crosswind) and vertically, whilst travelling with the mean windspeed u and falling at settling speed S.

A solution to Equation (5.71) is constructed from the solution for a single trapping point on page 68:

$$\begin{aligned} c\left(x, y, z, t\right) &= Qf\left(x, y, z, t; X_0, Y_0, H\right) \\ &\quad - \sum_{n=1}^{N}\sum_{l=1}^{L}\sum_{m=1}^{M}\int_0^t kc\left(X_n, Y_l, Z_m, \tau\right) f\left(x, y, z, t - \tau; X_n, Y_l, Z_m\right)\, d\tau \end{aligned} \quad (5.72)$$

where

$$\begin{aligned} f\left(x, y, z, t; X, Y, Z\right) &= \frac{e^{-\frac{(x-X-ut)^2}{4D_L t} - \frac{(y-Y)^2}{4D_T t}}}{4\pi t\sqrt{D_L D_T}}\left[\frac{e^{-\frac{S^2 t}{4D_V} - \frac{S(z-Z)}{2D_V}}}{2\sqrt{\pi D_V t}}\left(e^{-\frac{(z-Z)^2}{4D_V t}} + e^{-\frac{(z+Z)^2}{4D_V t}}\right)\right. \\ &\quad \left. - \frac{Se^{-\frac{SZ}{D_V}}}{2D_V}\operatorname{erfc}\left(\frac{z + Z + St}{2\sqrt{D_V t}}\right)\right]. \end{aligned} \quad (5.73)$$

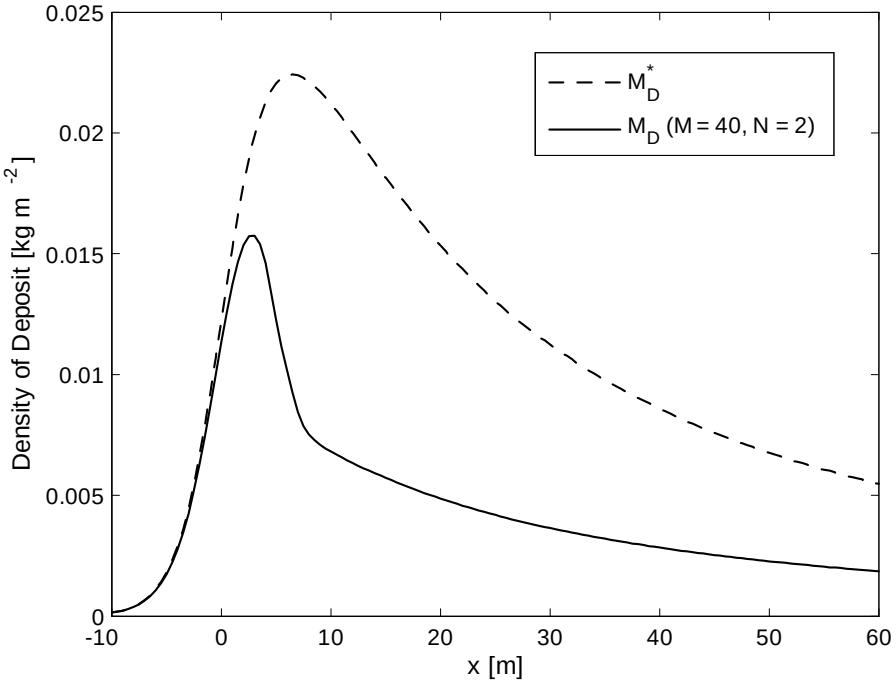

Figure 5.9: Cross-section of the density of deposit [kg m^{-2}], resulting from a line release with non-zero vertical dispersion and an $N \times M$ array of trapping lines. M_D denotes the density of deposit with trapping, and M_D^* denotes the corresponding value without trapping. Parameter values are as given in Table 5.3.

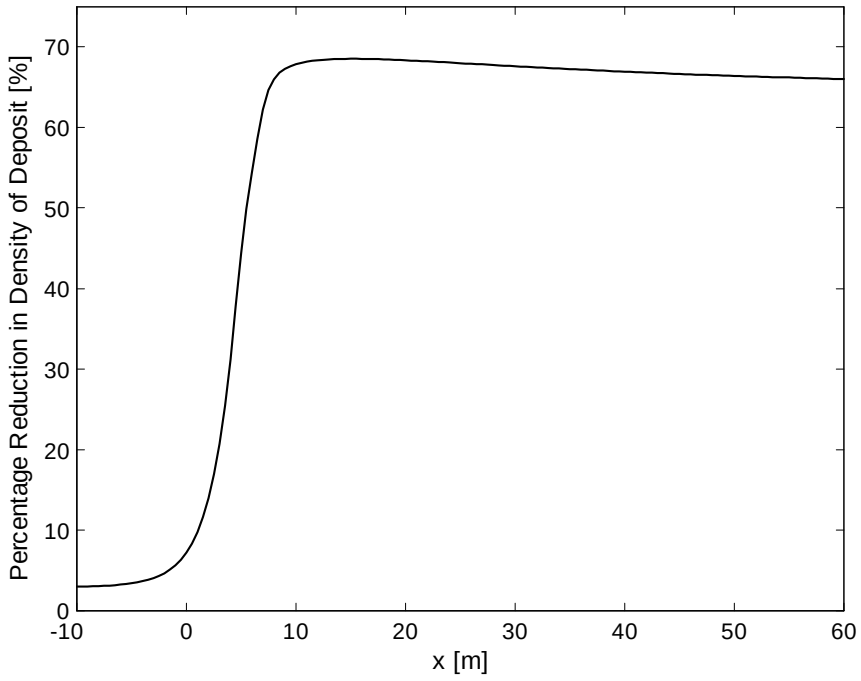

Figure 5.10: Cross-section of the percentage reduction in density of deposit as a result of the trapping in Figure 5.9. Parameter values are the same as for Figure 5.10.

The $N \times L \times M$, as yet unknown values of $c(X_1, Y_1, Z_1, t), \ldots, c(X_N, Y_L, Z_M)$ appear inside the integrand in Equation (5.72). Setting $(x, y, z) = (X_n, Y_l, Z_m)$ gives

$$\begin{aligned} c(X_n, Y_l, Z_m, t) &= Qf(X_n, Y_l, Z_m, t; X_0, Y_0, H) \\ &\quad - \sum_{j=1}^{N}\sum_{r=1}^{L}\sum_{i=1}^{M}\int_0^t kc(X_j, Y_r, Z_i, \tau)\, f(X_n, Y_l, Z_m, t-\tau; X_j, Y_r, Z_i)\; d\tau. \end{aligned} \tag{5.74}$$

Thus, the concentration at the n, l, m^{th} trapping point depends upon all of the other trapping points. The first term represents the concentration at the n, l, m^{th} trapping point purely due to the original release, and the second term compensates for the mass removal at all of the trapping points up until the present time.

This solution, being an extension from 2-D, also exhibits a negative concentration for a short time in the vicinity of the trapping. It is possible to resolve the issue by making the trapping continuous horizontally (both alongwind and crosswind), and this can be done by letting both N and $L \to \infty$ following the procedure described in 2-D for Case 1. We do not pursue this further here, as the issue has negligible effect on the total trapping and deposit with realistic trapping rates (see page 94).

Total Droplet Trapping and Deposition

Following Section 5.3, the total mass of droplets trapped by the discretised shelterbelt [kg] is

$$M_{TT} = \sum_{n=1}^{N}\sum_{l=1}^{L}\sum_{m=1}^{m} k\overline{c}(X_n, Y_l, Z_m, 0) \tag{5.75}$$

where

$$\begin{aligned} \overline{c}(X_n, Y_l, Z_m, 0) &= \frac{Q\overline{f}(X_n, Y_l, Z_m, 0; X_0, Y_0, H)}{1 + k\overline{f}(X_n, Y_l, Z_m, 0; X_n, Y_l, Z_m)} \\ &\quad - \sum_{\substack{j=1 \\ (j,r,i)\neq(n,l,m)}}^{N}\sum_{r=1}^{L}\sum_{i=1}^{M} \frac{k\overline{c}(X_j, Y_r, Z_i, 0)\,\overline{f}(X_n, Y_l, Z_m, 0; X_j, Y_r, Z_i)}{1 + k\overline{f}(X_n, Y_l, Z_m, 0; X_n, Y_l, Z_m)}. \end{aligned} \tag{5.76}$$

This leaves a total mass deposit on the ground of $M_{DT} = Q - M_{TT}$ [kg]. The density of deposit on the ground [kg m^{-2}] is

$$\begin{aligned} M_D(x, y) &= S\overline{c}(x, y, 0, 0) \\ &= SQ\overline{f}(x, y, 0, 0; X_0, Y_0, H) \\ &\quad - \sum_{n=1}^{N}\sum_{l=1}^{L}\sum_{m=1}^{M} Sk\overline{c}(X_n, Y_l, Z_m, 0)\,\overline{f}(x, y, 0, 0; X_n, Y_l, Z_m). \end{aligned} \tag{5.77}$$

To evaluate the total trapping M_{TT} and the density of deposit M_D, one must solve the system of simultaneous equations formed by Equation (5.76) at each trapping point.

For $(x,y,z) \neq (X,Y,Z)$, the required transform is

$$\begin{aligned}\overline{f}\,(x,y,z,0;X,Y,Z) &= \frac{e^{\frac{u(x-X)}{2D_L}}}{4\pi\sqrt{D_L D_T D_V}}\left[e^{-\frac{S(z-Z)}{2D_V}}\left(\frac{e^{-\frac{1}{2}\alpha\beta_1(x,y,z)}}{\beta_1\,(x,y,z)}+\frac{e^{-\frac{1}{2}\beta_2(x,y,z)}}{\beta_2\,(x,y,z)}\right)\right.\\ &\left.-\frac{S}{D_V}\int_z^\infty e^{-\frac{S(\xi-Z)}{2D_V}}\frac{e^{-\frac{1}{2}\alpha\beta_2(x,y,\xi)}}{\beta_2\,(x,y,\xi)}\,d\xi\right] \qquad (5.78)\end{aligned}$$

where

$$\alpha=\sqrt{\frac{u^2}{D_L}+\frac{S^2}{D_V}},\quad \beta_1\,(x,y,z)=\sqrt{\frac{(x-X)^2}{D_L}+\frac{(y-Y)^2}{D_T}+\frac{(z-Z)^2}{D_V}},\text{ and}$$

$$\beta_2\,(x,y,z)=\sqrt{\frac{(x-X)^2}{D_L}+\frac{(y-Y)^2}{D_T}+\frac{(z+Z)^2}{D_V}}.$$

Otherwise, for $(x,y,z)=(X,Y,Z)$ the required transform is

$$\begin{aligned}\overline{f}\,(X,Y,Z,0;X,Y,Z) &= \frac{1}{4\pi\sqrt{D_L D_T D_V}}\left[-\frac{\alpha}{2}+\frac{\sqrt{D_V}}{2Z}e^{-\frac{\alpha Z}{\sqrt{D_V}}}\right.\\ &\left.-\frac{S}{\sqrt{D_V}}\int_Z^\infty\frac{1}{(\xi+Z)}e^{-\frac{S(\xi-Z)}{2D_V}-\frac{\alpha(\xi+Z)}{2\sqrt{D_V}}}\,d\xi\right]. \qquad (5.79)\end{aligned}$$

with α as given above.

An Illustrative Example of the Three-Dimensional Solution

The following example is intended to illustrate the 3-D solution with discretised trapping. The parameter set used here is given in Table 5.4. A settling speed of $S = 0.2$ m s^{-1} corresponds to droplets of approximate diameter $d = 44$ μm, and dominant turbulence length scales of $(L_L, L_T, L_V) = (2,2,1)$ m give dispersion coefficients $(D_L, D_T, D_V) = u\,(L_L, L_T, L_V) = (2,2,1)$ m^2 s^{-1}. The shelterbelt extends vertically between $Z_B = 0.5$ m and $Z_A = 8.5$ m, alongwind between $X_A = 4$ m $X_B = 8$ m, and crosswind between $Y_A = -4$ m and $Y_B = 4$ m. The size of the array of trapping points into which the shelterbelt is divided is $N \times L \times M = 2 \times 4 \times 40$, thus there are 320 trapping points and the effective trapping rate for each is $k = 0.4$ m^3 s^{-1}.

Table 5.4: Parameter set used to generate Figures 5.11, 5.12 and 5.13.

u	S	(L_L, L_T, L_V)	Q	(X_0, Y_0, H)	k_b	$N \times L \times M$	$\Delta x \Delta y \Delta z$
1 m s^{-1}	0.2 m s^{-1}	$(2, 2, 1)$ m	1 kg	$(0, 0, 4)$ m	0.5 s^{-1}	$2 \times 4 \times 40$	0.8 m^3

Figure 5.11 shows contours of the density of deposit [kg m^{-2}] without trapping, calculated by setting $k = 0$ in Equation (5.77). Note the oval shape of the contours; they are elongated in the downwind direction as a result of the vertical dispersion – droplets which are dispersed upwards spend longer in the air, and are blown further before depositing. The corresponding contours of the density of deposit with trapping are shown in Figure 5.12; the contour lines are compressed and bent as the density is reduced behind the trapping points.

Figure 5.13 shows the percentage reduction in density of deposit as a result of the trapping; the shadow area of reduced deposit downwind of the shelterbelt is clearly visible. According to Equation (5.75), the total mass trapped here is $M_{TT} = 0.45$ kg.

5.6 Chapter Summary

In this chapter we took the solution to our advection-dispersion model with a point representation for trapping, described in Chapter 4, and used it to construct a solution for trapping in a discretised shelterbelt. The discretisation was achieved by dividing the shelterbelt into a 3-D array of smaller blocks, with the trapping in each block concentrated to the point at its centre.

As for the single trapping point in the previous chapter, we analysed the model with trapping in a discretised shelterbelt for two separate cases: zero and non-zero vertical dispersion. In each case we presented solutions in 1-D and 2-D, building up to a full 3-D solution. In 1-D, we were also able to determine analytic solutions with continuous trapping for comparison with our discretised solutions. It was observed that the 2-D and 3-D solutions exhibit negative concentrations in the vicinity of the trapping – this is an artefact of the point representation for trapping carried over from Chapter 4, and caused by focusing the trapping at an infinitely small point. We showed how the problem can be resolved by making the trapping continuous horizontally within the shelterbelt, thus spreading it out over a finite area rather than an infinitely small point.

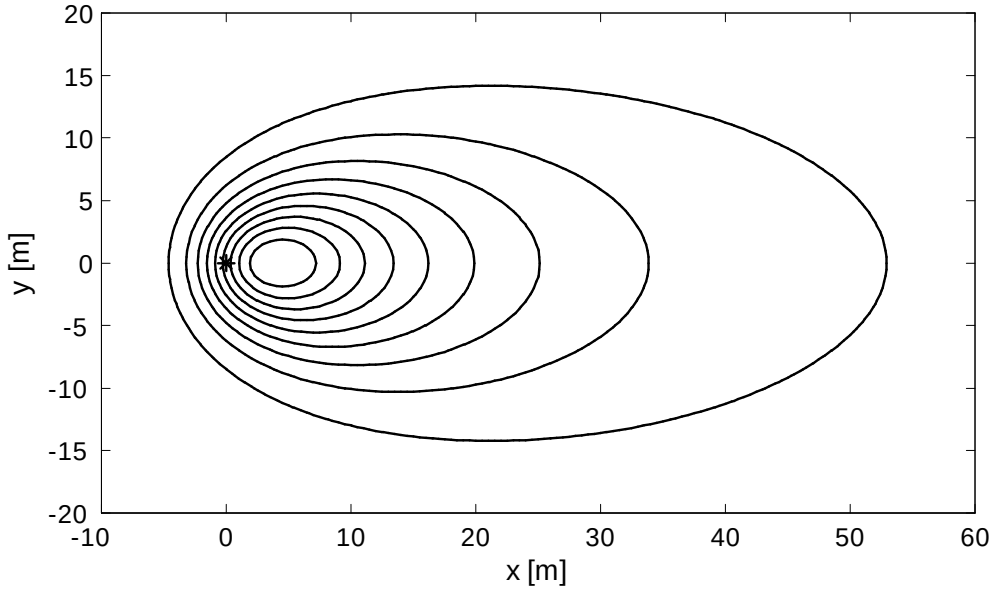

Figure 5.11: Contours of the density of deposit M_D [kg m^{-2}], resulting from a point release (marked with a $*$) with non-zero vertical dispersion and no trapping. The spacing between contour lines is 0.00018 kg m^{-2}, the outermost contour has value $M_D = 0.00018$ kg m^{-2}, and the innermost contour has value $M_D = 0.0016$ kg m^{-2}. Parameter values are as given in Table 5.4.

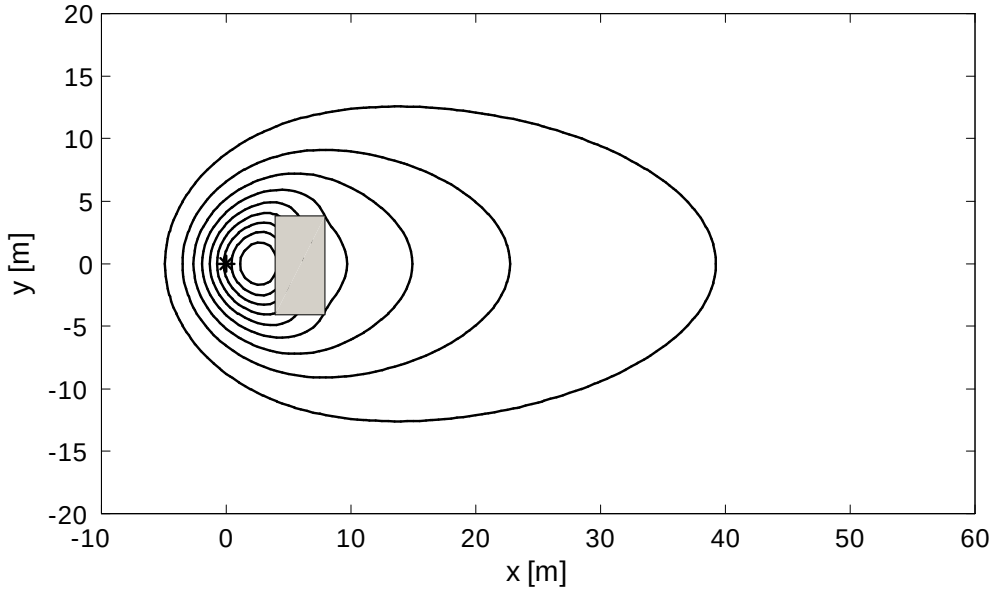

Figure 5.12: Contours of the density of deposit M_D [kg m^{-2}], resulting from a point release (marked with a $*$), with non-zero vertical dispersion and trapping at a $2 \times 4 \times 40$ array of points. The region containing the trapping points is shaded in grey. The spacing between contours is 0.00015 kg m^{-2}, the outermost contour has value $M_D = 0.00015$ kg m^{-2}, and the innermost contour has value $M_D = 0.0014$ kg m^{-2}. Parameter values are as given in Table 5.4.

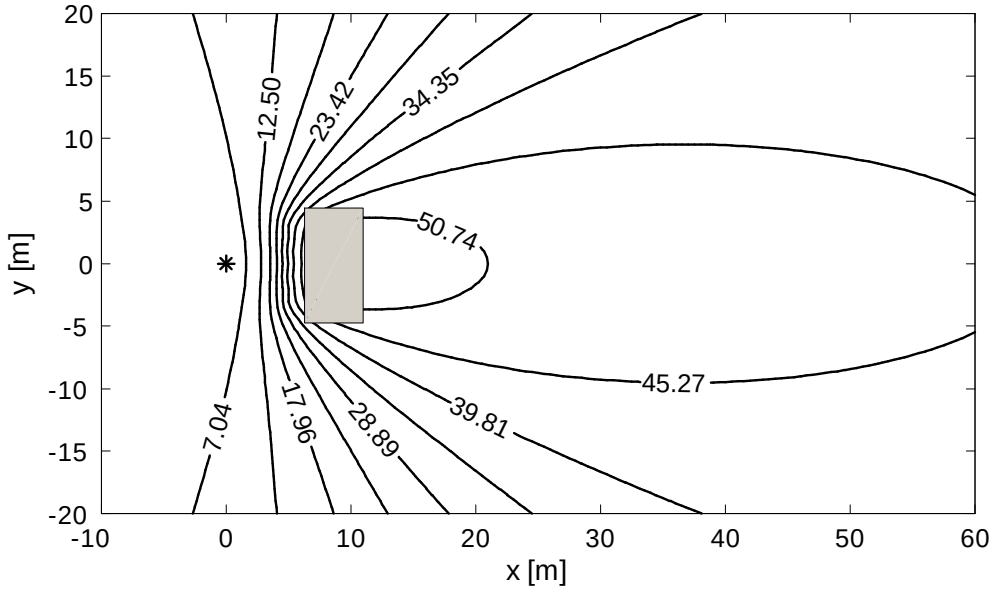

Figure 5.13: Contours of the percentage reduction in density of deposit between Figures 5.11 and 5.12 as a result of the trapping. The release point is marked with a $*$, and the region containing the trapping points is shaded grey. Parameter values are the same as for Figure 5.11 and Figure 5.12.

However, comparative examples showed very little difference in the total trapping and deposit because the region in which the concentration is negative is very small.

One could spend a considerable length of time experimenting with various parameter values and array sizes for the discretisation of the shelterbelt, and we leave this as a subject for further study.

Chapter 6

Trapping With Evaporation

The previous models in Chapters 3 – 5 apply to droplets which are not evaporating. In this chapter, we take the information on droplet evaporation from Chapter 2, and incorporate it into our advection-dispersion model with the point representation for trapping from Chapter 4.

We begin by setting up the model with evaporation, and then introduce approximations for the droplet mass and settling speed to simplify calculation later in the chapter. Following the analysis of the previous models we seek analytic solutions, first in the simple case where vertical dispersion is negligible compared to horizontal dispersion, and then in the more realistic but also more difficult case of significant vertical dispersion. For each case, we present solutions in one and two dimensions, working towards a full three-dimensional solution. Fully analytic solutions for the case of significant vertical dispersion could not be found; instead the solutions are embedded in integral equations which we evaluate numerically.

The solutions in this chapter also inherit the issue of a negative concentration in the vicinity of the trapping, which was identified in Chapter 4 as an artefact of the point representation for trapping. We do not discuss the issue any further in this chapter, as it was shown in the previous chapter to have little effect with realistic trapping rates (see pages 91 – 95).

6.1 Advection-Dispersion Model with Trapping and Evaporation

With evaporation of the droplets, it is convenient to solve our advection-dispersion model in terms of the number concentration rather than the mass concentration. The advantage of using the number concentration is that there is no evaporation (or mass loss) term in the model. All

droplets count the same in the number concentration no matter their mass; in fact, we continue to count even droplets which have completely evaporated – these are just considered as droplets with zero mass.

A cloud of evaporating droplets is still advected by the wind and dispersed by turbulence, all whilst falling under the influence of gravity, however the rate at which the droplets fall decreases with time as they become smaller and lighter. We assume that the relative humidity and ambient temperature are uniform, and that the evaporating droplets do not affect the relative humidity; as a result, the amount of evaporation from a droplet is only dependent on the length of time it spends in the air. The number concentration of droplets per unit volume of air is denoted $C(x, y, z, t)$ [# m^{-3}]; our advection-dispersion model in terms of C, with evaporation and a point representation for trapping, is:

$$\begin{aligned}\frac{\partial C}{\partial t} + u\frac{\partial C}{\partial x} - S(t)\frac{\partial C}{\partial z} &= D_L\frac{\partial^2 C}{\partial x^2} + D_T\frac{\partial^2 C}{\partial y^2} + D_V\frac{\partial^2 C}{\partial z^2} \\ &\quad + \frac{Q}{m_0}\delta(x - X_0)\,\delta(y - Y_0)\,\delta(z - H)\,\delta(t) \\ &\quad - kC(X_1, Y_1, Z_1, t)\,\delta(x - X_1)\,\delta(y - Y_1)\,\delta(z - Z_1) \qquad (6.1)\end{aligned}$$

where m_0 is the initial mass of each droplet, and the remaining parameters are as defined in the previous models in Chapters 3 – 5. The unit of k [m^3 s^{-1}] is the same as in the previous models (since it is defined by $k = k_b\Delta x\Delta y\Delta z$, and k_b is a ratio of droplets trapped per unit time). In theory, the size of k should change with time as the droplets evaporate (smaller droplets are less efficiently trapped, see Section 3.3). At present, we assume that k remains constant; this could be a topic for future research. The initial and boundary conditions are also the same as those for the previous models. Note that evaporation only appears indirectly in Equation (6.1) via the settling speed $S(t)$, which decreases with time as the droplets become smaller and lighter.

Equation (6.1) may be derived following the argument in Chapter 3, but with conservation of number rather than mass. Some important points to note are: (i) we assume that evaporation does not affect the dispersion, that is, the droplets are dispersed independently of their size, and (ii) the situation is greatly simplified by the choice of an instantaneous release, which means that at any given instant, all of the droplets have been in the air for the same length of time, therefore they have all experienced the same amount of evaporation, and consequently all have the same settling speed. If the release were not instantaneous, the air would contain droplets which have been airborne for differing lengths of time, and so there would be a distribution of droplet sizes with an associated distribution of settling speeds.

At any time t, the mass concentration $c(x, y, z, t)$ [kg m^{-3}] is related to the number concentration by $c = m(t) C$. Multiplying Equation (6.1) by the mass $m(t)$, our advection dispersion model with evaporation and a point representation for trapping becomes, in terms of the mass concentration:

$$\begin{aligned} \frac{\partial c}{\partial t} + u\frac{\partial c}{\partial x} - S(t)\frac{\partial c}{\partial z} - E(t)c &= D_L\frac{\partial^2 c}{\partial x^2} + D_T\frac{\partial^2 c}{\partial y^2} + D_V\frac{\partial^2 c}{\partial z^2} \\ &\quad + Q\delta(x - X_0)\delta(y - Y_0)\delta(z - H)\delta(t) \\ &\quad - kc(X_1, Y_1, Z_1, t)\delta(x - X_1)\delta(y - Y_1)\delta(z - Z_1) \end{aligned} \quad (6.2)$$

where $E(t)c = \frac{1}{m}\frac{dm}{dt}c$ is the evaporation term. The evaporation term acts as a mass sink, where the rate of removal depends upon the local concentration. If there is no evaporation, then $E(t) = 0$ and $S(t) = S =$ constant, and Equation (6.2) is the same as the model in Chapter 4.

6.2 Total Droplet Trapping and Deposition

Once again, the quantities of particular interest are the total amount trapped at the point and the subsequent deposit on the ground. Whilst in the previous models these quantities were evaluated using Laplace transforms (see Section 4.2), the time-dependent mass and settling speed rule out that technique here.

Total Droplet Trapping

The number of droplets trapped per unit time, per unit volume, [# s^{-1} m^{-3}] is

$$kC(X_1, Y_1, Z_1, t)\delta(x - X_1)\delta(y - Y_1)\delta(z - Z_1).$$

The total number of droplets trapped at the point, N_{TT} [#], is the integral of this rate per unit volume with respect to space and time:

$$\begin{aligned} N_{TT} &= \int_0^{t_s}\int_0^{\infty}\int_{-\infty}^{\infty}\int_{-\infty}^{\infty} kC(X_1, Y_1, Z_1, t)\delta(x - X_1)\delta(y - Y_1)\delta(z - Z_1)\ dx\ dy\ dz\ dt \\ &= \int_0^{t_s} kC(X_1, Y_1, Z_1, t)\ dt \end{aligned} \quad (6.3)$$

where t_s is the disappearance time, that is, the time at which the droplets have evaporated completely. Since all of the droplets have the same mass at any given time, the total mass of droplets trapped at the point, M_{TT} [kg], is

$$M_{TT} = \int_0^{t_s}\int_0^{\infty}\int_{-\infty}^{\infty}\int_{-\infty}^{\infty} m(t)\, kC(X_1, Y_1, Z_1, t)\, \delta(x - X_1)\, \delta(y - Y_1)\, \delta(z - Z_1)\ dx\ dy\ dz\ dt$$
$$= \int_0^{t_s} m(t)\, kC(X_1, Y_1, Z_1, t)\ dt. \tag{6.4}$$

Deposition on the Ground

At ground level, the downward number flux of droplets per unit area [# m^{-2} s^{-1}] is

$$S(t)\, C(x, y, 0, t).$$

The number density of deposit on the ground, N_D [# m^{-2}], is the integral with respect to time:

$$N_D(x, y) = \int_0^{t_s} S(t)\, C(x, y, 0, t)\ dt. \tag{6.5}$$

Once again, since all of the droplets have the same mass at any given time, the mass density of deposit on the ground M_D [kg m^{-2}] is

$$M_D(x, y) = \int_0^{t_s} m(t)\, S(t)\, C(x, y, 0, t)\ dt. \tag{6.6}$$

6.3 Approximations for the Mass and Settling Speed

Expressions for the settling speed and evaporation rate of a droplet were given in Chapter 2 (Equations 2.5 and 2.19), however these expressions both require numerical evaluation. To simplify calculation in this chapter we use approximations for the mass and settling speed; it should be noted, though, that the solutions presented later in the chapter could be used with formulae other than these approximations.

Referring back to Section 2.4 (Equation 2.19), the evaporation rate of a droplet of radius a is given by

$$\frac{dm}{dt} = -\frac{4\pi a f_w M_W D_W}{R_g}\left(\frac{p_{sat}(T_a)}{T_a} - \phi\frac{p_{sat}(T_\infty)}{T_\infty}\right). \tag{6.7}$$

The ventilation coefficient f_w is very close to one for droplets with diameter less than around 100 μm, rising to around 1.7 at diameter 200 μm (see Figure 2.6); for the purposes of this chapter we will assume that $f_w = 1$, and write $\frac{dm}{dt} = -Ea$ where

$$E = \frac{4\pi M_W D_W}{R_g}\left(\frac{p_{sat}(T_a)}{T_a} - \phi\frac{p_{sat}(T_\infty)}{T_\infty}\right) = \text{ constant}. \tag{6.8}$$

The droplet mass is $m = \frac{4}{3}\rho_w \pi a^3$; differentiating with respect to time gives $4\rho_w \pi a^2 \frac{da}{dt} = -Ea$, and therefore

$$a(t)^2 = a_0^2 \left(1 - \frac{t}{t_s}\right) \tag{6.9}$$

for $0 \leq t \leq t_s$, where $a_0 = a(0)$ is the initial droplet radius, and

$$t_s = \frac{2\rho_w \pi a_0^2}{E} \tag{6.10}$$

is the disappearance time, or the time at which the radius is zero and the droplet evaporates completely. The droplet mass as a function of time is then

$$m(t) = m_0 \left(1 - \frac{t}{t_s}\right)^{3/2} \tag{6.11}$$

where $m_0 = m(0) = \frac{4}{3}\rho_w \pi a_0^3$ is the initial mass.

We approximate the settling speed by the Stokes flow settling speed. Stokes flow describes very low Reynolds number flows, where viscous forces dominate inertial forces; this is appropriate for small droplets moving at low speed. In Stokes flow the drag force is equal to $-3\pi\mu d(\mathbf{v} - \mathbf{u})$ (Reist, 1993), notation as in Chapter 2, and Equation (2.5) for the settling speed becomes

$$S(a) = \frac{4ga^2}{18\mu}(\rho_w - \rho_a). \tag{6.12}$$

Substituting Equation (6.9) for the droplet radius, the settling speed as a function of time is

$$S(t) = S_0 \left(1 - \frac{t}{t_s}\right) \tag{6.13}$$

where $S_0 = S(0) = \frac{4ga_0^2}{18\mu}(\rho_w - \rho_a)$ is the initial settling speed. Figure 6.1 compares the settling speed calculated according to Equation (2.5) with the Stokes flow settling speed calculated from Equation (6.12); the two compare well up to around 100 μm in diameter, where the difference is approximately 26 %; for larger droplets, the Stokes flow approximation increasingly overestimates the settling speed.

6.4 Case 1: Zero Vertical Dispersion

In this section we present 1-D, 2-D and 3-D solutions to our advection-dispersion model, with evaporation and a point representation for trapping, in the case of negligible vertical dispersion. As in the models without evaporation in Chapters 4 and 5, this is a special case where the droplets

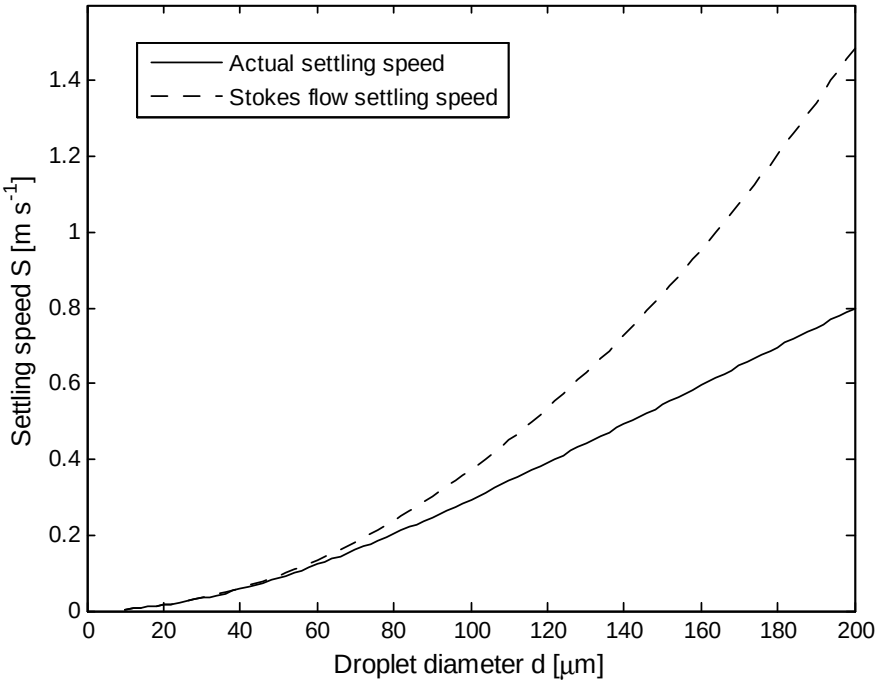

Figure 6.1: Comparing the actual settling speed (Equation 2.5), with the Stokes flow settling speed (Equation 6.12), for droplets with diameter between 10 μm and 200 μm.

can disperse only horizontally, and the boundary condition on the ground is automatically satisfied. Since the droplets do not spread vertically there are two possibilities: either they will all deposit on the ground, having lost only part of their mass by evaporation, or they will all evaporate completely during flight, in which case there is no deposit on the ground.

We obtain the solutions presented here by changing to a coordinate system which moves downwards with the droplets; this eliminates the time-dependent settling term from the model, and makes the solution process quite straightforward. Also, this method is flexible in that it may be applied independently of the form of the settling speed $S(t)$.

One-Dimensional Solution

In 1-D, and with $D_V = 0$, our advection-dispersion model with evaporation and a point representation for trapping is

$$\frac{\partial C}{\partial t} - S(t)\frac{\partial C}{\partial z} = \frac{Q}{m_0}\delta(z - H)\,\delta(t) - kC(Z_1, t)\,\delta(z - Z_1) \tag{6.14}$$

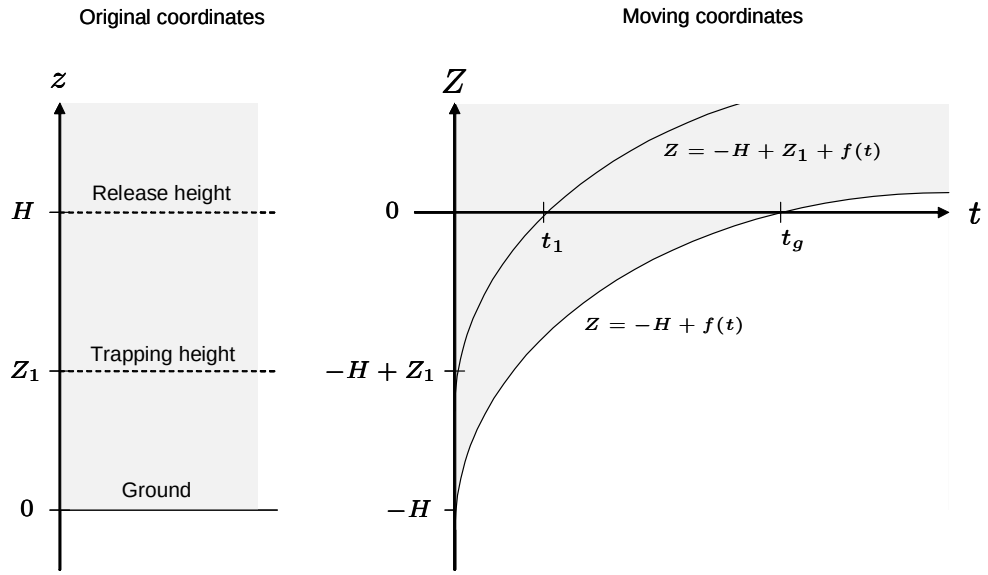

Figure 6.2: Illustration of the 1-D model in the moving coordinate system (Z,t). The droplets are at height $Z=0$. The ground and the trapping plane are rising at the same rate; after time t they are at heights $Z=-H+f(t)$ and $Z=Z_1-H+f(t)$ respectively. Time t_1 is when the trapping plane and the droplets meet, and time t_g is when the ground and the droplets meet.

with initial and boundary conditions

$$C\left(z,0^{-}\right)=0 \text{ and } C\left(\infty,t\right)=0.$$

The conceptual situation here is a plane release with a plane representation for trapping, as described for the 1-D model in Chapter 4 (see Section 4.3). To solve Equation (6.14) we change to a moving coordinate system (Z,t), where $Z=z-H+f(t)$ with $f(t)=\int_0^t S(\tau)\ d\tau$. In this coordinate system, we denote the number concentration by $C^*(Z,t)$, and Equation (6.14) becomes

$$\frac{dC^*}{dt}=\frac{Q}{m_0}\delta(Z)\,\delta(t)-kC^*\left(Z_1-H+f(t),t\right)\delta\left(Z-Z_1+H-f(t)\right) \tag{6.15}$$

with initial and boundary conditions $C^*(Z,0^-)=0$ and $C^*(\infty,t)=0$. Relative to the new coordinate system the droplets are no longer falling; however the ground and the trapping plane are moving upwards to meet them. The droplets are released at time $t=0$ from height $Z=0$ and remain there; the ground is initially at height $Z=-H$ and the trapping plane is initially at height $Z=-H+Z_1$, and both move upwards with speed $S(t)$. After time t, the height of the ground is $Z=-H+f(t)$ and the height of the trapping plane is $Z=Z_1-H+f(t)$. See Figure 6.2 for a sketch of this scenario.

Using the property of the delta function that

$$\delta\left(g\left(t\right)\right)=\sum_{i}\frac{\delta\left(t-t_{i}\right)}{\left|g'\left(t_{i}\right)\right|} \tag{6.16}$$

where the t_i's are the zeros of the function $g\left(t\right)$, Equation (6.15) can be re-written as

$$\frac{dC^{*}}{dt}=\frac{Q}{m_{0}}\delta\left(Z\right)\delta\left(t\right)-\frac{kC^{*}\left(Z,t_{Z}\right)}{S\left(t_{Z}\right)}\delta\left(t-t_{Z}\right) \tag{6.17}$$

where $t_Z = F\left(Z+H-Z_1\right)$ is the time at which the trapping plane reaches height Z, with F being the inverse of function f, as defined on page 123. Integrating with respect to time:

$$C^{*}\left(Z,t\right)=\frac{Q}{m_{0}}\delta\left(Z\right)\mathcal{H}\left(t\right)-\frac{kC^{*}\left(Z,t_{Z}\right)}{S\left(t_{Z}\right)}\mathcal{H}\left(t-t_{Z}\right). \tag{6.18}$$

The, as yet unknown $C^{*}\left(Z,t_{Z}\right)$ is the concentration at height Z at the time at which the trapping plane arrives there. To determine $C^{*}\left(Z,t_{Z}\right)$ we let $t\rightarrow t_{Z}^{-}$, since this gives the concentration which the trapping plane meets upon arrival.

$$\begin{aligned}C^{*}\left(Z,t_{Z}\right) &= \lim_{t\rightarrow t_{Z}^{-}}C^{*}\left(Z,t\right)\\ &= \frac{Q}{m_{0}}\delta\left(Z\right)H\left(t_{Z}\right).\end{aligned} \tag{6.19}$$

Substituting Equation (6.19) back into Equation (6.18) gives

$$C^{*}\left(Z,t\right)=\frac{Q}{m_{0}}\delta\left(Z\right)\mathcal{H}\left(t\right)-\frac{kQ}{m_{0}S\left(t_{1}\right)}\delta\left(Z\right)\mathcal{H}\left(t_{1}\right)\mathcal{H}\left(t-t_{1}\right) \tag{6.20}$$

where $t_1 = F\left(H-Z_1\right)$ is the time at which the trapping plane and the droplets meet. Looking at the sketch in Figure 6.2: if $-H+Z_1<0$ as shown then $t_1>0$, but if $-H+Z_1>0$ then $t_1<0$. In other words, if the trapping plane is below the release height ($Z_1<H$) then $t_1>0$, but if the trapping plane is above the release height ($Z_1>H$) then $t_1<0$. Returning to the original coordinate system:

$$\text{For } Z_{1}>H,\quad C\left(z,t\right)=\begin{cases}0, & t<0,\\ \dfrac{Q}{m_{0}}\delta\left(z-H+f\left(t\right)\right), & t>0,\end{cases} \tag{6.21}$$

$$\text{and for } Z_{1}<H,\quad C\left(z,t\right)=\begin{cases}0, & t<0,\\ \dfrac{Q}{m_{0}}\delta\left(z-H+f\left(t\right)\right), & 0<t<t_{1},\\ \dfrac{Q}{m_{0}}\left(1-\dfrac{k}{S\left(t_{1}\right)}\right)\delta\left(z-H+f\left(t\right)\right), & t>t_{1}.\end{cases} \tag{6.22}$$

The concentration is zero until the release at $t = 0$, and after that it is non-zero only at height $z = H - f(t)$ which is the height of the droplets at time t. At time t_1 some of the droplets are removed at the trapping plane (provided it is below the release height).

The solution above may be applied for general $S(t)$, however, use of the Stokes flow approximation from Equation (6.13) does lead to simple formulae for f and its inverse F as follows: if $A = f(t)$, so that consequently $t = F(A)$, then

$$f(t) = \int_0^t S(\tau)\ d\tau = S_0 t \left(1 - \frac{t}{2t_s}\right) \tag{6.23}$$

and

$$F(A) = t_s \left(1 - \sqrt{1 - \frac{2A}{S_0 t_s}}\right). \tag{6.24}$$

The examples in this chapter are calculated using the expressions above for f and F, and Equation (6.10) for the disappearance time t_s. In the case of no evaporation, $S(t) = S_0 =$ constant and $t_s = \infty$, and the expressions above reduce to $f(t) = S_0 t$ and $F(A) = \dfrac{A}{S_0}$.

Total Droplet Trapping and Deposition

The total amount trapped and the deposit on the ground are calculated according to Section 6.2. The total mass of droplets trapped at the plane per unit area [kg m^{-2}] is

$$\begin{aligned} M_{TT} &= \int_0^{t_s} m(t)\, kC(Z_1, t)\ dt \\ &= \begin{cases} 0, & Z_1 > H, \\ 0, & Z_1 < H,\ t_s < t_1 \\ \dfrac{m(t_1)\, kQ}{m_0 S(t_1)}, & Z_1 < H,\ t_s < t_1. \end{cases} \end{aligned} \tag{6.25}$$

There is no trapping if $Z_1 > H$ because no droplets move upwards from the release height. There is also no trapping for $Z_1 < H$ if the droplets completely evaporate before reaching the trapping plane (that is $t_s < t_1$).

The density of deposit on the ground [kg m^{-2}] is

$$M_D = \int_0^{t_s} m(t)\, S(t)\, C(0, t)\ dt.$$

For $Z_1 > H$ this gives

$$M_D = \begin{cases} 0, & t_s < t_g, \\ \dfrac{m\left(t_g\right) Q}{m_0}, & t_s > t_g, \end{cases} \tag{6.26}$$

and for $Z_1 < H$,

$$M_D = \begin{cases} 0, & t_s < t_g, \\ \dfrac{m\left(t_g\right) Q}{m_0}\left(1 - \dfrac{k}{S\left(t_1\right)}\right), & t_s > t_g \end{cases} \tag{6.27}$$

where $t_g = F\left(H\right)$ is the time for the droplets to reach the ground. There is no deposit if $t_s < t_g$, that is, if the droplets completely evaporate before reaching the ground. Otherwise the deposit depends upon the height of the trapping plane through the parameter t_1.

Two-Dimensional Solution

In 2-D, and with $D_V = 0$, our advection-dispersion equation with evaporation and a point representation for trapping becomes

$$\begin{aligned} \frac{\partial C}{\partial t} + u\frac{\partial C}{\partial x} - S\left(t\right)\frac{\partial C}{\partial z} &= D_L\frac{\partial^2 C}{\partial x^2} + \frac{Q}{m_0}\delta\left(x - X_0\right)\delta\left(z - H\right)\delta\left(t\right) \\ &\quad -kC\left(X_1, Z_1, t\right)\delta\left(x - X_1\right)\delta\left(z - Z_1\right) \end{aligned} \tag{6.28}$$

with initial and boundary conditions

$$C\left(x, z, 0^-\right) = 0, \text{ and}$$

$$C\left(x, z, t\right) \to 0 \text{ as } x \to \pm\infty, \text{ and } z \to +\infty.$$

This is now a line release with a line representation for trapping (see the description for the 2-D model in Chapter 4, Section 4.3). To solve Equation (6.28) we employ the moving coordinate system from the 1-D solution; so that $C\left(x, z, t\right) \to C^*\left(x, Z, t\right)$, where $Z = z - H + f\left(t\right)$ with $f\left(t\right) = \displaystyle\int_0^t S\left(\tau\right)\ d\tau$. Equation (6.28) becomes

$$\begin{aligned} \frac{\partial C^*}{\partial t} + u\frac{\partial C^*}{\partial x} &= D_L\frac{\partial^2 C}{\partial x^2} + \frac{Q}{m_0}\delta\left(x - X_0\right)\delta\left(Z\right)\delta\left(t\right) \\ &\quad -kC^*\left(X_1, Z_1 - H + f\left(t\right), t\right)\delta\left(x - X_1\right)\delta\left(Z - Z_1 + H - f\left(t\right)\right). \end{aligned} \tag{6.29}$$

Relative to this coordinate system, the droplets are released from the line at $(x, Z) = (X_0, 0)$ at time $t = 0$; they remain at that height whilst travelling with the wind and also dispersing alongwind. The ground and the trapping line rise with speed $S\left(t\right)$ to meet them.

Using the property of the delta function in Equation (6.16), Equation (6.29) can be rewritten as

$$\frac{\partial C^*}{\partial t}+u\frac{\partial C^*}{\partial x}=D_L\frac{\partial^2 C}{\partial x^2}+\frac{Q}{m_0}\delta\left(x-X_0\right)\delta\left(Z\right)\delta\left(t\right)-\frac{kC^*\left(X_1,Z,t_Z\right)}{S\left(t_Z\right)}\delta\left(x-X_1\right)\delta\left(t-t_Z\right) \quad (6.30)$$

where $t_Z=F\left(Z+H-Z_1\right)$ is the time at which the trapping line reaches height Z. Taking Fourier transforms with respect to x, integrating with respect to t, and then inverting the Fourier transforms:

$$\begin{aligned} C^*\left(x,Z,t\right) &= \frac{Q}{2m_0\sqrt{\pi D_L t}}e^{-\frac{\left(x-X_0-ut\right)^2}{4D_L t}}\delta\left(Z\right)\mathcal{H}\left(t\right) \\ &\quad -\frac{kC^*\left(X_1,Z,t_Z\right)}{2S\left(t_Z\right)\sqrt{\pi D_L\left(t-t_Z\right)}}e^{-\frac{\left(x-X_1-u\left(t-t_Z\right)\right)^2}{4D_L\left(t-t_Z\right)}}\mathcal{H}\left(t-t_Z\right) \end{aligned} \quad (6.31)$$

The, as yet unknown $C^*\left(X_1,Z,t_Z\right)$ is the concentration which the trapping line encounters when it arrives at height Z. To determine $C^*\left(X_1,Z,t_Z\right)$ we set $x=X_1$ and let $t\rightarrow t_Z^-$, to correspond with the concentration met by the trapping line on arrival.

$$\begin{aligned} C^*\left(X_1,Z,t_Z\right) &= \lim_{t\rightarrow t_Z} C^*\left(X_1,Z,t\right) \\ &= \frac{Q}{2m_0\sqrt{\pi D_L t_Z}}e^{-\frac{\left(X_1-X_0-ut_Z\right)^2}{4D_L t_Z}}\delta\left(Z\right)\mathcal{H}\left(t_Z\right). \end{aligned} \quad (6.32)$$

Substituting this result back into Equation (6.31) gives

$$\begin{aligned} C^*\left(x,Z,t\right) &= \frac{Q\mathcal{H}\left(t\right)}{2m_0\sqrt{\pi D_L t}}e^{-\frac{\left(x-X_0-ut\right)^2}{4D_L t}}\delta\left(Z\right) \\ &\quad -\frac{kQ\mathcal{H}\left(t_1\right)\mathcal{H}\left(t-t_1\right)}{4m_0 S\left(t_1\right)\pi D_L\sqrt{t_1\left(t-t_1\right)}}e^{-\frac{\left(X_1-X_0-ut_1\right)^2}{4D_L t_1}-\frac{\left(x-X_1-u\left(t-t_1\right)\right)^2}{4D_L\left(t-t_1\right)}}\delta\left(Z\right). \end{aligned} \quad (6.33)$$

where $t_1=F\left(H-Z_1\right)$ is the time at which the trapping line and the droplets meet. As for the 1-D solution, $Z_1>H$ corresponds to $t_1<0$ and $Z_1<H$ corresponds to $t_1>0$. Returning to the original coordinate system:

For $Z_1>H$,

$$C\left(x,z,t\right) = \begin{cases} 0, & t<0, \\ \dfrac{Q}{2m_0\sqrt{\pi D_L t}}e^{-\frac{\left(x-X_0-ut\right)^2}{4D_L t}}\delta\left(z-H+f\left(t\right)\right), & t>0, \end{cases} \quad (6.34)$$

and for $Z_1 < H$,

$$C(x,z,t) = \begin{cases} 0, & t<0, \\ \dfrac{Q}{2m_0\sqrt{\pi D_L t}} e^{-\frac{(x-X_0-ut)^2}{4D_L t}} \delta\left(z-H+f(t)\right), & 0<t<t_1, \\ \left[\dfrac{Q}{2m_0\sqrt{\pi D_L t}} e^{-\frac{(x-X_0-ut)^2}{4D_L t}} - \dfrac{kQ}{4m_0\pi S(t_1) D_L \sqrt{t_1(t-t_1)}} \times \right. & \\ \left. e^{-\frac{(X_1-X_0-ut_1)^2}{4D_L t_1} - \frac{(x-X_1-u(t-t_1))^2}{4D_L(t-t_1)}}\right] \delta\left(z-H+f(t)\right), & t>t_1. \end{cases} \tag{6.35}$$

Again, as in the 1-D solution, the concentration is non-zero only after the release, and then only at height $z = -H + f(t)$ which is the height of the droplets at time t. Provided it is below the release, some of the droplets are removed at the trapping line when they reach it at time t_1.

Total Droplet Trapping and Deposition

The total mass of droplets trapped at the line per unit length [kg m^{-1}] is

$$\begin{aligned} M_{TT} &= \int_0^{t_s} m(t)\, kC(X_1, Z_1, t)\ dt \\ &= \begin{cases} 0, & Z_1 > H, \\ 0, & Z_1 < H,\ t_s < t_1, \\ \dfrac{m(t_1)\, kQ}{2m_0 S(t_1)\sqrt{\pi D_L t_1}} e^{-\frac{(X_1-X_0-ut_1)^2}{4D_L t_1}}, & Z_1 < H,\ t_s > t_1. \end{cases} \end{aligned} \tag{6.36}$$

Nothing is trapped if $Z_1 > H$ because the droplets do not move upwards. There is also nothing trapped for $Z_1 < H$ if $t_s < t_1$, because this means that the droplets evaporate completely before reaching the trapping line.

The density of deposit on the ground [kg m^{-2}] is

$$M_D(x) = \int_0^{t_s} m(t)\, S(t)\, C(x,0,t)\ dt.$$

For $Z_1 > H$ this gives

$$M_D(x) = \begin{cases} 0, & t_s < t_g, \\ \dfrac{m(t_g)\, Q}{2m_0 S(t_g)\sqrt{\pi D_L t_g}} e^{-\frac{(x-X_0-ut_g)^2}{4D_L t_g}}, & t_s > t_g, \end{cases} \tag{6.37}$$

and for $Z_1 < H$,

$$M_D(x) = \begin{cases} 0, & t_s < t_g, \\ \dfrac{m(t_g)\,Q}{2m_0\sqrt{\pi D_L t_g}} e^{-\frac{(x-X_0-ut_g)^2}{4D_L t_g}} - & \\ \dfrac{m(t_g)\,kQ}{4m_0\pi S(t_1)\,D_L\sqrt{t_1(t_g-t_1)}} e^{-\frac{(X_1-X_0-ut_1)^2}{4D_L t_1} - \frac{(x-X_1-u(t_g-t_1))^2}{4D_L(t_g-t_1)}}, & t_s > t_g. \end{cases} \tag{6.38}$$

where $t_g = F(H)$ is the time the droplets take to reach the ground. There is once again no deposit if $t_s < t_g$, since this means the droplets completely evaporate before reaching the ground.

An Illustrative Example of the Two-Dimensional Solution

The following example is intended to illustrate the 2-D solution described above. The parameter set used here is given in Table 6.1. The droplets, with initial diameter $d_0 = 100$ μm, have initial mass and settling speed $m_0 = 5.23 \times 10^{-10}$ kg and $S_0 = 0.37$ m s^{-1} respectively, and are at temperature $T_a = 14.7$ °C; they reach the height of the trapping line at $t_1 = 2.9$ s with mass $m(t_1) = 4.25 \times 10^{-10}$ kg, and deposit on the ground at $t_g = 10.6$ s with mass $m(t_g) = 2.0 \times 10^{-10}$ kg. The disappearance time according to Equation (6.10) is $t_s = 22.2$ s. Note that the background trapping rate $k_b = 25$ s^{-1} is unrealistically high, and we have inflated it to make the effect of trapping more visible; a realistic value would be < 2 s^{-1}.

Table 6.1: Parameter set used to generate Figure 6.3.

u	L_L	ϕ	T_∞	d_0	Q	(X_0, H)	k_b	$\Delta x \Delta z$	(X_1, Z_1)
1 m s^{-1}	2 m	60 %	20 °C	100 μm	1 kg m^{-1}	(0, 3) m	25 s^{-1}	0.04 m^2	(4, 2) m

Figure 6.3 shows cross-sections of the density of mass deposit on the ground, first with neither evaporation nor trapping, then with evaporation but no trapping, and finally with both evaporation and trapping. The deposit with evaporation is significantly lower than that without evaporation, since the droplets are smaller and lighter upon reaching the ground. Also, the peak in deposit with evaporation is shifted slightly downwind, as the smaller droplets are blown further by the wind. Trapping further reduces the deposit; with the parameter values chosen here there is a maximum reduction of around 43 % in the density of deposit with evaporation when the trapping line is added.

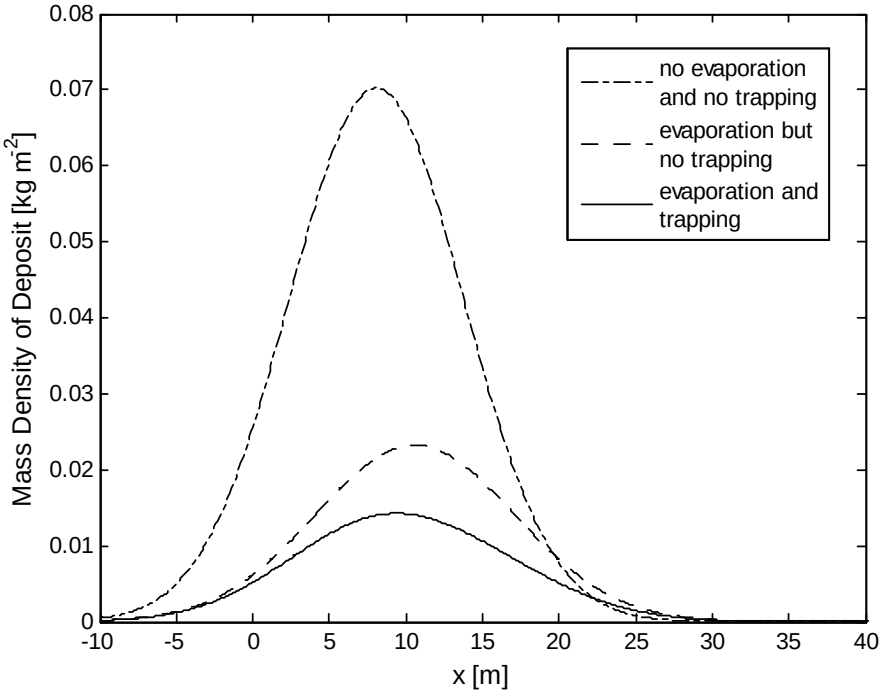

Figure 6.3: Cross-sections of the density of deposit on the ground [kg m^{-2}], with and without evaporation and/or trapping, resulting from a line release with zero vertical dispersion and a line representation for trapping. Parameter values are as given in Table 6.1.

Three-Dimensional Solution

In all three spatial dimensions, but with $D_V = 0$, our advection-dispersion model with evaporation and a point representation for trapping becomes

$$\begin{aligned}\frac{\partial C}{\partial t} + u\frac{\partial C}{\partial x} - S(t)\frac{\partial C}{\partial z} &= D_L\frac{\partial^2 C}{\partial x^2} + D_T\frac{\partial^2 C}{\partial y^2} + \frac{Q}{m_0}\delta(x - X_0)\,\delta(y - Y_0)\,\delta(z - H)\,\delta(t) \\ &\quad -kC(X_1, Y_1, Z_1, t)\,\delta(x - X_1)\,\delta(y - Y_1)\,\delta(z - Z_1) \qquad (6.39)\end{aligned}$$

with initial and boundary conditions

$$C\left(x, y, z, 0^-\right) = 0, \text{ and}$$

$$C(x, y, z, t) \to 0 \text{ as } x, y \to \pm\infty \text{ and } z \to +\infty.$$

Once again, we employ the moving coordinate system from the 1-D solution; so that $C(x, y, z, t) \to C^*(x, y, Z, t)$, where $Z = z - H + f(t)$ with $f(t) = \int_0^t S(\tau)\ d\tau$. Equation (6.39) then becomes

$$\begin{aligned}\frac{\partial C^*}{\partial t} + u\frac{\partial C^*}{\partial x} &= D_L\frac{\partial^2 C^*}{\partial x^2} + D_T\frac{\partial^2 C^*}{\partial y^2} + \frac{Q}{m_0}\delta(x - X_0)\,\delta(y - Y_0)\,\delta(Z)\,\delta(t) \\ &\quad -kC^*(X_1, Y_1, Z_1 - H + f(t), t)\,\delta(x - X_1)\,\delta(y - Y_1)\,\delta(Z + H - Z_1 + f(t)) \\ &\qquad (6.40)\end{aligned}$$

The droplets are released at time $t = 0$ from $(x, y, Z) = (X_0, Y_0, 0)$ in the new coordinate system. Relative to this coordinate system the droplets do not fall, but are transported by the wind and disperse horizontally, while the ground and the trapping point rise with speed $S(t)$.

Following the procedure laid out for the 2-D solution, Equation (6.40) may be rewritten using the property of the delta function (Equation 6.16), and then solved by taking Fourier transforms and integrating with respect to t. The result is

$$\begin{aligned} C^*(x,y,Z,t) &= \frac{Q}{4m_0\pi t\sqrt{D_L D_T}} e^{-\frac{(x-X_0-ut)^2}{4D_L t}-\frac{(y-Y_0)^2}{4D_T t}} \delta(Z)\,\mathcal{H}(t) \\ &\quad -\frac{kC^*(X_1,Y_1,Z,t_Z)}{4\pi(t-t_Z)S(t_Z)\sqrt{D_L D_T}} e^{-\frac{(x-X_1-u(t-t_Z))^2}{4D_L(t-t_Z)}-\frac{(y-Y_1)^2}{4D_T(t-t_Z)}} \mathcal{H}(t-t_Z) \end{aligned} \tag{6.41}$$

where $C^*(X_1, Y_1, Z, t_Z)$ is the, as yet unknown concentration met by the trapping point when it reaches height Z. We set $(x, y, Z) = (X_1, Y_1, Z)$ and let $t \to t_Z^-$ to correspond with the concentration met by the trapping point on arrival:

$$\begin{aligned} C^*(X_1,Y_1,Z,t_Z) &= \lim_{t\to t_Z^-} C^*(X_1,Y_1,Z,t) \\ &= \frac{Q}{4m_0\pi t_Z\sqrt{D_L D_T}} e^{-\frac{(X_1-X_0-ut_Z)^2}{4D_L t_Z}-\frac{(Y_1-Y_0)^2}{4D_T t_Z}} \delta(Z)\,\mathcal{H}(t_Z) \end{aligned} \tag{6.42}$$

where $t_Z = F(Z + H - Z_1)$ is the time at which the trapping point rises to height Z, with F being the inverse of function f. Consequently,

$$\begin{aligned} C^*(x,y,Z,t) &= \frac{Q\mathcal{H}(t)}{4m_0\pi t\sqrt{D_L D_T}} e^{-\frac{(x-X_0-ut)^2}{4D_L t}-\frac{(y-Y_0)^2}{4D_T t}} \delta(Z) - \frac{kQ\mathcal{H}(t_1)\,\mathcal{H}(t-t_1)}{16m_0\pi^2 S(t_1)\,t_1\,(t-t_1)\,D_L D_T} \times \\ &\quad e^{-\frac{(X_1-X_0-ut_Z)^2}{4D_L t_Z}-\frac{(x-X_1-u(t-t_1))^2}{4D_L(t-t_1)}-\frac{(Y_1-Y_0)^2}{4D_T t_1}-\frac{(y-Y_1)^2}{4D_T(t-t_1)}} \delta(Z) \end{aligned} \tag{6.43}$$

where $t_1 = F(H - Z_1)$ is the time when the trapping point and the droplets meet. As for the 1-D and 2-D solutions, $Z_1 > H$ corresponds to $t_1 < 0$ and $Z_1 < H$ corresponds to $t_1 > 0$. Returning to the original coordinate system:

For $Z_1 > H$,

$$C(x,y,z,t) = \begin{cases} 0, & t < 0, \\ \dfrac{Q}{4m_0\pi t\sqrt{D_L D_T}} e^{-\frac{(x-X_0-ut)^2}{4D_L t}-\frac{(y-Y_0)^2}{4D_T t}} \delta(z-H+f(t)), & t > 0, \end{cases} \tag{6.44}$$

and for $Z_1 < H$,

$$C(x,y,z,t) = \begin{cases} 0, & t < 0, \\ \dfrac{Q}{4m_0\pi t\sqrt{D_L D_T}} e^{-\frac{(x-X_0-ut)^2}{4D_L t} - \frac{(y-Y_0)^2}{4D_T t}} \delta\left(z - H + f(t)\right), & 0 < t < t_1, \\ \left[\dfrac{Q}{4m_0\pi t\sqrt{D_L D_T}} e^{-\frac{(x-X_0-ut)^2}{4D_L t} - \frac{(y-Y_0)^2}{4D_T t}} - \dfrac{kQ}{16m_0\pi^2 S(t_1) D_L D_T t_1 (t-t_1)} \times \right. & \\ \left. e^{-\frac{(X_1-X_0-ut_1)^2}{4D_L t_1} - \frac{(Y_1-Y_0)^2}{4D_T t_1} - \frac{(x-X_1-u(t-t_1))^2}{4D_L(t-t_1)} - \frac{(y-Y_1)^2}{4D_T(t-t_1)}} \right] \delta\left(z - H + f(t)\right), & t > t_1. \end{cases} \tag{6.45}$$

The concentration is once again zero before the release, and only non-zero after the release at height $z = -H + f(t)$ which is the height of the droplets after time t. Some of the droplets are removed at the trapping point when they reach it at time t_1 (provided it is below the release height).

Total Droplet Trapping and Deposition

Following Section 6.2, the total mass of droplets trapped at the point [kg] is

$$\begin{aligned} M_{TT} &= \int_0^{t_s} m(t)\, kC(X_1, Y_1, Z_1, t)\ dt \\ &= \begin{cases} 0, & Z_1 > H, \\ 0, & Z_1 < H,\ t_s < t_1, \\ \dfrac{m(t_1)\, kQ}{4m_0\pi S(t_1)\, t_1\sqrt{D_L D_T}} e^{-\frac{(X_1-X_0-ut_1)^2}{4D_L t_1} - \frac{(Y_1-Y_1)^2}{4D_T t_1}}, & Z_1 < H,\ t_s > t_1. \end{cases} \end{aligned} \tag{6.46}$$

Once again, there is no trapping if $Z_1 > H$ because the droplets do not move upwards, and there is also no trapping for $Z_1 < H$ if $t_s < t_1$ because this means that the droplets evaporate completely before reaching the trapping point.

The density of deposit on the ground [kg m^{-2}] is

$$M_D(x,y) = \int_0^{t_s} m(t)\, S(t)\, C(x,y,0,t)\ dt. \tag{6.47}$$

For $Z_1 > H$ this gives

$$M_D(x,y) = \begin{cases} 0, & t_s < t_g, \\ \dfrac{m(t_g)\,Q}{4m_0\pi S(t_g)\,t_g\sqrt{D_L D_T}} e^{-\frac{(x-X_0-ut_g)^2}{4D_L t_g} - \frac{(y-Y_0)^2}{4D_T t_g}}, & t_s > t_g, \end{cases} \tag{6.48}$$

and for $Z_1 < H$,

$$M_D(x,y) = \begin{cases} 0, & t_s < t_g, \\ \dfrac{m(t_g)\,Q}{4m_0\pi t_g\sqrt{D_L D_T}} e^{-\frac{(x-X_0-ut_g)^2}{4D_L t_g} - \frac{(y-Y_0)^2}{4D_T t_g}} - \dfrac{m(t_g)\,kQ}{16m_0\pi^2 S(t_1)\,t_1\,(t_g-t_1)\,D_L D_T} \times \\ e^{-\frac{(X_1-X_0-ut_1)^2}{4D_L t_1} - \frac{(Y_1-Y_0)^2}{4D_T t_1} - \frac{(x-X_1-u(t_g-t_1))^2}{4D_L(t_g-t_1)} - \frac{(y-Y_1)^2}{4D_T(t_g-t_1)}}, & t_s > t_g. \end{cases} \tag{6.49}$$

where $t_g = F(H)$ is the time the droplets take to reach the ground. Again, there is no deposit if $t_s < t_g$, since this means the droplets completely evaporate before reaching the ground.

6.5 Case 2: Non-Zero Vertical Dispersion

In this section, we present 1-D, 2-D and 3-D solutions to our advection-dispersion model, with evaporation and a point representation for trapping, in the case where vertical dispersion is significant ($D_V \neq 0$). As in the previous models without evaporation, the boundary condition of zero vertical dispersive flux on the ground requires $\dfrac{\partial C}{\partial t}(x,y,0,t) = 0$.

With evaporation and $D_V \neq 0$, the non-constant settling speed $S(t)$ combined with the boundary condition on the ground make it extremely difficult to solve the model analytically. We attempted a number of different methods with a varying degree of progress. The method which proved the most successful, described in the 1-D, 2-D and 3-D solutions below, combines a Greens function with the moving coordinate system from Case 1. Unfortunately the solutions obtained are embedded in integral equations, and require the numerical inversion of a Fourier transform, however they still allow for easy parameter variation and are not specific to a particular form for $S(t)$.

Solution Approaches

We tried a number of approaches in solving our advection-dispersion model with evaporation and $D_V \neq 0$. Two methods which were ultimately unsuccessful but warrant a little discussion are (i) Laplace transforms with respect to z rather than t, and (ii) a time-varying "underground" image source.

Laplace Transforms

Initially we experimented with solving the model by taking Laplace transforms with respect to z. Interestingly, this results in a transform which cannot be inverted. As a simple example, consider the model in 1-D and with dispersion only (that is $S(t) = 0$ and $k = 0$); in this case the model is

$$\frac{\partial C}{\partial t} = D_V \frac{\partial^2 C}{\partial z^2} + \frac{Q}{m_0} \delta(z - H)\, \delta(t) \tag{6.50}$$

for which the known solution is

$$C(z,t) = \frac{Q}{2m_0\sqrt{\pi D_V t}} \left(e^{-\frac{(z-H)^2}{4D_V t}} + e^{-\frac{(z+H)^2}{4D_V t}} \right). \tag{6.51}$$

Taking the Laplace transform of the model with respect to z $\left(C(z,t) \rightarrow \overline{C}(p,t)\right)$, gives an integral equation for $\overline{C}(p,t)$:

$$\overline{C}(p,t) = \frac{Q}{m_0} e^{p^2 D_V t - pH} \mathcal{H}(t) - \int_0^t p D_V C(0,\tau)\, e^{p^2 D_V (t-\tau)}\, d\tau. \tag{6.52}$$

As it stands, the transform $\overline{C}(p,t)$ cannot be inverted because $e^{p^2 D_V t}$ has no inverse transform. There is a way around the problem, however, if the integration in time is carried out first using the form of $C(0,t)$ from Equation (6.51); the transform can then be inverted to give the same answer as Equation (6.51). Unfortunately, for the full model with settling, trapping and evaporation, $C(0,t)$ is unknown and no way around the problem could be found.

Method of Images

A method of images approach, with a time varying image source placed underneath the ground, worked well in 1-D but not in 2-D or 3-D. The solution is of the form $C = C_s + C_i$, where C_s is the contribution from the original source, and C_i is the contribution from the image source. Because there is no vertical dispersive flux at $z = 0$, none of the droplets from the image source

will cross into the aboveground domain, and therefore the image source does not affect the solution other than to ensure the boundary condition on the ground is met.

The 1-D model is

$$\frac{\partial C}{\partial t} - S(t)\frac{\partial C}{\partial z} = D_V \frac{\partial^2 C}{\partial z^2} + \frac{Q}{m_0}\delta(z-H)\,\delta(t) - kC(Z_1,t)\,\delta(z-Z_1) \tag{6.53}$$

with initial and boundary conditions $C(z,0^-) = 0$, $C(\infty,t) = 0$ and $\dfrac{\partial C}{\partial z}(0,t) = 0$. The contribution from the original source, C_s, is found by solving Equation (6.53) with homogeneous boundary conditions $C(\pm\infty,t) = 0$:

$$C_s(z,t) = \frac{Q}{2m_0\sqrt{\pi D_V t}} e^{-\frac{(z-H+f(t))^2}{4D_V t}} - \int_0^t \frac{kC(Z_1,\tau)}{2\sqrt{\pi D_V (t-\tau)}} e^{-\frac{(z-Z_1+f(t)-f(\tau))^2}{4D_V(t-\tau)}}\, d\tau. \tag{6.54}$$

The contribution from the image source, C_i, is found by solving

$$\frac{\partial C_i}{\partial t} - S(t)\frac{\partial C_i}{\partial z} = D_V \frac{\partial^2 C_i}{\partial z^2} + q(t)\,\delta(z+H) \tag{6.55}$$

with initial and boundary conditions $C_i(z,0^-) = 0$, and $C_i(\pm\infty,t) = 0$, where $q(t)$ [kg m^{-2} s^{-1}] is the strength of the time-varying plane source (placed at $z = -H$, however the placement is arbitrary provided it is below the ground):

$$C_i(z,t) = \int_0^t \frac{q(\tau)}{2\sqrt{\pi D_V (t-\tau)}} e^{-\frac{(z+H-f(t)-f(\tau))^2}{4D_V(t-\tau)}}\, d\tau. \tag{6.56}$$

A system of equations to evaluate $q(t)$ and $C(Z_1,t)$ is formed from $C(z,t) = C_s(z,t) + C_i(z,t)$ by applying the boundary condition $\dfrac{\partial C}{\partial z}(0,t) = 0$, and by setting $z = Z_1$; the system can then be evaluated numerically at discrete time steps using, for instance, a trapezium rule integration. This method generally works well in 1-D, although the numerical evaluation is sensitive to the parameter D_V.

Unfortunately, the method does not work so well in 2-D (or 3-D). For example, a time-varying line source of strength $q(t)$ [kg m^{-1} s^{-1}] placed at $(x,z) = (X_0,-H)$ gives

$$\begin{aligned} C(x,z,t) \;=\; & \frac{Q}{4m_0\pi t\sqrt{D_L D_V}} e^{-\frac{(x-X_0-ut)^2}{4D_L t} - \frac{(z-H+f(t))^2}{4D_V t}} \\ & + \int_0^t \frac{q(t)}{4\pi(t-\tau)\sqrt{D_L D_V}} e^{-\frac{(x-X_0-u(t-\tau))^2}{4D_L(t-\tau)} - \frac{(z+H+f(t)-f(\tau))^2}{4D_V(t-\tau)}}\, d\tau \\ & - \int_0^t \frac{kC(X_1,Z_1,\tau)}{4\pi(t-\tau)\sqrt{D_L D_V}} e^{-\frac{(x-X_1-u(t-\tau))^2}{4D_L(t-\tau)} - \frac{(z-Z_1+f(t)-f(\tau))^2}{4D_V(t-\tau)}}\, d\tau \end{aligned} \tag{6.57}$$

but the subsequent expression for $q(t)$ obtained by applying the boundary condition $\frac{\partial C}{\partial z}(x,0,t) = 0$ is not independent of x. An alternative may be to make the time-varying source a planar source, with strength $q(x,t)$ [kg m^{-2} s^{-1}]; however this has not been pursued.

One-Dimensional Solution

In 1-D, and with $D_V \neq 0$, our advection-dispersion model with evaporation and a point representation for trapping becomes

$$\frac{\partial C}{\partial t} - S(t)\frac{\partial C}{\partial z} = D_V \frac{\partial^2 C}{\partial z^2} + \frac{Q}{m_0}\delta(z-H)\,\delta(t) - kC(Z_1,t)\,\delta(z-Z_1) \tag{6.58}$$

with initial and boundary conditions

$$C\left(z,0^-\right) = 0,$$
$$C(\infty,t) = 0, \text{ and } \frac{\partial C}{\partial z}(0,t) = 0.$$

This is conceptually a plane release with a plane representation for trapping (see the description for the the 1-D model without evaporation in Section 4.4). Our solution to Equation (6.58) involves two stages; first, the moving coordinate system as used in Case 1 reduces the problem to a diffusion equation, which we then solve by modifying a powerful Greens function technique. A full working of the solution may be found in Appendix A.3.

In the moving coordinate system as used in Case 1, the number concentration is denoted $C^*(Z,t)$ where $Z = z - H + f(t)$ with $f(t) = \int_0^t S(\tau)\ d\tau$, and Equation (6.58) becomes

$$\frac{\partial C^*}{\partial t} = D_V \frac{\partial^2 C^*}{\partial Z} + \frac{Q}{m_0}\delta(Z)\,\delta(t) - kC^*(Z_1 - H + f(t),t)\,\delta(Z + H - Z_1 - f(t)) \tag{6.59}$$

with initial and boundary conditions

$$C^*\left(Z,0^-\right) = 0,$$
$$C^*(\infty,t) = 0 \text{ and } \frac{\partial C^*}{\partial Z}(-H + f(t),t) = 0.$$

The problem is now one of diffusion only, but with a moving boundary. The droplets are released from $Z = 0$, at time $t = 0$, and disperse vertically whilst the ground and trapping plane rise with speed $S(t)$ to meet them. The boundary condition requires zero vertical dispersive flux on the moving ground.

We note that Equation (6.4) is similar in many ways to a Stefan problem. Stefan problems usually involve heat transfer with a phase change that results in a moving boundary; for example

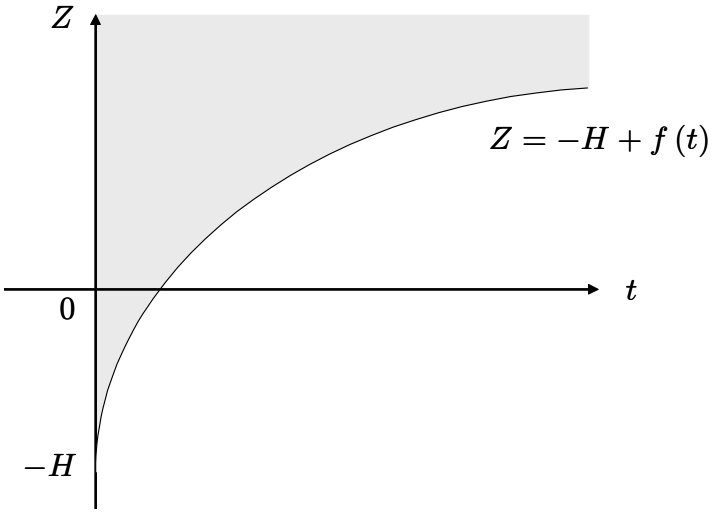

Figure 6.4: Solution space (shaded in grey) in the moving coordinate system (Z, t).

a melting block of ice – the boundary of the ice recedes as the block melts. Generally the objective is to determine the path of the moving boundary, however, in our case, we know the path of the moving boundary and wish to use it to solve for the concentration. With some modification, a Greens function method described for Stefan problems in Crank (1984) will work to provide a solution, albeit one nestled in an integral equation.

The solution space is $t > 0$ and $-H + f(t) \leq Z < \infty$, as shown by the grey-shaded region in Figure 6.4. The method as described in Crank (1984, pp. 117-119) requires a Greens function which obeys the boundary conditions. There is no (known) Greens function matching the condition on the moving boundary; instead, we modify the technique by knowingly using a Green function which does not match, and this results in an extra term in the integral equation. The Green function used is

$$G_{X00}(Z, t|\xi, \tau) = \frac{1}{2\sqrt{\pi D_V (t-\tau)}} e^{-\frac{(Z-\xi)^2}{4D_V(t-\tau)}} H(t-\tau) \tag{6.60}$$

(Beck *et al.*, 1992) which is for the infinite space $-\infty < Z < \infty$, and obeys boundary conditions $G_{X00}(\pm\infty, t|\xi, \tau) = 0$. Beck *et al.* (1992, pp. 40-43) show how to combine G_{X00} and $C^*(\xi, \tau)$ to give

$$\begin{aligned} G\frac{\partial C^*}{\partial \tau} + C^*\frac{\partial G_{X00}}{\partial \tau} &= D_V\left(G_{X00}\frac{\partial^2 C^*}{\partial \xi^2} - C^*\frac{\partial^2 G_{X00}}{\partial \xi^2}\right) \\ &\quad + \frac{Q}{m_0} G_{X00}\delta(\xi)\,\delta(\tau) - C^*\delta(\xi - z)\,\delta(\tau - t) \\ &\quad - kC^*(Z_1 - H + f(\tau), \tau)\, G_{X00}\delta(\xi + H - Z_1 - f(\tau)). \end{aligned} \tag{6.61}$$

Now, following Crank (1984), we integrate with respect to ξ between $-H+f(t) \leq \xi < \infty$, and with respect to τ between 0 and $t+\varepsilon$ where ε is a small positive number:

$$\begin{aligned}\int_0^{t+\varepsilon}\int_{-H+f(\tau)}^{\infty}\frac{\partial}{\partial\tau}\left(C^*G_{X00}\right)\,d\xi\,d\tau &= \int_0^{t+\varepsilon}\int_{-H+f(\tau)}^{\infty}D_V\left(G_{X00}\frac{\partial^2 C^*}{\partial\xi^2}-C^*\frac{\partial^2 G_{X00}}{\partial\xi^2}\right)\,d\xi\,d\tau\\ &+\int_0^{t+\varepsilon}\int_{-H+f(\tau)}^{\infty}\left(\frac{Q}{m_0}G_{X00}\delta\left(\xi\right)\delta\left(\tau\right)-C^*\delta\left(\xi-Z\right)\delta\left(\tau-t\right)\right)\,d\xi\,d\tau\\ &-\int_0^{t+\varepsilon}\int_{-H+f(\tau)}^{\infty}kC^*\left(Z_1-H+f\left(\tau\right),\tau\right)G_{X00}\delta\left(\xi+H-Z_1-f\left(\tau\right)\right)\,d\xi\,d\tau\end{aligned} \tag{6.62}$$

The first term of Equation (6.62) is simplified by changing the order of integration. The second term is simplified using integration by parts, and the third and fourth terms may be integrated directly. Letting $\varepsilon \to 0$, the result is

$$\begin{aligned}&C^*\left(Z,t\right)\mathcal{H}\left(Z+H-f\left(t\right)\right)=\frac{Q}{m_0}G_{X00}\left(Z,t|0,0\right)\\ &+\int_0^t C^*\left(-H+f\left(\tau\right),\tau\right)\left(D_V\frac{\partial G_{X00}}{\partial\xi}\left(Z,t|-H+f\left(\tau\right),\tau\right)-\frac{G_{X00}\left(Z,t|-H+f\left(\tau\right),\tau\right)}{F'\left(f\left(\tau\right)\right)}\right)\,d\tau\\ &-\int_0^t kC^*\left(Z_1-H+f\left(\tau\right),\tau\right)G_{X00}\left(Z,t|Z_1-H+f\left(\tau\right),\tau\right)\,d\tau\end{aligned} \tag{6.63}$$

where F is once again the inverse of f. Returning to the original coordinate system, and substituting Equation (6.61) for G_{X00}, the integral equation solution to our advection-dispersion model with evaporation and a point representation for trapping is

$$\begin{aligned}C\left(z,t\right)\mathcal{H}\left(z\right)&=\frac{Q}{2m_0\sqrt{\pi D_V t}}e^{-\frac{\left(z-H+f(t)\right)^2}{4D_V t}}\\ &+\int_0^t\frac{C\left(0,\tau\right)}{2\sqrt{\pi D_V\left(t-\tau\right)}}e^{-\frac{\left(z+f(t)-f(\tau)\right)^2}{4D_V(t-\tau)}}\left(\frac{z+f\left(t\right)-f\left(\tau\right)}{2\left(t-\tau\right)}-\frac{1}{F'\left(f\left(\tau\right)\right)}\right)\,d\tau\\ &-\int_0^t\frac{kC\left(Z_1,\tau\right)}{2\sqrt{\pi D_V\left(t-\tau\right)}}e^{-\frac{\left(z-Z_1+f(t)-f(\tau)\right)^2}{4D_V(t-\tau)}}\,d\tau.\end{aligned} \tag{6.64}$$

The, as yet unknowns, $C\left(0,t\right)$ and $C\left(Z_1,t\right)$ appear inside the integrals, which are not true convolution integrals, and the term involving $C\left(0,t\right)$ occurs as a consequence of G_{X00} not obeying the boundary condition on the ground. Note, too, the definition of the Heaviside function as in Abramowitz (1964):

$$\mathcal{H}(z) = \begin{cases} 0, & z < 0, \\ \frac{1}{2}, & z = 0, \\ 1, & z > 0, \end{cases} \tag{6.65}$$

so that on the ground $\mathcal{H}(z) = \mathcal{H}(0) = 1/2$. Though not an ideal solution (as the integrals must be evaluated numerically), Equation (6.64) is at least mostly analytical. A relatively simple numerical procedure is described below, based upon the method in Chapter 4 (page 60), which gives good accuracy with minimum computational difficulty.

A Numerical Evaluation Method

The following is a simple numerical scheme for evaluating $C(0,t)$ and $C(Z_1,t)$. From Equation (6.64), the system for $C(0,t)$ and $C(Z_1,t)$ is

$$\begin{aligned} C(0,t) &= 2g_1(0,t) + \int_0^t \left(2C(0,\tau)\, g_2(0,t,\tau) - 2kC(Z_1,\tau)\, g_3(0,t,\tau)\right)\, d\tau \\ C(Z_1,t) &= g_1(Z_1,t) + \int_0^t \left(C(0,\tau)\, g_2(Z_1,t,\tau) - kC(Z_1,\tau)\, g_3(Z_1,t,\tau)\right)\, d\tau \end{aligned} \tag{6.66}$$

where

$$g_1(z,t) = \frac{Qe^{-\frac{(z-H+f(t))^2}{4D_V t}}}{m_0\sqrt{\pi D_V t}},\ g_2(z,t,\tau) = \frac{e^{-\frac{(z+f(t)-f(\tau))^2}{4D_V(t-\tau)}}}{2\sqrt{\pi D_V(t-\tau)}}\left(\frac{z+f(t)-f(\tau)}{2(t-\tau)} - \frac{1}{F'(f(\tau))}\right)$$

$$\text{and } g_3(z,t,\tau) = \frac{e^{-\frac{(z-Z_1+f(t)-f(\tau))^2}{4D_V(t-\tau)}}}{2\sqrt{\pi D_V(t-\tau)}}. \tag{6.67}$$

When $z = 0$, g_2 is singular at the upper end-point of the integration $\tau = t$, and when $z = Z_1$, it is g_3 that is singular at the upper end-point. The same product integration technique as described in Chapter 4 can be used here for the singular integrals, whilst the non-singular integrals can be handled by a trapezium integration (see pages 60 – 61). Given discrete time-steps

$$t_1 = 0,\ t_2 = \Delta t,\ t_3 = 2\Delta t,\ \ldots\ t_i = (i-1)\,\Delta t, \tag{6.68}$$

the system in Equation (6.66) is approximated by

$$\begin{aligned} C(0,t_i) \simeq 2g_1(0,t_i) + \sum_{j=2}^{i-1} &\left[4C(0,t_j)\,\beta_0(t_i,t_j)\left(\sqrt{t_i-t_j} - \sqrt{t_i-t_{j+1}}\right)\right. \\ &\left. -2k\Delta t C(Z_1,t_j)\, g_3(0,t_i,t_j)\ \right] \\ C(Z_1,t_i) \simeq g_1(Z_1,t_i) + \sum_{j=2}^{i-1} &\left[\Delta t C(0,t_j)\, g_2(Z_1,t_i,t_j)\right. \\ &\left. -2kC(Z_1,t_j)\,\beta_1(t_i,t_j)\left(\sqrt{t_i-t_j} - \sqrt{t_i-t_{j+1}}\right)\right] \end{aligned} \tag{6.69}$$

where $\beta_0(t_i, t_j)$ and $\beta_1(t_i, t_j)$ are the parts of $g_2(0, t_i, t_j)$ and $g_3(Z_1, t_i, t_j)$ that are non-singular when $t_j = t_i$; that is

$$\beta_0(t_i, t_j) = \frac{e^{-\frac{(f(t)-f(\tau))^2}{4D_V(t-\tau)}}}{2\sqrt{\pi D_V}} \left(\frac{f(t) - f(\tau)}{2(t-\tau)} - \frac{1}{F'(f(\tau))} \right), \text{ and } \beta_1(t_i, t_j) = \frac{e^{-\frac{(f(t)-f(\tau))^2}{4D_V(t-\tau)}}}{2\sqrt{\pi D_V}}. \quad (6.70)$$

With this method of numerical evaluation, both $C(0, t_i)$ and $C(Z_1, t_i)$ are calculated using only values from previous time steps, so there is no need to solve simultaneously.

Total Droplet Trapping and Deposition

Following Section 6.2, the total mass of droplets trapped per unit area [kg m^{-2}] is

$$M_{TT} = \int_0^{t_s} m(t)\, kC(Z_1, t)\ dt. \quad (6.71)$$

Equation (6.71) must also be evaluated numerically; this can be done using any numerical integration scheme, with values for $C(Z_1, t)$ at discrete time steps calculated according to Equation (6.69).

The density of deposit on the ground [kg m^{-2}] is

$$M_D = \int_0^{t_s} m(t)\, S(t)\, C(0, t)\ dt. \quad (6.72)$$

Similarly, this must be evaluated numerically using values for $C(0, t)$ at discrete time steps calculated according to Equation (6.69).

Two-Dimensional Solution

In 2-D, and with $D_V \neq 0$, our advection-dispersion model with evaporation and a point representation for trapping becomes

$$\begin{aligned} \frac{\partial C}{\partial t} + u\frac{\partial C}{\partial x} - S(t)\frac{\partial C}{\partial z} &= D_L\frac{\partial^2 C}{\partial x^2} + D_V\frac{\partial^2 C}{\partial z^2} + \frac{Q}{m_0}\delta(x - X_0)\,\delta(z - H)\,\delta(t) \\ &\quad -kC(X_1, Z_1, t)\,\delta(x - X_1)\,\delta(z - Z_1) \end{aligned} \quad (6.73)$$

with initial and boundary conditions

$$C\left(x, z, 0^-\right) = 0,$$

$$C(x, z, t) \to 0 \text{ as } x \to \pm\infty \text{ and } z \to +\infty,$$

$$\text{and } \frac{\partial C}{\partial z}(x, 0, t) = 0.$$

The conceptual situation is a line release with a line representation for trapping (see page 62). We solve Equation (6.73) using Fourier transforms combined with the method described for the 1-D solution. Taking Fourier transforms with respect to x (so that $C(x,z,t) \rightarrow \widehat{C}(\omega,z,t)$), and then substituting $\widehat{C}(\omega,z,t) = \widehat{V}(\omega,z,t)\, e^{-\left(\omega^2 D_L + i\omega u\right)t}$ gives

$$\frac{\partial \widehat{V}}{\partial t} - S(t)\frac{\partial \widehat{V}}{\partial z} = D_V \frac{\partial^2 \widehat{V}}{\partial z^2} + \frac{Q}{m_0} e^{-i\omega X_0}\delta(Z)\,\delta(t) - kC(X_1,Z_1,t)\, e^{-i\omega(X_1-ut)+\omega^2 D_L t}\delta(z-Z_1) \tag{6.74}$$

with initial and boundary conditions

$$\widehat{V}\left(\omega,z,0^-\right) = 0,\ \widehat{V}(\omega,z,t) \rightarrow 0 \text{ as } z \rightarrow \infty, \text{ and } \frac{\partial \widehat{V}}{\partial z}(\omega,0,t) = 0.$$

Equation (6.74) is now in the same form as Equation (6.59) in the 1-D solution; by following the method laid out for the 1-D solution we obtain

$$\begin{aligned}\widehat{V}(\omega,z,t)\,\mathcal{H}(z) = {} & \frac{Q}{2m_0\sqrt{\pi D_V t}} e^{-i\omega X_0 - \frac{(z-H+f(t))^2}{4D_V t}} \\ & + \int_0^t \frac{\widehat{V}(\omega,0,\tau)}{2\sqrt{\pi D_V (t-\tau)}} e^{-\frac{(z+f(t)-f(\tau))^2}{4D_V(t-\tau)}} \left(\frac{z+f(t)-f(\tau)}{2(t-\tau)} - \frac{1}{F'(f(\tau))}\right) d\tau \\ & - \int_0^t \frac{kC(X_1,Z_1,\tau)}{2\sqrt{\pi D_V (t-\tau)}} e^{-i\omega(X_1-u\tau)+\omega^2 D_L \tau - \frac{(z-Z_1+f(t)-f(\tau))^2}{4D_V(t-\tau)}}\, d\tau \end{aligned} \tag{6.75}$$

and subsequently,

$$\begin{aligned}\widehat{C}(\omega,z,t)\,\mathcal{H}(z) = {} & \frac{Q}{2m_0\sqrt{\pi D_V t}} e^{-i\omega(X_0+ut)-\omega^2 D_L t - \frac{(z-H+f(t))^2}{4D_V t}} \\ & + \int_0^t \frac{\widehat{C}(\omega,0,\tau)}{2\sqrt{\pi D_V (t-\tau)}} e^{-\left(\omega^2 D_L + i\omega u\right)(t-\tau) - \frac{(z+f(t)-f(\tau))^2}{4D_V(t-\tau)}} \left(\frac{z+f(t)-f(\tau)}{2(t-\tau)} - \frac{1}{F'(f(\tau))}\right) d\tau \\ & - \int_0^t \frac{kC(X_1,Z_1,\tau)}{2\sqrt{\pi D_V (t-\tau)}} e^{-i\omega(X_1+u(t-\tau))-\omega^2 D_L (t-\tau) - \frac{(z-Z_1+f(t)-f(\tau))^2}{4D_V(t-\tau)}}\, d\tau. \end{aligned} \tag{6.76}$$

The integrals in Equation (6.76) have singularities of the form $(t-\tau)^{-1/2}$ at the upper end-point. Inverting the Fourier transform at this point results in integrals in the inverse transform which have singularities of the form $(t-\tau)^{-1}$ at the upper end-point. The difficulty of numerical evaluation around these singularities is avoided by following the procedure described below, where the integration in time is carried out before inverting the transform.

Numerical Evaluation

As in the 1-D solution, both integrals in Equation (6.76) have singularities of the form $(t-\tau)^{-1/2}$ at the upper end-point (the first integral when $z=0$ and the second when $z=Z_1$); accordingly, we evaluate Equation (6.76) using the same numerical procedure as on page 137.

Discrete ω values $\omega_n = \omega_1 + (n-1)\,\Delta\omega$, where $n = 1, \ldots, N$, are chosen to cover a broad enough range between $-\infty$ and ∞ so that $\widehat{C}\,(\omega_1, z, t)$ and $\widehat{C}\,(\omega_N, z, t)$ are both very small in magnitude. Then, at discrete time-steps $t_i = (i-1)\,\Delta t$ where $i = 1, 2, 3, \ldots$

$$\begin{aligned}\widehat{C}\,(\omega_n, 0, t_i) \simeq{}& 2g_1\,(0, t_i)\,e^{-i\omega_n(X_0+ut_i)-\omega_n^2 D_L t_i} \\ &+\sum_{j=2}^{i-1}\Big[4\widehat{C}\,(\omega_n, 0, t_j)\,e^{-\left(\omega_n^2 D_L + i\omega_n u\right)(t_i-t_j)}K_0\,(t_i, t_j)\,(\sqrt{t_i-t_j}-\sqrt{t_i-t_{j+1}}) \\ &-2k\Delta t C\,(X_1, Z_1, t_j)\,e^{-\omega_n^2 D_L(t_i-t_j)-i\omega_n(X_1+u(t_i-t_j))}g_3\,(0, t_i, t_j)\Big]\end{aligned} \tag{6.77}$$

and,

$$\begin{aligned}\widehat{C}\,(\omega_n, Z_1, t_i) \simeq{}& g_1\,(Z_1, t_i)\,e^{-i\omega_n(X_0+ut_i)-\omega^2 D_L t_i} \\ &+\sum_{j=2}^{i-1}\Big[\Delta t\widehat{C}\,(\omega_n, 0, t_j)\,e^{-\left(\omega_n^2 D_L t_i + i\omega_n u\right)(t_i-t_j)}g_2\,(Z_1, t_i, t_j) \\ &-2kC\,(X_1, Z_1, t_j)\,K_1\,(t_i, t_j)\,e^{-\omega_n^2 D_L(t_i-t_j)-i\omega_n(X_1+u(t_i-t_j))}\,(\sqrt{t_i-t_j}-\sqrt{t_i-t_{j+1}})\Big]\end{aligned} \tag{6.78}$$

with g_1, g_2, g_3, K_0 and K_1 as on page 137. At each time step t_i, after calculation of Equation (6.78), the Fourier transform must be numerically inverted to obtain $C\,(X_1, Z_1, t_i)$ for use at the next time step. We use a trapezium integration to invert the Fourier transform, so that for any (x, z)

$$C\,(x, z, t_i) \simeq \frac{\Delta\omega}{2\pi}\sum_{n=2}^{N-1}\widehat{C}\,(\omega_n, z, t_i)\,e^{i\omega_n x}. \tag{6.79}$$

Total Droplet Trapping and Deposition

The total mass of droplets trapped per unit area [kg m^{-1}] is

$$M_{TT} = \int_0^{t_s} m\,(t)\,kC\,(X_1, Z_1, t)\;\,dt \tag{6.80}$$

which we evaluate using discrete values of $C\,(X_1, Z_1, t)$ calculated from the numerical inverse Fourier transform of Equation (6.78).

The density of deposit on the ground [kg m^{-2}] is

$$M_D(x) = \int_0^{t_s} m(t)\, S(t)\, C(x, 0, t)\ dt \tag{6.81}$$

which is similarly evaluated using discrete values of $C(x, 0, t)$, calculated according to Equation (6.77) with a numerical inversion of the Fourier transform.

An Illustrative Example of the Two-Dimensional Solution

The following illustrative example uses the same parameters as the previous example in Case 1, but with $D_V \neq 0$. The initial values for the droplets are diameter $d_0 = 100$ μm, mass $m_0 = 5.23{\times}10^{-10}$ kg and settling speed $S_0 = 0.37$ m s^{-1}, and the remaining parameters are summarised in Table 6.2. To reiterate, the unrealistically high value for $\overline{k}$ is used only to make the effect of trapping more visible. According to Equation (6.10), the disappearance time is $t_s = 22.2$ s

Table 6.2: Parameter set used to generate Figure 6.3.

u	(L_L, L_V)	ϕ	T_∞	Q	(X_0, H)	$\overline{k}$	$\Delta x \Delta z$	(X_1, Z_1)
1 m s^{-1}	$(2, 1)$ m	60 %	20 °C	1 kg m^{-1}	$(0, 3)$ m	25 s^{-1}	0.04 m^2	$(4, 2)$ m

Figure 6.5 shows that the mass density of deposit, obtained by numerically evaluating Equation (6.81) without evaporation ($S(t) = S_0$, $t_s = \infty$), is the same as that obtained from the analytical result in Chapter 4.

Figure 6.6 illustrates the effect of evaporation on the deposition profile. The highest of the dashed lines represents the mass density of deposit with neither evaporation nor trapping. The second of the dashed lines is with evaporation but without trapping, and the solid line is with both evaporation and trapping. One again, the deposit with evaporation is significantly reduced over that without. Adding the trapping further reduces the deposit, however the degree of reduction is less than in the previous example where $D_V = 0$. Here the maximum reduction is around 23 % as opposed to around 43 % with $D_V = 0$.

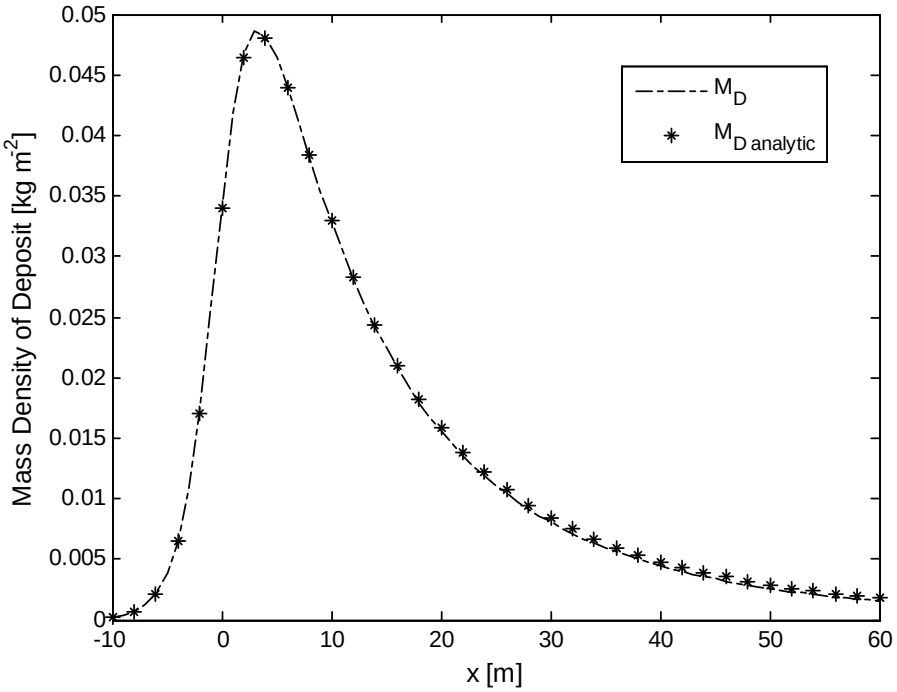

Figure 6.5: Cross-sections of the density of deposit M_D [kg m^{-2}] obtained from the numerical evaluation of Equation (6.81), with no evaporation and no trapping, compared with the analytic result from Chapter 4 ($M_{D\ analytic}$, Equation 4.73). Parameter values are as given in Table 6.2.

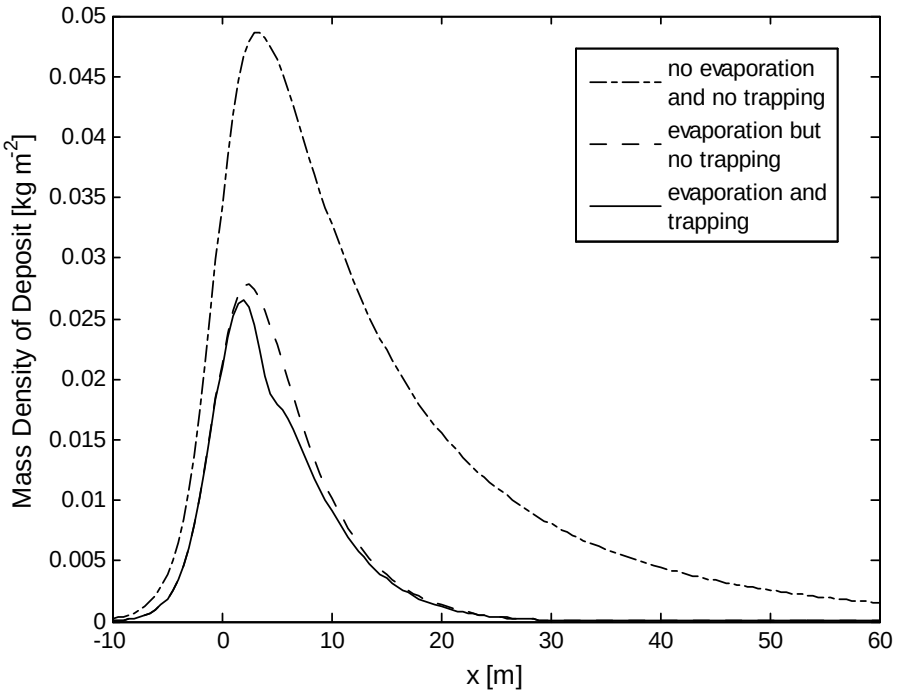

Figure 6.6: Cross-section of the density of deposit on the ground [kg m^{-2}], with and without evaporation and/or trapping, resulting from a line release with non-zero vertical dispersion and a line representation for trapping. Parameter values are the same as for Figure 6.5.

Three-Dimensional Solution

In all three spatial dimensions, and with $D_V \neq 0$, our advection-dispersion model with evaporation and a point representation for trapping is as given by Equation (6.1), that is

$$\begin{aligned}\frac{\partial C}{\partial t}+u\frac{\partial C}{\partial x}-S\left(t\right)\frac{\partial C}{\partial z} &= D_L\frac{\partial^2 C}{\partial x^2}+D_T\frac{\partial^2 C}{\partial y^2}+D_V\frac{\partial^2 C}{\partial z^2}\\ &\quad +\frac{Q}{m_0}\delta\left(x-X_0\right)\delta\left(y-Y_0\right)\delta\left(z-H\right)\delta\left(t\right)\\ &\quad -kC\left(X_1,Y_1,Z_1,t\right)\delta\left(x-X_1\right)\delta\left(y-Y_1\right)\delta\left(z-Z_1\right)\end{aligned} \tag{6.82}$$

with initial and boundary conditions

$$\begin{gathered}C\left(x,y,z,0^-\right)=0,\\ C\left(x,y,z,t\right)\rightarrow 0 \text{ as } x,y\rightarrow\pm\infty \text{ and } z\rightarrow+\infty,\\ \text{and } \frac{\partial C}{\partial z}\left(x,y,0,t\right)=0.\end{gathered}$$

We solve Equation (6.82) following the same method as used in the 2-D solution; that is, by taking Fourier transforms with respect to x and y (so that $C\left(x,y,z,t\right)\rightarrow\widetilde{\widehat{C}}\left(\omega,\psi,z,t\right)$), and then making the substitution $\widetilde{\widehat{C}}\left(\omega,\psi,z,t\right)=\widetilde{\widehat{V}}\left(\omega,\psi,z,t\right)e^{-\left(\omega^2D_L+i\omega u+\psi^2D_T\right)t}$. The result is

$$\begin{aligned}\widetilde{\widehat{V}}\left(\omega,\psi,z,t\right)\mathcal{H}\left(z\right) &= \frac{Q}{2m_0\sqrt{\pi D_V t}}e^{-i\omega X_0-i\psi Y_0-\frac{\left(z-H+f(t)\right)^2}{4D_V t}}\\ &\quad +\int_0^t\frac{\widetilde{\widehat{V}}\left(\omega,\psi,0,\tau\right)}{2\sqrt{\pi D_V\left(t-\tau\right)}}e^{-\frac{\left(z+f(t)-f(\tau)\right)^2}{4D_V(t-\tau)}}\left(\frac{z+f\left(t\right)-f\left(\tau\right)}{2\left(t-\tau\right)}-\frac{1}{F'\left(f\left(\tau\right)\right)}\right)d\tau\\ &\quad -\int_0^t\frac{kC\left(X_1,Y_1,Z_1,\tau\right)}{2\sqrt{\pi D_V\left(t-\tau\right)}}e^{-i\omega(X_1-u\tau)+\omega^2D_L\tau-i\psi Y_1+\psi^2D_T\tau-\frac{\left(z-Z_1+f(t)-f(\tau)\right)^2}{4D_V(t-\tau)}}d\tau\end{aligned} \tag{6.83}$$

and subsequently,

$$\begin{aligned}\widetilde{\widehat{C}}\left(\omega,\psi,z,t\right)\mathcal{H}\left(z\right) &= \frac{Q}{2m_0\sqrt{\pi D_V t}}e^{-i\omega(X_0+ut)-i\psi Y_0-\left(\omega^2D_L+\psi^2D_T\right)-\frac{\left(z-H+f(t)\right)^2}{4D_V t}}\\ &\quad +\int_0^t\frac{\widehat{C}\left(\omega,\psi,0,\tau\right)}{2\sqrt{\pi D_V\left(t-\tau\right)}}e^{-\left(\omega^2D_L+i\omega u+\psi^2D_T\right)(t-\tau)-\frac{\left(z+f(t)-f(\tau)\right)^2}{4D_V(t-\tau)}}\left(\frac{z+f\left(t\right)-f\left(\tau\right)}{2\left(t-\tau\right)}-\frac{1}{F'\left(f\left(\tau\right)\right)}\right)d\tau\\ &\quad -\int_0^t\frac{kC\left(X_1,Y_1,Z_1,\tau\right)}{2\sqrt{\pi D_V\left(t-\tau\right)}}e^{-i\omega(X_1+u(t-\tau))-i\psi Y_1-\left(\omega^2D_L+\psi^2D_T\right)(t-\tau)-\frac{\left(z-Z_1+f(t)-f(\tau)\right)^2}{4D_V(t-\tau)}}d\tau.\end{aligned} \tag{6.84}$$

As in the 2-D solution, the integrals in Equation (6.84) have singularities of the form $(t-\tau)^{-1/2}$ at the upper end-point, and inverting the Fourier transforms at this point results in integrals in

the inverse transform which have singularities of the form $(t-\tau)^{-3/2}$ at the upper end-point. We avoid the difficulty caused by these singularities by numerically evaluating Equation (6.84) using the same procedure as described for the 2-D solution (the only difference is that two Fourier transforms must be inverted after each time step).

Total Droplet Trapping and Deposition

The total mass of droplets trapped [kg] is

$$M_{TT} = \int_0^{t_s} m(t)\, kC(X_1, Y_1, Z_1, t)\ dt \tag{6.85}$$

and the density of deposit on the ground [kg m^{-2}] is

$$M_D(x,y) = \int_0^{t_s} m(t)\, S(t)\, C(x,y,0,t)\ dt, \tag{6.86}$$

both of which are evaluated numerically using discrete values of $C(X_1, Y_1, Z_1, t)$ and $C(x,y,0,t)$ calculated according to the numerical procedure from the 2-D solution.

6.6 Partial Evaporation (Solid Core)

In reality the droplets will be a mix of water and an active ingredient; the active ingredient does not evaporate, thus, after all of the water has evaporated, a small "solid core" of active ingredient will remain. Generally it is assumed that evaporation occurs as though the droplets were purely water, until only the solid core remains, after which there is no further evaporation (Thompson & Ley, 1983; Miller & Hadfield, 1989).

We include the solid core phenomenon in our model by using piecewise functions for the droplet mass and settling speed. The initial volume of each droplet is $V_0 = \frac{4}{3}\pi a_0^3$; if the volume fraction of active ingredient in the droplet is I [-], then the radius of the droplet when only the active ingredient remains is

$$a_I = \left(\frac{3IV_0}{4\pi}\right)^{1/3} = I^{1/3} a_0. \tag{6.87}$$

Using Equations (6.9) – (6.13), the time at all of the water evaporates is

$$t_I = t_s\left(1 - I^{2/3}\right), \tag{6.88}$$

the mass of each droplet at this time is

$$m_I = m_0 \left(1 - \frac{t_I}{t_s}\right)^{2/3} \tag{6.89}$$

and the settling speed is

$$S_I = S_0 \left(1 - \frac{t_I}{t_s}\right). \tag{6.90}$$

We define piecewise functions for the mass and settling speed, so that up until time t_I the mass and settling speed decrease as the droplet evaporates, and after time t_I they remain constant as there is no further evaporation:

$$m(t) = \begin{cases} m_0 \left(1 - \dfrac{t}{t_s}\right)^{3/2}, & t < t_I, \\ m_I, & t \geq t_I \end{cases} \tag{6.91}$$

and

$$S(t) = \begin{cases} S_0 \left(1 - \dfrac{t}{t_s}\right), & t < t_I, \\ S_I, & t \geq t_I. \end{cases} \tag{6.92}$$

Each of the solutions in the previous sections may be calculated with these piecewise functions for $m(t)$ and $S(t)$.

The volume fraction of active ingredient in the droplets I can vary widely with different applications; less than 10 % would be a reasonable value [A. Forster, personal communication, 24 September, 2008]. The example below is in 2-D, with $D_V \neq 0$, and is calculated for droplets which have $I = 5$ %. The droplets have initial diameter 100 μm with initial mass $m_0 = 5.23 \times 10^{-10}$ kg and initial settling speed $S_0 = 0.37$ m s^{-1}; the time at which all of the water evaporates leaving only the active ingredient is $t_I = 19.2$ s, with $m_I = 2.62 \times 10^{-11}$ kg and $S_I = 0.05$ m s^{-1}. The remaining parameters are the same as those in Table 6.2. Figures 6.7 and 6.8 show the number and mass densities of deposit respectively. The droplets with a solid core (partial evaporation) deposit over a greater distance, because the core is small and light and therefore carried further by the wind. The effect is not easily visible for the mass deposition density however, as the core is so much lighter than the original droplet.

6.7 Chapter Summary

In this chapter we took our advection-dispersion model with the point representation for trapping from Chapter 4, and redefined it in terms of the droplet number concentration to include the

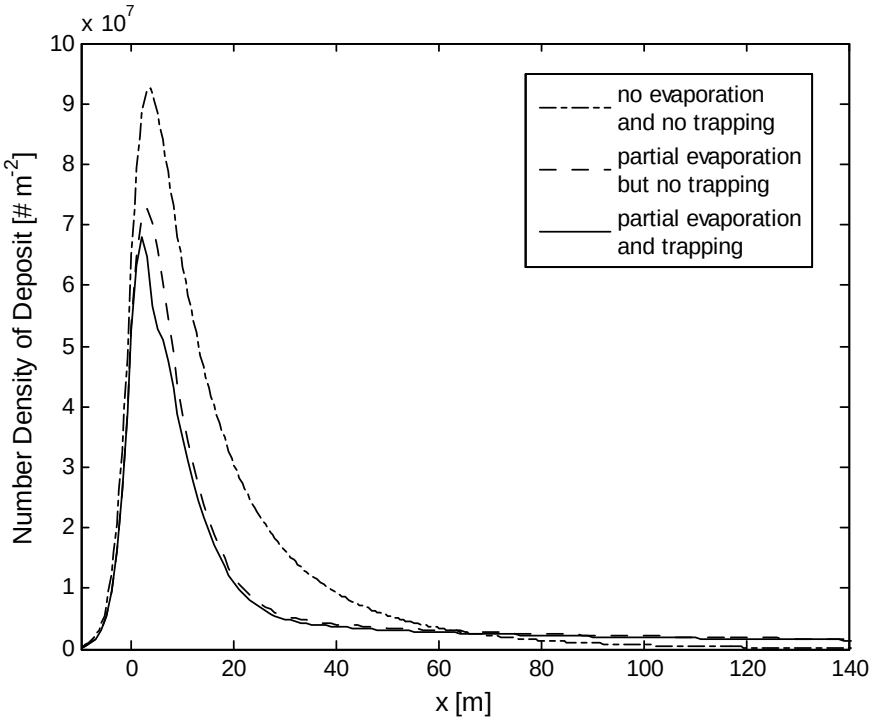

Figure 6.7: Cross-section of the number density of deposit N_D [# m^{-2}] for droplets which evaporate only partially, leaving a small "solid core" of active ingredient. Parameter values are as given in the text.

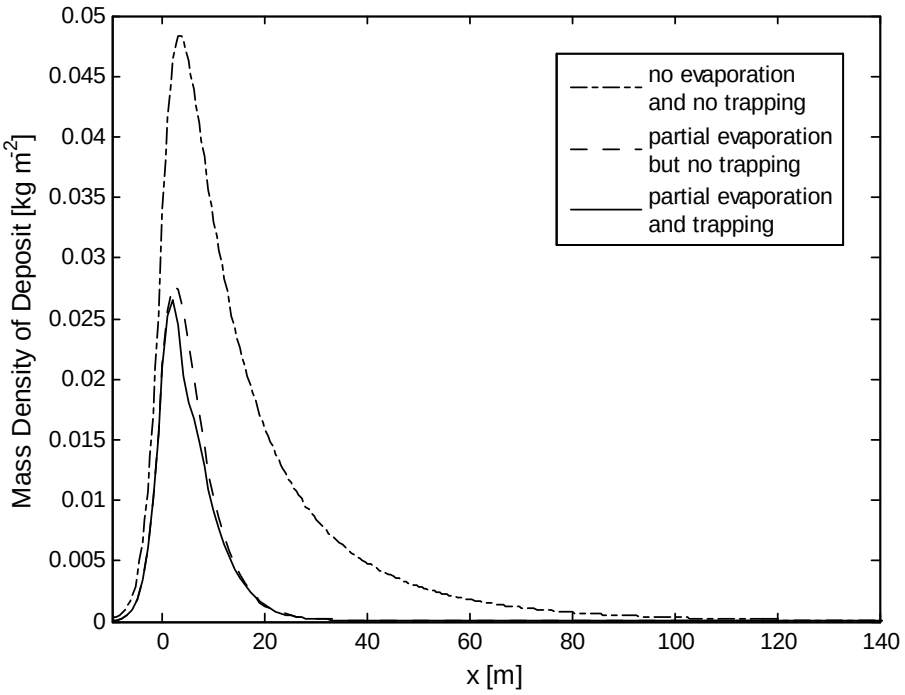

Figure 6.8: Cross-section of the mass density of deposit M_D [kg m^{-2}] for droplets which only partially evaporate, leaving a small "solid core". Parameter values are the same as for Figure 6.7.

effect of evaporation. Using the number concentration, rather than the mass concentration, meant that evaporation only influenced the model via the time-dependent settling speed.

We began by establishing the model in terms of the number concentration and relating it back to the mass concentration. Subsequently, we presented solutions in one, two and three dimensions for two separate cases: zero vertical dispersion, and non-zero vertical dispersion. The case of zero vertical dispersion was relatively straightforward, and the solutions were obtained by introducing a moving coordinate system. In the case of non-zero vertical dispersion the model was very difficult to solve analytically; we achieved the most success by combining the moving coordinate system with a Green function technique.

For each case, we presented an example to show the significant reduction in the mass density of deposit as a result of evaporation. These examples were calculated for droplets which were 100 % water, and therefore could evaporate until nothing remained. Approximations for the droplet mass and settling speed, based on the information in Chapter 2, were used to make the calculation simpler. To conclude the chapter, we considered a further example with only partial evaporation since, realistically, droplets contain a small amount of pesticide, and this remains as a solid core after all of the water has evaporated. With partial evaporation, the drift distances of droplets were much greater, since the solid core which remains after all of the water has evaporated is very small and light, and is therefore blown far by the wind before depositing.

Chapter 7

Thesis Summary

7.1 Summary

The object of this thesis was to develop a simple analytical model for the transport of drifting spray droplets, including the trapping of these droplets within a shelterbelt. Building on the approach of McKibbin (2006) in previous analysis of particle transport within a forest canopy, we applied an advection-dispersion model for the droplet transport and added a sink term to represent trapping within the shelterbelt.

The model was derived under the assumptions that:

- The rate at which droplets are removed by trapping is proportional to the local concentration. The proportionality constant is related to the shelterbelt characteristics and the droplet size.
- The mean wind flow through and around the shelterbelt is horizontal and uniform in both speed and direction.
- Turbulence in the airflow is characterised by some dominant length scales alongwind, crosswind and vertically, and that these length scales are uniform in space and time.
- The ground is approximately horizontal, and is impervious to the droplets so that they cannot disperse through it.
- The droplets are all of the same mass and are released instantaneously from a point source. To simulate a distribution of droplet sizes we would run the model for a number of different droplet sizes and superpose the results. Results for different source types can also be constructed from those for the point release.

In order to solve the model analytically we discretised the shelterbelt. This was done by representing the shelterbelt as a three-dimensional array of blocks, with the trapping in each block concentrated to the point at its centre. First, we considered the more straightforward case where there was no evaporation of the droplets; we determined solutions to the model with just a single point representation for trapping, and then built upon those results to determine a solution for trapping in the discretised shelterbelt. Finally, we considered the more difficult case where there was evaporation; in this case we analysed only the single point representation for trapping.

In each case above we determined solutions in one, two and three dimensions for: (i) zero vertical dispersion, and (ii) non-zero vertical dispersion of the droplets. For the model without evaporation, the solutions with zero vertical dispersion were obtained using standard transform methods. With non-zero vertical dispersion the solutions obtained were embedded in integral equations, however, we were able to use Laplace transforms to explicitly evaluate the total amount trapped and the deposit on the ground. In two and three dimensions some of the Laplace transforms had to be sourced from generalised calculus. To solve the model with evaporation we introduced a moving coordinate system; it was relatively straightforward to obtain solutions with zero vertical dispersion, but with non-zero vertical dispersion the solutions obtained were nestled in integral equations which had to be evaluated numerically.

As a consequence of focusing all of the trapping within a volume to an infinitely small point, we observed that in the solutions to our model the concentration of droplets became negative in the vicinity of the trapping. In this vicinity the model does not accurately reflect the conceptual situation. However, with realistic trapping rates this issue has very little effect on the calculated total amount trapped and the deposit on the ground, since the vicinity in which the concentration is negative is very small.

7.2 Analyses

In each of the solutions described above, we were able to write expressions for the total amount trapped and the subsequent deposit on the ground. In two and three dimensions, we presented calculated examples of the deposition profile on the ground, and the percentage reduction in deposit as a result of trapping. A shadow area of reduced deposit was clearly visible downwind of the trapping in each example; the reduction was greater with zero vertical dispersion, but persisted much further downwind with non-zero vertical dispersion.

7.3 Further Research

Some suggestions for future research following this thesis include:

- Extension of the model with evaporation to include trapping in a discretised shelterbelt. At this stage solutions to the model with evaporation have only been determined for the single point representation for trapping. These solutions could be combined to construct solutions to the model with trapping in a discretised shelterbelt, in the same manner as in Chapter 5.

- Possible use of an alternative boundary condition. In an advection-dispersion model for volcanic ashfall McKibbin *et al.* (2005) used an infinite solution space $-\infty < z < \infty$, with the concentration set to zero at $z = \pm\infty$. This did not ensure that the condition of zero vertical dispersive flux at ground level is met, however the form of the solution was much simpler, and the deposit on the ground was not greatly altered. This approach may result in a simpler form for the solution to our model with evaporation and non-zero vertical dispersion; if so, and if the deposit on the ground is not greatly altered, this may provide a better alternative.

- Experimentation with the shelterbelt discretisation. In Chapter 5 we discretised the shelterbelt by dividing it into a three-dimensional array of blocks; N blocks wide by L blocks long by M blocks high. For a given shelterbelt, there are many possible combinations for N, L and M; it appears from the examples in Chapter 5 that the number of blocks used vertically has a greater effect on the total trapping and deposit than the number of blocks used horizontally. Possible questions include: is there an optimum number of blocks, and, if so, how does this change with shelterbelt size?

- Exploration of the parameter space. Most of the solutions presented in this thesis result in expressions for the total trapping and deposition which are explicitly expressed in terms of the influencing parameters. These expressions could be used to explore the effects of variations in these parameters, and to identify which parameters have the greatest effect.

7.4 Publications

The author has presented material from this thesis at a number of New Zealand and international conferences, and was recipient of the T. M. Cherry Prize, awarded for the best student presentation, at the annual Australia and New Zealand Industrial and Mathematics (ANZIAM)

conference in Fremantle, Australia, 2007. The author also received highly commended in the Aitken Prize, awarded for the best student presenation at the New Zealand Mathematics Colloquium in Palmerston North, New Zealand, 2005, and highly commended in the T. M Cherry Prize at the annual ANZIAM conference in Sydney, Australia, 2008.

Material from Chapter 5 of this thesis may be found published in the *Gazette of the Australian Mathematical Society* (Harper, 2007), subsequent to the award of the T. M. Cherry Prize, and further material from this thesis will be published at a later date.

Appendix A

Selected Workings

A.1 The Dispersion Tensor

This section contains a derivation of the dispersion tensor $\underline{\mathbf{D}}$ as used in Section 3.1 [R. McKibbin, personal communication, 15 September, 2006].

Figure A.1 shows the mean wind velocity $\mathbf{u} = (u, v, 0)$ in the horizontal plane; $\mathbf{L}$ is a unit vector parallel to the wind, and $\mathbf{N}$ is a unit vector perpendicular to the wind.

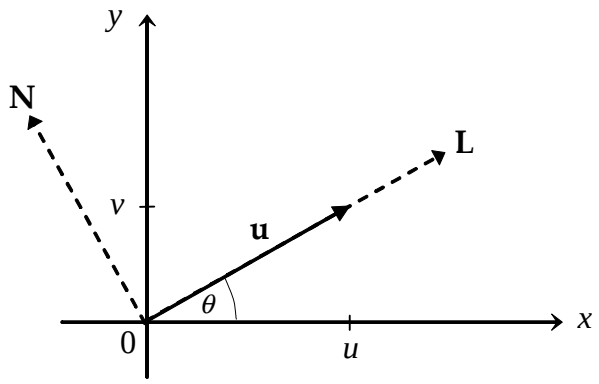

Figure A.1: Mean wind velocity $\mathbf{u}$ in the horizontal plane

Unit vectors $\mathbf{L}$ and $\mathbf{N}$ are given by

$$\mathbf{L} = \frac{u}{|\mathbf{u}|}\mathbf{i} + \frac{v}{|\mathbf{u}|}\mathbf{j} + 0\mathbf{k}, \text{ and} \tag{A.1}$$

$$\mathbf{N} = -\frac{v}{|\mathbf{u}|}\mathbf{i} + \frac{u}{|\mathbf{u}|}\mathbf{j} + 0\mathbf{k}. \tag{A.2}$$

Assuming that the dispersion may be described according to Fick's Law, the dispersive fluxes of droplets alongwind, crosswind and vertically are

$$\mathbf{q}_L = -D_L\left(\mathbf{L}\cdot\nabla c\right)\mathbf{L},$$
$$\mathbf{q}_T = -D_T\left(\mathbf{N}\cdot\nabla c\right)\mathbf{N} \text{ and}$$
$$\mathbf{q}_V = -D_V\left(\mathbf{k}\cdot\nabla c\right)\mathbf{k},$$

where D_L, D_T, and D_V are the dispersion coefficients in each direction, and $\mathbf{L}\cdot\nabla c$, $\mathbf{N}\cdot\nabla c$ and $\mathbf{k}\cdot\nabla c$ are the concentration gradients. The result is:

$$\mathbf{q}_L = -\frac{D_L}{|\mathbf{u}|^2}\left(u^2\frac{\partial c}{\partial x} + uv\frac{\partial c}{\partial y}\right)\mathbf{i} - \frac{D_L}{|\mathbf{u}|^2}\left(uv\frac{\partial c}{\partial x} + v^2\frac{\partial c}{\partial y}\right)\mathbf{j}, \tag{A.3}$$

$$\mathbf{q}_T = -\frac{D_T}{|\mathbf{u}|^2}\left(v^2\frac{\partial c}{\partial x} - uv\frac{\partial c}{\partial y}\right)\mathbf{i} + \frac{D_T}{|\mathbf{u}|^2}\left(uv\frac{\partial c}{\partial x} - u^2\frac{\partial c}{\partial y}\right)\mathbf{j} \text{ and} \tag{A.4}$$

$$\mathbf{q}_V = -D_V\frac{\partial c}{\partial z}\mathbf{k}. \tag{A.5}$$

The total dispersive flux of droplets per unit area, $\mathbf{q}_D = \mathbf{q}_L + \mathbf{q}_T + \mathbf{q}_V$, is then

$$\begin{aligned}\mathbf{q}_D \;=\; & -\left(D_L\frac{u^2}{|\mathbf{u}|^2} + D_T\frac{v^2}{|\mathbf{u}|^2}\right)\frac{\partial c}{\partial x}\mathbf{i} - \left(D_L\frac{uv}{|\mathbf{u}|^2} - D_T\frac{uv}{|\mathbf{u}|^2}\right)\frac{\partial c}{\partial y}\mathbf{i} \\ & -\left(D_L\frac{uv}{|\mathbf{u}|^2} - D_T\frac{uv}{|\mathbf{u}|^2}\right)\frac{\partial c}{\partial x}\mathbf{j} - \left(D_L\frac{v^2}{|\mathbf{u}|^2} + D_T\frac{u^2}{|\mathbf{u}|^2}\right)\frac{\partial c}{\partial y}\mathbf{j} - D_T\frac{\partial c}{\partial z}\mathbf{k}.\end{aligned} \tag{A.6}$$

If the x, y and z components of $\mathbf{q}_D$ are denoted q_x, q_y and q_z (so that $\mathbf{q}_D = q_x\mathbf{i} + q_y\mathbf{j} + q_z\mathbf{k}$), then Equation (A.6) may be rewritten as follows:

$$\begin{bmatrix} q_x \\ q_y \\ q_z \end{bmatrix} = -\begin{bmatrix} D_{xx} & D_{xy} & D_{xz} \\ D_{yx} & D_{yy} & D_{yz} \\ D_{zx} & D_{zy} & D_{zz} \end{bmatrix}\begin{bmatrix} \dfrac{\partial c}{\partial x} \\ \dfrac{\partial c}{\partial y} \\ \dfrac{\partial c}{\partial z} \end{bmatrix} = -\underline{\mathbf{D}}\nabla c \tag{A.7}$$

where the dispersion tensor $\underline{\mathbf{D}}$ has components

$$\begin{aligned} D_{xx} &= D_L\frac{u^2}{|\mathbf{u}|^2} + D_T\frac{v^2}{|\mathbf{u}|^2}, & D_{xy} &= D_{yx} = (D_L - D_T)\frac{uv}{|\mathbf{u}|^2}, \\ D_{yy} &= D_L\frac{v^2}{|\mathbf{u}|^2} + D_T\frac{u^2}{|\mathbf{u}|^2}, & D_{xz} &= D_{zx} = 0, \\ D_{zz} &= D_V, & D_{yz} &= D_{zy} = 0. \end{aligned}$$

If the wind is blowing at angle θ (as shown in Figure A.1) then $u = |\mathbf{u}|\cos\theta$ and $v = |\mathbf{u}|\sin\theta$; the dispersion tensor becomes

$$\underline{\mathbf{D}} = \begin{bmatrix} D_L\cos^2\theta + D_T\sin^2\theta & (D_L - D_T)\sin\theta\cos\theta & 0 \\ (D_L - D_T)\sin\theta\cos\theta & D_L\sin^2\theta + D_T\cos^2\theta & 0 \\ 0 & 0 & D_V \end{bmatrix}. \tag{A.8}$$

A.2 A Point Representation for Trapping with $D_V \neq 0$

This section contains a full working of the 1-D solution, as presented in Section 4.4, for the advection-dispersion model with $D_V \neq 0$ and a point representation for trapping.

One-Dimensional Solution (Section 4.4, page 57)

In 1-D, our advection-dispersion model for the droplet mass concentration $c(z,t)$ is

$$\frac{\partial c}{\partial t} - S\frac{\partial c}{\partial z} = D_V \frac{\partial^2 c}{\partial z^2} + Q\delta(z-H)\,\delta(t) - kc(Z_1,t)\,\delta(z-Z_1) \tag{A.9}$$

with initial and boundary conditions

$$c\left(z,0^-\right) = 0,$$
$$c(\infty,t) = 0, \text{ and } \frac{\partial c}{\partial z}(0,t) = 0.$$

Applying the method used for a similar model in Lim (2005, Chap. 2), we begin by writing

$$c(z,t) = U(z,t)\, e^{-\frac{Sz}{2D_V} - \frac{S^2 t}{4D_V}} \tag{A.10}$$

so that Equation (A.9) becomes

$$\frac{\partial U}{\partial t} - D_V \frac{\partial^2 U}{\partial z^2} = P(z,t) \tag{A.11}$$

with

$$\begin{aligned} P(z,t) &= e^{\frac{Sz}{2D_V} + \frac{S^2 t}{4D_V}} \left(Q\delta(z-H)\,\delta(t) - kc(Z_1,t)\,\delta(z-Z_1)\right) \\ &= Qe^{\frac{SH}{2D_V}}\delta(z-H)\,\delta(t) - kc(Z_1,t)\, e^{\frac{SZ_1}{2D_V} + \frac{S^2 t}{4D_V}}\delta(z-Z_1). \end{aligned} \tag{A.12}$$

We then write

$$V(z,t) = \frac{\partial U}{\partial z} - \frac{SU}{2D_V} \tag{A.13}$$

and apply the operator $\left(\frac{\partial}{\partial t} - D_V\frac{\partial^2}{\partial z^2}\right)$ to obtain a diffusion equation with zero boundary conditions; that is

$$\begin{aligned} \frac{\partial V}{\partial t} - D_V\frac{\partial^2 V}{\partial z^2} &= \frac{\partial}{\partial z}\left(\frac{\partial U}{\partial t} - D_V\frac{\partial^2 U}{\partial z^2}\right) - \frac{S}{2D_V}\left(\frac{\partial U}{\partial t} - D_V\frac{\partial^2 U}{\partial z^2}\right) \\ &= \frac{\partial P}{\partial z} - \frac{SP}{2D_V} \end{aligned} \tag{A.14}$$

with $V(z,0^-) = 0$, and $V(0,t) = V(\infty,t) = 0$. This form of diffusion equation has a known Green's function; following Beck *et al.* (1992, p. 43) the solution is

$$V(z,t) = \int_0^t d\tau \int_0^\infty \left(\frac{\partial P}{\partial \xi}(\xi,\tau) - \frac{S}{2D_V}P(\xi,\tau)\right) G_{X10}(z,t \mid \xi,\tau)\; d\xi \tag{A.15}$$

where

$$G_{X10}\left(z,t \mid \xi,\tau\right) = \frac{1}{\sqrt{4\pi D_V\left(t-\tau\right)}}\left(e^{-\frac{(z-\xi)^2}{4D_V(t-\tau)}} - e^{-\frac{(z+\xi)^2}{4D_V(t-\tau)}}\right). \tag{A.16}$$

Integrating by parts in Equation (A.15) gives

$$V\left(z,t\right) = \int_0^t d\tau\left(\Big[P\left(\xi,\tau\right)\Big]_0^\infty - \int_0^\infty P\left(\xi,\tau\right)\left(\frac{SG_{X10}}{2D_V} + \frac{\partial G_{X10}}{\partial\xi}\right)\,d\xi\right), \tag{A.17}$$

and since $P\left(0,\tau\right) = P\left(\infty,\tau\right) = 0$ this becomes

$$V\left(z,t\right) = -\int_0^t d\tau\int_0^\infty P\left(\xi,\tau\right)\left(\frac{SG_{X10}}{2D_V} + \frac{\partial G_{X10}}{\partial\xi}\right)\,d\xi. \tag{A.18}$$

Substituting for $P\left(\xi,\tau\right)$ from (A.12):

$$\begin{aligned} V\left(z,t\right) &= -\int_0^t d\tau\int_0^\infty Qe^{\frac{SH}{2D_V}}\delta\left(\xi-H\right)\delta\left(\tau\right)\left(\frac{SG_{X10}}{2D_V} + \frac{\partial G_{X10}}{\partial\xi}\right)\,d\xi \\ &\quad + \int_0^t d\tau\int_0^\infty kc\left(Z_1,\tau\right)e^{\frac{SZ_1}{2D_V}+\frac{S^2\tau}{4D_V}}\delta\left(\xi-Z_1\right)\left(\frac{SG_{X10}}{2D_V} + \frac{\partial G_{X10}}{\partial\xi}\right)\,d\xi \\ &= -Qe^{\frac{SH}{2D_V}}\mathcal{H}\left(t\right)\left[\frac{SG_{X10}}{2D_V} + \frac{\partial G_{X10}}{\partial\xi}\right]_{\substack{\tau=0,\\ \xi=H}} \\ &\quad + \int_0^t kc\left(Z_1,\tau\right)e^{\frac{SZ_1}{2D_V}+\frac{S^2\tau}{4D_V}}\left[\frac{SG_{X10}}{2D_V} + \frac{\partial G_{X10}}{\partial\xi}\right]_{\xi=Z_1}d\tau. \end{aligned} \tag{A.19}$$

After inserting G_{X10} and $\dfrac{\partial G_{X10}}{\partial\xi}$ and doing a little rearranging we obtain

$$\begin{aligned} V\left(z,t\right) &= -\frac{Qe^{\frac{SH}{2D_V}}\mathcal{H}\left(t\right)}{\sqrt{4\pi D_V t}}\left[\left(\frac{S}{2D_V} + \frac{z-H}{2D_V t}\right)e^{-\frac{(z-H)^2}{4D_V t}} + \left(-\frac{S}{2D_V} + \frac{z+H}{2D_V t}\right)e^{-\frac{(z+H)^2}{4D_V t}}\right] \\ &\quad + \int_0^t \frac{kc\left(Z_1,\tau\right)e^{\frac{SZ_1}{2D_V}+\frac{S^2\tau}{4D_V}}}{\sqrt{4\pi D_V\left(t-\tau\right)}}\left[\left(\frac{S}{2D_V} + \frac{z-Z_1}{2D_V\left(t-\tau\right)}\right)e^{-\frac{(z-Z_1)^2}{4D_V(t-\tau)}}\right. \\ &\quad \left. + \left(-\frac{S}{2D_V} + \frac{z+Z_1}{2D_V\left(t-\tau\right)}\right)e^{-\frac{(z+Z_1)^2}{4D_V(t-\tau)}}\right]\,d\tau. \end{aligned} \tag{A.20}$$

Armed now with a solution for $V\left(z,t\right)$, we work backwards to obtain the desired result $c\left(z,t\right)$. First, we return to Equation (A.13) and solve for $U\left(z,t\right)$ using the integrating factor technique:

$$e^{-\frac{Sz}{2D_V}}U\left(z,t\right) = \int_0^z e^{-\frac{S\xi}{2D_V}}V\left(\xi,t\right)\,d\xi + U\left(0,t\right). \tag{A.21}$$

Next, we require an expression for $U\left(0,t\right)$. Differentiating Equation (A.13) with respect to z and then setting $z = 0$:

$$\frac{\partial V}{\partial z}\left(0,t\right) = \frac{\partial^2 U}{\partial z^2}\left(0,t\right) - \frac{S}{2D_V}\frac{\partial U}{\partial z}\left(0,t\right). \tag{A.22}$$

Also, setting $z = 0$ in Equation (A.11):

$$\frac{\partial U}{\partial t}(0,t) - D_V \frac{\partial^2 U}{\partial z^2}(0,t) = P(0,t). \tag{A.23}$$

Equations (A.22) and (A.23) combine to give

$$\frac{\partial U}{\partial t}(0,t) = \frac{S}{2}\frac{\partial U}{\partial z}(0,t) + D_V \frac{\partial V}{\partial z}(0,t) + P(0,t), \tag{A.24}$$

which simplifies to

$$\frac{\partial U}{\partial t}(0,t) - \frac{S^2}{4D_V} U(0,t) = D_V \frac{\partial V}{\partial z}(0,t) \tag{A.25}$$

since $P(0,t) = 0$ and $V(0,t) = 0$, therefore $\frac{\partial U}{\partial z}(0,t) = \frac{S}{2D_V} U(0,t)$ by Equation (A.13). An expression for $U(0,t)$may be found by solving Equation (A.25) using the integrating factor technique:

$$U(0,t) = e^{\frac{S^2 t}{4D_V}} \int_0^t D_V \frac{\partial V}{\partial z}(0,\tau)\, e^{-\frac{S^2 \tau}{4D_V}}\, d\tau. \tag{A.26}$$

Returning now to Equation (A.21), we have for $U(z,t)$

$$e^{-\frac{Sz}{2D_V}} U(z,t) = \int_0^z e^{-\frac{S\xi}{2D_V}} V(\xi,t)\, d\xi + e^{\frac{S^2 t}{4D_V}} \int_0^t D_V \frac{\partial V}{\partial z}(0,\tau)\, e^{\frac{S^2 \tau}{4D_V}}\, d\tau. \tag{A.27}$$

Back-substituting this into Equation (A.10):

$$\begin{aligned} c(z,t) &= U(z,t)\, e^{-\frac{Sz}{2D_V} - \frac{S^2 t}{4D_V}} \\ &= e^{-\frac{S^2 t}{4D_V}} \int_0^z e^{-\frac{S\xi}{2D_V}} V(\xi,t)\, d\xi + \int_0^t D_V \frac{\partial V}{\partial z}(0,\tau)\, e^{\frac{S^2 \tau}{4D_V}}\, d\tau. \end{aligned} \tag{A.28}$$

Inserting $V(z,t)$ from Equation (A.20):

$$\begin{aligned} c(z,t) = & -\frac{Q e^{-\frac{S^2 t}{4D_V}}}{\sqrt{4\pi D_V t}} \int_0^z e^{-\frac{S(\xi - H)}{2D_V}} \left[\left(\frac{S}{2D_V} + \frac{\xi - H}{2D_V t} \right) e^{-\frac{(\xi - H)^2}{4D_V t}} \right. \\ & \left. + \left(-\frac{S}{2D_V} + \frac{\xi + H}{2D_V t} \right) e^{-\frac{(\xi + H)^2}{4D_V t}} \right] d\xi \\ & + \int_0^z \int_0^t \frac{kc(Z_1,\tau)\, e^{-\frac{S(\xi - Z_1)}{2D_V} - \frac{S^2 (t-\tau)}{4D_V}}}{\sqrt{4\pi D_V (t-\tau)}} \left[\left(\frac{S}{2D_V} + \frac{\xi - Z_1}{2D_V (t-\tau)} \right) e^{-\frac{(\xi - Z_1)^2}{4D_V (t-\tau)}} \right. \\ & \left. + \left(-\frac{S}{2D_V} + \frac{\xi + Z_1}{2D_V (t-\tau)} \right) e^{-\frac{(\xi + Z_1)^2}{4D_V (t-\tau)}} \right] d\tau\, d\xi + \int_0^t D_V \frac{\partial V}{\partial z}(0,\tau)\, e^{\frac{S^2 \tau}{4D_V}}\, d\tau. \end{aligned} \tag{A.29}$$

Equation(A.29) above may be further simplified; in lines 1 and 2 we perform the following integrations by parts:

$$\int_0^z \frac{S}{2D_V} e^{-\frac{S(\xi - H)}{2D_V} - \frac{(\xi - H)^2}{4D_V t}}\, d\xi = -e^{-\frac{S(z-H)}{2D_V} - \frac{(z-H)^2}{4D_V t}} + e^{\frac{SH}{2D_V} - \frac{H^2}{4D_V t}} - \int_0^z \frac{(\xi - H)}{2D_V t} e^{-\frac{S(\xi - H)}{2D_V} - \frac{(\xi - H)^2}{4D_V t}}\, d\xi$$

and

$$\int_0^z \frac{(\xi+H)}{2D_V t} e^{-\frac{S(\xi-H)}{2D_V}-\frac{(\xi+H)^2}{4D_V t}}\,d\xi = -e^{-\frac{S(z-H)}{2D_V}-\frac{(z+H)^2}{4D_V t}} + e^{\frac{SH}{2D_V}-\frac{H^2}{4D_V t}} - \int_0^z \frac{S}{2D_V} e^{-\frac{S(\xi-H)}{2D_V}-\frac{(\xi+H)^2}{4D_V t}}\,d\xi,$$

then in lines 3 and 4 we interchange the order of integration and perform the same integrations by parts, but with H replaced by Z_1 and t replaced by $t-\tau$. After simplifying,

$$\begin{aligned} c(z,t) &= \frac{Qe^{-\frac{S^2 t}{4D_V}}}{\sqrt{4\pi D_V t}}\left[e^{-\frac{S(z-H)}{2D_V}}\left(e^{-\frac{(z-H)^2}{4D_V t}}+e^{-\frac{(z+H)^2}{4D_V t}}\right)-2e^{\frac{SH}{2D_V}-\frac{H^2}{4D_V t}}\right. \\ &\quad \left.+\frac{S}{D_V}\int_0^z e^{-\frac{S(\xi-H)}{2D_V}-\frac{(\xi+H)^2}{4D_V t}}\,d\xi\right]-\int_0^t \frac{kc(Z_1,\tau)\,e^{-\frac{S^2(t-\tau)}{4D_V}}}{\sqrt{4\pi D_V(t-\tau)}}\left[e^{-\frac{S(z-Z_1)}{2D_V}}\left(e^{-\frac{(z-Z_1)^2}{4D_V(t-\tau)}}\right.\right. \\ &\quad \left.\left.+e^{-\frac{(z+Z_1)^2}{4D_V(t-\tau)}}\right)-2e^{\frac{SZ_1}{2D_V}-\frac{Z_1^2}{4D_V(t-\tau)}}+\frac{S}{D_V}\int_0^z e^{-\frac{S(\xi-Z_1)^2}{2D_V}-\frac{(\xi+Z_1)^2}{4D_V(t-\tau)}}\,d\xi\right]d\tau \\ &\quad +\int_0^t D_V\frac{\partial V}{\partial z}(0,\tau)\,e^{-\frac{S^2\tau}{4D_V}}\,d\tau. \end{aligned} \tag{A.30}$$

This is as far as Lim's 2005 method takes us, but we are able to go one step further by applying the boundary condition $c(\infty,t)=0$; this gives us an expression for the terms which are dependent only on t. Applying the boundary condition to Equation (A.30) gives

$$\begin{aligned} 0 &= \frac{Qe^{-\frac{S^2 t}{4D_V}}}{\sqrt{4\pi D_V t}}\left[-2e^{\frac{SH}{2D_V}-\frac{H^2}{4D_V t}}+\frac{S}{D_V}\int_0^\infty e^{-\frac{S(\xi-H)}{2D_V}-\frac{(\xi+H)^2}{4D_V t}}\,d\xi\right] \\ &\quad -\int_0^t \frac{kc(Z_1,\tau)\,e^{-\frac{S^2(t-\tau)}{4D_V}}}{\sqrt{4\pi D_V(t-\tau)}}\left[-2e^{\frac{SZ_1}{2D_V}-\frac{Z_1^2}{4D_V(t-\tau)}}+\frac{S}{D_V}\int_0^\infty e^{-\frac{S(\xi-Z_1)}{2D_V}-\frac{(\xi+Z_1)^2}{4D_V(t-\tau)}}\,d\xi\right]d\tau \\ &\quad +\int_0^t D_V\frac{\partial V}{\partial z}(0,\tau)\,e^{-\frac{S^2\tau}{4D_V}}\,d\tau. \end{aligned} \tag{A.31}$$

Using this result to substitute for the terms dependent only on t in Equation (A.30), then simplifying:

$$\begin{aligned} c(z,t) &= \frac{Qe^{-\frac{s^2 t}{4D_V}}}{\sqrt{4\pi D_V t}}\left[e^{-\frac{S(z-H)}{2D_V}}\left(e^{-\frac{(z-H)^2}{4D_V t}}+e^{-\frac{(z+H)^2}{4D_V t}}\right)-\frac{S}{D_V}\int_z^\infty e^{-\frac{S(\xi-H)}{2D_V}-\frac{(\xi+H)^2}{4D_V t}}\,d\xi\right] \\ &\quad -\int_0^t \frac{kc(Z_1,\tau)\,e^{-\frac{S^2(t-\tau)}{4D_V}}}{\sqrt{4\pi D_V(t-\tau)}}\left[e^{-\frac{S(z-Z_1)}{2D_V}}\left(e^{-\frac{(z-Z_1)^2}{4D_V(t-\tau)}}+e^{-\frac{(z+Z_1)^2}{4D_V(t-\tau)}}\right)\right. \\ &\quad \left.-\frac{S}{D_V}\int_z^\infty e^{-\frac{S(\xi-Z_1)}{2D_V}-\frac{(\xi+Z_1)^2}{4D_V(t-\tau)}}\,d\xi\right]d\tau. \end{aligned} \tag{A.32}$$

Alternatively, the integrals in ξ may be written as complementary error functions, so that

$$\begin{aligned} c(z,t) &= \frac{Qe^{-\frac{S^2t}{4D_V}-\frac{S(z-H)}{2D_V}}}{\sqrt{4\pi D_V t}}\left(e^{-\frac{(z-H)^2}{4D_V t}}+e^{-\frac{(z+H)^2}{4D_V t}}\right)-\frac{QS}{2D_V}e^{\frac{SH}{D_V}}\operatorname{erfc}\left(\frac{z+H+St}{2\sqrt{D_V t}}\right) \\ &\quad -\int_0^t \frac{kc(Z_1,\tau)\,e^{-\frac{S^2(t-\tau)}{4D_V}-\frac{S(z-Z_1)}{2D_V}}}{\sqrt{4\pi D_V(t-\tau)}}\left(e^{-\frac{(z-Z_1)^2}{4D_V(t-\tau)}}+e^{-\frac{(z+Z_1)^2}{4D_V(t-\tau)}}\right) \\ &\quad -\frac{kc(Z_1,\tau)\,S}{2D_V}e^{\frac{SZ_1}{D_V}}\operatorname{erfc}\left(\frac{z+Z_1+S(t-\tau)}{2\sqrt{D_V(t-\tau)}}\right). \end{aligned} \tag{A.33}$$

Note that many of the terms inside the convolution integral are the same as those outside, but with H replaced by Z_1 and t replaced by $t-\tau$. Thus, in a much simpler form

$$c(z,t) = Qf(z,t;H) - \int_0^t kc(Z_1,\tau)\,f(z,t-\tau;Z_1)\;d\tau \tag{A.34}$$

where

$$f(z,t;Z) = \frac{e^{-\frac{S^2t}{4D_V}-\frac{S(z-Z)}{2D_V}}}{2\sqrt{\pi D_V t}}\left(e^{-\frac{(z-Z)^2}{4D_V t}}+e^{-\frac{(z+Z)^2}{4D_V t}}\right)-\frac{S}{2D_V}e^{\frac{SZ}{D_V}}\operatorname{erfc}\left(\frac{z+Z+St}{2\sqrt{D_V t}}\right). \tag{A.35}$$

A.3 A Point Representation for Trapping With Evaporation and $D_V \neq 0$

This section contains a full working of the 1-D solution, as presented in Section 6.5, for the advection-dispersion model with $D_V \neq 0$ and a point representation for trapping.

One-Dimensional Solution (Section 6.5, page 134)

In 1-D, our advection-dispersion model for the droplet number concentration $C(z,t)$ with evaporation is

$$\frac{\partial C}{\partial t} - S(t)\frac{\partial C}{\partial z} = D_V \frac{\partial^2 C}{\partial z^2} + \frac{Q}{m_0}\delta(z-H)\,\delta(t) - kC(Z_1,t)\,\delta(z-Z_1) \tag{A.36}$$

with initial and boundary conditions

$$C\left(Z,0^-\right) = 0,$$
$$C(\infty,t) = 0, \text{ and } \frac{\partial C}{\partial z}(0,t) = 0.$$

We solve Equation (A.36) by changing to a moving coordinate system and employing a Greens function technique. In the moving coordinates $C(z,t) \rightarrow C^*(Z,t)$, where $Z = z - H + f(t)$ with $f(t) = \int_0^t S(\tau)\ d\tau$, and Equation (A.36) becomes

$$\frac{\partial C^*}{\partial t} = D_V \frac{\partial^2 C^*}{\partial Z^2} + \frac{Q}{m_0}\delta(Z)\,\delta(t) - kC^*(Z_1 - H + f(t), t)\,\delta(Z + H - Z_1 - f(t)) \tag{A.37}$$

with initial and boundary conditions

$$C^*\left(Z,0^-\right) = 0,$$
$$C^*(\infty,t) = 0, \text{ and } \frac{\partial C^*}{\partial Z}(-H + f(t), t) = 0.$$

In this coordinate system the problem is one of diffusion only, but with a moving boundary. The droplets are released at time $t = 0$ from $Z = 0$; they do not fall, but disperse (vertically) whilst the ground and trapping plane rise with speed $S(t)$ to meet them. Initially, the ground is at $Z = -H$ and the trapping plane is at $Z = Z_1 - H$; their positions after time t are $Z = -H + f(t)$ and $Z = Z_1 - H + f(t)$ respectively. A diagram of the solution space is given in Figure 6.4 on page 135.

We now employ a Green function technique modified from Crank (1984, pp. 117-119). The technique as described by Crank requires a Green function which obeys the boundary conditions.

As there is no (known) Green function which satisfies these conditions, we modify the technique by knowingly using a Green function which does not satisfy the condition on the moving ground boundary.

Take the Green function for a 1-D diffusion equation in an infinite region $-\infty < Z < \infty$ with zero boundary conditions:

$$G_{X00}\left(Z,t|\xi,\tau\right)=\frac{1}{2\sqrt{\pi D_V\left(t-\tau\right)}}e^{-\frac{(Z-\xi)^2}{4D_V(t-\tau)}}\mathcal{H}\left(t-\tau\right) \tag{A.38}$$

(Beck *et al.*, 1992). This Green function is a solution to

$$\frac{\partial G_{X00}}{\partial t}=D_V\frac{\partial^2 G_{X00}}{\partial Z^2}+\delta\left(Z-\xi\right)\delta\left(t-\tau\right),\ t>\tau \tag{A.39}$$

with boundary and initial conditions

$$G_{X00}\left(Z,0^-|\xi,\tau\right)=0,\text{ and } G_{X00}\left(\pm\infty,t|\xi,\tau\right)=0.$$

Note that it does not satisfy $\dfrac{\partial G_{X00}}{\partial Z}\left(-H+f\left(t\right),t|\xi,\tau\right)$, which is the condition on the moving ground boundary.

We combine Equations (A.37) and (A.39) following Beck *et al.* (1992, pp. 40-43). First, the reciprocity relation $G_{X00}\left(Z,t|\xi,\tau\right)=G_{X00}\left(\xi,-\tau|Z,-t\right)$ is applied to Equation (A.39) to give

$$-\frac{\partial G_{X00}}{\partial \tau}=D_V\frac{\partial^2 G_{X00}}{\partial \xi^2}+\delta\left(\xi-Z\right)\delta\left(\tau-t\right). \tag{A.40}$$

Next, the change of variables $Z=\xi$ and $t=\tau$ is applied to Equation (A.37) so that

$$\frac{\partial C^*}{\partial \tau}=D_V\frac{\partial^2 C^*}{\partial \xi^2}+\frac{Q}{m_0}\delta\left(\xi\right)\delta\left(\tau\right)-kC^*\left(Z_1-H+f\left(\tau\right),\tau\right)\delta\left(\xi+H-Z_1-f\left(\tau\right)\right). \tag{A.41}$$

Multiplying Equation (A.40) by $C^*\left(\xi,\tau\right)$, and Equation (A.41) by $G_{X00}\left(Z,t|\xi,\tau\right)$, then subtracting the two:

$$\begin{aligned} G_{X00}\frac{\partial C^*}{\partial \tau}+C^*\frac{\partial G_{X00}}{\partial \tau} &= D_V\left(G_{X00}\frac{\partial^2 C^*}{\partial \xi^2}-C^*\frac{\partial^2 G_{X00}}{\partial \xi^2}\right) \\ &\quad +\frac{Q}{m_0}G_{X00}\delta\left(\xi\right)\delta\left(\tau\right)-C^*\delta\left(\xi-Z\right)\delta\left(\tau-t\right) \\ &\quad -kC^*\left(Z_1-H+f\left(\tau\right),\tau\right)G_{X00}\delta\left(\xi+H-Z_1-f\left(\tau\right)\right). \end{aligned} \tag{A.42}$$

Now, following Crank (1984, pp. 117-119), we integrate only over the domain of interest, that is $-H+f\left(\tau\right)\leq\xi<\infty$ and $0^-<\tau<t+\varepsilon$ where ε is a small positive number:

$$\int_0^{t+\varepsilon}\int_{-H+f(\tau)}^{\infty}\frac{\partial}{\partial\tau}\left(C^*G_{X00}\right)\,d\xi\,d\tau=\int_0^{t+\varepsilon}\int_{-H+f(\tau)}^{\infty}D_V\left(G_{X00}\frac{\partial^2C^*}{\partial\xi^2}-C^*\frac{\partial^2G_{X00}}{\partial\xi^2}\right)\,d\xi\,d\tau$$
$$+\int_0^{t+\varepsilon}\int_{-H+f(\tau)}^{\infty}\left(\frac{Q}{m_0}G_{X00}\delta\left(\xi\right)\delta\left(\tau\right)-C^*\delta\left(\xi-Z\right)\delta\left(\tau-t\right)\right)\,d\xi\,d\tau$$
$$-\int_0^{t+\varepsilon}\int_{-H+f(\tau)}^{\infty}kC^*\left(Z_1-H+f\left(\tau\right),\tau\right)G_{X00}\delta\left(\xi+H-Z_1-f\left(\tau\right)\right)\,d\xi\,d\tau. \tag{A.43}$$

The left-hand side of Equation (A.43) may be simplified by changing the order of integration:

$$\begin{aligned}&\int_0^{t+\varepsilon}\int_{-H+f(\tau)}^{\infty}\frac{\partial}{\partial\tau}\left(C^*G_{X00}\right)\,d\xi\,d\tau\\&=\int_{-H}^{-H+f(t+\varepsilon)}\int_0^{F(\xi+H)}\frac{\partial}{\partial\tau}\left(C^*G_{X00}\right)\,d\tau\,d\xi+\int_{-H+f(t+\varepsilon)}^{\infty}\int_0^{t+\varepsilon}\frac{\partial}{\partial\tau}\left(C^*G_{X00}\right)\,d\tau\,d\xi\\&=\int_{-H}^{-H+f(t+\varepsilon)}\left[C^*G_{X00}\right]_0^{F(\xi+H)}\,d\xi+\int_{-H+f(t+\varepsilon)}^{\infty}\left[C^*G_{X00}\right]_0^{t+\varepsilon}\,d\xi\end{aligned} \tag{A.44}$$

where F is the inverse of function f, so that if $\xi=f\left(\tau\right)$ then $\tau=F\left(\xi\right)$. Equation (A.44) reduces to

$$\begin{aligned}&\int_0^{t+\varepsilon}\int_{-H+f(\tau)}^{\infty}\frac{\partial}{\partial\tau}\left(C^*G_{X00}\right)\,d\xi\,d\tau\\&=\int_{-H}^{-H+f(t+\varepsilon)}C^*\left(\xi,F\left(\xi+H\right)\right)G_{X00}\left(Z,t|\xi,F\left(\xi+H\right)\right)\,d\xi\end{aligned} \tag{A.45}$$

because of the initial condition $C^*\left(\xi,0^-\right)=0$, and also because $G_{X00}\left(Z,t|\xi,t+\varepsilon\right)=0$. We introduce the change of variable $\tau=F\left(\xi+H\right)$; then $f\left(\tau\right)=\xi+H$ and $\dfrac{d\tau}{d\xi}=F'\left(\xi+H\right)=F\prime\left(f\left(\tau\right)\right)$, and Equation (A.45) becomes

$$\begin{aligned}&\int_0^{t+\varepsilon}\int_{-H+f(\tau)}^{\infty}\frac{\partial}{\partial\tau}\left(C^*G_{X00}\right)\,d\xi\,d\tau\\&=\int_0^{t+\varepsilon}C^*\left(-H+f\left(\tau\right),\tau\right)G_{X00}\left(Z,t|-H+f\left(\tau\right),\tau\right)\,\frac{d\tau}{F'\left(f\left(\tau\right)\right)}.\end{aligned} \tag{A.46}$$

Returning to Equation (A.43), the first double integral on the right-hand side may be simplified using integration by parts:

$$\int_0^{t+\varepsilon}\int_{-H+f(\tau)}^{\infty} D_V\left(G_{X00}\frac{\partial^2 C^*}{\partial\xi^2}-C^*\frac{\partial^2 G_{X00}}{\partial\xi^2}\right)\,d\xi\,d\tau$$
$$=\int_0^{t+\varepsilon} D_V\left[G_{X00}\frac{\partial C^*}{\partial\xi}-C^*\frac{\partial G_{X00}}{\partial\xi}\right]_{-H+f(\tau)}^{\infty}\,d\tau$$
$$=\int_0^{t+\varepsilon} D_V C^*\left(-H+f\left(\tau\right),\tau\right)\frac{\partial G_{X00}}{\partial\xi}\left(Z,t|-H+f\left(\tau\right),\tau\right)\,d\tau. \tag{A.47}$$

The second double integral on the right-hand side of Equation (A.43) may be integrated directly:

$$\int_0^{t+\varepsilon}\int_{-H+f(\tau)}^{\infty}\left(\frac{Q}{m_0}G_{X00}\delta\left(\xi\right)\delta\left(\tau\right)-C^*\delta\left(\xi-Z\right)\delta\left(\tau-t\right)\right)\,d\xi\,d\tau$$
$$=\frac{Q}{m_0}G_{X00}\left(Z,t|0,0\right)-C^*\left(Z,t\right)\mathcal{H}\left(Z+H-f\left(t\right)\right). \tag{A.48}$$

Note that we use the definition of the Heaviside function as in Abramowitz (1964), that is

$$\mathcal{H}\left(Z+H-f\left(t\right)\right)=\begin{cases}0, & Z<-H+f\left(t\right),\\ \frac{1}{2}, & Z=-H+f\left(t\right),\\ 1, & Z>-H+f\left(t\right).\end{cases} \tag{A.49}$$

The value of $\mathcal{H}\left(Z+H-f\left(t\right)\right)=\frac{1}{2}$ at $Z=-H+f\left(t\right)$ results from the definition of the Dirac delta function $\delta\left(\xi-Z\right)$ as a Gaussian distribution which is centred at $\xi=Z$ and has zero variance, that is

$$\delta\left(\xi-Z\right)=\lim_{\sigma\to 0^+}\frac{e^{-\frac{(\xi-Z)^2}{\sigma^2}}}{\sigma\sqrt{\pi}}.$$

If $Z=-H+f\left(t\right)$, then

$$\int_{-H+f(t)}^{\infty}\delta\left(\xi-Z\right)\,d\xi=\frac{1}{2} \tag{A.50}$$

because the distribution is centred at $\xi=-H+f\left(t\right)$ and so the integral is capturing only half of the area under the distribution.

Returning once again to Equation (A.43), the third double integral on the right-hand simplifies to

$$-\int_0^{t+\varepsilon}\int_{-H+f(\tau)}^{\infty} kC^*\left(Z_1-H+f\left(\tau\right),\tau\right)G_{X00}\delta\left(\xi+H-Z_1-f\left(\tau\right)\right)\,d\xi\,d\tau$$
$$=-\int_0^{t+\varepsilon} kC^*\left(Z_1-H+f\left(\tau\right),\tau\right)G_{X00}\left(Z,t|Z_1-H+f\left(\tau\right),\tau\right)\mathcal{H}\left(Z_1\right)\,d\tau. \tag{A.51}$$

We will assume that $Z_1>0$ so that $\mathcal{H}\left(Z_1\right)=1$.

Substituting the results from Equations (A.46) – (A.48) and (A.51) back into Equation (A.43), then letting $\varepsilon \to 0$ and rearranging gives

$$\begin{aligned} C^*(Z,t)\,\mathcal{H}(Z+H-f(t)) &= \frac{Q}{m_0} G_{X00}(Z,t|0,0) \\ &+ \int_0^t C^*(-H+f(\tau),\tau)\left(D_V \frac{\partial G_{X00}}{\partial \xi}(Z,t|-H+f(\tau),\tau) - \frac{G_{X00}(Z,t|-H+f(\tau),\tau)}{F'(f(\tau))}\right) d\tau \\ &- \int_0^t kC^*(Z_1-H+f(\tau),\tau)\, G_{X00}(Z,t|Z_1-H+f(\tau),\tau)\; d\tau, \qquad Z_1>0. \end{aligned} \tag{A.52}$$

Returning to the original coordinate system (z,t) and substituting Equation (A.38) for G_{X00}:

$$\begin{aligned} C(z,t)\,\mathcal{H}(z) &= \frac{Q}{2m_0\sqrt{\pi D_V t}} e^{-\frac{(z-H+f(t))^2}{4D_V t}} \\ &+ \int_0^t \frac{C(0,\tau)}{2\sqrt{\pi D_V (t-\tau)}} e^{-\frac{(z+f(t)-f(\tau))^2}{4D_V(t-\tau)}} \left(\frac{z+f(t)-f(\tau)}{2(t-\tau)} - \frac{1}{F'(f(\tau))}\right) d\tau \\ &- \int_0^t \frac{kC(Z_1,\tau)}{2\sqrt{\pi D_V (t-\tau)}} e^{-\frac{(z-Z_1+f(t)-f(\tau))^2}{4D_V(t-\tau)}}\; d\tau, \qquad Z_1>0. \end{aligned} \tag{A.53}$$

Appendix B

Laplace and Fourier Transforms

B.1 Laplace Transforms

Table B.1 contains formulae for the Laplace transforms which have been used in this thesis. Numbers $1-9$ are from Roberts & Kaufman (1966), and Numbers $10-11$ are generalised Laplace transforms from Zemanian (1987).

Table B.1: Table of Laplace transforms

	$f(t)$	$\overline{f}(p) = \int_0^\infty e^{-pt} f(t)\ dt$	Conditions
1	$f'(t)$	$p\overline{f}(p) - f(0)$	
2	$f''(t)$	$p^2\overline{f}(p) - pf'(0) - f(0)$	
3	$e^{-at} f(t)$	$\overline{f}(p+a)$	
4	$\int_0^t f(\tau)\, g(t-\tau)\ d\tau$	$\overline{f}(p)\,\overline{g}(p)$	
5	$\delta(t-a)$	e^{-ap}	$a \geq 0$, $\mathrm{Re}\, p > -\infty$

	$f(t)$	$\overline{f}(p) = \int_0^\infty e^{-pt} f(t)\ dt$	Conditions
6	$\frac{1}{\sqrt{t}} e^{-\frac{a}{t}}$	$\sqrt{\frac{\pi}{p}} e^{-2\sqrt{ap}}$	$\operatorname{Re} a \geq 0$, $\operatorname{Re} p > 0$
7	$\frac{1}{t^{3/2}} e^{-\frac{a}{t}}$	$\sqrt{\frac{\pi}{a}} e^{-2\sqrt{ap}}$	$\operatorname{Re} a > 0$, $\operatorname{Re} p > 0$
8	$t^\nu e^{-\frac{a}{t}}$	$2\left(\frac{a}{p}\right)^{\frac{\nu+1}{2}} K_{\nu+1}\left(2\sqrt{ap}\right)$	$\operatorname{Re} a > 0$, $\operatorname{Re} p > 0$, K_ν = modified Bessel function of order ν.
9	$e^{a^2 t} \operatorname{erfc}\left(a\sqrt{t} + \frac{b}{\sqrt{t}}\right)$	$\frac{1}{\sqrt{p}\left(\sqrt{p}+a\right)} e^{-2b\left(\sqrt{p}+a\right)}$	$\operatorname{Re} b^2 \geq 0$, $\operatorname{Re} p > 0$ if $\operatorname{Re} a \geq 0$, $\operatorname{Re} p > \max\left(0, \operatorname{Re} a^2\right)$ if $\operatorname{Re} a < 0$.
10	$\frac{1}{t}$	$-\gamma - \ln(p)$	$\operatorname{Re} p > 0$, γ = Euler's constant
11	$\frac{1}{t^{3/2}}$	$-2\sqrt{\pi p}$	$\operatorname{Re} p > 0$

B.2 Fourier Transforms

Table B.2 contains formulae for the Fourier transforms which have been used in this thesis. These formulae are from Haberman (1998).

Table B.2: Table of Fourier transforms

	$f(x)$	$\widehat{f}(\omega) = \int_{-\infty}^{\infty} f(x)\, e^{-i\omega x}\, dx$
1	$f'(x)$	$i\omega \widehat{f}(\omega)$
2	$f''(x)$	$-\omega^2 \widehat{f}(\omega)$
3	$\delta(x-a)$	$e^{-i\omega a}$
4	$e^{-\frac{x^2}{2\sigma^2}}$	$\sqrt{2\pi}\sigma e^{-\frac{\omega^2\sigma^2}{2}}$

References

Abramowitz, M. (1964). *Handbook of mathematical functions with formulas, graphs, and mathematical tables* (M. Abramowitz & I. A. Stegun, Eds.). Washington: U.S. Govt. Print. Off.

Asman, W., Jorgensen, A., & Jensen, P. K. (2003). Dry deposition of spray drift of pesticides to nearby water bodies. *Pesticide Research*, *66*. (Retrieved May 12, 2008 from http://www2.mst.dk/common/Udgivramme/Frame.asp?http://www2.mst.dk/udgiv/Publications/2003/87-7972-945-2/html/indhold_eng.htm)

Beck, J. V., Cole, K. D., Haji-Sheikh, A., & Litkouhi, B. (1992). *Heat conduction using green's functions*. Hemisphere.

Bhalwankar, R. V., Sathe, A. B., & Kamra, A. K. (2004). The evaporation of the charged and uncharged water drops suspended in a wind tunnel. *Proc. Indian Acad. Sci. (Earth Planet. Sci.)*, *113*(2), 129–138.

Bilanin, A. J., Teske, M. E., Barry, J. W., & Ekbald, R. B. (1989). AGDISP: The aircraft spray dispersion model, code development and experimental validation. *Transactions of the ASAE*, *32*(1), 327–334.

Brown, R. B., & Sidhamed, M. M. (2001). Simulation of spray dispersal and deposition from a forestry airblast sprayer - part II: Droplet trajectory model. *Transactions of the ASAE*, *44*(1), 11–17.

Calder, K. L. (1961). Atmospheric diffusion of particulate material, considered as a boundary value problem. *Journal of Meteorology*, *18*, 413–416.

Cleugh, H. A. (1998). Effects of windbreaks on airflow, microclimates and crop yields. *Agroforestry Systems*, *41*, 55–84.

Craig, I. P. (2004). The GDS model - a rapid computational technique for the calculation of aircraft spray drift buffer distances. *Computers and Electronics in Agriculture*, *43*, 235–250.

Crank, J. (1984). *Free and moving boundary problems*. New York: Oxford University Press.

Davies, C. N. (1978). Evaporation of airborne droplets. In D. T. Shaw (Ed.), *Fundamentals of aerosol science* (pp. 135–164). New York: Wiley.

Eltayeb, I. A., & Hassan, M. H. A. (2000). Diffusion of dust particles from a point source above ground level and a line source at ground level. *Geophys. J. Int.*, *142*, 426–438.

Essa, K. S. M., Etman, S. M., & Embaby, M. (2007). New analytical solution of the dispersion equation. *Atmospheric Research*, *84*, 337–344.

Finnigan, J. (2000). Turbulence in plant canopies. *Annu. Rev. Fluid Mech.*, *32*, 519–571.

Gradshteyn, I. S., & Ryzhik, I. M. (2000). *Table of integrals, series and products* (6th ed.; A. Jeffrey, Ed.). San Diego: Academic Press.

Green, D. W., & Perry, R. H. (2008). *Perry's chemical engineers' handbook* (8th ed.). New York: McGraw-Hill.

Haberman, R. (1998). *Elementary applied partial differential equations with fourier series and boundary value problems* (3rd ed.). Prentice Hall.

Harper, S. A. (2007). Modelling droplet transport and interception by a shelterbelt: a continuum approach. *Gazette of the Australian Mathematical Society*, *34*(4). (Available online at http://www.austms.org.au/Publ/Gazette/)

Hewitt, A. J. (2001). *Drift filtration by natural and artifical collectors: a literature review* (Report No. T00-008). Spray Drift Task Force. (Available online at http://www.agdrift.com/PDF_FILES/drift%20filtration.PDF)

Holland, P., & Maber, J. (1991). Little spray goes past the shelter. *NZ Kiwifruit Journal*, *September 1991*, 8–9.

Holland, P., May, B., & Maber, J. (n.d.). *Hortresearch publication - spray drift from orchards.* (Retrieved December 22, 2005, from http://www.hortnet.co.nz/publications/science/sprydrft.htm)

Holland, P. T., Maber, J. F., May, W. A., & Malcolm, C. P. (1997). Drift from orchard spraying. In *Proceedings of the New Zealand plant protection conference* (Vol. 50, pp. 112–118).

Holterman, H. J., van de Zande, J. C., Porskamp, H. A. J., & Huijsmans, J. F. M. (1997). Modelling spray drift from boom sprayers. *Computers and Electronics in Agriculture*, *19*, 1–22.

Incompressible flow. (n.d.). In *McGraw-Hill Encyclopedia of Science and Technology.* (Retrieved November 16, 2007, from Answers.com, http://www.answers.com/topic/incompressible-flow)

Lazzaro, L., Otto, S., & Zanin, G. (2008). Role of hedgerows in intercepting spray drift: Evaluation and modelling of the effects. *Agriculture, Ecosystems and Environment*, *123*, 317–327.

Lim, L. L. (2005). *Modelling of volcanic ashfall.* Phd thesis, Massey University. (Retrieved November 9, 2006, from Massey University Library)

Lin, J., & Hildemann, L. M. (1996). Analytical solutions of the atmospheric diffusion equation with multiple sources and height-dependent wind speed and eddy diffusivities. *Atmospheric Environment*, *30*(2), 239–254.

Lin, J., & Hildemann, L. M. (1997). A generalized mathematical scheme to analytically solve the atmospheric diffusion equation with dry deposition. *Atmospheric Environment*, *31*(1), 59–71.

Lindstrom, F. T., & Boersma, L. (1989). Analytical solutions for convective-dispersive transport in confined aquifers with different initial and boundary conditions. *Water Resources Research*, *25*(2), 241–256.

Linz, P. (1985). *Analytical and numerical methods for volterra equations.* Philadelphia: SIAM.

Lorenzini, G. (2006). Water droplet dynamics in an irrigation spray. *Transactions of the ASABE*, *49*(2), 545–549.

Manktelow, D., Gaskin, R., & May, B. (2006). You won't get my drift! *NZ Kiwifruit Journal*, *July/August 2006*, 31–35.

McKibbin, R. (2006). Modelling pollen distribution by wind through a forest canopy. *JSME International Journal, Series B*, *49*(3), 583–589.

McKibbin, R., Lim, L. L., Smith, T. A., & Sweatman, W. L. (2005). A model for dispersal of eruption ejecta. In *Proceedings world geothermal congress.* (Retrieved December 13, 2007, from http://ifs.massey.ac.nz/staff/smith/WGC2005.PDF)

Mercer, G. N. (n.d.). Modelling to determine the optimal porosity of shelterbelts for the capture of agricultural spray drift. *Submission to Environmental Modelling & Software.*

Mercer, G. N., & Roberts, T. (2005). Predicting off-site deposition of spray drift from horticultural spraying through porous barriers on soil and plant surfaces. In G. Wake (Ed.), *Proceedings of the 2005 Mathematics in Industry study Group* (pp. 27–52).

Miller, P. C. H., & Hadfield, D. J. (1989). A simulation model of the spray drift from hydraulic nozzles. *J. Agric. Engng Res.*, *42*, 135–147.

Ministry of Agriculture and Forestry. (2006). *SFF project summary: Minimising off-target impacts of kiwifruit orchard sprays.* (Retrieved January 22, 2007, from http://www.maf.govt.nz/sff/about-projects/search/06-090/index.htm)

Moreira, D. M., Rizza, U., Vilhena, M. T., & Goulart, A. (2005). Semi-analytical model for pollution dispersion in the planetary boundary layer. *Atmospheric Environment*, *39*, 2673–2671.

Palmer, J. W., Snelgar, W. P., & Manson, P. J. (1993). Shade cast by shelterbelts around kiwifruit orchards; validation of a computer model. *Agricultural and Forest Meteorology*, *66*, 21–30.

Peters, K., & Eiden, R. (1992). Modelling the dry deposition velocity of aerosol particles to a spruce forest. *Atmospheric Environment*, *26A*(14), 2555–2564.

Pruppacher, H. R., & Klett, J. D. (1978). *Microphysics of clouds and precipitation.* Dordrecht: D. Reidel.

Raupach, M. R., Briggs, P. R., Ahmad, N., & Edge, V. E. (2001). Endosulfan transport: II. modeling airborne dispersal and deposition by spray and vapor. *J. Environ. Qual.*, *30*, 729–740.

Raupach, M. R., Leys, J. F., Woods, N., Dorr, G., & Cleugh, H. A. (2000). *Modelling the effects of riparian vegetation on spray drift and dust: the role of local protection* (Technical Report No. 29/00). CSIRO Land and Water.

Raupach, M. R., Woods, N., Dorr, G., Leys, J. F., & Cleugh, H. A. (2001). The entrapment of particles by windbreaks. *Atmospheric Environment*, *35*, 3373–3383.

Reist, P. C. (1993). *Aerosol science & technology* (2nd ed.). New York: Wiley.

Roberts, G. E., & Kaufman, H. (1966). *Table of laplace transforms.* Philadelphia: W. B. Saunders.

Rogers, G. F. C., & Mayhew, Y. R. (1980). *Thermodynamic and transport properties of fluids SI units* (3rd ed.). Basil Blackwell.

The MathWorks^{TM}. (n.d.). *MATLAB® - the language of technical computing.* (Retrieved May 5, 2008, from http://www.mathworks.com/products/matlab/)

Thompson, N., & Ley, A. J. (1983). Estimating spray drift using a random-walk model of evaporating drops. *J. Agric. Engng Res.*, *28*, 419–435.

Ucar, T., & Hall, F. R. (2001). Windbreaks as a pesticide drift mitigation strategy: a review. *Pest Management Science*, *57*, 663–675.

Ucar, T., Hall, F. R., Tew, J. E., & Hacker, J. K. (2003). Wind tunnel studies on spray deposition on leaves of tree species used for windbreaks and exposure of honey bees. *Pest Management Science*, *59*, 358–364.

Walklate, P. J. (1992). A simulation study of pesticide drift from an air-assisted orchard sprayer. *J. agric. Engng Res.*, *51*, 263–283.

Walklate, P. J. (1993). The effect of orchard crop structure on the integral length-scale of turbulence. *Boundary-Layer Meteorology*, *63*, 1–22.

Wang, H., Takle, E. S., & Shen, J. (2001). Shelterbelts and windbreaks: Mathematical modeling and computer simulations of turbulent flows. *Annu. Rev. Fluid Mech.*, *33*, 549–586.

Wang, Y. S., Miller, D. R., & Anderson, D. E. (1992). A spatial length scale analysis of turbulent temperature and velocity fluctuations within and above an orchard canopy. *Boundary-Layer Meteorology*, *59*, 125–139.

Weisstein, E. W. (2002). Modified bessel function of the second kind. In *Mathworld - A Wolfram Web Resource.* (Retrieved January 13, 2008 from http://mathworld.wolfram.com/ModifiedBesselFunctionoftheSecondKind.html)

Wolf, R. (1997). *Strategies to reduce spray drift.* Retrieved April 21, 2008, from http://www.pesticidesafety.uiuc.edu/facts/strategies.pdf.

Zemanian, A. H. (1987). *Distribution theory and transform analysis.* New York: Dover. (Reprint, slightly corrected. Originally published: New York: Mc Graw-Hill, 1965)